VOLUME 14 (1959) No. 1

NUCLEAR PHYSICS

JOURNAL DEVOTED TO THE EXPERIMENTAL AND THEORETICAL STUDY OF THE FUNDAMENTAL CONSTITUENTS OF MATTER AND THEIR INTERACTIONS

EDITOR: L. ROSENFELD · COPENHAGEN

C. J. GALLAGHER Jr. and T. D. THOMAS, Vibrational states in U^{234} excited by Np^{234} decay and evidence for an E0-transition between states with $I \neq 0$ . . 1

D. W. LANG and K. J. LE COUTEUR, Pairing energy effects in excited nuclei . . 21

D. KLEITMAN, On the parity of K-baryon vertices 33

D. M. VAN PATTER, E2 transitions from the second 2+ level of even-even nuclei 42

N. MACDONALD, Even nuclei without an axis of symmetry 70

N. NATH, M. A. ROTHMAN, D. M. VAN PATTER and C. E. MANDEVILLE, Inelastic neutron scattering in Nb^{93} 78

R. BLANKENBECLER, A contraction rule for composite particles 97

MASATO MORITA, γ_5 symmetries and relativistic corrections in beta decay . . 106

E. W. CYBULSKA and L. MARQUEZ, Gamma rays in the decay of ^{141}Nd 117

J. M. LEBLANC, R. E. COTÉ and L. M. BOLLINGER, On the splitting of the peak in the neutron strength function near $A = 55$ 120

J. DULAR, G. KERNEL, M. KREGAR, M. V. MIHAILOVIĆ, G. PREGL, M. ROSINA and Č. ZUPANČIČ, Nuclear absorption of gamma rays in Al, Si, P, S and Ca . . 131

R. K. SHELINE, H. L. NIELSEN and A. SPERDUTO, An aid in the determination of nuclear spins 140

P. BOSKMA and H. DE WAARD, Decay of ^{140}Ba 145

SEITARO NAKAMURA, The universal Fermi interaction and heavy mesons . . . 155

News Items 169

Book Reviews 172

NORTH-HOLLAND PUBLISHING COMPANY-AMSTERDAM

December (1) 1959

EDITORIAL BOARD

AUSTRALIA & NEW ZEALAND:	H. Messel (Sydney), M. L. Oliphant (Canberra)
AUSTRIA:	B. Karlik, (Vienna), H. Thirring (Vienna)
BELGIUM:	M. de Hemptinne (Louvain), J. Verhaeghe (Ghent)
CANADA:	G. Volkoff (Vancouver)
DENMARK:	C. Møller (Copenhagen), S. Rozental (Copenhagen)
FINLAND:	L. Simons (Helsinki)
FRANCE:	A. Berthelot (Saclay), S. Gorodetzky (Strasbourg)
GERMANY (DEM. REP.):	G. Hertz (Leipzig)
GERMANY (FED. REP.):	W. Gentner (Freiburg i. B.), J. H. D. Jensen (Heidelberg)
GREAT BRITAIN:	S. Devons (Manchester), T. H. R. Skyrme (Harwell)
HUNGARY:	L. Janossy (Budapest)
INDIA:	H. Bhabha (Bombay), R. Ramanna (Trombay)
IRISH REPUBLIC:	J. McConnell (Maynooth)
ISRAEL:	G. Racah (Jerusalem)
ITALY:	E. Amaldi (Rome)
JAPAN:	S. Kikuchi (Tokyo), S. Tomonaga (Tokyo)
MEXICO:	M. Moshinsky (Mexico)
NETHERLANDS:	H. Brinkman (Groningen), S. R. de Groot (Leiden)
NORWAY:	E. Hylleraas (Oslo), A. Lundby (Oslo), H. Wergeland (Trondheim)
POLAND:	L. Infeld (Warsaw)
PORTUGAL:	J. M. Araújo (Porto), J. R. de Almeida Santos (Coimbra)
SOUTH AMERICA:	G. Beck (Saõ Paulo), J. Leite Lopes (Rio de Janeiro)
SPAIN:	J. M. Otero (Madrid), C. Sanchez del Rio (Madrid)
SWEDEN:	O. Klein (Stockholm), K. Siegbahn (Uppsala), I. Waller (Uppsala)
SWITZERLAND:	P. Huber (Basel), P. Scherrer (Zürich)
U.A.R. & ARAB COUNTRIES:	F. El Bedewi (Alexandria), M. G. Nooh (Cairo)
U.S.A.	H. H. Barschall (Madison, Wisconsin), V. Weisskopf (Cambridge, Mass.)
U.S.S.R.:	M. A. Markov (Moscow), I. S. Shapiro (Moscow), D. V. Skobeltzyn (Moscow)
YUGOSLAVIA:	I. Supek (Zagreb)

CONTRIBUTIONS may be sent to the Editor, Professor L. Rosenfeld, NORDITA, Blegdamsvej 17, Copenhagen Ø, either directly, or preferably through the intermediary of one of the members of the Editorial Board of the country or region in which the author is working. They may be written in English, French or German.

NUCLEAR PHYSICS is published in fortnightly issues. The subscription price per volume of 700 pages is fl 57.00; 114s; $ 15.00. Post-free.

SUBSCRIPTIONS should be sent to the publishers, NORTH-HOLLAND PUBLISHING COMPANY, P.O.Box 103, Amsterdam or to any subscription-agent.

BOOKS FOR REVIEW should be sent to Professor Rosenfeld.

No part of this issue may be reproduced in any form, by print, photoprint, microfilm or any other means without written permission from the publisher. Reprints, photoprints or microfilms are obtainable at cost from the publisher.

Printed in the Netherlands

1.D.2:1.E.1:
1.E.4:3.B

Nuclear Physics **14** (1959/60) 1—20; © *North-Holland Publishing Co., Amsterdam*
Not to be reproduced by photoprint or microfilm without written permission from the publisher

VIBRATIONAL STATES IN U^{234} EXCITED BY Np^{234} DECAY AND EVIDENCE FOR AN E0-TRANSITION BETWEEN STATES WITH $I \neq 0$

C. J. GALLAGHER Jr.

Norman Bridge Laboratory of Physics, California Institute of Technology, Pasadena, California

and

T. D. THOMAS

Lawrence Radiation Laboratory and Department of Chemistry, University of California, Berkeley, California †

Received 4 August 1959

Abstract: Transitions following the EC-capture decay of 4.4-day Np^{234} have been investigated with 99-, 160- and 350-gauss permanent magnets, a solenoidal "long lens" spectrometer, and NaI(Tl) scintillation detectors with a 100-channel analyzer. Many internal conversion electron lines were observed, and assigned to transitions at 43.49, 99.70, 233.6, 234.6, 238.6, 247.9, 297.6, 450.5, 482.8, 485.1, 515.7, 525.9, 556.8, 744.1, 751.7, 767.9, 787.8, 793.8, 810.0, 812, 854, 1003, 1105, 1196, 1240, 1395, 1439, 1531, 1562, 1575 and 1606 keV. A few other weak electron lines were observed, but not assigned to transitions. Transitions following Np^{236}, Np^{238}, and Np^{239} decay were also observed on the same plates and identified, helping to insure correctness of the isotopic assignment of the U^{234} transitions. The above transitions have been interpreted to establish levels in U^{234} at 43.49, 143.2, 788, 812, 854, 1049, 1090, 1092, 1240, 1340, 1439, 1575 and 1606 keV. The 812-keV E0 transition has been resolved into two components, one of which is interpreted to be an E0-transition between two 2^+ states. Transition multipolarities and possible level spin and parity assignments are discussed. A comparison of the known data on relative energies of vibrational states indicates that the β-vibrational states have lower energies than the γ-vibrational states in the few nuclei where the energies of both are known.

1. Introduction

The spectra of deformed even nuclei in the rare earth and heavy element regions of the periodic table have been shown to be remarkably similar. Qualitative understanding of these spectra has been achieved largely on the basis of the Bohr-Mottelson model [1]), which describes these states as due to collective rotational and vibrational motions of many nucleons. The rotational states have been extensively studied [2]), whereas considerably less is known about the vibrational states [2, 3, 4]) ††. When this work was begun no spectra had been reported in which both the theoretically predicted "β" and "γ" vibrational states had been observed. The present study was undertaken in an attempt to

† This work was supported by the United States Atomic Energy Commission.

†† See for example the decay schemes of Ta^{182}, Re^{182}, Re^{184}, Tb^{160}, Th^{228}, and Np^{238} in ref. [2]) for data on γ-vibrational states. See also the decay scheme of Ho^{166} shown in ref. [2]). Ref. [2]) and [3]) contain what information was available until recently on β-vibrational states.

obtain information on the relative energies of the β and γ vibrational levels in a single nucleus, and also perhaps the rotational states based upon them. Np^{234} was chosen because earlier work [5, 6, 7]) on the decay of this nucleide had shown strong cascade transitions, suggesting possible excitation of vibrational states decaying through lower lying vibrational states, and also that a 0+ level in U^{234} at approximately 800 keV is populated.

2. Previous Results on the Levels of U^{234}

Before beginning the discussion of the present experiment, let us review the previous work on the levels of U^{234}, as populated by the EC decay of Np^{234}, the β^--decay of the Pa^{234} isomers, and the alpha decay of Pu^{238}.

The 4.40-day electron capturing isotope Np^{234} was first reported by Hyde, Studier and Ghiorso [8]). Early spectroscopic studies were made by Orth [5]) who reported 0.177-, 0.442-, 0.803- and 1.42-MeV transitions. Hoff [6]) remeasured the spectrum and reported 0.76-, 0.81-, and 1.57-MeV transitions and a K/L X-ray ratio of $\frac{10}{7}$, from which he concluded a K/L electron-capture ratio of ≈ 1. Prestwood, Smith, Brown and Hoffman [9]) reported the presence of a β^+ group of 0.8-MeV endpoint and a β^+/EC ratio of $4.6 \pm 1 \times 10^{-4}$. The decay energy of 1.8 MeV determined by this method agrees with the closed-cycle calculations of Foreman [10]).

The most recent work on this isotope was done by Huizenga, Engelkemeir, Freedman, Porter and Gindler [9]), who reported evidence for 18 gamma transitions on the basis of scintillation spectroscopy and internal conversion data. The transitions they reported are shown in table 1. They also reported the

TABLE 1

Transitions reported by Huizenga *et al.* [7]) following the decay of Np^{234}

Energies of transitions deduced from internal conversion data (keV)	Energies of additional transitions observed with scintillation detector (keV)
43	500
109	720
234	905
247	1010
449	1190
517(?)	1540
752	
813	
1567	

coincidence data shown in table 2. They did not, however, postulate a definitc decay scheme for Np^{234}. Thus no definite U^{234} level scheme has been proposed on the basis of Np^{234} decay.

TABLE 2
Coincidence measurements reported by Huizenga *et al.* [7]) in Np^{234} decay to U^{234}

Energy of gate (keV)	Energy of coincident transitons (keV)
500	445, 720, 905, 1010
720	445, ≈750
1190	235
1540	excess LX-rays

Studies of the beta decay of UX complex by many workers [2]) have indicated that these nucleides populate many levels in U^{234}. The latest work on the isomers has been reported by Ong, Verschoor and Born [11]), who reported evidence for 24 transitions based on conversion electron and gamma scintillation studies. The transitions were interpreted to establish the U^{234} level scheme shown in fig. 4.

Almost all of the authors mentioned above reported that the 812 keV transition (our energy value) was probably an E0, as its K-internal conversion coefficient was too large to assign it other than E0 multipolarity. This assignment was checked in $Pa^{234}(UX_2)$ decay by Cross and Eastwood [12]), and later rechecked by Ong *et al.* [11]). The latter measured both internal and external conversion lines, and reported no evidence for gamma rays of ≈ 0.80 MeV. It is interesting to note here that Ong *et al.* apparently resolved the 812-keV transition into two components, of which they concluded at least one had to be appreciably E0.

In addition to these studies of the decays of the Pa^{234} isomers and Np^{234}, studies of the alpha decay of Pu^{238} have established [2]) the 43.5-, 143.2- and 812-keV levels in U^{234}. The level energies we quote are those determined in the present study.

The population of the 812-keV 0+ state following Pu^{238} alpha decay has been measured by Perlman, Asaro, Harvey and Stephens [3]). They were able to set limits on the conversion coefficient of the ≈ 800-keV transition, essentially ruling out everything except E0 multipolarity, and thus confirming the results of the earlier workers.

3. Experimental

3.1. INSTRUMENTS AND EXPERIMENTAL TECHNIQUES

Three permanent magnet spectrographs [13]) of 0.1 % and a "long lens" annular focussing spectrometer at 2.2 % momentum resolution were used to study the electron spectrum. The detector in the spectrometer was a $\frac{3}{4}$-inch-diameter, $\frac{1}{8}$-inch-thick anthracene crystal attached by a 1-inch diameter Lucite light pipe 6 inches long to a DuMont 6292 phototube. Eastman Kodak No-

Screen X-ray film was used in the spectrographs. No attempt was made to obtain numerical intensities from the photographic plates; we report only visual estimates on these intensities. A $1\frac{1}{2} \times 1$ inch NaI(Tl) scintillation spectrometer of $\approx 8\,\%$ resolution (at 1 MeV) with a Penco 100-channel analyzer was used to obtain gamma intensities.

3.2. SOURCE PREPARATION

Approximately 1 mC of Np^{234} was prepared by the U^{235}(d, 3n)Np^{234} reaction in the Berkeley 60-inch cyclotron. The isotopic composition of the U^{235} was $\approx 93\,\%$ U^{235} and $\approx 7\,\%$ U^{238}. The rigorous chemical method used to isolate the neptunium fraction is described in the appendix. The carrier-free activity obtained was deposited on 0.010-inch platinum wires by cathodic electrodeposition from $1M(NH_4)_2C_2O_4$ plating solution at 150 mA and 5 V for 15 minutes. The source for the long-lens spectrometer was made by evaporating approximately 50 μl containing 0.2 mC of Np activity on a Tygon film of approximately 100 $\mu g/cm^2$ thickness.

3.3. EXPERIMENTAL RESULTS

3.3.1. *Permanent Magnets*

Spectra taken with the permanent magnets indicated the presence of Np^{236}, Np^{238} and Np^{239} activities in addition to the Np^{234}. Fortunately these isotopes have been studied at high resolution and their spectra are well known. The lines of Np^{236}, Np^{238} and Np^{239} which we observed are indicated in table 7, 8 and 9. A tabulation of the electron spectrum in order of increasing electron line energy, and also the electron line energies supporting the transition assignments, will be made available later in a Lawrence Radiation Laboratory Report. The Np^{236} spectrum contained two new lines, corresponding to a new level in U^{236} at 688 keV. A separate bombardment was made to show that the activity producing these lines decayed with a 22-hour half-life. The Np^{236} assignments were based on the work of Gray [14]), the Np^{238} on the summary of data by Albridge and Hollander [15]) and the Np^{239} on the results of Hollander, Smith and Mihelich [16]). A rough check of the half-lives of the individual lines was made by taking a series of exposures at four-day intervals for a period of approximately 3 weeks following the irradiation.

The Np^{234} electron spectrum proved to be extremely complex, especially in the high energy region. The portion of the electron spectrum which yielded to analysis, and which could be assigned to transitions, is reported in table 3. Only visual intensity estimates are reported. The energy calibration of the lines below 500-keV was made relative to the reported energies of the Np^{239} transitions. Because of the less accurate calibration of the high energy spectrograph the values reported for high energy transitions are estimated to have an absolute error of $\pm 0.2\,\%$. The transitions of Np^{238} were not used to calibrate

TABLE 3

Transitions in U^{234} following Np^{234} decay. Transition assignments are based on the internal conversion data tabulated below. The isotope assignment is based on the decay of the lines observed in a series of five exposures at 4.4-day intervals over an approximately three week period. Visual intensities listed are vvs = very very strong, vs = very strong, s = strong, ms = moderately strong, m = moderate, mw = moderately weak, w = weak, vw = very weak, vvw = very very weak, ew = extremely weak, ew? = extremely weak and questionable, −d = diffuse

Assignment	Energy of gamma (keV)	Subshell conversion										Multipolarity
		K	L_I	L_{II}	L_{III}	M_I	M_{II}	M_{III}	N_I	N_{II}	N_{III}	
BA	43.49±0.05 [a]			mw	m [b]		m [c]	ms [d]		w	vw	E2
CB	99.7 ±0.1 [a]			vw	ew?		ew?					E2
—	233.6 ±0.2 [e]	ew?	ew									
MK	234.6 ±0.2 [e]	vvw	w [f]			ew?			ew?			
IF	238.6 ±0.4 [g]	ew?										
KI	247.9 ±0.2 [e]	vvw−d	ew			ew						
NK	265.8 ±0.5 [g]	ew?										
—	297.6 ±0.5 [g]	ew?										
JD	450.5 ±0.5	ms	vw	ew	ew?	ew?						
MI	482.8 ±1 [g]	ew?										
MH	485.1 ±1 [g]	ew?										
NH	515.7 ±0.5	mw	ew									
MG	525.9 ±0.5	ew−d										
NG	556.8 ±0.6	m	ew−d [h]									
DB	744.1 ±0.7	w										
NF	751.7 ±0.8	w	ew?									
EB	768.0 ±0.8	ew−d	ew?									
DA	787.8 ±0.8	vvw										
NE	793.8 ±0.8	vw										
FB	810.0 ±0.8	s	mw			ew						(E0)
EA	811.6 ±0.8	vvs	ms			w			ew−d			E0
FA	853.6 ±1	ew?										
—	1003 ±2	vvw	ew?									
—	1105 ±2	ew?										
JB	1196 ±2	ew										
JA	1240 ±2 [i]	ew??										
LB	1395 ±3 [i]	ew??										
LA	1439 ±3	ew										
MB	1531 ±3	vw										
NB	1562 ±3	m	vvw			ew						
MA	1575 ±3	vw	ew									
NA	1606 ±3	w	ew									

[a] Electron lines observed on 99-gauss magnet.
[b] L_{III} 43.49 (U^{234}), L_I 49.38 (Pu^{239}) superimposed.
[c] M_{II} 43.49 (U^{234}), L_I 61.42 (Pu^{239}) superimposed.
[d] M_{III} 43.49 (U^{234}), L_{III} 57.26 (Pu^{239}) superimposed.
[e] K lines observed 99-gauss magnet. L and M lines observed on the 160- and 350-gauss magnets.
[f] L_I 234.6 (U^{234}), K 333.4 (Pu^{239}) superimposed.
[g] Lines observed on the 160-gauss magnet and read only by TDT.
[h] All succeeding intensities (underlined) observed on the 350-gauss magnet.
[i] Lines observed on the 350-gauss magnet and read only by TDT. Lines were also observed on the ring-focussing spectrometer.

the spectrum because they had been measured on the same instrument and in addition did not extend to as high energies as the transitions of Np^{234} decay. However, if the Np^{238} lines are used to calibrate the spectrograph field, the energies reported in table 3 for the transitions above about 800 keV should be decreased by approximately 1 keV. Regardless of the absolute error, the overall relative energies have excellent internal agreement, and the sums which serve as the basis for the decay scheme are shown in table 4. The electron binding energies reported by Hill [17]) were used in analyzing the data.

TABLE 4

Sums and differences supporting the U^{234} level assignments

Transition 1	Transition 2	Sum or difference	Transition 3	Level energy (keV)	Level designation
1562.2	43.49	1605.69	1605.8	1606	N
1531	43.49	1574.49	1574.5	1575	M
1394.8	43.49	1438.29	1438.6	1439	L
1605.8	265.8	1340.0	—	1340	K
1574.5	234.6	1339.9	—	1340	K
1196.1	43.49	1239.59	1239.6	1240	J
787.8	450.5	1238.3	1239.6 [a]	1240	J
853.6	238.6	1092.2	—	1092	I
1574.5	482.8	1091.7	—	1092	I
1605.8	515.7	1090.1	—	1090	H
1574.5	485.2	1089.3	—	1090	H
1605.8	556.8	1049.0	—	1049	G
1574.5	525.9	1048.6	—	1049	G
1605.8	751.7	854.1	853.6	854	F
809.9	43.49	853.4	853.6	854	F
1605.8	793.8	812.0	811.6	812	E
768.0	43.49	811.49	811.6	812	E
744.1	43.49	787.59	787.8	788	D

[a] The difference in energy between the sum and this crossover transition is the worst in the table, 1.3 keV. This is probably a result of the calibration used because the low energy transitions are calibrated relative to the Np^{239} transitions, whereas the high-field spectrograph has not been calibrated absolutely in this experiment.

Electron lines which could not be readily assigned to transitions are tabulated in table 5. In most cases these are probably due to KLM and KLN Auger electrons.

3.3.2. *Ring Focussing Spectrometer and Gamma Scintillation Detector Measurements*

The electron spectrum measured in the ring-focussing spectrometer above about 650 keV is shown in fig. 1. The spectrum shown is a composite spectrum of data gathered over a period of approximately 3 weeks. The data were correct-

TABLE 5

Electron lines observed which are probably due to Np^{234} decay but which are not sufficiently well established to be assigned to transitions. Intensity code as in table 3

Electron energy (keV)	Electron intensity	Comments or possible assignment
79.87	vvw	Pu Auger (KL_IL_{II})
88.38 [a]	vw	Probably uranium KLX Augers.
89.18 [a]	vw—d	
90.09 [a]	m	
90.42 [a]	vw	
92.95 [a]	s—d	
93.54 [a]	s	
96.10 [a]	vvw	
97.53 [a]	m	
108.73 [a]	vvw	
109.96 [a]	vvw	
161.64 [a]	ew?	
178.96 [a]	ew?	
192.51 [a]	ew?	
195.93 [a]	ew	
330.11 [a]	ew—d	
345.55 [a]	ew?	
356.37 [a]	ew?	
690.6	ew	Probably due to extremely intense line at 696.5.
1318.9 [a]	vvw	

[a] Lines read only by TDT on spectrograph plates exposed later in the series than those from which most of the data were taken.

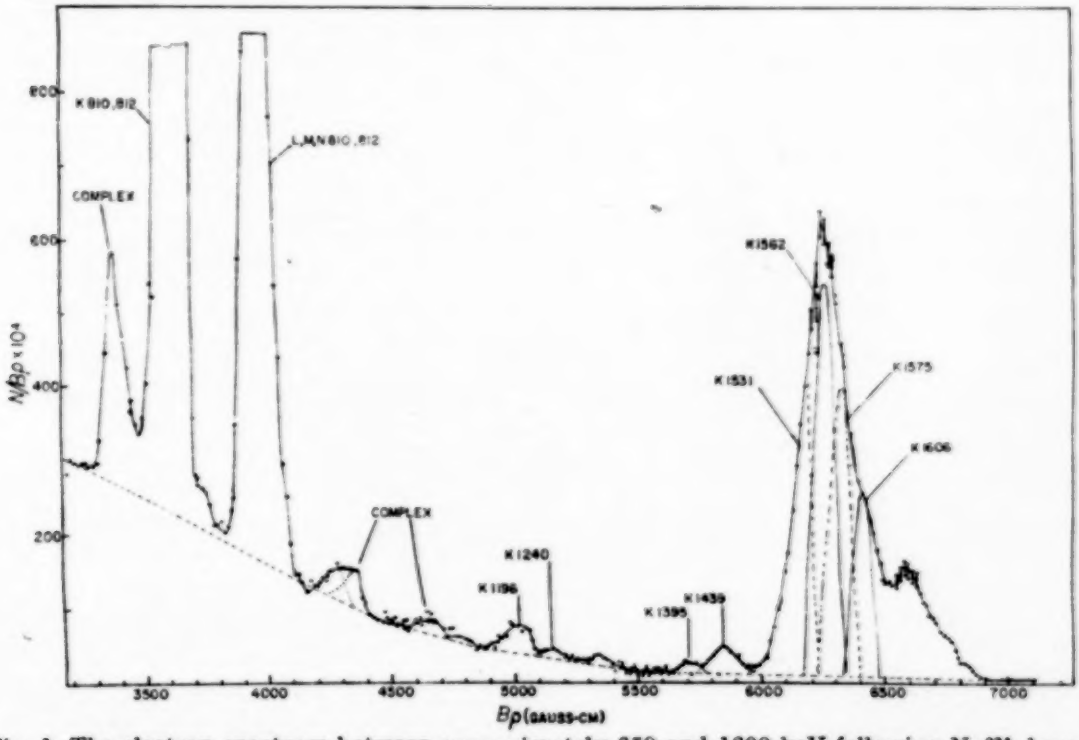

Fig. 1. The electron spectrum between approximately 650 and 1600 keV following Np^{234} decay. The resolution is 2.2 %. The curve represents the average of 3 runs over the spectrum using constant counts. (Hence the variation in statistics.) The data were corrected for the decay of Np^{234} and therefore the Np^{238} beta spectrum causes some distortion of the background.

TABLE 6

Intensity measurements from the instruments with low resolution. The electron intensities were measured with the long lens spectrometer at 2.2 % resolution. (See fig. 1). The gamma data were measured with a NaI(Tl) scintillation spectrometer. (See fig. 2.) Only the most intense gamma peaks are reported, as the complexity of the spectrum makes an accurate analysis of the gamma spectrum difficult

Electron energy (keV)	Assignment	Corresponding transitions from 350 gauss-magnet	Gross electron intensity I_K	Gross electron intensity I_L	Gross gamma intensity I_γ	Gross conversion coefficient $\bar{\alpha}_{abs}$
		K 482.8				
		K 485.1				
408	K 523	K 515.7	36			
		K 525.9				
		L 450.5				
440	K 556	K 556.8	33			
		L 482.8				
		L 485.1				
496	L 523	L 515.7		5.6		
		L 525.9				
537	L 559	L 556.8		3.6		
		K 744.1				
638	K 754	K 751.7	20			$\geqq 0.01$
		K 768.0				
		K 787.8			1	
		K 793.8				
695	K 811	K 810.0	529			$\geqq 0.26$
		K 811.6				
		L 744.1				
		L 751.7				
731	L 752	L 768.0		2.3		
		K 853.6				
		L 787.8				
		L 793.8				
796	L 817	L+M 810.0	136			
		L+M 811.6				
		K 986 [a]				
881	K 997	K 1002				
		K 1027 [a]	5.8			
899	K 1015	K 1029 [a]				
		L 1002				
988	L 1010	K 1104	1.8			
		L 1027 [a]				
1018	L 1041	L 1029 [a]		0.25		
1090	K 1206	K 1196	3.7			
1124	K 1240	K 1240	0.6			
1178	L 1200	L 1196		0.5		
1287	K 1402	K 1395	0.7			
1331	K 1447	K 1437	3.2			
1408	K 1523	K 1531				
1435	K 1550	K 1562	116		5.7	$(\geqq 0.01)$ [b]
1462	K 1577	K 1575				
1495	K 1610	K 1606				
		L 1531				
1536	L 1558	L 1562				
1561	L 1583	L 1575	25.8			
1585	L 1607	L 1606				
		M 1562				

[a] Transitions in Pu^{238} from Np^{238} decay.

[b] Absolute value measured by Stephens [18]) and used for normalization.

ed only for background and the decay of 4.40-day Np^{234}. As a consequence, the presence of Np^{238} causes the beta spectrum shown.

The intensities of the lines measured in this spectrometer are reported in table 6. Many of these "lines" are unresolved groups. In addition we have reported two gamma intensities in this table. These low resolution data have

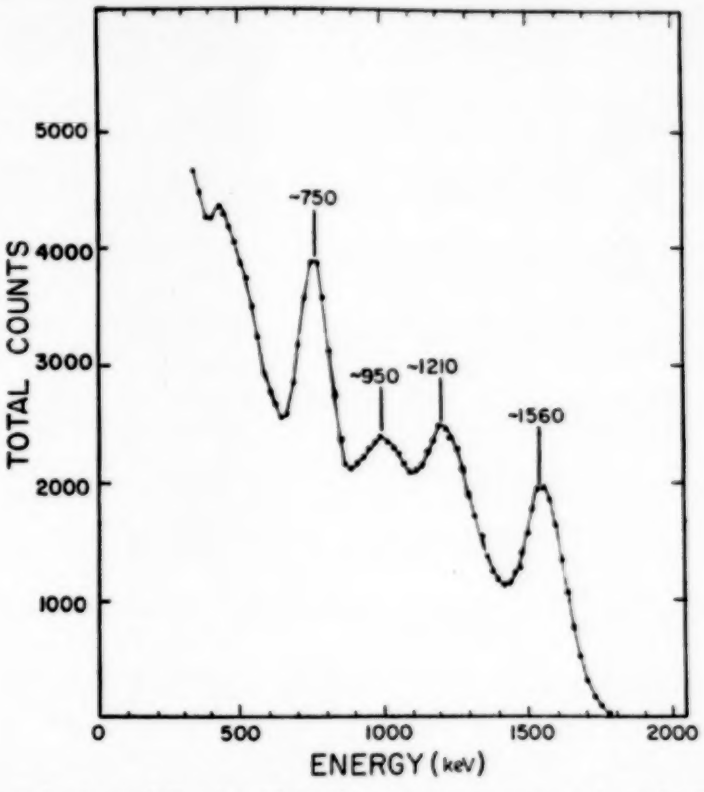

Fig. 2. The gamma spectrum following Np^{234} decay between approximately 650 and 1700 keV. The data shown were taken with 1 gram of lead between source and crystal.

been normalized absolutely to give the limits on the gross line conversion coefficient shown. The absolute normalization was made possible by the $\geqq 1$ % limit on the absolute conversion coefficient reported by Stephens [18]) for the gross 1560-keV transition. A gamma-ray spectrum, similar to that on which these intensities are based, is shown in fig. 2. The spectrum shows a cutoff at about 1600 keV. Such a result supports the 1800-keV decay energy obtained by closed-cycle calculations [10]) and the reported positron endpoint of 0.8 MeV [9]). We have not attempted to calculate log *ft* values for primary branching to the various levels because we do not believe our intensity data are sufficiently good to warrant such calculations.

4. Interpretation of Results

4.1. THE PROPOSED LEVEL SCHEME OF U^{234}

The level scheme proposed on the basis of present results is shown in fig. 3. The 43.49-, 143.2- and 812-keV levels have been observed in Pu^{238} alpha decay.

On the basis of the sums in table 4 the levels at 788, 854, 1240, 1439, 1575 and 1606 keV are reasonably well established. The levels at 1049, 1090 and 1340 keV are based on the energy difference between the transitions populating these levels from levels M and N, which are in excellent agreement with the energy NM. The 1092 level is then fixed. It is noteworthy that the proposed level

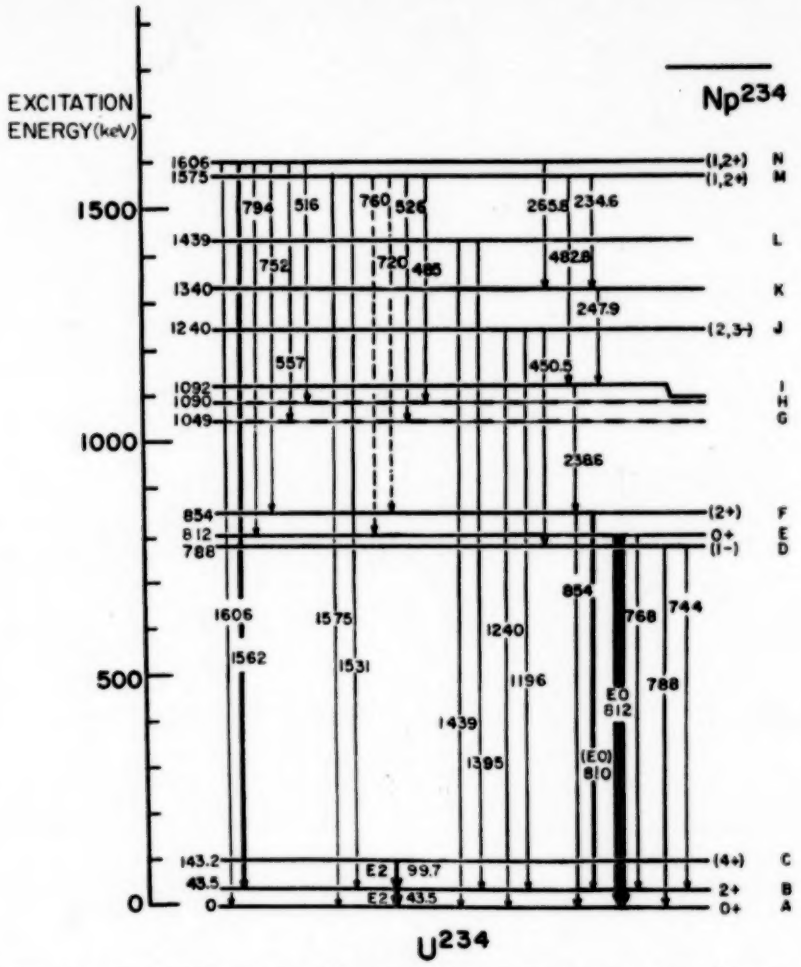

Fig. 3. Some of the levels of U^{234} populated by Np^{234} decay. The dashed transitions appeared on the spectrograph plates, but were too weak to be read accurately. They are not reported in table 1. The dashed levels are so represented because no transitions are observed to depopulate them.

scheme accounts for all of the definite transitions except the 233.6, 297.6, 1003 and 1105. The 1003 and 1105 transitions probably depopulate a level at 1146 keV; we have not indicated it in the figure, as its assignment is considerably less certain than that of the other levels.

4.2. TRANSITIONS SUPPORTING THE LEVEL SCHEME

In the introduction we stated that the purpose of this study was to obtain more information on the β-vibrational levels of nuclei. Experimentally this usually means observing an E0 transition. Thus our resolution of the conversion

lines of the 812-keV E0 transition into two components, both of which are quite strong, presented us with an interesting problem to interpret. First it was

TABLE 7

Electron lines observed in the sample which decayed with the Np^{236} half-life and which were assigned to Np^{236} on this basis. Intensity code as in table 3

Energy of gamma (keV)	Subshell conversion									
	K	L_I	L_{II}	L_{III}	M_I	M_{II}	M_{III}	N_I	N_{II}	N_{III}
A. From electron capture to U^{236}										
45.32			vvw	vvw–d		vw	vvw–d		vvw	ew?
643.0 [a]	m	vw								
688.2 [a]	mw	ew?								
B. From β^- decay to Pu^{236}										
44.6			vvw? [b]	ew [b]						

[a] This is the first time these transitions have been reported.

[b] L_{II}, L_{III} 44.6 (Pu^{236}) superimposed on L_{II}, L_{III} 44.64 (Pu^{239}). The intensity of these transitions is not consistent with the β^--branching of Np^{236} reported by Gray [14]). They appear to be considerably weaker than previously reported.

TABLE 8

Electron lines observed in the sample which agreed in energy with reported Pu^{238} transitions following Np^{238} decay. The transition energies used in the table are taken from the compilation of Np^{238} data by Albridge and Hollander [15]). Intensity code as in table 3

Energy of gamma (keV) [a]	Subshell conversion						
	K	L_I	L_{II}	L_{III}	M_I	M_{II}	M_{III}
44.11 [b]			vvw–d	vw		ew?	
101.7		not observed					
870.6		not observed					
884.6		not observed					
925.4		not observed					
940.4 [c]	ew						
943.3		not observed					
985.7 [c]	vw	ew?					
988.3		not observed					
1027.2 [c]	ew						
1029.9 [c]	vvw	ew?					

[a] Energies as reported in summary of Np^{238} data by Albridge and Hollander [15]).

[b] Electron lines observed with 99-gauss magnet.

[c] Electron lines observed with 160-gauss magnet.

necessary to determine whether both components were E0; if they were, they would then have to be interpreted on the basis of a level scheme.

TABLE 9

Electron lines observed in the sample which agreed in energy with the reported Pu^{239} transitions following Np^{239} decay. The transition energies used in the table are taken from Hollander, Smith and Mihelich [16]). The observed relative intensities are in excellent agreement with those reported by these authors. Intensity code as in table 3

Energy of gamma (keV) [a]	Subshell conversion										
	K	L_I	L_{II}	L_{III}	M_I	M_{II}	M_{III}	N_I	N_{II}	N_{III}	0
44.64		vvw	vvw? [b]	ew [b]	ew??						
49.38		m [c]	vvw–d	vvw	ew [d]	vvw [e]	vvw	ew–d			
57.25		ew?	m	ms [f]		mw	w		vvw	ew	ew–d
61.42		m [g]									
67.82			mw	mw		w	w		ew	ew	ew–d
106.12		mw	mw	– [h]	vvw	vvw	ew?				
106.43			ew?	ew?							
125.3		not observed									
181.8	ew–d										
209.9	s	w	ew		ew			w [i]			
226.4	vw				ew?						
228.4	vvs	m	ew	ew				ew			
254.6	ew?	ew									
273.1		not observed									
277.7	vs	mw	ew		vvw			mw			vw
285.6	ew??		vvw	ew–d		ew–d					
316.1		not observed									
334.5	w										

[a] Energies as reported by Hollander, Smith and Mihelich. All intensities except those otherwise indicated were obtained on the 99-gauss magnets.
[b] L_{II}, L_{III} 44.64 (Pu^{239}) and L_{II}, L_{III} 44.6 (Pu^{236}) superimposed.
[c] L_I 49.38 (Pu^{239}), L_{III} 43.49 (U^{234}) superimposed.
[d] M_I 49.38 (Pu^{239}), O_{III} 43.49 (U^{234}) superimposed.
[e] M_{II} 49.38 (Pu^{239}), N_{II} 45.32 (U^{236}) superimposed.
[f] L_{III} 47.26 (Pu^{239}), M_{III} 43.49 (U^{234}) superimposed.
[g] L_I 61.42 (Pu^{239}), M_{II} 43.49 (U^{234}) superimposed.
[h] May be masked.
[i] All intensities underlined were observed on the 160-gauss permanent magnet.

In order to answer the first question, we obtained a limit on the conversion coefficients of the 812-keV transition. We measured that the ratio of the relative gross conversion coefficients $e^-_{\overline{640}}/\gamma_{\overline{760}}$, $e^-_{\overline{690}}/\gamma_{\overline{760}}$ and $e^-_{\overline{1440}}/\gamma_{\overline{1560}}$ (where the bar indicates that the energy is the average energy of the composite peak, and the electron energies are the K-conversion line energies) was 1 : 26 : 1. Stephens [18]) has measured a limit on the absolute value of the gross $e^-_{\overline{1440}}/\gamma_{\overline{1560}}$ conversion coefficient and determined that it is $\geqq 0.01$. This value corresponds to an M1 or a higher-magnetic-multipole transition. Normalizing the value above this number yields conversion coefficients of $\geqq 0.01$ and $\geqq 0.26$, for the two other transitions.

To determine whether the two components are E0 we had to estimate the relative K conversion-line intensities of the 810- and 812-keV transitions and what fraction of the 760-keV peak could be attributed to a gamma ray of 812 keV. We visually estimated that the relative intensities of the K conversion lines of the 810- and 812-keV transitions (which were resolved on the spectrographic plate) are in the ratio $1 : (4 \pm 1)$. The estimate was based on the relative intensities of these lines in a series of 4.0 day exposures. Knowing the inherent resolution of the NaI crystal from a study of calibration sources, we were able to estimate that the maximum fraction of the 760 peak intensity that could be attributed to a gamma of 810 keV was $\leqq \frac{1}{3}$. Such a reduction of the 760 gamma intensity raises the limit on the second gross conversion coefficient to $\geqq 0.78$. On the basis of the high resolution electron data, we divide this 0.78 between the two transitions yielding limits on the conversion coefficients of $\geqq 0.15$ and $\geqq 0.62$. The second is consistent only with a very large E0 admixture. The first must be M2 or higher magnetic multipolarity ($\alpha_K(M2) \approx 0.15$ for this Z and energy). Because there are 3 transitions, at 788, 793 and 854 keV, which must also be included in considering a gamma peak at 810 keV (thus reducing the fraction of $\frac{1}{3}$ appreciably, and hence raising the limit on the conversion coefficient) and because the $K/L_I/M_I$ ratio of the 810 and 812 transitions are identical to within the accuracy of the visual estimate, we believe the 810-keV transition has a large E0 admixture also. The K/(L+M) ratio of 3.9 for the gross peaks measured in the long-lens spectrometer is consistent with the K/(L+M) ratio of an E0 transition of this Z and energy as calculated by Church and Weneser [19]) and by Listengarten and Band [20]).

The second question, as to the position of the transition in the decay scheme, was to a large extent settled by sums and differences based on the many transitions observed, which established the 854-keV state with little ambiguity. The interpretation will be discussed below.

The gross conversion coefficient $e^-_{\overline{640}}/\gamma_{\overline{760}}$ lies between the values for E1 and E2 radiations, and the interpretation of these transitions in the decay scheme is consistent with such a value. If the 810 and 812 are E0 transitions all the 760 gamma intensity must of course be assigned to the other transitions. Sliv and

Band's [21]) K and L shell internal conversion coefficients were used for comparison of the experimental data to theory. The 43.49 and 99.7 are E2 on the basis of their $L_I/L_{II}/L_{III}$ conversion ratios. The 233.6, 234.6 and 238.6 have very weak L-conversion, hence they are probably E1. The 247.9 has strong L_I and M_I conversion and is therefore probably magnetic. The 450.5 appears to convert in the L_I, L_{II} and L_{III} shells and hence is probably E2, although since the L_{II} and L_{III} lines are extremely weak the assignment must be tentative. We have not ruled out the possibility that these are K lines of unidentified transitions. Little can be said about the other transitions.

4.3. BASIS OF THE LEVEL SPIN AND PARITY ASSIGNMENTS

From the present data and the data on the alpha decay of Pu^{238} the levels at 43.49, 143.2 and 812 are assigned 2+, 4+ and 0+ spins and parities. On the basis of the reported β^+ group we assume Np^{234} has a spin 0, 1 or 2, assuming beta decay to the 0+ and/or 2+ state. We will discuss the possible spin assignments of Np^{234} in more detail below. The very strong decay of the 1575 and 1606 levels to ground, plus the gross conversion coefficient of $\geqq 0.01$ reported by Stephens [18]) for the 1560-keV peak suggests spins 1 or 2, positive parity, for both the 1575- and 1606-keV levels.

The level at 812 is 0+. The level at 854 agrees in energy with a 2+ rotational state based upon such a state. The branching from the 1606 level to the 854 and 812 levels is also similar to that from the 1606 to the 43.49 and ground state levels, which seems consistent. If we now combine this information with the at-least-partial E0 nature of the 810-keV transition, we can state that the 810-keV transition is an E0 transition between two states with $I \neq 0$. The interpretation of the 854 state as a $K = 0$, 2+ state implies, however, that there should be an E2 transition to the 4^+ state of the ground state rotational band, of intensity 2.57 to 1 relative to the E2 transition to the first 2^+ rotational state [1, 22]). The conversion electrons of this transition were looked for on the photographic plates but were not observed, although the conversion electrons of the theoretically weaker transition to the ground state were. Therefore, there remains some uncertainty as to the correct interpretation of this state because, if selection rules are not obeyed, either the assignment is wrong or K is not a good quantum number for these states.

The 1— assignment to the 788-keV level is tentative. However, the relative K conversion electron intensities for the 744 and 788 transitions are in the ratio 2 : 1, in agreement with the theoretical ratio of 2 for the decay of $K = 0, I = 1$ states to $K = 0, I = 2$ and $K = 0, I = 0$ states [22]). We assumed in making this calculation that the 788- and 744-keV transitions are pure E1.

The levels at 1049 and 1090 (G and H) are uncertain because no transitions have been observed which depopulate them. If the levels are the expected 2+ and 3+ ($K = 2$) states, and the populating transitions are M1 and E2,

the expected pure E2 radiations depopulating them would not be observed. We favour such an interpretation for these states.

Levels I, J, and K probably have negative parity and low spin. The parity assignments are based on the comments made regarding the probable multipolarities of the low energy transitions populating and depopulating them. Level L probably has low spin as it decays directly to the 0+ and 2+ states. Its parity is uncertain.

5. Discussion of Results

5.1. COMPARISON TO PREVIOUS RESULTS

The decay scheme we report is consistent with the results reported from Pu^{238} alpha decay. The gamma transitions reported by Huizenga *et al.* [7]) agree to

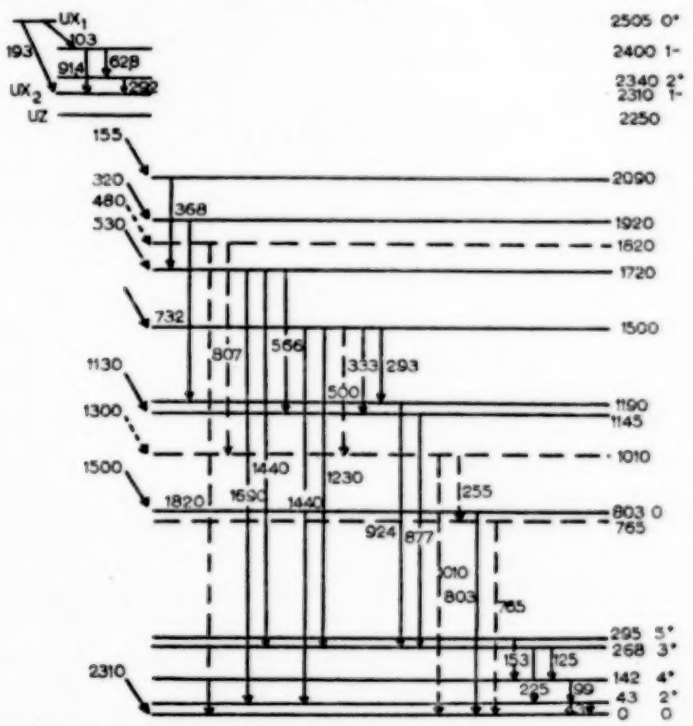

Fig. 4. Level scheme of U^{234} as previously reported by Ong, Verschoor and Born from Pa^{234} decay.

within the limits of error with the present results, (although we have observed many more transitions) except for the 109-, 905-, and 1010-keV transitions. On the basis of our high resolution studies of the ≈ 87-keV region of the electron spectrum we believe we can rule out the 109-keV transition. The conversion lines of the 905 and 1010 were not observed in our electron spectrum, but a definite peak appears in our gamma spectrum at this energy (see fig. 2). Furthermore our level scheme predicts several transitions of approximately these energies. It therefore seems likely that they are present and were not observed in the electron spectrum owing to either small internal conversion

coefficients or weak intensities, or both. We report the presence of a very weak line at 1440 which would not have been seen by Huizenga *et al.* [7, 23]), who reported that there was no line at this energy. However, in agreement with both Hoff [6]) and Huizenga *et al.*, our data rule out the strong ≈ 1450-keV transition reported by Orth [5]). The coincidence data of Huizenga *et al.* are consistent with our proposed level scheme, with the possible exception of the 445—500 keV coincidence.

A comparison of figs. 3 and 4 shows that the U^{234} level schemes postulated by Ong *et al.* [11]) from Pa^{234} decay and our own proposals are not in good agreement. Whether this discrepancy is the result of an actual difference in the primary branching of the different nuclei or of differences in interpretation is not certain as the lower resolution used in the Pa^{234} study make the data difficult to compare. However, the levels at ≈ 43, ≈ 142 and ≈ 800 keV are common to both decay schemes, and several of the transitions following Pa^{234} decay have nearly the energies of transitions reported here. In UX_2 these are the 230-, 255-, 770-, 803-, 807-, (1010-), 1240- and 1440-keV transitions; in UZ decay they are the 293-, 566-, 732-, 803- and 1240-keV transitions. It would thus appear that a high-resolution electron spectroscopic study of these isomers is in order. It is expected that such a study would yield much new information on the levels of U^{234}, besides removing some of the differences which now appear to exist.

5.2. THE Np^{234} GROUND STATE.

An aspect of the decay scheme which deserves further study is the determination of the primary electron-capture branching to the levels of U^{324}, which we have not attempted. The log $ft \approx 8.4$ calculated for the β^+ transition to the ground state band suggests an appreciable hindrance for the beta decay, and would probably indicate a unique first-forbidden transition if only single particle rates were considered. However, the log ft's for decay of odd nuclei have not been clearly classified, and it is doubtful that strong arguments for spin assignments can be based on them at present. A direct comparison with the log $ft = 7.2$ reported for the EC decay of $Np^{236}(1+)$ to the U^{236} ground state [14]) indicates that the Np^{234} decay is probably more hindered than the Np^{236} decay, and hence suggests negative parity for Np^{234}. This, coupled with the fact that the states Np^{234} populates in U^{234} appear to have low spin, can be interpreted consistently if Np^{234} has a spin in the range 0—2, negative parity.

Because Np^{234} is strongly deformed, the coupling rules proposed by Gallagher and Moszkowski [24]) should apply. From Mottelson and Nilsson [25]) the most probable proton levels are $642\uparrow$ and $523\downarrow$, and the most probably neutron levels are $633\downarrow$ and $743\uparrow$. On the basis of these most probable states and the coupling rules, the states available for the Np^{234} ground state should be 5−, 6−, 0+ or 1+. The experimental data therefore indicate a violation of the coupling rules. Assuming the coupling rules are violated, it is likely that the

Np^{234} ground state is 0−. This would correspond to coupling states $523\downarrow$ and $633\downarrow$ with intrinsic spins antiparallel. Such a suggestion is made because states $523\uparrow$ and $633\uparrow$, coupled antiparallel, have been postulated [24]) to be the Ho^{166} ground state. In this respect the log $ft = 8.0$ for the ground state to ground state transition in Ho^{166} β^- decay is analogous to the log $ft = 8.4$ observed in Np^{234}. A direct measurement of the Np^{234} spin will apparently be necessary to settle this problem.

5.3. VIBRATIONAL LEVELS

What can we say about the energies of the various vibrational states in U^{234} as a consequence of the present work? Primarily, we have checked the energy of the β vibrational state and established the energy of its first rotational state. A comparison of the energies of the first rotational states of the $K = 0$ levels shows that the excited state apparently has a greater moment of inertia then the ground state. We have some evidence for the energies of the γ vibrational state and its first rotational state, although we have not observed the transitions depopulating them. Again in this case, the apparent moment of inertia is larger than that of the ground state.

In addition we believe we have established the energy of the $K = 0$, 1− state. The energy of this 787-keV state is approximately three times the energies of the corresponding levels in the thorium and radium isotopes [26]). The energies of the 1− states in Pu are only 200 keV less ,however [2]). If our assignment is correct, this maximum in the energies of the 1− states in uranium can be interpreted to mean that the stability against octupole modes of deformation passes through a maximum in the uranium isotopes.

On the basis of the present data, U^{234} is now the second nucleus in the heavy element region in which the relative energies of the β and γ vibrational states are known. In Pu^{238}, the other, the β vibrational state is also at lower energy than the γ-vibrational state. It thus appears experimentally that the β vibrational bands lie lower in energy than the γ vibrational bands in the heavy elements, at least at the onset of the region where the strong-coupling approximation holds. The work of Nathan and Hultberg [27]) suggests that the β vibrational bands also lie lower at the onset of the strong coupling region around $N = 88$. Other evidence in this region (the work of King and Johns [28]) on the levels of Os^{188}, and the relatively high energy of the 0+ level in Er^{166}) suggests that the level ordering may invert as the shell fills. The data on the relative energies of the β, γ and 1− vibrational states in these nuclei are shown in fig. 5.

5.4. E0 TRANSITIONS

In our opinion the most interesting experimental result in the present study is the probable identification of an E0-admixed transition between two states with $I \neq 0$. Church and Weneser [19]) have predicted such transitions, but until

recently no experimental evidence for such transitions had been observed. In addition to the present study, however, Nathan and Hultberg [27]), have recently reported the possible presence of an E0-admixed transition between two $2+(K=0)$ states in Sm^{152}, and have postulated, on the basis of some coincidence data and a highly-converted transition in Eu^{154} reported by Juliano and Stephens [29]), that there is also one in Ge^{154}. At present time no half-lives for the states from which these transitions arise have been measured, and thus a direct comparison of the E0-rates to the Church-Weneser "strength factor" is not possible.

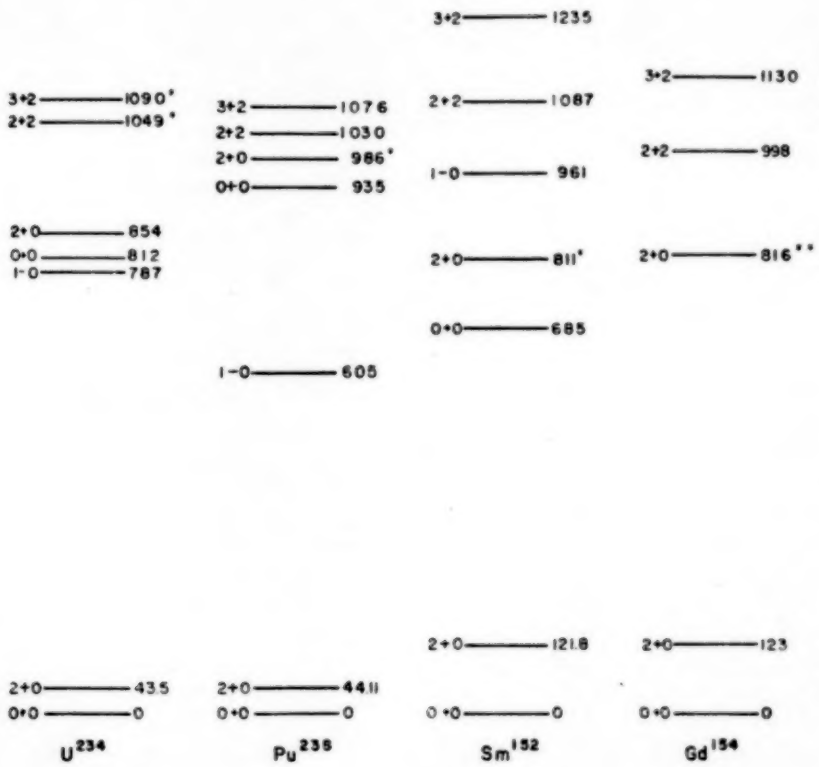

Fig. 5. Comparison of β-, γ- and 1-vibrational state energies in nucleides where they are known. The Np^{238} data are from ref. [15]); the Sm^{152} and Gd^{154} data from ref. [27]). The single asterisk indicates the level assignment is uncertain. The double asterisk on the Gd^{154} level indicates the assignment was postulated by Nathan and Hultberg [27]) on the basis of the work of Juliano and Stephens [29]).

Let us speculate briefly on an interesting aspect of the appearance of E0 transitions between states which have some of the expected properties of rotational states based upon $K=0$ vibrational states. On the basis of simple considerations, if E0 transitions appear between the 2+ states, there is no apparent reason why they should not also occur between the 4+, 6+ and higher-spin rotational states. If this is indeed the case, the presence of E0 transitions may serve the very useful purpose of yielding more information on the excited

β vibrational bands, which appear to be populated only weakly in the decay of most odd nuclei and have been difficult to observe experimentally. Such a possibility would support the conclusions of Albridge and Hollander [15]) on some apparently highly converted transitions observed in Np^{238} decay including the evidence for the $K = 0$, $2+$ state of Pu^{238} shown in fig. 5.

We thank Professor J. O. Rasmussen and Dr. G. Manning for critically reading the manuscript. One of us (C. J. G.) acknowledges an interesting discussion with Professor S. A. Moszkowski, and also the continued interest of Professor J. W. M. DuMond in this work.

Appendix

CHEMICAL PROCEDURE

The U_3O_8 target was dissolved in aqua regia. Lanthanum and zirconium carriers were added, the solution evaporated to dryness and taken up in $1M$ HNO_3. Saturation of the solution with SO_2 caused the reduction of neptunium and plutonium to the IV and III states respectively. Lanthanum fluoride was precipitated, carrying neptunium and plutonium. The precipitate was dissolved in $6M$ HNO_3 saturated with H_3BO_3. $La(OH)_3$ was precipitated and then redissolved in conc. HCl. Neptunium and plutonium were adsorbed on an ion-exchange column of Dowex A–1 anion exchange resin, and were stripped from the column in $3M$ HCl.

The neptunium and plutonium were oxidized with bromate and the solution scavenged with LaF_3. Another reduction with SO_2 was made and the neptunium and plutonium were again carried on LaF_3. The precipitate was converted to the hydroxide by treatment with KOH, and the hydroxide was dissolved in $1M$ HNO_3. After the neptunium and plutonium had again been oxidized with bromate, $Mg(NO_3)_2$ was added to the solution, and the neptunium and plutonium were extracted into ethyl ether. The activity was back extracted into water, reduced with SO_2, and again carried on LaF_3. The fluoride precipitate was metathesized to $La(OH)_3$ with KOH. The $La(OH)_3$ was dissolved in conc. HCl. The solution was passed through a column packed with Dowex A–1 ion exchange resin. The neptunium was eluted in a minimum volume of $0.1M$ HCl. The activity was then ready for source preparation.

Note added in proof: Some recent work by E. Arbman and O. B. Nielsen (private communication to CJG) on the levels of Th^{230} has shown that the γ vibrational level is higher in energy than the β vibrational level in this nucleus. The $0+$ level in Gd^{154} has been observed by O. Nathan (private communication to CJG) who has also checked the existence of the 816-keV level.

References

1) A. Bohr and B. R. Mottelson, Mat. Fys. Medd. Dan. Vid. Selsk. **27**, No. 16 (1953)
2) See Strominger, Hollander and Seaborg, Revs. Mod. Phys. **30** (1958) 585
3) Perlman, Asaro, Harvey and Stephens, Bull. Amer. Phys. Soc., **2** (1957) 394
4) Alder, Bohr, Huus, Mottelson and Winther, Revs. Mod. Phys. **28** (1956) 432
5) D. A. Orth, Ph. D. thesis, University of California Radiation Laboratory Report, UCRL 1059 (Sept. 1953)
6) R. W. Hoff, Ph. D. thesis, University of California Radiation Laboratory Report, UCRL-2325 (Nov. 1952)
7) Huizenga, Engelkemeir, Freedman, Porter and Gindler, Bull. Amer. Phys. Soc. **1** (1956) 171
8) Hyde, Studier and Ghiorso, NNES-PPR **14B** (1949) 1622
9) Prestwood, Smith, Brown and Hoffman, Phys. Rev. **98** (1955) 1324
10) B. M. Foreman, University of California Radiation Laboratory Report UCRL-8223 (April 1958)
11) Ong, Verschoor, and Born, Physica **22** (1956) 465
12) W. G. Gross and T. A. Eastwood, Phys. Rev. **95** (1954) 628A
13) W. G. Smith and J. M. Hollander, Phys. Rev. **101** (1956) 746
14) P. Gray, Phys. Rev. **101** (1956) 1306
15) R. G. Albridge and J. M. Hollander, University of California Radiation Laboratory Report UCRL-8034 (November 1957); Bull. Amer. Phys. Soc. **2** (1957) 395
16) Hollander, Smith and Mihelich, Phys. Rev. **102** (1956) 740
17) R. D. Hill, in Beta- and Gamma-Ray Spectroscopy, edited by K. Siegbahn (North-Holland Publishing Company, Amsterdam, 1955) Appendix VI, p. 914
18) F. S. Stephens (unpublished data, 1956)
19) E. L. Church and J. Weenser, Phys. Rev. **103** (1956) 1035
20) M. A. Listengarten and I. M. Band, Izvestia Akad. Nauk SSSR, Fiz. Ser. **23** (1959) 235 (In Russian)
21) L. A. Sliv and I. M. Band, Table of K-conversion coefficients, Issued in USA as Report 57 ICC Kl, Physics Department, University of Illinois, Urbana, Illinois.
22) Alaga, Alder, Bohr and Mottelson, Mat. Fys. Medd. Dan. Vid. Selsk. **29**, No. 9 (1955)
23) J. R. Huizenga (private communication)
24) C. J. Gallagher, Jr. and S. A. Moszkowski, Phys. Rev. **111** (1958) 1282
25) B. R. Mottelson and S. G. Nilsson, Mat. Fys. Skr. Dan. Vid. Selsk **1**, No. 8 (1959)
26) Stephens, Asaro and Perlman, Phys. Rev. **96** (1954) 1568; **100** (1955) 1543
27) O. Nathan and S. Hultberg, Nuclear Physics **10** (1958) 118
28) W. J. King and M. W. Johns, Canadian J. Phys. **37** (1959) 755
29) J. O. Juliano and F. S. Stephens, Jr., Phys. Rev. **108** (1957) 341

2.D *Nuclear Physics* **14** (1959/60) 21—32; © *North-Holland Publishing Co., Amsterdam*
Not to be reproduced by photoprint or microfilm without written permission from the publisher

PAIRING ENERGY EFFECTS IN EXCITED NUCLEI

D. W. LANG and K. J. LE COUTEUR
Australian National University, Canberra

Received 26 July 1959

Abstract: The nucleus is considered as a Fermi gas with pairs of degenerate single particle states and a coupling energy Δ between the two states of a pair. A statistical treatment gives expressions for the density of excited states and the expected value of the total angular momentum. Suitable approximations for purposes of calculation are indicated. All the formulae become equivalent to those of a simple Fermi gas at high enough excitations.

1. Introduction

Measurement of level densities in excited nuclei by different methods have become accurate enough in recent years for some conflicts to be noted [1, 2, 3]) in the nuclear parameters on which the densities depend. Many of these conflicts can be resolved if the level density at low excitations, particularly in even nuclei, is assumed to depart from the simplest form which is adequate to explain high energy behaviour. It has been suggested that the discrepancy may be due to

(1) a gap in the levels available to a single particle at the highest occupied level [4]),

(2) shell effects [5, 6]),

(3) pairing of nucleons whose states differ only in having opposite projections of angular momentum on the symmetry axis of a non-spherical nucleus.

The third hypothesis has the advantage that it brings in the even-odd effects in the ground state energy of the nucleus and in the level density in a natural way. It has been particularly considered by Ericson [7]) but the results obtained still require awkward numerical calculations before they can be compared with experiment. It is the purpose of this paper to obtain simpler forms for numerical calculation. By a more direct approach some unification is achieved between excited pair states and rotational states, and the moment of inertia of the nucleus in such states is calculated. A reduction of the pairing energy with temperature may be required to give a reasonable fit to experiment.

2. The Partition Function with Pairing Energy

For a given pair $s+$, $s-$ of degenerate single particle states, such as occur in the unified nuclear model [8,9,10]) according to Nilsson's[11]) level scheme with components $\pm m_s$ of angular momentum along the symmetry axis of the nucleus, there are four possible configurations, viz. both empty, one or other filled, both filled. Assuming that residual interactions within the nucleus lead to a coupling energy of magnitude Δ_s between members of a pair, these four configurations have energies 0, $a_s+\frac{1}{2}\Delta_s$ and $2a_s$, respectively, for neutrons and likewise 0, $b_r+\frac{1}{2}\Delta_r$ and $2b_r$ for protons. The pairing energy leads to characteristic differences $\frac{1}{2}\Delta$, Δ between the ground state energies of even and of odd mass and odd nuclei, and the magnitude of Δ may be taken from Stolovy and Harvey's [12]) empirical estimate of these differences:

$$\Delta_0 = 3.36-0.0084A \text{ MeV} \quad \text{for } A > 40. \tag{2.1}$$

The partition function for the neutron-proton assembly is then given by

$$\begin{aligned} e^{-\beta\Phi} = \prod_{s,r} &\{1+2e^{\beta(\mu_1-a_s-\frac{1}{2}\Delta_s)}+e^{2\beta(\mu_1-a_s)}\} \\ &\times \{1+2e^{\beta(\mu_2-b_r-\frac{1}{2}\Delta_r)}+e^{2\beta(\mu_2-b_r)}\}, \end{aligned} \tag{2.2}$$

where μ_1 and μ_2 are the Fermi levels for neutrons and protons and $\beta = 1/t$ is the reciprocal of the thermodynamic temperature. This expression must be identical with

$$e^{-\beta\Phi} = \sum_{N'Z'} \int_0^\infty dE'\, P(N', Z', E') e^{\beta(\mu_1 N' + \mu_2 Z' - E')} \tag{2.3}$$

if $P(N', Z', E')$ is the density of excited levels of a nucleus of N' neutrons and Z' protons in the neighbourhood of energy E'.

The neutron contribution to $\beta\Phi$ in (2.2) is

$$-\beta\Phi_n = \sum_s \log\,[1+2e^{\beta(\mu_1-a_s-\frac{1}{2}\Delta_s)}+e^{2\beta(\mu_1-a_s)}] \tag{2.4}$$

$$\begin{aligned} &= \sum_{a_s \leqq \mu_1} \{2\beta(\mu_1-a_s)+ \log\,[1+2e^{\beta(a_s-\mu_1-\frac{1}{2}\Delta_s)}+e^{2\beta(a_s-\mu_1)}]\} \\ &+ \sum_{a_s > \mu_1} \log\,[1+2e^{\beta(\mu_1-a_s-\frac{1}{2}\Delta_s)}+e^{2\beta(\mu_1-a_s)}]. \end{aligned} \tag{2.5}$$

We will assume that the value of Δ_s is the same for all states and that the densities of pairs of states available to neutrons and protons can be described by two continuous functions $g_n(a)$ and $g_p(b)$ respectively.

Equation (2.5) can be written more simply if g_n is symmetric about μ_1 as

$$-\beta\Phi_n = \sum_{a_s \leqq \mu_1} 2\beta(\mu_1-a_s)+\frac{1}{\beta}I_n \tag{2.6}$$

where

$$I_n = 2\int_0^\infty g_n(x) \log\,(1+2\cos\lambda e^{-x}+e^{-2x})dx, \tag{2.7}$$

$$\cos\lambda = e^{-\frac{1}{2}\beta\Delta}; \tag{2.8}$$

and x is the magnitude $|\beta(a_s-\mu_1)|$.

We define I_p similarly and $I = (I_n+I_p)$. If $g_n(x)$ and $g_p(x)$ are constant for the range of orbits whose occupation state is likely to change, the integral is

$$I = 2(g_n+g_p)(\tfrac{1}{6}\pi^2-\tfrac{1}{2}\lambda^2) \tag{2.9}$$

and we have, collecting results

$$e^{-\beta\Phi} = \exp\left\{\frac{I}{\beta}+\sum_{a_s\lesssim\mu_1} 2\beta(\mu_1-a_s)+\sum_{b_r\lesssim\mu_2} 2\beta(\mu_2-b_r)\right\}. \tag{2.10}$$

At high temperatures $\lambda \to 0$ and (2.10) reduces to the result of the single particle treatment [13]) because

$$2g_n+2g_p = g \tag{2.11}$$

is the total density of single particle states.

3. Reversing the Summation

To evaluate $P(N, Z, E')$ for a particular N and Z we evaluate the residues of $\exp(-\beta\Phi-\mu_1\beta(N+1))$ and $\exp(-\beta\Phi-\mu_1\beta(N+1)-\mu_2\beta(Z+1))$ in turn. The saddle point for the first is given by

$$\frac{\partial\Phi}{\partial\mu_1} = -N = \sum_{a_s\lesssim\mu_1} 2. \tag{3.1}$$

If N is odd we must adopt the convention that μ_1 is equal to the energy of the last occupied level and take half the last term of the summation. This follows from the original definition of Φ whence

$$\frac{\partial\Phi}{\partial\mu_1} = \sum_s \frac{2e^{\beta(\mu_1-a_s-\frac{1}{2}\Delta)}+2e^{\beta(\mu_1-a_s)}}{1+2e^{\beta(\mu_1-a_s-\frac{1}{2}\Delta)}+e^{2\beta(\mu_1-a_s)}} \tag{3.2}$$

$$= \sum_s \frac{2\{1+e^{\beta(a_s-\mu_1-\frac{1}{2}\Delta)}\}}{1+2e^{\beta(a_s-\mu_1-\frac{1}{2}\Delta)}+e^{2\beta(a_s-\mu_1)}} = \sum_s n_s. \tag{3.3}$$

If $\beta \to \infty$, i.e. at low excitation, each term
$\to 2$ for $a_s < \mu_1$
$\to 0$ for $a_s > \mu_1$
and for $a_s = \mu_1$ the term $= \dfrac{2(1+\exp(-\frac{1}{2}\Delta))}{2(1+\exp(-\frac{1}{2}\Delta))} = 1$,
i.e. for N even μ_1 must lie between the last occupied level and the next unoccupied, and for N odd μ_1 is the last (singly) occupied level.

Then, if the residues for N and Z are evaluated by saddle point integration, we have

$$\int_0^\infty dE'\,P(N, Z, E')e^{-\beta E'} = \frac{\beta}{2\pi\left(\dfrac{\partial N}{\partial\mu_1}\dfrac{\partial Z}{\partial\mu_2}\right)^{\frac{1}{2}}} e^{-\beta(\Phi+\mu_1 N+\mu_2 Z)} \tag{3.4}$$

The total energy of neutrons is

$$E_n = \sum_{n_s=2} 2a_s + \sum_{n_s=1} (a_s + \tfrac{1}{2}\Delta), \tag{3.5}$$

and similarly for the energy E_p of the protons. Using the above convention about the contribution of the highest occupied level, the summation in (2.10) reduces to

$$\sum_{a_s \leqq \mu_1} 2\beta(\mu_1 - a_s) + \sum_{b_r \leqq \mu_2} 2\beta(\mu_2 - b_r) = \beta(\mu_1 N + \mu_2 Z - E^*), \tag{3.6}$$

where $E^* = E_0$, the ground state energy for even nuclei
$= E_0 - \frac{1}{2}\Delta_0$ for odd mass nuclei
$= E_0 - \Delta_0$ for odd nuclei (3.7)

and we write Δ_0, in case Δ should subsequently become temperature dependent, because in (3.7) we want the value for the ground state.

We can now simplify (3.4) by replacing the energy E by the excitation energy $U = E - E_0$, and, using (2.10),

$$\int_0^\infty P(N, Z, U') e^{-\beta U'} dU' = \exp\left\{\frac{I}{\beta} + \log\frac{\beta}{2\pi} - \tfrac{1}{2}\log 4 g_n g_p + \beta(E_0 - E^*)\right\} \tag{3.8}$$

since

$$\frac{\partial N}{\partial \mu_1} = 2g_n \quad \text{and} \quad \frac{\partial Z}{\partial \mu_2} = 2g_p. \tag{3.9}$$

We define (3.8) to be $e^{-\beta F}$ for the system with exactly N neutrons and Z protons. Reversing the Laplace transform over the saddle point gives

$$P(N, Z, U) = e^S / (-2\pi \partial U / \partial \beta)^{\frac{1}{2}} \tag{3.10}$$

where $S = \beta(U - F)$ is the entropy of the system. Then

$$\begin{aligned} U = \partial(\beta F)/\partial\beta &= It^2 - t\partial I/\partial\beta - t - (E_0 - E^*) \\ &= gt^2(\tfrac{1}{6}\pi^2 - \tfrac{1}{2}\lambda^2) + \tfrac{1}{2}tg\Delta\lambda \cot\lambda - t - (E_0 - E^*) \end{aligned} \tag{3.11}$$

and

$$P(N, Z, U) = \frac{\beta^2 \exp\{2It - \partial I/\partial\beta - 1\}}{(2\pi)^{\frac{1}{2}}\{4g_n g_p(2It - 2\partial I/\partial\beta + \beta\partial^2 I/\partial\beta^2 - 1\}^{\frac{1}{4}}}. \tag{3.12}$$

4. Distribution of Levels over Angular Momentum

The interpretation of the first of equations (3.2) is that

$$p_s(+\text{or}-) = \frac{2e^{\beta(\mu_1 - a_s - \frac{1}{2}\Delta)}}{1 + 2e^{\beta(\mu_1 - a_s - \frac{1}{2}\Delta)} + e^{2\beta(\mu_1 - a_s)}} \tag{4.1}$$

is the probability that one or other, but not both, of the states a_s is occupied and

$$p_s(+-) = \frac{e^{2\beta(\mu_1-a_s)}}{1+2e^{\beta(\mu_1-a_s-\frac{1}{2}\Delta)}+e^{2\beta(\mu_1-a_s)}} \tag{4.2}$$

is the probability that both are occupied.

These formulae remain true if $\Delta = 0$ and, in order to recover some familiar results, we first consider the simple case of a Fermi gas of independent particles in which the states a_s may be labelled $j \pm m$ *with* m *measured in an arbitrary direction of quantization*. For the pair a_s the average over the probability distribution (4.1), (4.2) is

$$\langle \sum m \rangle = 0, \langle (\sum m)^2 \rangle = m_s^2 p_s(+ \text{ or } -). \tag{4.3}$$

Let $M_N = \sum m$, taken over all neutrons, then $\langle M_N \rangle = 0$ and, since the different levels a_s are uncorrelated,

$$\langle M_N^2 \rangle = \sum_s m_s^2 p_s(+ \text{ or } -). \tag{4.4}$$

Thus for $\Delta = 0$,

$$\langle M_N^2 \rangle = 2\sum_s \frac{m_s^2 e^{\beta(\mu_1-a_s)}}{[1+e^{\beta(\mu_1-a_s)}]^2} = 2\sum_m m^2 g_n(m) \int_{-\infty}^{\infty} \frac{e^{\beta x} dx}{[1+e^{\beta x}]^2}, \tag{4.5}$$

where $g_n(m)$ is the density of neutron levels with quantum number m in the neighbourhood of the Fermi level, and so

$$\langle M_N^2 \rangle = 2g_n \overline{m^2}/\beta \tag{4.6}$$

where $\overline{m^2}$ is the average m^2 value for single particles near the Fermi level.

Combining effects of neutrons and protons, the mean square component of the resultant angular momentum of the nucleus is

$$\langle M^2 \rangle = \overline{m^2} gt = ct \quad \text{where} \quad c\hbar^2 = \overline{m^2} g\hbar^2 \tag{4.7}$$

is equal to the moment of inertia of the nucleus, considered as a rigid body.

The distribution of M is

$$p(M) = (2\pi ct)^{-\frac{1}{2}} e^{-M^2/2ct} \tag{4.8}$$

and the other components of total angular momentum have the same distribution, since M is measured in an arbitrary direction. Therefore the probability of a state with total angular momentum J is

$$\frac{4\pi(J+\frac{1}{2})^2}{(2\pi ct)^{\frac{3}{2}}} e^{-J(J+1)/2ct} \tag{4.9}$$

and the probability of a nuclear level with angular momentum J is accordingly

$$\frac{2J+1}{\pi^{\frac{1}{2}}(2ct)^{\frac{3}{2}}} e^{-J(J+1)/2ct}, \tag{4.10}$$

which are well known results.

Now consider $\Delta > 0$. The pairing of states $\pm m$ now has important dynamical effects and the nuclear model to which it seems most appropriate is the unified model of Bohr and Mottelson [8, 9, 10]) and Nilsson [11]) in which m may be measured along the axis S of a non-spherical nucleus with axial symmetry. (See fig. 1.)

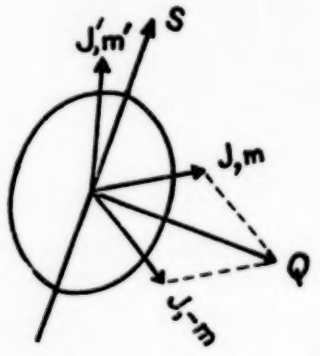

Fig. 1. The symmetry axis S of a deformed nucleus, with two paired particles j, $\pm m$; and the unpaired single particle j', m', angular momentum vectors. The resultant angular momentum Q of the pair is non zero, although the projection on S cancels.

The resultant angular momentum, in the direction S, of the neutrons has mean zero but the mean square is still determined by (4.4) which now gives

$$\begin{aligned}\langle M_N{}^2\rangle &= 2\sum_s \frac{m_s{}^2 e^{\beta(\mu_1-a_s-\frac{1}{2}\Delta)}}{1+2e^{\beta(\mu_1-a_s-\frac{1}{2}\Delta)}+e^{2\beta(\mu_1-a_s)}}\\ &= 2\overline{m^2}\sum_s \frac{e^{\beta(\mu_1-a_s-\frac{1}{2}\Delta)}}{1+2e^{\beta(\mu_1-a_s-\frac{1}{2}\Delta)}+e^{2\beta(\mu_1-a_s)}} \qquad (4.11)\\ &= 2\overline{m^2}\,\partial(\beta\Phi_N)/\partial(\beta\Delta),\end{aligned}$$

from (2.4). For even nuclei this comes to

$$\begin{aligned}\langle M_N{}^2\rangle &= 2\overline{m^2}g_n t\partial\lambda^2/\partial(\beta\Delta)\\ &= 2\overline{m^2}g_n t\lambda\cot\lambda. \qquad (4.12)\end{aligned}$$

Combining the contributions of neutrons and protons, the mean square component of the resultant angular momentum in the direction S is, *for even nuclei*,

$$\langle M^2\rangle = \lambda\cot\lambda\,\overline{m^2}gt = \lambda\cot\lambda\; ct = c't. \qquad (4.13)$$

At high temperatures $\lambda \to 0$ as $(\Delta/t)^{\frac{1}{2}}$ and $c' \to c$ so that (4.7) and (4.10) hold approximately. But at low temperatures, the expression (4.13) is less than (4.7) by the factor $\lambda/\tan\lambda$ which can be very small because the pairing energy inhibits the excitation of single particles when $\Delta \gg t$. In such circumstances it is worthwhile to note that if the total number of neutrons is odd there must be at least one unpaired neutron which contributes $\overline{m^2}$ to $\langle M_N{}^2\rangle$. Accordingly (4.13) should be generalized to

$$\langle M^2\rangle = \lambda\cot\lambda\overline{m^2}gt+\begin{cases}0 & \text{for even nuclei}\\ \overline{m^2} & \text{for odd mass nuclei}\\ 2\overline{m^2} & \text{for odd nuclei}\end{cases} \qquad (4.14)$$
$$= c't.$$

We must now evaluate the mean particle angular momentum in the plane x, y perpendicular to S. First considering the neutron contribution, we have obviously

$$\langle J_{Nx}\rangle = \langle J_{Ny}\rangle = 0$$

because the direction is random.

For an even nucleus we can assume that if all the occupation numbers n_{s+}, n_{s-} simultaneously have precisely their mean values in the Gibbs ensemble, the total angular momentum has magnitude zero and this includes in particular the assumption that the ground state has total angular momentum zero. Fluctuations of the occupation numbers away from their mean values give rise to a non-zero magnitude for the total angular momentum determined by

$$\langle J_{Nx}^2+J_{Ny}^2\rangle = \sum_s (j_x{}^2+j_y{}^2)\{\langle n_{s+}^2\rangle-\langle n_{s-}\rangle^2+\langle n_{s+}^2\rangle-\langle n_{s-}\rangle^2\}, \qquad (4.15)$$

for the components of angular momentum in the x, y plane are not paired and the states $s+$ and $s-$ contribute independently to the mean square. Accordingly for n_{s+} we may take the mean occupation numbers from (3.2) or (4.1, 4.2) as

$$\langle n_{s+}\rangle = \langle n_{s+}^2\rangle = \langle n_{s-}\rangle = \langle n_{s-}^2\rangle$$
$$= \frac{e^{\beta(\mu_1-a_s-\frac{1}{2}\Delta)}+e^{2\beta(\mu_1-a_s)}}{1+2e^{\beta(\mu_1-a_s-\frac{1}{2}\Delta)}+e^{2\beta(\mu_1-a_s)}}. \qquad (4.16)$$

Then from (3.2) and (4.11) we can evaluate terms of (4.15) as,

$$2\sum_s\{\langle n_{s+}^2\rangle-\langle n_{s+}\rangle^2\} = \tfrac{1}{2}\frac{\partial^2(\beta\Phi_N)}{\partial(\beta\mu_1)^2}+\frac{\partial(\beta\Phi_N)}{\partial(\beta\Delta)} = g_n t(1+\lambda\cot\lambda) \qquad (4.17)$$

after use of (2.10) and (4.12).

Now unless the shape of the nucleus is very far from spherical, we may take $\langle j_x{}^2+j_y{}^2\rangle = 2\overline{m^2}$ and find, after combining neutron and proton contributions,

$$\langle J_x{}^2+J_y{}^2\rangle = \overline{m^2}gt(1+\lambda\cot\lambda) = (c+c')t \qquad (4.18)$$

in the notation of (4.7) and (4.14).

If Δ/t is large, that is at low excitation energies, excitation of pairs is more important than excitation of single particles and $\lambda\cot\lambda$ and c' are small. Then most of the nuclear angular momentum is carried by excited pairs of particles or pairs of holes, which may have a resultant angular momentum Q, perpendicular to S, as indicated in fig. 1. It is noteworthy that in this case (4.18) gives

$$\langle J^2\rangle = ct \qquad (4.19)$$

which is the mean square angular momentum at temperature t appropriate to a rotator with moment of inertia $\frac{1}{2}c$, just half the rigid body value. Furthermore the exclusion principle requires the resultant angular momentum of the pairs to be even and, as remarked above, symmetries and residual interactions between particles produce the value zero in the ground state.

Now it is known [9]) that the collective rotation of a distorted nucleus must be about an axis like Q perpendicular to S and that the spacings of levels of spin 0, 2, 4 correspond to nuclear moments of inertia ranging up to about half the rigid body value. These results suggest that it may be possible to associate the rotational angular momentum of the collective model with the angular momentum of excited pairs in a pairing model. Elliott [14]) has previously shown how the collective rotational bands in some light nuclei are built up from the individual particle motions. This point of view also relieves a difficulty in the work of Bohr, Mottelson and Pines [4]), who introduced a pairing energy to account for the difficulty of exciting single particles in even nuclei, but observed that this does not prevent excitation of pairs. The excited pairs need not be suppressed if they can be used to account for low energy rotational levels.

Of course the pairing model will not account for the observed regularities of rotational energy spectra without further elaboration and assumptions about the interaction between particles. But the correspondence seems close enough to justify the belief that in counting up the number of excited pair states, we are counting up the rotational states.

In view of these results and Elliott's work, we consider that the level density P of (3.12), which certainly contains all possible arrangements of the particles, must include all the rotational states. This point of view differs from Ericson's [7]) who used a formula equivalent to (3.12) to determine the number of "intrinsic states", each of which was considered as the parent of a rotational band, and so multiplied the total number of states. By this procedure, using conventional values of g and Δ, he was able to find sufficient levels of low angular momentum to agree with the experimental values at neutron binding energy. But in § 6 it will be shown that if we are limited to a total of P states, the number of levels at neutron binding energy is too small to agree with experiment unless Δ is decreased below its value for the ground state.

If the direction of the symmetry axis is not specified, equations (4.14) and (4.18) imply that the expression (4.10) for the probability of a level with total angular momentum J is modified to

$$\frac{2J+1}{\pi^{\frac{1}{2}}(2c''t)^{\frac{3}{2}}}\,\mathrm{e}^{-J(J+1)/2c''t} \tag{4.20}$$

with c'' determined by

$$(2c'')^{\frac{3}{2}} = (2c')^{\frac{1}{2}}(c+c') \quad \text{or} \quad c'' = (c')^{\frac{1}{3}}(\tfrac{1}{2}c+\tfrac{1}{2}c')^{\frac{2}{3}}, \tag{4.21}$$

since the normalisation constant is fixed by the product of the standard deviations of the three components of J. At $t = \frac{1}{2}\Delta$, we find, from § 5, $c'' \approx \frac{1}{2}c$ and the distribution (4.20) slightly increases the proportion of states with low angular momentum in comparison with the distribution (4.10).

For comparison we quote Ericson's [7]) formula

$$\rho(U, N, Z, J) = \frac{(J+\frac{1}{2})}{K_{\mathrm{m}}}\left(\frac{3}{\pi v}\right)^{\frac{1}{2}} \exp -\left\{\frac{2(J+\frac{1}{2})^2}{3\tau}\left(\frac{\hbar^2}{\mathscr{I}}+\frac{3\tau}{2vK_{\mathrm{m}}{}^2}\right)\right\} P(U, N, Z, 0) \tag{4.22}$$

in which $\mathscr{I}$ is the moment of inertia about an axis perpendicular to the symmetry axis, K_{m} the highest value expected of the angular momentum of a single particle and v the number of unpaired particles.

We have discussed the effects of pairing energy in relation to non-spherical nuclei because that seems its most natural application. However, *for spherical nuclei*, the dependence of the total energy on the 'seniority' quantum number may be crudely represented as a tendency for like nucleons to couple together in pairs with *total angular momentum zero*. If we represent the coupling energy by Δ, eq. (4.14) gives an estimate of the mean square angular momentum in *any* direction, not as before only in the direction of the symmetry axis S. Therefore, the probability of a nuclear level with total angular momentum J is represented approximately by (4.10) or (4.20) using the smaller moment of inertia c' for spherical nuclei.

5. Approximate Forms

Solving the equation $e^{i\Delta\beta} = \cos\lambda$ we obtain

$$\lambda^2 = \Delta\beta[1-\tfrac{1}{3}(\tfrac{1}{2}\Delta\beta)+\tfrac{2}{45}(\tfrac{1}{2}\Delta\beta)^2+\tfrac{1}{315}(\tfrac{1}{2}\Delta\beta)^3-\tfrac{2}{1575}(\tfrac{1}{2}\Delta\beta)^4\ldots] \tag{5.1a}$$

or

$$\Delta\beta = \lambda^2[1+\tfrac{1}{6}\lambda^2+\tfrac{2}{45}\lambda^4\ldots]. \tag{5.1b}$$

This will be a good approximation at high excitation and $\lambda = \frac{1}{2}\pi-\cos\lambda-\frac{1}{6}\cos^3\lambda$ is valid at low excitations. From these, at high excitations,

$$U = \tfrac{1}{6}\pi^2 gt^2 - t - \frac{g\Delta^2}{12}+\frac{g\Delta^3}{90t}+\frac{g\Delta^4}{1680t^2}+\ldots-(E_0-E^*) \tag{5.2}$$

and

$$P(N, Z, U) = \frac{\exp\left\{\frac{1}{3}\pi^2 gt-1-\frac{1}{2}g\Delta+\frac{g\Delta^3}{180t^2}+\frac{g\Delta^4}{2520t^3}\cdots\right\}}{12(\pi t)^{\frac{1}{2}}(\frac{1}{6}g)^{\frac{3}{2}}} \tag{5.3}$$

or

$$P(N, Z, U) \approx \frac{\exp\{2(\frac{1}{6}\pi^2 g U')^{\frac{1}{2}} - \frac{1}{2}g\Delta\}}{12(\frac{1}{6}g)^{\frac{1}{4}}(U'+t)^{\frac{5}{4}}}, \tag{5.4}$$

where

$$U' = U + (E_0 - E^*) + \tfrac{1}{12}g\Delta^2. \tag{5.5}$$

For equations (4.20) and (4.21) a simple expression for $c''t$ will be required. From (4.14) we see that at high temperatures the even-odd dependence of c' is slight and find approximately

$$c' = \overline{m^2} g t[1 - (\Delta/3t)]. \tag{5.6}$$

Any too rapid variation of the bracketted term indicates that the range of the approximation has been exceeded. It would be expected that $t > \frac{1}{2}\Delta$ would be a suitable limit for most purposes. This in turn gives the first three terms of (5.2), the first three terms of the exponential in (5.3), or (5.4) as sufficient approximation wherever the approximation is valid. Comparison of (5.4) with (A-10) of ref.[13]) shows that at high temperature the level density is like that of a free Fermi gas except that U' replaces U.

The approximation to (2.8) and (2.9)

$$I = g(\tfrac{1}{6}\pi^2 - \tfrac{1}{2}\lambda^2) \approx \tfrac{1}{24}g\pi^2(1 + 3e^{-0.437\beta\Delta}) \tag{5.7}$$

has been found to be very close over almost the whole range of Δ and directly shows the transition between the low temperature and high temperature limits. From this formula more widely valid formulae for U, P, and $c't$ in terms of t can be found:

$$U = \tfrac{1}{6}g\pi^2 t^2\{\tfrac{1}{4} + \tfrac{3}{4}(1 + a/t)e^{-a/t}\} - t; \tag{5.8}$$

$$P = \frac{\exp\{\frac{1}{3}\pi^2 g t[\frac{1}{4} + \frac{3}{4}(1 + a/2t)e^{-a/t}] - 1\}}{12(\pi t)^{\frac{3}{2}}(\frac{1}{6}g)^{\frac{3}{2}}}, \tag{5.9}$$

where

$$a = 0.437\Delta; \tag{5.10}$$

then, from (4.12, 4.13), for even nuclei,

$$c't = \overline{m^2} g \tfrac{1}{4}\mu\pi^2 t(0.437e^{-a/t}) \approx cte^{-a/t}, \tag{5.11}$$

and according to (4.14) $c't$ must be increased by $\overline{m^2}$ for odd mass and $2\overline{m^2}$ for odd nuclei. These formulae have the advantage of being accurate over a wide range of t.

6. Comparison with Experiment

Results of scattering and evaporation experiments depend on the temperature $\tau = \mathrm{d}U/\mathrm{d}(\log P)$ and are thus much more sensitive to the form of the entropy than to any of the slowly varying factors in the expression for the

level density. From (5.3) we find that τ is related to t by $\tau \approx t+\frac{1}{2}g$ so that (5.2) can be written

$$U = \tfrac{1}{6}\pi^2 g\tau^2 - \tfrac{5}{2}\tau - \tfrac{1}{12}g\Delta^2 - (E_0 - E^*); \qquad (6.1)$$

although this approximation would be expected to be accurate only for energies at which $t > \frac{1}{2}\Delta$, i.e. $U > \frac{1}{3}g\Delta^2$, it should nevertheless give a useful indication in predicting the variation of τ with U. The results of computation from the accurate forms displayed in fig. 2 confirm this.

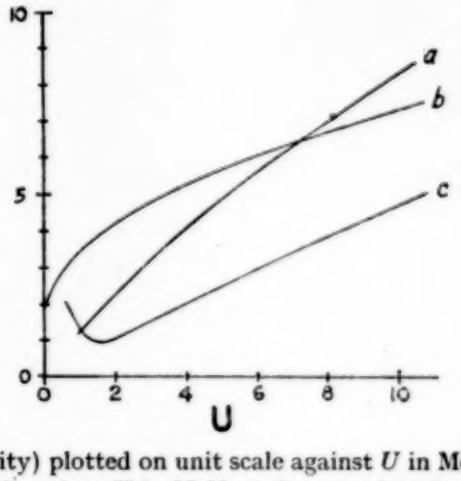

Fig. 2. a) $\log_{10}$ (level density) plotted on unit scale against U in MeV. b) Nuclear temperature τ in units 0.1 MeV plotted against U in MeV. c) Square of nuclear temperature τ^2 plotted in units 0.1 MeV^2 against $(U+\frac{5}{2}\tau)$ in MeV. All three graphs are for $g = 15\,\mathrm{MeV}^{-1}$, $\Delta = 1.145\,\mathrm{MeV}$.

It is seen that some estimates of the pairing energies required can be obtained from the intercept of a graph of τ^2 against U. An attempt was made to carry out this measurement from the results of J. S. Levin and L. Cranberg[15]), but the accuracy of the experiment is still insufficient to give conclusive evidence either for or against an intercept of the required magnitude for a pairing energy constant with respect to t. It should be noted that any system whose free energy can be approximated by a form like $F = at^2 e^{-\Delta/kt}$ will give a positive intercept on the τ^2 axis.

Measurements of total absorption cross section for 1 MeV neutrons and individual resonances with thermal neutrons give an absolute knowledge of the level density of a compound nucleus near the binding energy of the last neutron added. To predict this accurately requires that all the factors involved in (4.20) and (4.21) must be evaluated. From ref. [16]) we obtain $\overline{m^2} \approx 0.146A^{\frac{5}{3}}$ and hence, using (5.4) and (5.11),

$$\rho(N, Z, U, J) = (J+\tfrac{1}{2})e^{-J(J+1)/2c''t}\,\frac{\exp\{2(\frac{1}{6}\pi^2 gU')^{\frac{1}{2}} - \frac{1}{2}g\Delta + a/t\}}{0.0636\,A^2(U'+t)^2} \qquad (6.2)$$

if we use the dispersion c'' of angular momentum. The last term in the exponential is omitted if we use c. We have here assumed that approxima-

tions to Δ, g in the denominator will suffice to determine the value of the exponential term if ρ is known experimentally. As a result of Ericson's work, however, it was suspected that the value of g required would have to be large and the value of Δ smaller than that used in correcting the ground state energies. Some calculations were therefore done using values of level spacing, pairing energy and neutron binding energy taken from Stolovy and Harvey[12]) and assuming [1]) that $\frac{1}{6}g\pi^2 = \frac{1}{7}A$. Despite the fact that this is an upper limit on g [1]) the values obtained for the level spacing were still too small by a factor of about 3 using c'' and about 10 using the wider angular momentum distribution c. Further, with the value of Δ assumed and the consequent value of t, the entropy is insensitive to the value of Δ(5.4). To introduce a factor 3 in the level density will then require the assumption of a pairing energy differing by thirty percent from that to correct the odd-even effect in the ground state. It was therefore not considered worth while to make a least squares fit to the data, especially as it would not be surprising if the correlation Δ between states of individual particles were less in excited states than in the ground state of the nucleus.

References

1) K. J. Le Couteur and D. W. Lang, Nuclear Physics **13** (1959) 32
2) D. L. Livesey, Can. J. Phys. **33** (1955) 391
3) G. Igo and H. E. Wegner, Phys. Rev. **102** (1956) 1364 (L)
4) A. Bohr, B. R. Mottelson and D. Pines, Phys. Rev. **110** (1958) 936
5) Torleif Ericson, Nuclear Physics **8** (1958) 265
6) N. Rosenzweig, Phys. Rev. **108** (1957) 817
7) Torleif Ericson, Nuclear Physics **6** (1958) 62
8) A. Bohr and B. R. Mottelson, Mat. Fys. Medd. Dan. Vid. Selsk. **27**, No. 16 (1953)
9) A. Bohr, Rotational States of Atomic Nuclei (København, Ejnar Munksgaards Forlag, 1954)
10) A. Bohr, Nuovo Cimento, Supplemento, **4** (1956) 1091
11) S. G. Nilsson, Mat. Fys. Medd. Dan. Vid. Selsk. **29**, No. 16 (1955)
12) A. Stolovy and J. A. Harvey, Phys. Rev. **108** (1957) 353
13) J. M. B. Lang and K. J. Le Couteur, Proc. Phys. Soc. A **67** (1954) 585
14) J. P. Elliott, Proc. Roy. Soc. A **245** (1958) 128, 562
15) J. S. Levin and L. Cranberg, O.R.N.L. 2309 (1957) 84
16) J. H. D. Jensen and J. M. Luttinger, Phys. Rev. **86** (1952) 907

8.B

Nuclear Physics **14** (1959/60) 33—41; © *North-Holland Publishing Co., Amsterdam*

Not to be reproduced by photoprint or microfilm without written permission from the publisher

ON THE PARITY OF K-BARYON VERTICES

D. KLEITMAN †

Universitetes Institut for Teoretisk Fysik, Copenhagen

Received 3 August 1959

Abstract: The baryon mass spectrum is examined for a set of theories in which π mesonic interactions are universal and K mesonic interactions distinguish between nucleons and cascade particles only through their having opposite space inversion properties. The nucleon-cascade particle mass splittings for such theories are evaluated through use of the approximations that vertex corrections in the mass operator may be ignored, and that only the leading divergent terms in the mass renormalization need be considered. It is shown that this splitting only has the correct sign if nucleon-K meson vertices are scalar rather than pseudoscalar.

1. Introduction

The point of view that π mesonic interactions among the baryons maintain complete symmetry among them, and that K interactions are responsible for the observed deviations from such symmetry was first suggested by Schwinger [1]) and, independently, by Gell-Mann [2]). Schwinger, in addition, advanced the hypothesis that the comparatively large difference in mass between the nucleon and cascade particle pointed to a more fundamental origin to it than to that, say, between the masses of the Λ and Σ particles. Thus, he conjectured that the nucleon and cascade particles might have opposite space inversion properties and that this distinction might underlie all others between them through the difference in their K interactions induced by this parity difference. More recently, a double hyperfragment event has been observed at Oxford [3]) which seems at present to be most easily interpretable if nucleons and cascade particles have opposite parity.

In this paper we assume this conjecture to be correct and concern ourselves with determining the relative parities of these particles or, more precisely, the forms of the nucleon-hyperon-K meson vertices that are implied by it. In this connection we examine the sign of the nucleon—cascade-particle mass splitting produced by theories satisfying the conjecture.

Thus, we start from the following three assumptions:

1) Complete symmetry among the baryons is maintained by their π-mesonic interactions.

2) The only differences between nucleons and cascade particles arise through

† National Science Foundation Postdoctoral Fellow. Present address: Physics Dept. Harvard University, Cambridge, Mass.

the difference in their K interactions that is required by their having opposite parity.

3) All mesonic interactions are either scalar or pseudoscalar.

We proceed to calculate the nucleon—cascade-particle mass splittings produced by theories satisfying these assumptions. To do so we make use of the following three additional assumptions:

4) In the general expression of the baryon mass operator in terms of particle propagators and vertex operators, the vertex operator may be approximated in lowest order of perturbation theory for the purpose of predicting the sign of the difference in nucleon and cascade-particle mass renormalization.

5) The mass renormalization calculated by use of assumption 4) is logarithmically divergent. We assume that the sign referred to in 4) is adequately represented by considering only the leading divergent terms in such mass shift predictions.

6) We assume that the mass parameter in the Lagrange operator has the same sign as the observed mass of the various baryons.

We then discover that the observed mass spectrum requires that the K meson and Λ (or Σ) hyperon combination have even relative parity with respect to the nucleon, in S states.

It is hoped that future experiments will permit a testing of this prediction.

In the next section the class of Lagrange operators that will be considered in the calculation is explicitly exhibited. We then proceed to describe and discuss our approximations in further detail. Finally, the computation itself is outlined.

2. The Lagrange Operator

Assumptions 1) to 3) of the previous section imply that the system can be described by a Lagrange operator of the form

$$L = L_{\text{kin}\cdot\text{F}}+L_{\text{kin}\cdot\text{B}}+L_{\text{M}}+L_{\pi-\text{F}}+L_{\text{K}-\text{F}}, \tag{2.1}$$

with

$$L_{\text{kin}\cdot\text{F}} = -\tfrac{1}{2}\psi\cdot\beta\gamma^{\mu}\frac{1}{i}\partial_{\mu}\psi, \tag{2.2}$$

$$L_{\text{kin}\cdot\text{B}} = -\tfrac{1}{2}[\phi^{\lambda}\cdot\partial_{\lambda}\phi-\phi\cdot\partial_{\lambda}\phi^{\lambda}-\phi^{\lambda}\phi_{\lambda}], \tag{2.3}$$

$$L_{\text{M}} = -\tfrac{1}{2}m_0\psi\cdot\beta\psi-\tfrac{1}{2}\mu_{\text{K}0}^2\phi_{\text{K}}{}^2-\tfrac{1}{2}\mu_{\pi 0}^2\phi_{\pi}{}^2, \tag{2.4}$$

and

$$\begin{aligned} L_{\pi-\text{F}} = g_{\pi}\phi_{\pi}\tfrac{1}{2}[&\psi_{\text{N}}\beta\gamma_5\nu\tau\psi_{\text{N}}+\psi_{\Xi}\beta\gamma_5\nu\tau\psi_{\Xi} \\ &+\psi_{\Lambda}\beta\gamma_5 i\nu\psi_{\Sigma}-\psi_{\Sigma}\beta\gamma_5 i\nu\psi_{\Lambda}+\psi_{\Sigma}\beta\gamma_5\nu\frac{1}{i}\times\psi_{\Sigma}. \end{aligned} \tag{2.5}$$

For simplicity we refer only to strong interactions. The notations used here are described in detail in several previous papers on this general subject [1,4]). Various signs in the π-baryon coupling term $L_{\pi-\text{F}}$ could be altered without

affecting any of the arguments below though some of the physical predictions of the resulting theories would in fact be modified.

The K-baryon interactions may take either of the general forms

$$\begin{aligned} L^{(1)}_{\mathrm{K-F}} &= g_{\mathrm{K}\Lambda}\phi_{\mathrm{K}}[\psi_{\Lambda}\beta\psi_{\mathrm{N}}+\psi_{\Lambda}\beta\gamma_5\psi_{\Xi}] \\ &\quad +g_{\mathrm{K}\Sigma}\phi_{\mathrm{K}}[\psi_{\Sigma}\beta i\tau\psi_{\mathrm{N}}+\psi_{\Sigma}\beta\gamma_5 i\tau\psi_{\Xi}] \end{aligned} \tag{2.6}$$

and

$$\begin{aligned} L^{(2)}_{\mathrm{K-F}} &= g_{\mathrm{K}\Lambda}\phi_{\mathrm{K}}[\psi_{\Lambda}\beta\gamma_5\psi_{\mathrm{N}}+\psi_{\Lambda}\beta\psi_{\Xi}] \\ &\quad +g_{\mathrm{K}\Sigma}\phi_{\mathrm{K}}[\psi_{\Sigma}\beta i\tau\gamma_5\psi_{\mathrm{N}}+\psi_{\Sigma}\beta i\tau\psi_{\Xi}]. \end{aligned} \tag{2.7}$$

Here $g_{\mathrm{K}\Lambda}$ and $g_{\mathrm{K}\Sigma}$ need not be identical.

The presence of additional strong interaction terms in the Lagrange operator involving a π—K interaction or perhaps some of the unobserved mesons that have been suggested in the past few years, will not alter any of the arguments below so long as such terms themselves do not destroy nucleon-cascade particle symmetry when the K-baryon interaction is ignored.

3. Approximations

We seek to calculate the mass shifts induced in the various baryons by introduction of K interaction terms into the Lagrange operator. The physical mass of a particle may be identified by the location of the lowest energy pole of the corresponding one-particle propagator. Thus, with

$$\begin{aligned} G_{\mathrm{A}}(x, x') &= i\langle(\psi_{\mathrm{A}}(x)\bar{\psi}_{\mathrm{A}}(x'))_+\rangle\varepsilon(x-x') \\ &= \frac{1}{(2\pi)^4}\int \mathrm{d}^4p\, \mathrm{e}^{ip(x-x')}G_{\mathrm{A}}(\gamma p) \end{aligned} \tag{3.1}$$

and

$$G_{\mathrm{A}}(\gamma p) = (\gamma p + M_{\mathrm{A}}(\gamma p))^{-1}, \tag{3.2}$$

the mass m_{A} of particle A can be identified by the requirement that $G_{\mathrm{A}}(\gamma p)$ have a pole at m_{A}:

$$\gamma p + M_{\mathrm{A}}(\gamma p)|_{\gamma p=-m_{\mathrm{A}}} = 0 \tag{3.3}$$

or

$$M_{\mathrm{A}}(-m_{\mathrm{A}}) = m_{\mathrm{A}}. \tag{3.4}$$

Now, in general, the mass operator may be expressed in terms of particle propagators and vertices according to

$$M_{\mathrm{A}}(\gamma p) = \frac{ig^2}{(2\pi)^4}\int \gamma_{i\mathrm{AP}}G_{\mathrm{B}}(\gamma(p-k))\Gamma_{i\mathrm{BA}}(k, p-k, p)(\mathrm{d}^4k)\Delta_i(k^2)+m_0 \tag{3.5}$$

$$= \frac{ig_{\pi}^2}{(2\pi)^4}\int \gamma_{\pi\mathrm{AB}}\Delta_{\pi}G_{\mathrm{B}}\Gamma_{\pi\mathrm{BA}}(\mathrm{d}k)+\frac{ig_{\mathrm{K}}^2}{(2\pi)^4}\int \gamma_{\mathrm{KAC}}\Delta_{\mathrm{K}}G_{\mathrm{C}}\Gamma_{\mathrm{KCA}}(\mathrm{d}k)+m_0 \tag{3.6}$$

Here Δ_i represents the propagator for the boson whose virtual emission can contribute to the self energy M_A, while G_B is the propagator for the fermion that is produced when such a boson is emitted from a fermion of type A. The operator γ_{iAB} is the lowest order perturbation theory vertex, while Γ_{iBA} is the so-called vertex operator.

In our calculation below we shall approximate this exact relation by the following equation:

$$M_A - m_0 = \frac{ig_\pi^2}{(2\pi)^4}\int \gamma_{\pi AB}\Delta_\pi G_B \gamma_{\pi BA}(dk) + \frac{ig_K^2}{(2\pi)^4}\int \gamma_{KAC}\Delta_K G_C \gamma_{KCA}(dk) + \frac{ig_\pi^2}{(2\pi)^4}\int \gamma_{\pi AB}\Delta_\pi G'_B(\Gamma'_{\pi BA} - \gamma_{\pi BA})(dk). \tag{3.7}$$

Here G'_B and $\Gamma'_{\pi BA}$ are the operators that would be propagators and vertex if K-baryon interactions were ignored. Thus we are omitting from consideration the effects of the terms

$$\frac{ig_\pi^2}{(2\pi)^4}\int (dk)\gamma_{\pi AB}\Delta_\pi[G_B(\Gamma-\gamma)_{\pi AB} - G'_B(\Gamma'-\gamma)_{\pi BA}] + \frac{ig_K^2}{(2\pi)^4}\int \gamma_{ACK}\Delta_K G_C(\Gamma-\gamma)_{KCA}(dk) \tag{3.8}$$

in the mass operator. In words, we are omitting the contributions of those parts of the vertex corrections to the mass operator which involve virtual emission of at least one K meson.

Formally, that is, in terms of diagrams, the mass operator can be pictured as in fig. 1,

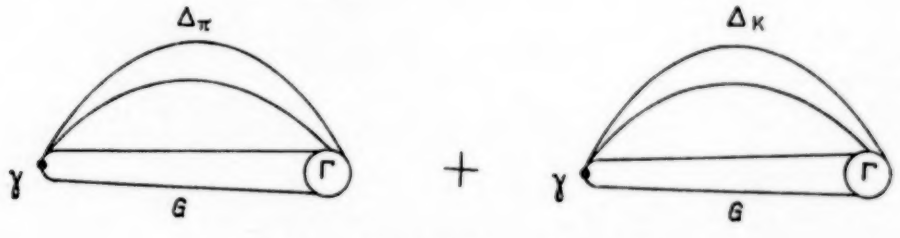

Fig. 1. The exact mass operator.

while our approximation can be represented as including the diagrams of fig. 2. Thick lines and points in these figures represent corrected operators; shaded lines represent operators for which π-corrections only have been included.

The simplest diagrams that are omitted in our approximation are shown in fig. 3.

In general, correction of the propagators alone as done in eq. (3.7) does not necessarily represent an improvement over use of ordinary perturbation theory. Thus, in quantum electrodynamics it is well known that corrections to

the electron propagator give rise to infinite charge renormalizations which are exactly compensated by corrections to the vertex operator. In other theories and for other predictions we have no particular reason to believe that vertex corrections are any smaller than propagator corrections.

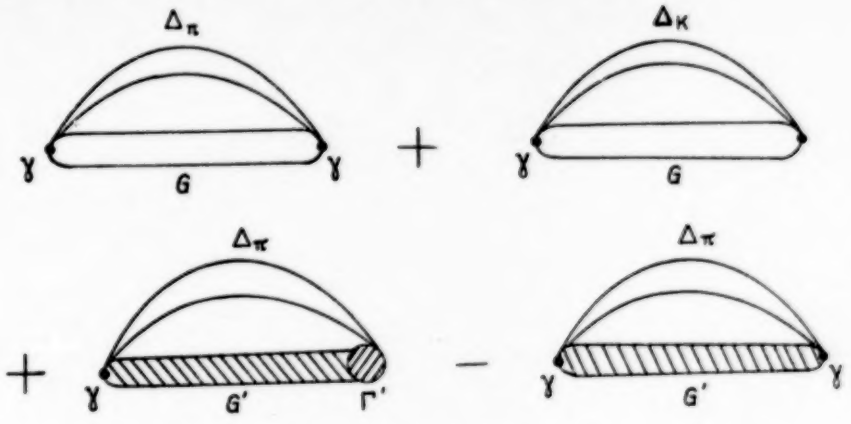

Fig. 2. Approximation (3.1) to the mass operator.

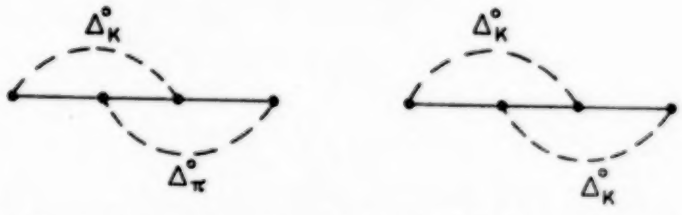

Fig. 3. Simplest Feynman diagrams omitted in approximation (3.1).

In the particular case under consideration here we have two extenuating circumstances which make the use of this approximation perhaps more satisfactory. First, the form of our argument is not really affected by the inclusion of corrections to the particle propagators; we could as well proceed to the same conclusions by use of perturbation theory, or by correcting either one of the propagators. Thus, if vertex corrections are only as harmless as the others, we are justified in neglecting them.

Secondly, the approximation can be justified here if one accepts the philosophy which led to our assumption about nucleon and cascade particle parities. For, if vertex corrections give the dominant contribution to the nucleon-cascade mass splitting, the assumption about parity no longer serves as an explanation for the comparatively large size of the splitting. Conversely, if the parity difference is to provide an understanding of the relative size of this splitting in the manner suggested by Schwinger [1]), vertex corrections must not dominate (and we must start from a Lagrange operator in which $g_{K\Lambda}$ and $g_{K\Sigma}$ are identified).

We have noted in the introduction that the mass renormalizations calculated on the basis of the approximation just described are found to be proportional

to logarithmically divergent integrals. In order to estimate these integrals we introduce a cutoff and consider only contributions which are proportional to the logarithm of the cutoff. Use of such an approximation is justified only if the actual cutoff is significantly greater than any if the other relevant masses that appear in the integral.

This approximation is quite as intangible as the previous one. As we are only interested in the sign of the mass splitting, however, we shall actually need only to assume that the approximation gives the correct sign of the integrals involved. It is quite reasonable that most of the contributions to the baryon mass spectrum arise from masses that are well below the cutoff, so that our procedure may well give this sign correctly.

We also assume below that the terms in our approximation to the mass operator that are independent of the presence of the K meson field cannot contribute to a mass splitting between nucleon and cascade particle. This is not strictly true, however, as the mass operator is evaluated at different values of its momentum argument according to eq. (3.4), for the two particles. We must therefore assume that such contributions to the mass difference are small, or modify our approximation to exclude the pionic vertex corrections included in the last two terms of eq. (3.7).

4. The Calculation

In order to evaluate the mass renormalizations implied by eq. (3.7) we make use of spectral representations of the propagators. From very general principles [5]) it is possible to show that the various particle propagators can be expressed according to

$$G_{\mathrm{A}}(\gamma p) = \frac{A_{0\mathrm{A}}}{\gamma p + m_{\mathrm{A}}} + \int_{m_{\mathrm{A}}+\mu_\pi}^{\infty} \mathrm{d}k \left(\frac{A_{+\mathrm{A}}(k)}{\gamma p + k - i\varepsilon} + \frac{A_{-\mathrm{A}}(k)}{\gamma p - k + i\varepsilon} \right) \equiv \int_{-\infty}^{\infty} \mathrm{d}k \, \frac{A_{\mathrm{A}}(k)}{\gamma p + k}, \tag{4.1}$$

$$\Delta_i(k^2) = \int_{\mu_i^2}^{\infty} \frac{B_i(\lambda^2)\mathrm{d}\lambda^2}{k^2 + \lambda^2 - i\varepsilon}, \tag{4.2}$$

where the spectral densities $A_{\mathrm{A}}(k)$ and $B_i(\lambda^2)$ are required to satisfy the additional relations

$$\begin{aligned} &\int \mathrm{d}k A_{\mathrm{A}}(k) = 1, \qquad \int \mathrm{d}k \, k A_{\mathrm{A}}(k) = m_0; \\ &\int Bi(\lambda^2)\mathrm{d}\lambda^2 = 1, \qquad \int Bi(\lambda^2)\lambda^2 \mathrm{d}\lambda^2 = \mu_{0i}^2. \end{aligned} \tag{4.3}$$

We first drop the last two terms of eq. (3.7) since they do not distinguish nucleon and cascade particle. (But see the remarks of the previous section.) If these spectral forms are substituted into the remainder of eq. (3.7) we obtain

$$M_A(\gamma p) = m_0 + \frac{ig_\pi^2}{(2\pi)^4}\int_{-\infty}^{\infty} d\alpha \int_{\mu_\pi^2}^{\infty} d\beta \left[\int (dk)\gamma_{\pi AB}\frac{1}{\gamma(p-k)+\alpha}\gamma_{\pi BA}\frac{1}{k^2+\beta}\right] A_B(\alpha)B_\pi(\beta)$$
$$+ \frac{ig_K^2}{(2\pi)^4}\int_{-\infty}^{\infty} d\alpha \int_{\mu_K^2}^{\infty} d\beta \left[\int (dk)\gamma_{KAC}\frac{1}{\gamma(p-k)+\alpha}\gamma_{KCA}\frac{1}{k^2+\beta}\right] A_C(\alpha)B_K(\beta). \quad (4.4)$$

For simplicity we consider now only the K interaction described by $L_{K-F}^{(1)}$ of eq. (2.6). The nucleon cascade mass splitting can then be represented as

$$m_\Xi - m_N = \frac{i}{(2\pi)^4}\int_{-\infty}^{\infty} d\alpha \left\{[A_\Lambda g_{K\Lambda}^2 + 3A_\Sigma g_{K\Sigma}^2]\int_{\mu_K^2}^{\infty} d\beta B_K(\beta)\right.$$
$$\left.\cdot\left[\int (dk)\left[\gamma_5\frac{1}{\gamma(p-k)+\alpha}\gamma_5\frac{1}{k^2+\beta}\right]\Big|_{\gamma p=-m_\Xi} - \left[\frac{1}{\gamma(p-k)+\alpha}\frac{1}{k^2+\beta}\right]\Big|_{\gamma p=-m_N}\right]\right\} \quad (4.5)$$
$$+ \frac{3ig_\pi^2}{(2\pi)^4}\int_{-\infty}^{\infty} d\alpha \int_{\mu_\pi^2}^{\infty} d\beta \left[\int (dk)\gamma_5\frac{1}{\gamma(p-k)+\alpha}\gamma_5\frac{1}{k^2+\beta}\right] B_\pi(\beta)\{A_\Xi(\alpha)|_{\gamma p=-m_\Xi} - A_N(\alpha)|_{\gamma p=-m_N}\}.$$

The leading divergent terms of the integrals that appear here are given by

$$i\int (dk)\gamma_5\frac{1}{\partial(p-k)+\alpha}\gamma_5\frac{1}{k^2+\beta}\frac{\Lambda^2}{\Lambda^2+\dfrac{k^2}{\beta}} \to [\alpha+\tfrac{1}{2}(\gamma p)]\log\Lambda^2, \quad (4.6)$$

$$i\int (dk)\frac{1}{\gamma(p-k)+\alpha}\frac{1}{k^2+\beta}\frac{\Lambda^2}{\Lambda^2+\dfrac{k^2}{\beta}} \to [-\alpha+\tfrac{1}{2}(\gamma p)]\log\Lambda^2. \quad (4.7)$$

With use of eqs. (4.3) we may therefore represent the leading divergent contributions to the mass splitting as

$$m_\Xi - m_N = \frac{g_{K\Lambda}^2+3g_{K\Sigma}^2}{4\pi}\left(\frac{1}{2\pi}\right)m_0\log\Lambda^2 + \frac{g_{K\Sigma}^2+3g_{K\Sigma}^2+3g_\pi^2}{4\pi}\left(\frac{1}{8\pi}\right)(m_N-m_\Xi)\log\Lambda^2. \quad (4.8)$$

The effect of the last term on the right-hand side of this equation is simply to oppose the given mass difference. The sign of the splitting is determined by the first term, and is the correct one. The corresponding calculation for the K interaction of $L_{K-F}^{(2)}$ yields the result

$$m_\Xi - m_N = -\frac{(g_{K\Lambda}^2+3g_{K\Sigma}^2)}{4\pi}\left(\frac{1}{2\pi}\right)m_0\log\Lambda^2 + \frac{g_{K\Lambda}^2+3g_{K\Sigma}^2+3g_\pi^2}{4\pi}\left(\frac{1}{8\pi}\right)(m_N-m_\Xi)\log\Lambda^2, \quad (4.9)$$

and the sign of the mass splitting is seen to be incorrect.

Thus, on the basis of the assumptions listed in the first section, the nucleon

cascade particle mass spectrum indicates that the nucleon K meson hyperon vertex should be of the form

$$L_{KN} = g_{K\Lambda}\phi_K\psi_\Lambda\beta\psi_N + g_{K\Sigma}\phi_K\psi_\Sigma\beta i\tau\psi_N. \tag{4.10}$$

5. Additional Remarks

The approximations 4) and 5) of the introduction can be used to obtain additional statements about the baryon mass spectrum. The following list summarizes such remarks.

1) So long as the mass parameters m_0 are set equal for all the various baryons, if any baryon A is coupled only by pseudoscalar couplings, its mass m_A satisfies the inequalities

$$m_A \geqq m_0 \geqq \tfrac{1}{2}m_A. \tag{5.1}$$

In the theory described above, the cascade particle is coupled to mesons only through pseudoscalar interactions, so that its mass should satisfy this relation. This argument proves that assumption 6) of the introduction follows from 4) and 5).

2) If pionic couplings preserve the baryon symmetry assumed in 1), we have, in this approximation,

$$2m_N + 2m_\Xi = m_\Lambda + 3m_\Sigma. \tag{5.2}$$

3) If, further, the K coupling constants satisfy the relations $g^2_{K\Lambda N} = g^2_{K\Sigma N}$ and $g^2_{K\Lambda\Xi} = g^2_{K\Sigma\Xi}$, this approximation yields

$$m_\Lambda = m_\Sigma. \tag{5.3}$$

4) In the theories discussed in the body of this paper, for which the relation (4.8) can be derived, (5.1) can be used to obtain a relation among the coupling parameters that appear in (4.8). (These are not renormalized.) We can conclude that

$$g_\pi{}^2 < 15\bar{g}_K{}^2 \equiv \tfrac{15}{4}(g^2_{K\Lambda} + 3g^2_{K\Sigma}), \tag{5.4}$$

and if

$$(g_\pi{}^2/4\pi)(\log \Lambda^2)/2\pi \gg 1,$$

that

$$g_\pi{}^2 \approx 7\bar{g}_K{}^2. \tag{5.5}$$

In the opposite limit,

$$(g_\pi{}^2/4\pi)(\log \Lambda^2)/2\pi \ll 1,$$

we would have

$$(\bar{g}_K{}^2/4\pi)(\log \Lambda^2)/2\pi \approx \tfrac{1}{12}. \tag{5.6}$$

These remarks show that the approximations 4) and 5) give rise to expressions for the mass spectrum which are almost consistent with the observed

spectrum, and that they lead to statements about the coupling parameters (viz. (5.4) and (5.5)) which are consistent in order of magnitude with current estimations of the relative sizes of the K and π renormalized coupling constants.

This work is based upon part of a thesis submitted to Harvard University in partial fulfilment of the requirements for the degree of Doctor of Philosophy, in May 1958. Whe author would like to thank Professor Schwinger for suggesting this problem; he would also like to express his appreciation to Professor Niels Bohr for the hospitality extended to him at this institute.

References

1) J. Schwinger, Lectures on Fundamental Interactions, Harvard M.I.T. 1956 (unpublished); Annals of Physics **2** (1957) 407
2) M. Gell-Mann, Proceedings of the 1957 Rochester Conference; Phys. Rev. **106** (1957) 1296
3) Private communcication from the Oxford group
4) D. Kleitman, Phys. Rev. **107** (1957) 1453
5) G. Källén, Helv. Phys. Acta **25** (1952) 417;
H. Lehmann, Nuovo Cimento **11** (1954) 342

1.D.2:
1.E.4:6.D

Nuclear Physics **14** (1959/60) 42—69; © *North-Holland Publishing Co., Amsterdam*
Not to be reproduced by photoprint or microfilm without written permission from the publisher

E2 TRANSITIONS FROM THE SECOND 2+ LEVEL OF EVEN-EVEN NUCLEI

D. M. VAN PATTER

Bartol Research Foundation of the Franklin Institute, Swarthmore, Pa. †

Received 4 August 1959

Abstract: A survey has been made of available data for the γ-ray branching of the second 2+ level of over 50 even nuclei with $A > 30$, together with data for the E2−M1 mixing of the $(2' \rightarrow 2)$ cascade transition. In addition, presently available data for the Coulomb excitation cross sections for the second 2+ level of some 24 even nuclei have been collected. From these data, three ratios of reduced E2 transition probabilities have been calculated, and compared with the predictions of various theories. The comparisons indicate that by far the most successful theory to date for predicting such ratios is the recent asymmetric rotor model of Davydov and Filippov. Perhaps the most striking success of this theory is the prediction for the ratio $B(\text{E2}; 2' \rightarrow 0)/B(\text{E2}; 2 \rightarrow 0)$ as a function of the energy ratio $E_2(2+)/E_1(2+)$. However, there are some experimental results which remain unexplained, particularly for the ratio $B(\text{E2}; 2' \rightarrow 2)/B(\text{E2}; 2' \rightarrow 0)$.

1. Introduction

Knowledge of the systematic properties of the low-lying states of even nuclei has increased rapidly during the past eight years since Goldhaber and Sunyar [1]) first pointed out that the first excited state has usually a spin and parity of 2+. The energies and spins of the low-lying levels, and their smooth variation with A were first examined comprehensively [2,3]) in 1953. Since then there have been several more publications containing information of a similar nature [5–13]) ††, some of which were confined to studies of nuclei with a level scheme which can be classified either as "rotational" or "vibrational". These reports have usually provided either more complete information regarding known systematic properties, or have proposed the existence of new regularities. Despite the many publications in this field, there is still a strong continuing interest, and it is quite likely that further studies will reveal new regularities which are now unnoticed.

† This research was supported by the United States Air Force through the Air Force Office of Scientific Research of the Air Research and Development Command under contract AF49 (638)—512.

†† Ref. [8]) contains an excellent survey of the experimental data and theoretical results in the "vibrational region". Ref. [9]) contains a stimulating discussion, similar to ref. [8]), for nuclei with $A > 134$. Ref. [10]) contains an extensive compilation of the level energies, $B(\text{E2})$ values, and values of δ^2 for nuclei with "vibrational" spectra: $40 \leqq A \leqq 154$; $180 \leqq A \leqq 226$. Ref. [11]) contains similar information for $158 \leqq A \leqq 182$, $230 \leqq A$. Ref. [12]) contains similar information as refs. [10]) and [11]), also systematics for the sign of δ.

Studies of the systematic properties of γ-ray transitions between low-lying levels of nuclei exhibiting vibrational spectra were initiated by the discovery of Kraushaar and Goldhaber [14]) that the mixed (E2+M1) transition between the first two 2+ levels is usually $\approx 90\,\%$ E2 in character. The enhancement of the E2 transition probability is indicative of the collective nature of this transition. More recently there have been several surveys of the E2—M1 mixture in the $(2' \rightarrow 2)$ cascade transition [10–12, 15, 16]) and the γ-ray branching ratio for the second 2+ level [10–12, 17]), which together yield information concerning the ratio of the reduced E2 transition probabilities of the $(2' \rightarrow 2)$ and $(2' \rightarrow 0)$ transitions. A similar property was found by Sunyar [18]) for the E2 lifetime for the first 2+ level, which is found to be generally much shorter than expected on the basis of single-particle transitions. The advent of Coulomb excitation allowed determinations of the lifetimes of the first levels of many even nuclei [7]). More recently, possible regularities have been proposed for the lifetime (or B(E2) value) of the first 2+ level as a function of the level energy [10, 11, 19–21]).

At the same time that the experimental knowledge of the properties of even nuclei was increasing, there was a corresponding development in theories which could account for many of the observed properties, such as the Bohr-Mottelson unified nuclear model [22, 23]). Strong coupling solutions of this model have explained in great detail and to high accuracy [7, 24]) many of the properties of nuclei exhibiting "rotational" spectra ($N = 90$ to ≈ 114, $N \geqq 136$) [8, 9]). Weak coupling solutions of this model by Scharff-Goldhaber and Weneser [3]), and Raz [25]) have been investigated in order to account for some of the known properties of nuclei which exhibit "vibrational" spectra for the low-lying levels (roughly defined by $E_2(2+)/E_1(2+) \lesssim 3$).

A more recent theoretical development deals with the equilibrium shape of the nucleus, and the possibility that it may be represented by a triaxial ellipsoid [26]). Bohr [22]) specified the ellipsoidal shape of the nucleus with the parameters β and γ, which are related to the body-fixed co-ordinates a_μ which determine the shape of the nucleus as follows:

$$a_0 = \beta \cos\gamma, \quad a_1 = a_{-1} = 0, \quad a_2 = a_{-2} = (\beta/\sqrt{2}) \sin\gamma, \tag{1.1}$$

$$R(\theta, \phi) = R_0 \left\{ 1 + \sum_{\mu=-2}^{2} a_\mu Y_{2\mu}(\theta, \phi) \right\}. \tag{1.2}$$

For a fixed value of β, varying γ from 0 to $\frac{1}{3}\pi$ changes the shape of the nucleus from a prolate to oblate ellipscid of revolution; $\gamma = 30°$ corresponds to a shape intermediate between a prolate and oblate ellipsoid of revolution.

Gursky [27]) first demonstrated the possibility of axial asymmetry for the equilibrium shape of the nucleus. Marty [28]) and Wilets and Jean [5]) have calculated energy spectra for violation of axial symmetry. More quantitative predictions regarding the γ ray transition probabilities have been made recently by

Davydov and Filippov [26]) (henceforth referred to as DF) assuming an asymmetric rotor model. They calculated the energy states and γ-ray transition probabilities for rotation of an axially asymmetric nucleus without changes in its internal state. From a comparison of their predictions for ratios of energy levels and reduced E2 transition probabilities, they concluded that axial asymmetry had been demonstrated, particularly for medium-weight nuclei (or those having "vibrational" level schemes), with $E_2(2+)/E_1(2+) \gtrsim 2$ (which corresponds to values of γ close to 30°).

The apparent success of their model has encouraged DF to do further theoretical work [29]) † with the objective of demonstrating theoretically that the minimum energy for such nuclei does indeed correspond to an axially asymmetric shape. (In the case of their original model, it would then follow that a nucleus in an excited rotational state would have a similar shape.) They find that for a model with two nucleons with angular momentum j outside a core, the equilibrium shape is axially asymmetric for intermediate coupling of the nucleons to the surface, provided that $j > \frac{3}{2}$. In the limit of very weak or very strong coupling, the equilibrium shape approaches axial symmetry, as would be expected.

In view of the current interest in these recent theoretical developments, it seemed worthwhile to do a comprehensive survey of all the available data concerned with ratios of reduced E2 transition probabilities, and to compare these experimental results with the various theoretical predictions, particularly those of DF. In the publication containing their asymmetric rotor theory [26]), DF did make such comparisons with experiment; however, at that time, only a limited amount of information was available to them. During the past two years, a considerable amount of new results concerning the second 2+ state of even nuclei has been obtained from studies of both radioactivity and Coulomb excitation [32]). Much of the Coulomb excitation data had already been compiled by the author for an investigation of possible regularities for absolute B(E2) values, particularly for the first 2+ level of even nuclei [21]). Therefore it seemed appropriate to expand the survey to include available data for the γ-ray branching of the second 2+ level, and the E2-M1 mixing of the $(2' \rightarrow 2)$ cascade transition. A further reason for doing such a comprehensive survey was to draw attention to the wealth of new data in this field, and to point out the striking success of the DF theory in providing quantitative predictions which generally agree with the experimental data. A preliminary account of this work has been recently presented [33]).

† Theoretical calculations with a similar objective have been recently made by Daikin [30]) and Geilikman [31]).

2. Results of the Survey and Discussion

2.1. BRANCHING OF THE SECOND 2+ LEVEL; THE RATIO $B(E2; 2' \rightarrow 2)/B(E2; 2' \rightarrow 0)$

The first part of the survey consisted in accumulating all the data available to the author (until July 1, 1959) concerned with the γ-ray branching of the second 2+ level for even nuclei with $A > 30$. The information required includes measurements of the E2-M1 mixing in the $(2' \rightarrow 2)$ cascade transition from the second to first 2+ level, either from $\gamma-\gamma$ angular correlation measurements, or from measured conversion coefficients or K/L ratios. In a few cases, the γ-ray branching has been calculated from a measured ratio of intensities of conversion electrons, assuming 100 % E2 for the cascade transition if the E2-M1 mixture is not known. It is, of course, of paramount importance to know which γ-rays correspond to the decay of the second 2+ state, which requires a careful scrutiny of the data relating to each level scheme. For this survey, three recent compilations [34-36]) of radioactive decay schemes and energy level diagrams have been extremely helpful.

The information obtained in this survey for 55 even nuclei is summarized in table 1; these results are almost completely due to radioactive decay studies. The individual measurements (and corresponding references) which were used to obtain the weighted average values of the branching and E2-M1 mixture are listed in table 4 at the end of this article. From the average values for r = cross-overs/cascades and for the % E2 of the $(2' \rightarrow 2)$ transition, the ratio of reduced E2 transition probabilities $B(E2; 2' \rightarrow 2)/B(E2; 2' \rightarrow 0)$ is calculated, using the best values for the energies of the first two 2+ levels listed in table 1. In those cases where the % E2 is not known, it has been taken as 100 %. This assumption should not usually involve an error > 10 %, since when it is measured, the % E2 is generally > 90 %. However, for a few nuclei within 2 neutrons of closed shells (Xe^{136}, Ce^{142}) it is quite possible that the cascade transition will turn out to be predominately M1; therefore no value of $B(E2; 2' \rightarrow 2)/B(E2; 2' \rightarrow 0)$ has been calculated for these nuclei.

Some words of caution should be said concerning the associated errors listed for these ratios of $B(E2)$ values. The errors are primarily due to uncertainties in the γ-ray branching determinations, which in many cases have been estimated by the author from the deviations of individual measurements. However, it is quite possible that in some cases, systematic errors may be present, e.g. if the intensity of one of the γ-rays involved should be partially assigned to a transition between higher excited states. In the case of some nuclei, such a situation is known to exist (such as Ni^{60} and Se^{76}, as discussed in the remarks following table 4). It is likely that this situation will prove to be true for some of the nuclei listed in table 1, and therefore the quoted errors should be regarded as giving some indication of the uncertainty involved, but not as strict standard deviations. In addition, if any of the levels listed turn out not to be the second

TABLE I

Summary of available data for the γ-ray branching of the second 2+ level for 55 even nuclei

Nucleus	Neutron number N	First 2+ Level		Second 2+ Level		$\frac{E_2(2+)}{E_1(2+)}$	Average Cross-over / Cascade	Average % E2	$\frac{B(E2; 2' \to 2)}{B(E2; 2' \to 0)}$
		$E_1(2+)$ (keV)	Spin and parity	$E_2(2+)$ (keV)	Spin and parity				
S^{34}	18	2128 8	2+	3302 8	2+	1.55	0.42 ± 0.05	1.7±0.6	7 ± 3
Fe^{56}	30	845 3	2+	2657 5	2+	3.14	0.024 ± 0.003	0.4−2.5	1 − 7
Fe^{58}	32	806 4	2+	1663 5	2+	2.06	0.31 ± 0.11	84 ±6	75 ± 27
Ni^{60}	32	1332.5 3	2+	2159 3	2+	1.62	0.07	≧90	1800
Ni^{62}	34	1172 3	2+	2048 3	(0+, 2+)	1.75	<0.33		>210
Zn^{64}	34	990 4	2+	1799 5	(2+)	1.82	0.34		160
Zn^{66}	36	1039 3	2+	1871 8	(2+)	1.80	<0.04		>1300
Zn^{68}	38	1081 5	2+	1895 9	(2+)	1.75	≈1.4		≈50
Ge^{72}	40	834.5 <10	2+	1465 <1	2+	1.76	0.17 ± 0.03	≧95	400 ± 70
Ge^{74}	42	596 1	2+	1200 6	2+	2.01	3		10
Se^{76}	42	560.5 3	2+	1220 3	2+	2.18	0.8 ± 0.2	97 ±2	26 ± 7
Se^{78}	44	613 4	2+	1308 8	2+	2.13	0.8 ±(0.1)		30 ± (4)
Se^{80}	46	660 5	2+	1450 10	2+	2.20	1.0 ± 0.3		21 ± 6
Kr^{82}	46	776.9 2	2+	1475.3 4	2+	1.90	0.60 ± 0.03	E2+M1	70 ± 4
Kr^{84}	48	882 4	2+	1890 20	(2+, 1+)	2.14	1.7 ± 0.2	99.9	13.5 ± 1.6
Zr^{92}	52	934 1	2+	1830 10	2+	1.96	1.1 ± 0.6	<0.2	<0.06
Ru^{100}	56	535.3 <10	2+	1358 <1	2+	2.54	1.05 ±(0.15)		11.6 ± (1.7)
Ru^{102}	58	474 1	2+	1104 4	2+	2.33	?	99	
Pd^{104}	58	556.2 <10	2+	1340	(2+)	2.41	0.10		140
Pd^{106}	60	513.0 5	2+	1131 5	2+	2.20	0.46 ± 0.05		45 ± 5
Cd^{110}	62	656.3 3	2+	1473 ≈1	2+	2.24	0.67 ± 0.13		30 ± 6
Cd^{114}	66	556 1	2+	1208 4	2+	2.17	0.28 ±(0.06)	E2+M1	77 ±(16)
Sn^{116}	66	1272 5	2+	2090 10	(2+)	1.64	1.1 ± 0.2	92^{+3}_{-12}	38 ± 7
Te^{122}	70	563.9 2	2+	1257 5	2+	2.23	0.20 ± 0.03	92.4±1.4	91 ± 14
Te^{124}	72	603 1	2+	1326 2	(2+)	2.20	0.17 ± 0.03	50 ±4	61 ± 12
Te^{126}	74	662 3	2+	1415 15	(2+)	2.14	0.07 ± 0.01	97.6±1.7	330 ± 50
Xe^{126}	72	385 1	(2+)	865 10	(2+)	2.25	0.17 ± 0.02	>99	115 ± 15
Xe^{128}	74	451 2	2+	986 3	(2+)	2.19	0.17 ± 0.02		125 ± 15

Xe^{136}	82	1307	6	(2+)	2620	(20)	(2+)	2.00	0.50 ± 0.18	—	— [a]
Ba^{134}	78	604.7	2	(2+)	1167.4	15	(2+)	1.93	0.25 ± 0.04	E2	154 ± 25
Ce^{140}	82	1596	2	2+	2540	5	2+	1.59	0.40 ± 0.05	0.1 − 1.0	0.4 − 4
Ce^{142}	84	643	6	(2+)	1530	10	?	2.38	0.33	—	— [a]
Sm^{152}	90	121.85	3	2+	1086.6	10	2+	8.96	0.84 ± 0.03	98.3 ± 1.1	2.2 ± 0.3
Gd^{154}	90	123.1	1	2+	966.6	10	(2+)	7.85	≦0.9		≧1.8
Gd^{156}	92	88.97	3	2+	1140	10	?	12.8	0.8 ± 0.4		1.9 ± 0.9
Dy^{160}	94	86.6	2	2+	965.7	10	2+	11.2	0.77 ± 0.04	96.5 ± 3.5	2.0 ± 0.1
Er^{166}	98	80.57	2	2+	787.4	12	(2+)	9.77	0.86 ± 0.13		2.0 ± 0.3
Er^{168}	100	79.80	2	2+	822.0	12	(2+)	10.3	0.92 ± 0.15		1.8 ± 0.3
W^{182}	108	100.09	1	2+	1221.8	2	2+	12.21	0.85 ± 0.06		1.8 ± 0.1 [b]
W^{184}	110	111.13	6	2+	904	1	2+	8.14	1.1 ± 0.2	E2+M1	1.8 ± 0.3
W^{186}	112	122.48	8	2+	733	5	2+	5.98	1.0 ± 0.1		2.5 ± 0.3
Os^{186}	110	137.19	9	2+	768.2	10	2+	5.60	1.0 ± 0.2	99 ± 1	2.7 ± 0.6
Os^{188}	112	155.0	1	2+	633.0	1	2+	4.08	1.5 ± 0.1	99.6 ± 0.4	2.7 ± 0.2
Os^{190}	114	187.0	<10	2+	557	(2)	2+	3.00	1.1 ± 0.2	98	6.8 ± 1.2
Os^{192}	116	205.74	4	2+	489.0	2	2+	2.38	1.37 ± 0.2	(E2)	11.2 ± 1.6
Pt^{192}	114	316.46	9	2+	612.4	1	2+	1.93	0.23 ± 0.04	97.6 ± 1.0	161 ± 30
Pt^{194}	116	329.1	1	2+	622	1	2+	1.89	0.29 ± 0.04	≈99.9	150 ± 20
Pt^{196}	118	354.2	3	2+	685.5	4	2+	1.93	$<4\times10^{-4}$	95.8 ± 0.5	$<9\times10^{4}$
Hg^{198}	118	411.77	4	2+	1087.5	3	2+	2.64	0.19 ± 0.015	60 ± 6	34 ± 4
Hg^{202}	122	439.7	7	2+	963	2	(2+)	2.17	0.13 ± 0.03		160 ± 40
Po^{212}	128	727.2	5	2+	1512.6	5	(≦2)	2.08	1.6		17
Po^{214}	130	609.4	2	2+	1281.3		2+	2.10	≦1		≦25
Th^{228}	138	57.5	(1)	2+	965	1	(2+)	16.8	0.52 ± (0.1)		2.5 ± (0.5)
Th^{232}	142	52.8		2+	790	(10)	2+	15.0	0.65 ± (0.1)	?	2.1 ± (0.3)
Pu^{238}	144	44.03		2+	1031	1	2+	23.4	0.83 ± (0.13)	E2+(M1)	1.5 ± (0.2)

In column 3 is listed the present best value for the energy of the first 2+ level together with its associated error, which is the error in the last figure given for the energy (according to the convention adopted by the Nuclear Data group). In column 4 is presented information for the spin and parity of the first 2+ level, using the conventions adopted by the Nuclear Data group [34]). Similar data are listed for the second 2+ level in columns 5 and 6, while in column 7, the ratio of the best energies for the first two 2+ level is given.

(a) Since this nucleus is within 2 neutrons of a closed neutron shell, the cascade ($2' \rightarrow 2$) transition is likely to be mainly M1 (as in the cases of Fe^{56}, Zr^{92} and Ce^{140}). Therefore a calculation of $B(E2; 2' \rightarrow 2)/B(E2; 2' \rightarrow 0)$ is probably not meaningful without knowledge of the E2/M1 mixture.

(b) This value was calculated assuming 100 percent E2 for the 1121.6 keV cascade transition, despite the result of Williams and Roulston (see table 4) which indicated ≈ 90 % E2. From evidence obtained from neighbouring nuclei, it is expected that the cascade transition should be ≈ 99 % in W^{182}. If 90 % E2 had been assumed, then the calculated value of $B(E2; 2' \rightarrow 2)/B(E2; 2' \rightarrow 0)$ would have been 1.6 ± 0.2.

2+ level, the results for the corresponding nucleus would not be valid.

The 53 values of the ratio $B(\mathrm{E2}; 2' \to 2)/B(\mathrm{E2}; 2' \to 0)$ listed in table 1 are plotted, in fig. 1 as a function of the energy ratio $E_2(2+)/E_1(2+)$, in fig. 2 as a function of the neutron number N. These values cover a large range, from < 0.06 (Zr^{92}) to $> 9\times 10^4$ (Pt^{196}), with most of the values lying in the range of 1.5 to 500.

In fig. 1, a comparison is made between the experimental results and the prediction of the DF theory [26]), using the following relations from this theory (written in the notation of this paper):

$$\text{Energy level ratio: } \frac{E_2(2+)}{E_1(2+)} = \frac{3+\sqrt{9-8\sin^2(3\gamma)}}{2-\sqrt{9-8\sin^2(3\gamma)}}. \tag{2.1}$$

Relative reduced transition probabilities:

$$b(\mathrm{E2}; 2 \to 0) = \tfrac{1}{2}\left[1+\frac{3-2\sin^2(3\gamma)}{\sqrt{9-8\sin^2(3\gamma)}}\right], \tag{2.2}$$

$$b(\mathrm{E2}; 2' \to 0) = \tfrac{1}{2}\left[1-\frac{3-2\sin^2(3\gamma)}{\sqrt{9-8\sin^2(3\gamma)}}\right], \tag{2.3}$$

$$b(\mathrm{E2}; 2' \to 2) = \tfrac{10}{7}\frac{\sin^2(3\gamma)}{9-8\sin^2(3\gamma)}, \tag{2.4}$$

where γ is the asymmetry parameter defined in (1.1) and (1.2).

Following the procedure adopted by DF, a ratio of b(E2) values is equated to a ratio of B(E2) values, which can be experimentally determined. Since this ratio and the energy level ratio are both functions of γ, the DF predictions can be compared to experiment by plotting a ratio of B(E2) values as a function of $E_2(2+)/E_1(2+)$, as has been done in fig. 1. The DF prediction is then obtained from (2.1) and (2.4)/(2.3). For $\gamma \to 30°$, $E_2/E_1 \to 2$ and $B(\mathrm{E2}; 2' \to 2)/B(\mathrm{E2}; 2' \to 0) \to \infty$. For $\gamma \to 0°$, $E_2/E_1 \to \infty$ and $B(\mathrm{E2}; 2' \to 2)/B(\mathrm{E2}; 2' \to 0) \to 1.43$, which is the same value as that predicted by the Bohr-Mottelson theory [7, 24]).

Several comments can be made concerning the comparison between experiment and the DF theory shown in fig. 1:

(1) Qualitatively, the DF prediction gives the general behaviour of the experimental B(E2) ratios, which increase by a factor of $\approx 10^3$ as E_2/E_1 decreases from 23.4 (Pu^{238}) to 1.6 (Ni^{60}).

(2) The expected increase in the B(E2) ratio for decreasing E_2/E_1 according to the DF theory is quite well satisfied for nuclei with $A \geqq 152$; i.e., there does seem to be a correlation between the B(E2) ratio and E_2/E_1 from the experimental evidence for these nuclei.

(3) For nuclei in the regions of strong deformations, the agreement of the presently available data appears to be excellent. For nuclei with $152 \leqq A \leqq 184$ (6 cases, not including Gd^{154} and Gd^{156}) the average value for $B(E2; 2' \rightarrow 2)/B(E2; 2' \rightarrow 0)$ is $1.9 \pm \approx 0.2$, which seems to be in better agreement with the DF prediction of 2.0 (the average for these nuclei) than the Bohr-Mottelson prediction of 1.43†. This comparison is shown clearly in fig. 2. However, two of these results are preliminary (Er^{166} and Er^{168}) and it would be highly desirable to have more information to verify that the DF prediction is better for these strongly deformed nuclei. For nuclei with $N > 136$, predictions from the two

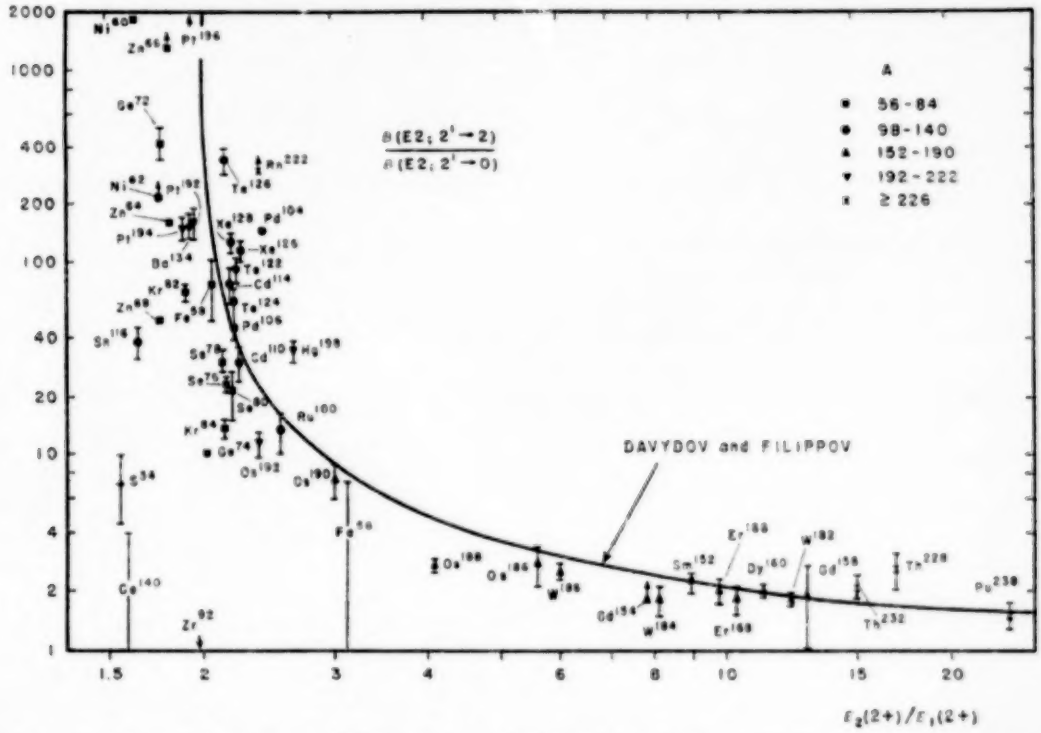

Fig. 1. Experimental data for $B(E2; 2' \rightarrow 2)/B(E2; 2' \rightarrow 0)$ for even nuclei as a function of the ratio of the energies of the first two 2+ levels, compared to the prediction of Davydov and Filippov. This ratio of reduced E2 transition probabilities is related to the E2 branching of the second 2+ level.

theories [7, 29]) are nearly the same, and few experimental data are available.

(4) For nuclei $58 \leqq A \leqq 134$ and $E_2/E_1 < 3$, the experimental values of this $B(E2)$ ratio fluctuate by a factor of 10—50 for given value of E_2/E_1, which seems to make any correlation with E_2/E_1 rather unlikely, in disagreement with the DF prediction.

(5) The DF theory cannot account for those nuclei with $E_2/E_1 < 2$, since the energy ratio predicted has a limiting value of 2 for $\gamma = 30°$. In addition to several nuclei with $32 \leqq N \leqq 40$ which are in this category, there are also Pt^{194} and

† *Note added in proof:* The Bohr-Mottelson prediction of 1.43 assumes no mixing between the $K = 0$ and $K = 2$ bands. Recent calculations given by Hansen *et al.*[39]) indicate that the experimental $B(E2)$ ratios for Gd^{156} can be accounted for if a correction for the effect of mixing of states of different K is included in the theoretical prediction.

Pt^{196}. Pt^{196} is an interesting case, since an anomalously high value of $> 9\times 10^4$ is observed for the B(E2) ratio (provided that the 685 keV level is correctly identified as the second 2+ level).

(6) Nuclei near closed shells (Fe^{56}, Zr^{92}, Ce^{140}) have values for this B(E2) ratio which fall well below the DF prediction, as would be expected.

The comparison in fig. 2 appears to indicate some effects and possible regularities which are not accounted for by any present theory:

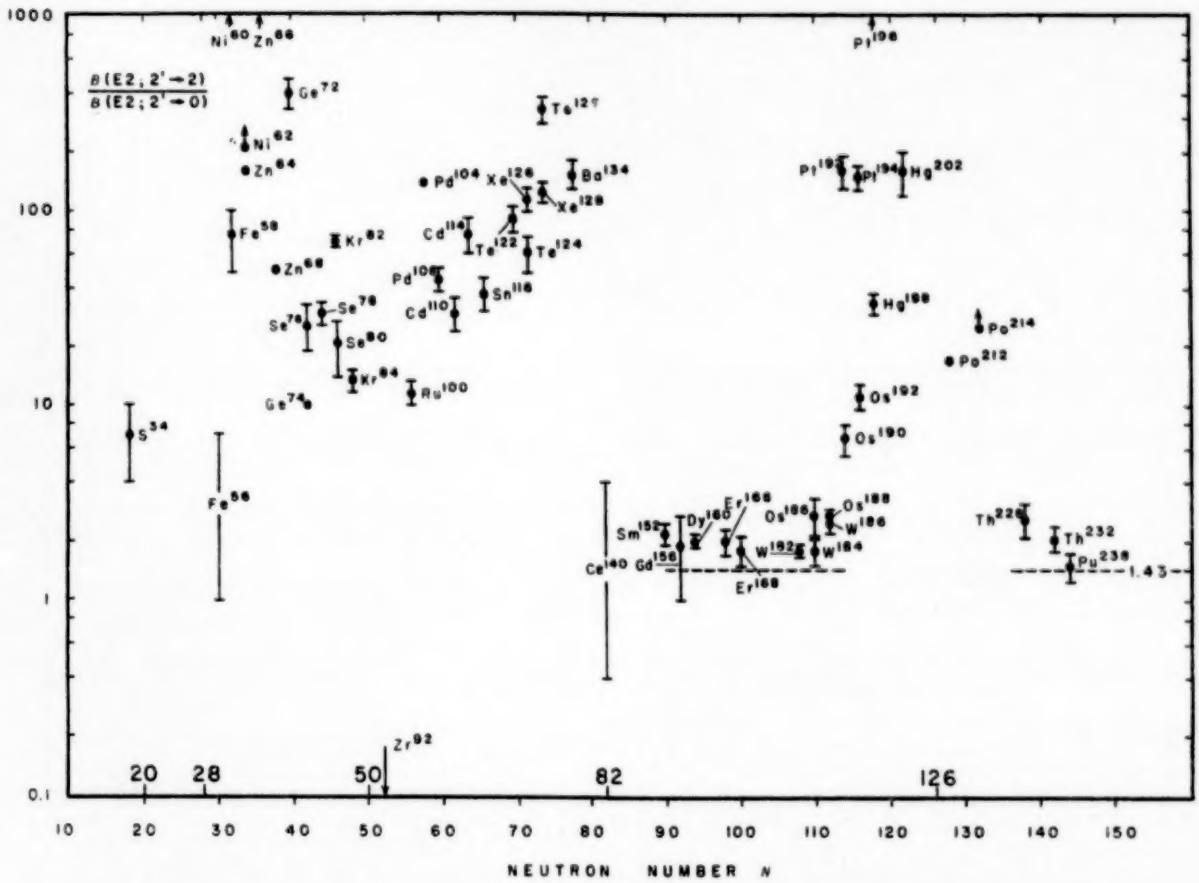

Fig. 2. Experimental data for $B(E2; 2' \rightarrow 2)/B(E2; 2' \rightarrow 0)$ for even-nuclei as a function of the neutron number N. This ratio of reduced E2 transition probabilities is related to the E2 branching of the second 2+ level.

(7) The sudden appearance of collective effects at $N = 32$ is quite striking (indicated by the increase in the B(E2) ratio of a factor of > 10 from Fe^{56} to Fe^{58}). A similar effect has been noted [37]) for the energy levels of even nuclei in this region, which may well be another symptom of the same nuclear property. Between $N = 30$ and $N = 32$, the second level changes from 4+ to 2+. The two effects seem to indicate that a collective state of excitation (the second 2+ level) suddenly appears at $N = 32$. [This is not true for the first level, since enhancement of the E2 transition probability persists down to $N = 26$ (Ti^{48}) [21]).]

TABLE 2

Coulomb excitation data of Stelson and McGowan for first two 2+ levels for medium weight nuclei, $A = 74$—122

Nucl.	$E_1(2+)$ (keV)	$E_2(2+)$ (keV)	$\frac{E_2}{E_1}$	$B(E2; 0 \to 2) \times 10^{50}$	$B(E2; 0 \to 2') \times 10^{50}$ cascade	$B(E2; 0 \to 2') \times 10^{50}$ total	$\frac{\text{Crossover}}{\text{Cascade}}$	$\frac{B(E2; 2' \to 0)}{B(E2; 2 \to 0)} \times 10^2$	$\frac{B(E2; 2' \to 2)}{B(E2; 2 \to 0)}$
Ge^{74}	600±6	1200± 8	2.00	31.7±3.2 [a])	0.44±0.09 [a])	1.74±0.56	3 ±(1)	5.5±1.8	0.57±0.14
Ge^{76}	576±6	1136± 8	1.99	26.3±2.6 [a])	0.43±0.09 [a])	—	—	>1.6	>0.49
Se^{76}	560±6	1220± 8	2.18	45.4±4.1 [a])	0.74±0.15 [a])	1.33±0.30	0.8 ± 0.2	2.9±0.7	0.76±0.18
Se^{78}	612±6	1307± 9	2.14	35.5±3.2 [a])	0.55±0.11 [a])	0.98±0.21	0.79±(0.1)	2.8±0.6	0.83±0.19
Se^{80}	665±7	1455±11	2.19	25.8±2.3 [a])	0.97±0.20 [a])	1.93±0.50	1.0 ± 0.3	7.5±2.0	1.56±0.43
Mo^{100}	530±5	1050± 9	1.98	61.4±6.1 [b])	1.75±0.26 [a])	—	—	>2.8	>0.96
Ru^{98}	654±6	1402±10	2.14	47.5±3.8 [b])	0.52±0.06 [a])	—	—	>1.1	>0.25
Ru^{100}	540±5	1355±16	2.51	57.2±4.0 [b])	1.16±0.14 [c])	2.38±0.34	1.05±(0.15)	4.2±0.7	0.48±0.08
Ru^{102}	475±5	1100± 9	2.31	73.3±5.1 [b])	1.17±0.09 [c])	—	—	>1.6	>0.26
Ru^{104}	358±3	893± 7	2.49	92.8±6.5 [b])	1.19±0.10 [c])	—	—	>1.3	>0.17
Pd^{106}	513±5	1120± 8	2.18	64.6±4.5 [b])	1.08±0.23 [c])	1.58±0.34	0.46± 0.05	2.6±0.6	1.09±0.25
Pd^{108}	433±4	941± 7	2.17	74.2±5.2 [b])	0.74±0.11 [c])	—	—	>1.0	>0.22
Pd^{110}	374±4	812± 7	2.17	86.0±6.0 [b])	0.94±0.08 [c])	—	—	>1.1	>0.24
Cd^{110}	656±6	1476	2.25	50.4±4.0 [b])	1.47±0.19 [c])	2.45±0.37	0.67± 0.13	4.9±0.8	1.47±0.29
Cd^{112}	610±6	1295±16	2.12	54.2±3.8 [b])	0.91±0.09 [c])	1.19±0.14	0.31±0.08	2.3±0.3	1.74±0.40
Cd^{114}	555±5	1200±10	2.16	58.4±4.1 [b])	0.79±0.06 [c])	1.02±0.10	0.28±(0.06)	1.74±0.2	1.33±0.26
Cd^{116}	517±5	1217±11	2.35	60.0±4.2 [b])	1.23±0.14 [c])	—	—	>2.0	>0.33
Te^{122}	564±5	1256± 9	2.23	65.2±5.2 [a])	1.77±0.35 [a])	2.12±0.43	0.20±0.03	3.3±0.7	3.0 ±0.7

$E_1(2+)$ and $E_2(2+)$ are the level energies for the first two 2+ levels, as determined from γ-ray energy measurements of Stelson and McGowan; E_2/E_1 is the ratio of these energies. Reduced E2 transition probabilities (columns 5 to 7) are given in units of $e^2 \times 10^{-50}$ cm^4. In column 6, values for $B'(E2; 0 \to 2')$ are listed for the excitation of the second 2+ level, for which only the cascade transition was observed. These values are not corrected for double E2 excitation and angular correlation effects from the triple cascade. When the branching of the second 2+ level is known, the value of the total $B(E2; 0 \to 2')$ is listed in column 7.

[a]) F. K. McGowan and P. H. Stelson, Bull. Am. Phys. Soc. **4** (1959) 232; ORNL-2610 (Feb. 26, 1959) 11; and private communication of error estimates

[b]) See ref. [20]).

[c]) P. H. Stelson and F. K. McGowan, Bull. Am. Phys. Soc. **2** (1957) 267; ORNL-2430 (April 8, 1958) 19; and private communication of revised values and errors

(8) A general trend towards lower values for $B(\mathrm{E2};\ 2' \rightarrow 2)/B(\mathrm{E2};\ 2' \rightarrow 0)$ of at least a factor 10 is noted for N increasing from 32 to 48. (There is possibly a decrease at the closing of the $N = 40$ subshell; however, the present data are not good enough to verify this possibility.) This is a surprising effect, since for $N = 32$—40, the E_2/E_1 ratio is generally 1.6—1.8, while for $N = 42$—48, E'/E_1 is generally > 2.0. The latter value is more typical of a "vibrational" spectrum [3]), and therefore nuclei with $N = 42$—48 might be expected to show a larger collective effect than the nuclei with $N = 32$—40; however, the opposite is in fact the case.

(9) There seems to be a general trend towards increasing values of this $B(\mathrm{E2})$ ratio of roughly a factor 10 as N increases from 60 to 78. This possible regularity, together with that mentioned in (8), seems to be the cause of lack of agreement with the DF theory for these nuclei, as discussed in (4).

(10) The reappearance of "vibrational" spectra for nuclei in the region $114 \leqq N \leqq 134$ is very marked, particularly for the isotopes of Os, Pt and Hg. This shows clearly how sensitively the γ-ray transition probabilities depend on the type of collective motion that is involved.

2.2. SURVEY OF COULOMB EXCITATION DATA

The second part of the survey consisted in collecting all the data presently available concerning Coulomb excitation of the second 2+ level in even nuclei, which come from the work of McGowan and Stelson, and Barloutaud *et al.*[32]). A considerable portion of these data is still preliminary in nature, with no corrections applied for double E2 excitation and angular correlation effects from the triple cascade. These data are shown in tables 2 and 3. Included are the Coulomb excitation measurements for the first 2+ level, for which the reduced E2 transition probability for excitation, $B(\mathrm{E2};\ 0 \rightarrow 2)$, is listed in column 5 of table 2. This is related to the $B(\mathrm{E2})$ value for decay by

$$B(\mathrm{E2};\ 0 \rightarrow 2) = 5B(\mathrm{E2};\ 2 \rightarrow 0),$$

and similarly,

$$B(\mathrm{E2};\ 0 \rightarrow 2') = 5B(\mathrm{E2};\ 2' \rightarrow 0).$$

The Coulomb excitation data in table 2 are obtained from the work of McGowan and Stelson. Their measurements for medium-weight nuclei ($A = 74$—122) consists of detecting the cascade $(2' \rightarrow 2)$ transitions by means of (γ, γ) coincidence measurements. The yield of the cross-over $(2' \rightarrow 0)$ γ-ray is too weak to be observed in the singles spectrum. Therefore, essentially they measure $B'(\mathrm{E2};\ 0 \rightarrow 2')$, defined by

$$B'(\mathrm{E2};\ 0 \rightarrow 2')(1+r) = B(\mathrm{E2};\ 0 \rightarrow 2'),$$

where r = crossovers/cascades. Hence we have listed values of $B'(\mathrm{E2};\ 0 \rightarrow 2')$ in column 6 of table 2. In order to establish the correct value of $B(\mathrm{E2};\ 0 \rightarrow 2')$ the branching of the second 2+ level must be known from other measurements.

TABLE 3

Coulomb excitation data for the first two 2+ levels of heavy nuclei, $A = 184$—232

Nucl.	$E_\gamma(2'\to0)$ (keV)	$E_\gamma(2'\to2)$ (keV)	$B(E2;\,0\to2)\times10^{50}$	$B(E2;\,0\to2')\times10^{50}$ cascade	$B(E2;\,0\to2')\times10^{50}$ total	Crossover / Cascade	$\frac{B(E2;\,2'\to0)}{B(E2;\,2\to0)}\times10^{2}$	Weighted Average $\frac{B(E2;\,2'\to0)}{B(E2;\,2\to0)}\times10^{2}$	Weighted Average $\frac{B(E2;\,2'\to2)}{B(E2;\,2\to0)}$
W^{184}	891 ± 9	780 ± 8	437 ± 44 [a]	8.5 ± 2.5 [d]	17 ± 5	1.07 ± 0.2	3.9 ± 1.2	3.8 ± 0.9	0.07 ± 0.02
	885	780	[420] [b]	7.5 ± 2.2 [h]	15.4 ± 5*		3.7 ± 1.2*		
W^{186}	730 ± 7	608 ± 6	356 ± 36 [a]	8.7 ± 1.5 [d]	17.5 ± 3	1.0 ± 0.1	4.9 ± 1.0	4.7 ± 0.7	0.12 ± 0.02
	750	615	[420] [b]	8.7 ± 2.6 [e]	17.5 ± 5		4.2 ± 1.3		
Os^{188}	633 ± 6	478 ± 5	280 ± 31 [a]	8.0 ± 2.4 [d]	20 ± 6	1.5 ± 0.1	7.1 ± 2.8	7.1 ± 2.8	0.19 ± 0.08
	(630)	480	348 ± 100 [c]	23 ± 9 [e]	58 ± 23		16.6 ± 6.6**		
Os^{190}	557 ± 6	370 ± 4	255 ± 26 [a]	7.9 ± 1.7 [d]	16.5 ± 4.5*	1.1 ± 0.2	6.5 ± 1.8*	6.3 ± 1.3	0.43 ± 0.12
	(566)	380	245 ± 60 [c]	7.0 ± 2.1 [e]	14.7 ± 4.6*		6.0 ± 1.8*		
Os^{192}	489 ± 5	283 ± 3	205 ± 21 [a]	6.0 ± 1.2 [d]	14.2 ± 3.1*	1.37 ± 0.2	6.9 ± 1.5*	6.7 ± 1.2	0.75 ± 0.17
	(486)	280	210 ± 50 [c]	5.6 ± 1.7 [e]	13.2 ± 4.1*		6.3 ± 2.0*		
Pt^{194}	(622)	292	194 ± 20 [d]	0.67 ± 0.15 [i]	0.87 ± 0.20	0.29 ± 0.04	0.45 ± 0.09	0.41 ± 0.08	0.60 ± 0.14
	(620)	293	125 ± 30 [e]	0.29 ± 0.12 [e]	0.38 ± 0.15*		0.30 ± 0.12*	0	
Pt^{196}	(688)	(330)	127 ± 13 [d]	< 0.13 [d]	< 0.13	$< 4\times10^{-4}$	< 0.10	< 0.10	—
Hg^{198}	(1090)	(675)	113 ± 34 [f]	< 12 [h]	< 14	0.19 ± 0.02	< 12	< 12	< 4.2
Th^{232}	790	740	665 ± 100 [j]	13.2 ± 1.7 [j]	21.8 ± 2.5	0.65 ± (0.1)	3.3 ± 0.6	2.1 ± (0.3)	0.068 ± 0.016

* This value has been corrected according to the branching ratio adopted (column 7) which differ from the ratio adopted in the original publication.

** This value has not been included in the weighted average value (column 9).

$E_\gamma(2'\to0)$ and $E_\gamma(2'\to2)$ are the γ-ray energies for the transitions from the second 2+ level to ground, and the second to first 2+ level, as measured in the Coulomb excitation experiments. Values enclosed in parentheses are the expected γ-ray energies in the cases where the γ-rays were not observed, or where they were too weak for accurate energy measurement.

[a]) F. K. McGowan and P. H. Stelson, Phys. Rev. **109** (1958) 901

[b]) This value was assumed by Barloutaud *et al.* from the measurements of T. Huus, J. H. Bjerregaard and B. Elbek, Mat. Fys. Medd. Dan. Vid. Selsk. **30**, No. 17 (1959)

[c]) R. Barloutaud, P. Lehmann and A. Lévêque, Comptes Rendus **245** (1957) 523; a revised $B(E2)$ value for the second 2+ level of Os^{190} is given in (h)

[d]) F. K. McGowan and P. H. Stelson, Bull. Am. Phys. Soc. **3** (1958) 228; ORNL-2501 (Feb. 15, 1958) p. 14

[e]) R. Barloutaud, A. Lévêque, P. Lehmann and J. Quidort, J. de Phys. et Radium **19** (1958) 60; a revised $B(E2)$ value for the second 2+ level of Pt^{194} is given in (h)

[f]) R. Barloutaud, T. Grjebine and M. Riou, Comptes Rendus **242** (1956) 1284

[g]) F. K. McGowan and P. H. Stelson, Bull. Am. Phys. Soc. **2** (1957) 207

[h]) See ref. [38])

[i]) F. K. McGowan and P. H. Stelson, Phys. Rev. **106** (1957) 522; also given in [d])

For those nuclei where the branching ratio is known (column 8), the total $B(\mathrm{E2}; 0 \rightarrow 2')$ is listed in column 7; otherwise only a lower limit is established. Then, using the values of McGowan and Stelson for $B(E2; 0 \rightarrow 2)$ for the excitation of the first level (column 5), the values of the $B(\mathrm{E2}; 2' \rightarrow 0)/B(\mathrm{E2}; 2 \rightarrow 0)$ are calculated (column 9), and plotted in fig. 3. Finally, taking the values for $B(\mathrm{E2}; 2' \rightarrow 2)/B(\mathrm{E2}; 2' \rightarrow 0)$ for these nuclei from table 1, values for the ratio $B(\mathrm{E2}; 2' \rightarrow 2)/B(\mathrm{E2}; 2 \rightarrow 0)$ are calculated (column 10), and plotted in fig. 4. Again, in the cases of nuclei where no branching is known, only a lower limit is established for this last $B(\mathrm{E2})$ ratio.

In table 3 are listed the Coulomb excitation results for the heavier nuclei ($A \geqq 184$). Results for six of these nuclei were obtained by both McGowan and Stelson, and Barloutaud *et al.* For some of the measurements, both the cascade and cross-over transitions were observed in the singles spectrum. For the remainder, only the cascade transition was clearly observed, by the use of $\gamma-\gamma$ coincidences. The same procedure was followed as for the preparation of table 2: the data were first reduced to the values of $B'(\mathrm{E2}; 0 \rightarrow 2')$ listed in column 5, since the same branching ratio was not adopted by both groups of workers. Then the value of $B(\mathrm{E2}; 0 \rightarrow 2') = (1+r)B'(\mathrm{E2}; 0 \rightarrow 2')$ was calculated (column 6) using the average branching ratio given in column 7. Since this branching ratio did not always coincide with that used originally, some of the $B(\mathrm{E2}; 0 \rightarrow 2')$ values listed in column 6 are different than reported by the authors (see references for table 3). Then values for the ratio $B(\mathrm{E2}; 2' \rightarrow 0)/B(\mathrm{E2}; 2 \rightarrow 0)$ are calculated, using the same values for $B(\mathrm{E2}; 0 \rightarrow 2)$ as originally given by the authors (column 4). The reason for this procedure is to preserve the original measurement, which is basically a measurement of the ratio $B'(\mathrm{E2}; 0 \rightarrow 2')/B(\mathrm{E2}; 0 \rightarrow 2)$ when only the cascade transition is observed. This fact also indicated that the best method of obtaining an average of the two results was to take a weighted average of the two determinations of $B(\mathrm{E2}; 2' \rightarrow 0)/B(\mathrm{E2}; 2 \rightarrow 0)$ for each nucleus which are given in column 8. (In the case of Os^{188} only, the value of Barloutaud *et al.* has been omitted from the average because of the possibility that the presence of annihilation radiation might make the value too large [38]). These average values are listed in column 9, and plotted in fig. 3, from which values for $B(\mathrm{E2}; 2' \rightarrow 2)/B(\mathrm{E2}; 2 \rightarrow 0)$ are calculated, listed in column 10, and plotted in fig. 4.

The ratio $B(\mathrm{E2}; 2' \rightarrow 0)/B(\mathrm{E2}; 2 \rightarrow 0)$

In fig. 3 are plotted 16 determinations for the ratio $B(\mathrm{E2}; 2' \rightarrow 0)/B(\mathrm{E2}; 2 \rightarrow 0)$, of which 9 correspond to medium-weight nuclei. (In addition, there are 8 lower limits for medium-weight nuclei.) This ratio gives the relative reduced E2 transition probabilities for decay (or excitation) of the first two levels to the ground state. Qualititative predictions for this ratio have been made from the strong coupling theories of Bohr and Mottelson [23, 24]), Wilets and Jean [5]), and

the weak coupling theory of Scharff-Goldhaber and Weneser [3]), which are all similar: the $(2' \rightarrow 0)$ transition is forbidden. However, the experimental result is that values of this ratio of up to a maximum of ≈ 0.08 are found. A quantitative prediction for this ratio has been obtained by Raz [25]), using a weak coupling theory. However, this prediction does not extend beyond $E_2/E_1 = 2.2$, and is not expected to apply to the region of strong collective motion.

The prediction of the DF theory is shown in fig. 3. The following remarks can be made about the comparison to the experimental results for $B(\mathrm{E2}; 2' \rightarrow 0)/B(\mathrm{E2}; 2 \rightarrow 0)$:

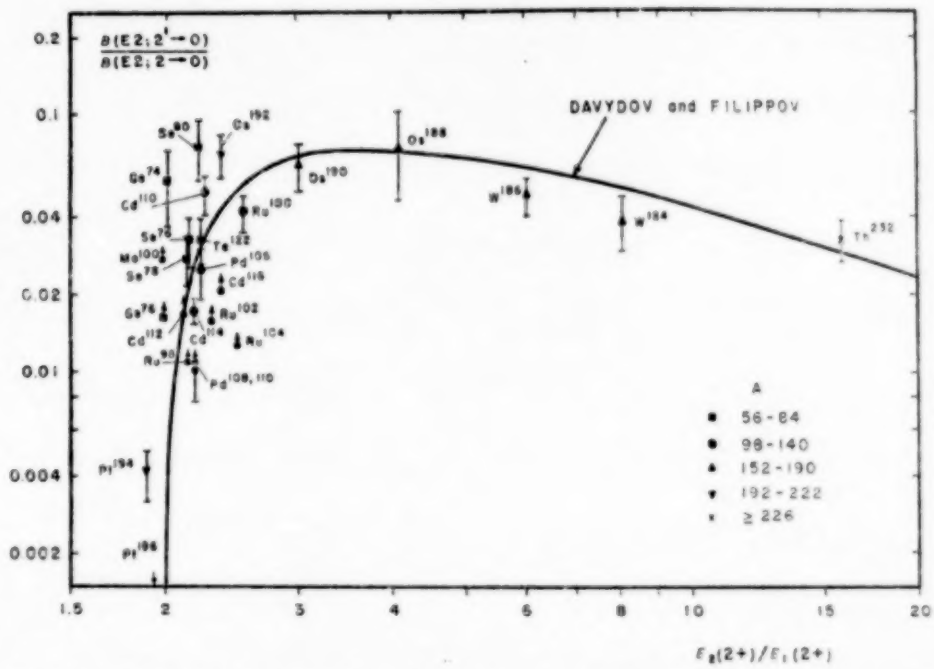

Fig. 3. Experimental data for $B(\mathrm{E2}; 2' \rightarrow 0)/B(\mathrm{E2}; 2 \rightarrow 0)$ for even nuclei compared to the prediction of Davydov and Filippov. This ratio of reduced E2 transition probabilities relates the decays of the first two 2+ levels to ground.

(1) The maximum value observed experimentally of ≈ 0.08 is in surprisingly good agreement with the maximum value of 0.072 predicted by the DF theory (which occurs at $E_2/E_1 \approx 3.5$).

(2) The experimental values are roughly consistent with the DF predicted curve; however, there is sufficient fluctuation in the experimental values, particularly for $E_2/E_1 < 3$, to prevent any verification of the predicted correlation of this $B(\mathrm{E2})$ value with E_2/E_1.

(3) Nuclei with $E_2/E_1 \approx 2.0$ (Ge^{74}, Ge^{76}, Mo^{100}) have values or lower limits which definitely exceed the DF prediction.

The ratio $B(\mathrm{E2}; 2' \rightarrow 2)/B(\mathrm{E2}; 2 \rightarrow 0)$

The final comparison between experimental data and predictions of various theories is shown in fig. 4. Again there are the same number of values and

lower limits as in fig. 3. The plotted ratio of $B(E2; 2' \rightarrow 2)/B(E2; 2 \rightarrow 0)$ relates the two transitions which are enhanced by collective motion. Quantitative predictions for this $B(E2)$ ratio are available from at least four theories. The weak coupling theory of Scharff-Goldhaber and Weneser [3]) and the strong coupling theory of Wilets and Jean [5]) both give a prediction of 2 for a small range of E_2/E_1, as shown in fig. 4. The predicted curve from the weak coupling theory of Raz [25]) is also shown, which may be applicable to nuclei in the region above calcium, where shell effects predominate. Since none of the nuclei shown in fig. 4 lie in this region, the predictions of Raz's theory may not apply to

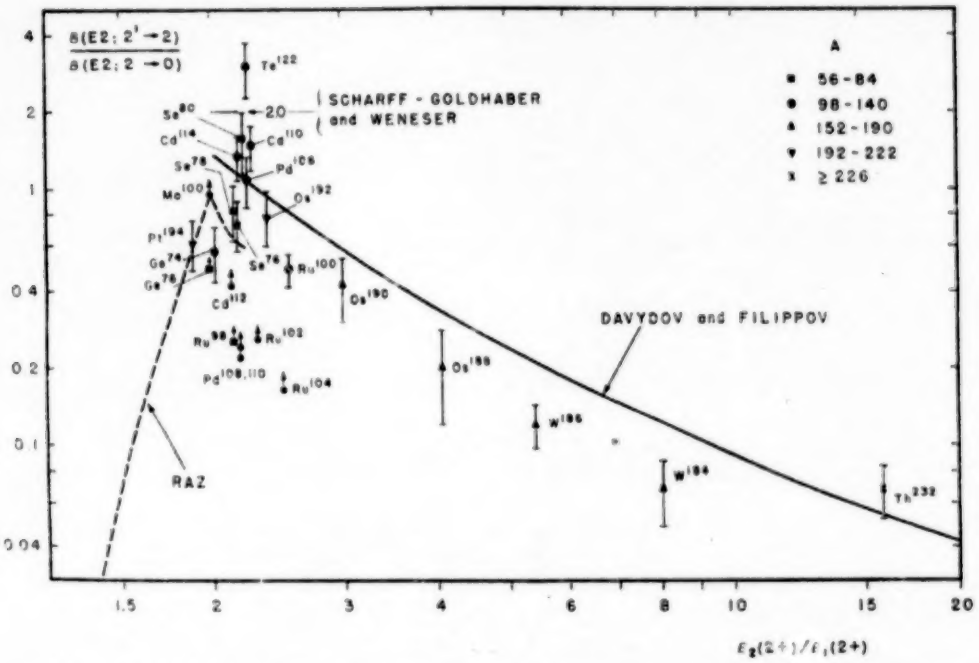

Fig. 4. Experimental data for $B(E2; 2' \rightarrow 2)/B(E2; 2 \rightarrow 0)$ for even nuclei compared to the theoretical predictions. This ratio of reduced E2 transition probabilities relates the E2 transitions from the second 2+ to first 2+ level, and the first 2+ level to ground.

them. Finally, the prediction of the DF theory is shown, which reaches a maximum value of 1.43 for $E_2/E_1 = 2$ ($\gamma = 30°$).

Several remarks can be made concerning the comparison of the experimental values of $B(E2; 2' \rightarrow 2)/B(E2; 2 \rightarrow 0)$ with the various theoretical predictions:

(1) The comparison with the DF prediction for nuclei in the transition region ($A = 184$—194) appears to be rather good, if it is remembered that systematic errors may well be present in the experimental data, so that the error bars should not be taken too seriously. The case of Th^{232} also seems to be in good agreement; however, there is at present some question concerning the multipolarity of the ($2' \rightarrow 2$) transition (see references for table 4).

(2) For medium-weight nuclei ($A = 74$—122) all the measured values for this $B(E2)$ ratio (except that of Te^{122}) fall below a value of 2.0, which definitely

disagrees with the prediction of two theories [3, 5]). Of the values which are not lower limits, the average of 8 determinations is 1.0 (omitting Te^{122}), which is nearly identical with the DF prediction of 1.1 (average value for these nuclei). However, in view of the rather large associated errors for these measurements, together with the fluctuation in the values, this close agreement appears to be somewhat fortuitous.

(3) It should be remembered that the three $B(E2)$ ratios shown in figs. 1, 3 and 4 are mutually dependent; therefore, if discrepancies between experimental values and the DF prediction appear in the comparison for one of these ratios, they should also appear in the comparison for at least one of the remaining two $B(E2)$ ratios. The comparison shown in fig. 1 (where the most experimental data are available) indicates quite clearly that definite departures from the DF prediction do exist, particularly for medium-weight nuclei with $E_2/E_1 < 3$. Similar departures would also be expected to appear in either or both figs. 3 and 4, if information were available for these nuclei. Such a departure may be present in fig. 4, where there may be a gradual increase in the ratio $B(E2; 2' \rightarrow 2)/B(E2; 2 \rightarrow 0)$ for A increasing from 74 to 122; corresponding to a similar possible trend in the values of $B(E2; 2' \rightarrow 2)/B(E2; 2' \rightarrow 0)$ shown in fig. 2 for this same range of A. Such a trend would account for the fact that Te^{122} has the highest value in fig. 4. Except for Se^{80} (for which the branching ratio is a preliminary value), the values for the $B(E2)$ ratio shown in fig. 4 may have a tendency to increase as A or N increases (see table 2, column 10). However, the present experimental information is not sufficient nor precise enough to verify this possible departure from the DF theory.

(4) It is interesting to note that for $E_2(2+)/E_1(2+) \approx 2-2.5$, the predictions of two weak-coupling [3, 25]) and two strong-coupling theories [5, 26]) for $B(E2; 2' \rightarrow 2)/B(E2; 2 \rightarrow 0)$ agree within a factor 4, and all lie within the range of fluctuation of the experimental values. This observation raises the possibility that for a prediction of a ratio of $B(E2)$ values in terms of a ratio of level energies, the theoretical results may be largely model-independent, with many of the nuclear model parameters disappearing when such ratios are considered. In any case, this observation might provide a clue concerning the question why the DF theory appears to be generally so successful in predicting these ratios of $B(E2)$ values.

3. Conclusions

The available experimental data for even nuclei with $A > 30$, from which ratios of reduced E2 transition probabilities can be calculated, have been compiled, and compared with the predictions of various theories [3, 5, 25, 26]). The recent asymmetric rotor theory of Davydov and Filippov [26, 29]) appears to be far the most successful in providing quantitative predictions, which appear to be in general agreement with the experimental results. Perhaps the most

striking success of their theory is the prediction for the ratio $B(\mathrm{E2}; 2' \to 0)/B(\mathrm{E2}; 2 \to 0)$, which relates the γ-ray transitions of the first two 2+ levels to ground, and for which their theory provides the only quantitative prediction. The comparisons made with the predictions of this theory indicate that it is applicable to a large class of nuclei, ranging from the "vibrational" to "rotational" regions, which cannot be said for most other theories.

Some of the experimental evidence is not accounted for by the DF theory. In particular, in its present form, it cannot account for the properties of even nuclei which have values of $E_2(2+)/E_1(2+) < 2$ (such as several nuclei with $N = 32$—40), and which appear to exhibit the same collective behaviour as nuclei whose ratios of reduced E2 transition probabilities are in good agreement with the predictions of this theory. In addition, there is a large scattering of the experimental values of the ratio $B(\mathrm{E2}; 2' \to 2)/B(\mathrm{E2}; 2' \to 0)$ of approximately a factor of 10—20 for a given value of E_2/E_1 for medium-weight nuclei, which is unexplained by this theory. Finally the DF theory predicts the energy ratio $E_1(4+)/E_1(2+)$ to be 3.33 for nuclei with $\gamma = 0°$, and to diminish to 2.67 for nuclei with $\gamma = 30°$. This energy ratio for the first 4+ level is approximately correct for nuclei in the "rotational" region, but is certainly not correct for medium-weight nuclei in the "vibrational" region, where values of $E_1(4+)/E_1(2+)$ of about 2 to 2.5 are generally observed.

Despite these objections, the apparent success of the Davydov-Filippov theory in providing quantitative predictions for a large amount of experimental data should encourage further theoretical and experimental investigations in this field.

The author is indebted to many physicists for communication and explanation of their unpublished or preliminary results, including Drs. R. Barloutaud, B. Harmatz, D. J. Horen, F. K. McGowan, M. Sakai, P. H. Stelson and R. van Lieshout. Stimulating discussions and helpful comments provided by Drs. R. D. Amado, C. A. Mallman, S. A. Moszkowski, B. J. Raz and G. T. Temmer have been a great encouragement. The advice of Mr. S. S. Malik and Dr. C. E. Mandeville concerning the measurements of the E2—M1 mixing of the $(2' \to 2)$ cascade transition was of considerable aid. The assistance and co-operation of Mrs. Helene M. Davis, Mrs. Marion Patterson, Miss Lillian Ries and Miss Barbara Smith in preparing the manuscript is acknowledged.

References

1) M. Goldhaber and A. Sunyar, Phys. Rev. **83** (1951) 906
2) G. Scharff-Goldhaber, Phys. Rev. **90** (1953) 587;
P. Stahelin and P. Preiswerk, Nuovo Cimento **10** (1953) 1219
3) G. Scharff-Goldhaber and J. Weneser, Phys. Rev. **98** (1955) 212L
4) M. Nagasaki and T. Tamura, Prog. in Theor. Phys. **12** (1954) 248L
5) L. Wilets and M. Jean, Phys. Rev. **102** (1956) 788

6) K. Way, D. N. Kundu, C. L. McGinnis and R. van Lieshout, Annual Rev. of Nucl. Sci. **6** (1956) 129
7) K. Alder, A. Bohr, T. Huus, B. Mottelson and A. Winther, Revs. Mod. Phys. **12** (1956) 432
8) G. Scharff-Goldhaber, Proc. of the University of Pittsburg Conference (June 6—8, 1957) p. 447
9) R. K. Sheline, Proc. of the University of Pittsburg Conference (June 6—8, 1957) p. 479
10) C. A. Mallman, A/Conf. 15/P/1971, 13 : 7004
11) W. Scheuer and E. Aisenberg, A/Conf. 15/P/2513 ; 13 : 7029
12) M. Sakai, Institute for Nuclear Study, Report no. 6, University of Tokyo (Feb. 24, 1958)
13) C. A. Mallman, Phys. Rev. Letters **2** (1959) 507
14) J. J. Kraushaar and M. Goldhaber, Phys. Rev. **89** (1953) 1081
15) T. Lindqvist and I. Marklund, Nuclear Physics **4** (1957) 189
16) S. S. Malik, V. R. Potnis and C. E. Mandeville, Nuclear Physics **11** (1959) 691
17) N. N. Deliagin and V. S. Shipnel, Zh. Eksp. Teor. Fiz. **32** (1957) 373L; Soviet Physics JETP **5** (1957) 309L
18) A. W. Sunyar, Phys. Rev. **98** (1955) 653
19) C. F. Coleman, Nuclear Physics **7** (1958) 488
20) P. H. Stelson and F. K. McGowan, Phys. Rev. **110** (1958) 489
21) D. M. Van Patter, preliminary report given in Journ. Franklin Inst. **266** (1958) 411; Bull. Am. Phys. Soc. **3** (1958) 360
22) A. Bohr, Mat. Fys. Medd. Dan. Vid. Selsk. **26**, No. 14 (1952)
23) A. Bohr and B. Mottelson Mat. Fys. Medd. Dan. Vid. Selsk. **27**, no. 16 (1953)
24) G. Alaga, K. Alder, A. Bohr and B. R. Mottelson, Mat. Fys. Medd. Dan. Vid. Selsk. **29**, no. 9 (1955)
25) B. J. Raz, Phys. Rev. **114 (1959) 1116**; Bull. Am. Phys. Soc. **3** (1958) 224
26) A. Davydov and G. Filippov, Zh. Eksp. Teor. Fiz. **35** (1958) 440; **35** (1958) 703; Nuclear Physics **8** (1958) 237
27) M. Gursky, Phys. Rev. **98** (1955) 1205A; results quoted by ref. [5])
28) C. Marty, Nuclear Physics **1** (1956) 85; **3** (1957) 193
29) A. Davydov and G. Filippov, Nuclear Physics **10** (1959) 654
30) D. A. Daikin, Zh. Eksp. Teor. Fiz. **35** (1958) 529; Soviet Physics JETP **8** (1959) 365
31) B. T. Geilikman, Zh. Eksp. Teor. Fiz. **35** (1958) 989; Soviet Physics JETP **8** (1959) 690
32) McGowan and Stelson, and Barloutaud *et al.*, refs. in tables 2 and 3
33) D. M. Van Patter, Bull. Am. Phys. Soc. **4** (1959) 233
34) C. L. McGinnis, G. Andersson, G. H. Fuller, J. B. Marion, K. Way, and M. Yamada, Nuclear Data Sheets (National Research Council, Washington, D. C.)
35) B. S. Dzhelepow and L. K. Peker, Decay Schemes of Radioactive Nuclei (Academy of Sciences of the USSR Press, Moscow, 1958)
36) D. Strominger, J. M. Hollander, and G. T. Seaborg, Revs. Mod. Phys. **30** (1958) 585
37) D. M. Van Patter, Bull. Am. Phys. Soc. **3** (1958) 212
38) R. Barloutaud, Ph. D. thesis, University of Paris (1958)
39) A. Bohr and B. Mottelson, Nuclear Physics **12** (1959) 389

TABLE 4

Accumulated data for the branching of the second 2+ level and the E2/M1 mixing of the ($2' \to 2$) cascade transition for even nuclei, $A > 30$.

Nucl.	$E_1(2+)$ (keV)	$E_2(2+)$ (keV)	$E_\gamma(2' \to 2)$ (keV)	$r = \frac{\text{Crossover}}{\text{Cascade}}$	Ref. r	δ	% E2	Ref. δ
S^{34}	2128	3302	1174	0.47 ± 0.07	Ha56	+0.13± 0.02	1.7± 0.6	Ha 56
	8	8	8	0.37 ± 0.06	St 56			
				0.42 ± 0.05				
Fe^{56}	845	2657	1812	0.010± 0.007	Gr 57	+0.15± 0.08	2.2± 2.2	Me 53
	3	5	4	0.07	Le 58	+0.16± 0.04	2.5±1.3	Le 58
				0.024± 0.003	Co 58	+0.06	0.4	St 59
				0.024± 0.003		+0.06− 0.16	0.4−2.5	
Fe^{58}	806	1663	857	0.31 ± 0.11	Fr 56	+2.3 ± 0.5	84 ±6	Fr 56
	4	5	5					
Ni^{60}	1332.5	2159	826	0.38 ± 0.11	Nu 54	$\geqq +3$	$\geqq 90$	Le 58
	0.3	3	3	0.29 ± 0.13	Da 56			
				0.067	Le 58			
				0.067 [a])				
Ni^{62}	1172	2048	876	<0.33	Bu 58			
	3	3	4					
Zn^{64}	990	1799	809	0.34	Ja 58a			
	4	5	6					
Zn^{66}	1039	1871	832	<0.04	Ho 58			
	3	8	8					
Zn^{68}	1081	1895	814	≈1.4	Ho 59			
	5	9	10					
Ge^{72}	834.5	1465	630.2	0.19 ± (0.03)	Jo 55	$\lvert\delta\rvert \gtrsim 4.4$	$\gtrsim 95$	Co 58a
	<1.0	<1	<1.0	0.13 ± (0.03)	Kr 56	$\lvert\delta\rvert \geqq 3.0$	$\geqq 90$	Ar 58
				0.17 ± 0.03			$\geqq 95$	
Ge^{74}	596	1200	604	≈4.2	Ho 59a			
	1	6	6	2.7 ±1.4	Mc 59			
				3.0 ±(1)				
Se^{76}	560.5	1220	659	1.05	Ku 55	−6.4 ± 2.4	93^{+4}_{-10}	Li 57
	0.3	3	3	0.89 ±(0.09)	Dz 56	−3.7 ± 1.9	$97.6^{+1.0}_{-4.9}$	Co 58a
				0.95	Gr 57a			
				0.62	Gu 58			
				0.8 ± 0.2 [b])		−5.5 ± 1.6	97 ± 2	
Se^{78}	613	1308	695	0.79 ±(0.1)	Sc 57			
	4	8	7					
Se^{80}	660	1450	790	1.0 ± 0.3	Ma 59a			
	5	10	8					
Kr^{82}	776.9	1475.3	698.4	0.49 ± 0.10	Wa 56		E2+M1 †	Wa 56
	0.2	0.4	0.3	0.64 ±(0.06)	Hu 57			
				0.59 ±(0.06)	Be 58			
				0.60 ± 0.03				
Kr^{84}	882	1890	1010	1.71 ± 0.25	Jo 57		99.9	Jo 57
	4	20	20	1.7	Jo 57			
				1.7 ± 0.2				
Sr^{88}	1832	3210	1380	0.23 ± 0.06	La 56			
	6	30	30					

Table 4

(Continued)

Nucl.	$E_1(2+)$ (keV)	$E_2(2+)$ (keV)	$E_\gamma(2'\to2)$ (keV)	$r = \frac{\text{Crossover}}{\text{Cascade}}$	Ref. r	δ	% E2	Ref. δ
Zr^{92}	934	1830 c)	900	1.7	Ha 55	$\lvert\delta\rvert < 0.11$	<1.2	Co 58a
	1	10	10	0.47	We 59		<0.2	We 59
				1.1 ± 0.6			<0.2	
Ru^{98}	654	1402	748	No 1.4 γ	Ka 58a			
	5	10	8					
Ru^{100}	535.3	1358	823	1.05 ± (0.15) e)	Ma 53			
	<1.0	<1	<1					
Ru^{102}	474	1104	630	≈0.8 d)	Hi 58			
	1	4	3	<0.1 d)	Go 57			
Pd^{104}	556.2	1340	780	0.10	Bu 55			
	<1.0							
Pd^{106}	513.0	1131	618	0.50 ± (0.1)	Al 55			
	0.5	5	5	0.44 ± 0.06	Ro 59			
				0.49 ± 0.14	Ro 59			
Cd^{110}	656.3	1473	817.4	0.67 ± 0.13	Dz 58			
	0.3	≈1	≈1.0					
Cd^{114}	556	1208	654	0.29	Ad 55		E2+M1 f)	Mo 56
	1	4	2	0.28	Mo 56			
				0.28 ± (0.06)				
Sn^{116}	1272	2090	818	1.1 ± 0.2	Gi 59	+3.5 ± 1.5	92^{+3}_{-12}	Sc 56
	5	10	10					
Te^{122}	563.9	1257	693	0.21 ± 0.05	Gl 55	+3.2 ± (1.0)	91.2 ± 2.5	Gl 55
	0.2	5	5	0.19 ± 0.04	Fa 55	+3.2 ± 0.5	91.2 ± 4.8	Li 57
				0.20 ± 0.03		+4.0 ± (0.7)	94.1 ± 1.9	Co 58a
						+3.5 ± 0.3	92.4 ± 1.4	
Te^{124}	603	1326	723	0.2	Zo 56	±1.00 ± 0.08	50 ± 10	Li 57
	1	2	1	0.14	Dz 58		M1 f)	Dz 58
				0.19 ± 0.03	Gi 59a			
				0.17 ± 0.03				
Te^{126}	662	1415	753	0.095 ± 0.02	Pe 54	+6.4 ± 0.9	97.6 ± 1.7	Sa 58
	3	15	15	<0.14	Ko 55			
				0.07 ± 0.01	Gi 59b			
				0.07 ± 0.01				
Xe^{126}	385	865	480	0.19 ± 0.04	Pe 54	$\lvert\delta\rvert > 10$	>99	Sa 58
	1	10	8	0.17 ± 0.02	Ko 55			
				0.17 ± 0.02				
Xe^{128}	451	986	535	0.16 ± 0.02	Be 56			
	2	3	2	0.19	Bo 58			
				0.17 ± 0.02				
Xe^{136}	1307	2620	1310	0.50 ± 0.18	Jo 59			
	6	(20)	(10)					
Ba^{134}	604.7	1167.4	562.8	0.27	Ve 54		E2 f)	Ke 55
	0.2	1.5	1.5	0.17 ± 0.06	Ba 54			
				0.22	Fo 55			
				0.33 ± 0.09	Ke 55			
				0.25 ± 0.04				

TABLE 4

(Continued)

Nucl.	$E_1(2+)$ (keV)	$E_2(2+)$ (keV)	$E_\gamma(2'\to2)$ (keV)	$r = \frac{\text{Crossover}}{\text{Cascade}}$	Ref. r	δ	% E2	Ref. δ
Ce^{140}	604.7	1167.4	562.8	≈ 0.36	Ba 54a		0.1 — 1.0	Co 55
	0.2	1.5	1.5	0.36 ± 0.16	Co 55			
				0.52	Dz 56a			
				0.39 ± (0.05)	Pr 58			
				0.40 ± 0.05				
Ce^{142}	643	1530	880	0.33	Sc 59			
	6	10	10					
Sm^{152}	121.85	1086.6	964.8	0.93	Gr 56	$\lvert\delta\rvert > 9$	> 98.8	Of 57
	0.03	1.0	1.0	0.84	Na 57	+7.68	98.3 ± 1.1	Li 59
				0.85 ± 0.03*	Bo 57		98.3 ± 1.1	
				0.82 ± 0.13	Dz 58			
				0.79 ± 0.14	Na 59			
				0.84 ± 0.03				
Gd^{154}	123.1	966.6	873.7	$\geqq 0.91$*	Bo 57			
	0.1	1.0	1.0					
Gd^{156}	88.97	1140	1050	0.8 ± 0.4	He 59			
	0.03	10	10					
Dy^{160}	86.6	965.7	879.1	0.60 ± 0.07*	Gr 58	> 60	> 99.9	Of 57a
	0.2	1.0	1.0	0.86 ± 0.20*	Gr 58		96.5 ± 3.5	Ar 59
				0.87 ± 0.09*	Ew59		96.5 ± 3.5	
				0.68 ± 0.10	Na 57a			
				0.90 ± 0.10	Of 57a			
				0.71 ± (0.15)[e]	Cl 57			
				0.90 ± 0.22[e]	Av 58			
				0.73 ± 0.06	Ar 59			
				0.77 ± 0.04				
Er^{166}	80.57	787.4	706.8	1.0*	Gr 57b			
	0.02	1.2	1.0	0.86 ± 0.13	Ja 58			
				0.86 ± 0.13				
Er^{168}	79,80	822.0	742.2	0.92 ± 0.15	Ja 58			
	0.02	1.2	1.1					
W^{182}	100.09	1221.8	1121.6	0.95*	Fo 54	−3	≈ 90 [f]	Wi 56
	0.01	0.2	0.2	0.71 ± 0.21*	Ga 59			
				0.95 ± 0.14	Mu 55			
				0.90	Su 57			
				0.75	Fr 57			
				0.85 ± 0.06[f]				
W^{184}	111.13	904	793	1.13 ± 0.32	Ga 58		E2+M1 [f]	Ga 58
	0.06	1	1	1.0 ± 0.25	Mc 58			
				1.07 ± 0.2				
W^{186}	122.48	733	611	≈ 1.4	Po 55			
	0.08	5	5	1.0 ± 0.1	Ba 58			
				1.0 ± 0.1	Mc 58			
				1.0 ± 0.1				

TABLE 4

(Continued)

Nucl.	$E_1(2+)$ (keV)	$E_2(2+)$ (keV)	$E_\gamma(2'\to2)$ (keV)	$r = \frac{\text{Crossover}}{\text{Cascade}}$	Ref. r	δ	% E2	Ref. δ
Os^{186}	137.19	768.2	630.8	0.51 ± 0.04	Po 56b	+10 ±2	99 1	Li 57
	0.09	1.0	8	1.00 ± 0.22	Jo 56	±10	99 ± 1	Ki 59
				1.00 ± 0.22[g]		−10	99	Ja 58b
							99 ± 1	
Os^{188}	155.0	633.0	478.2	1.59 ± 0.18	Jo 56	+15.7± 7.0	99.6±0.4	Po 56
	0.1	0.1	0.2	1.33	Po 56		99.7	Ki 59
				1.49	Po 56a		99.6± 0.4	
				1.5	Ni 58			
				1.5 ± 0.1				
Os^{190}	187.0	557	370	1.0	At 55		98	Ca 58
	<1.0	(2)	(2)	1.7	At 55			
				≈0.6	Ba 58			
				0.77	Mc 58			
				1.5 ±0.4	Ni 59			
				1.1 ±0.2[h]				
Os^{192}	205.74	489.0	283.35	1.25	Ba 58		(E2) †	Ba 55
	0.04	0.2	0.20	1.5	Mc 58			
				1.37 ± 0.2				
Pt^{192}	316.46	612.4	295.94	0.14	Ba 52		>95 †	Ba 55
	0.09	0.1	0.09	0.29	Jo 54		97.5	Ta 55
				0.23 ± 0.07	Ba 55		≧91	Ke 57
				0.25	Su 57a	−6.5 ± 1.5	97.7± 1.0	Mr 57
				0.23 ± 0.04			97.6± 1.0	
Pt^{194}	329.1	622	293.0	0.33	Jo 54	+29 ± 26	≈99.9	Ma 55
	0.1	1	0.3	0.25	Al 57			
				0.29 ± 0.04				
Pt^{196}	354.2	685.5	331.3	<4 ×10⁻⁴	Al 57		95 ± 1	St 53
	0.3	0.4	0.3				95.5± 0.8	St 56a
						+5.4 ± 0.5	96.7± 0.6	Po 56c
							95.8± 0.5	
Hg^{198}	411.77	1087.5	675.7	0.23 ± 0.07	Ca 51		68 ± 6 †	El 54
	0.04	0.3	0.3	0.20 ± 0.02	El 54		64 ±23 †	Vo 56
				0.16 ± 0.02	Vo 56		60 ±10	Sc 53
				0.19 ± 0.015		−0.96± 0.22	48 ±11	Sc 53a
							60 ± 6	
Hg^{200}	368.0	947.4	579.4	<0.05 [i]	He 57		E2+(M1) †	He 57
	0.2	0.4	0.3					
		≈950	580	≈1 [i]	Se 58			
			20					
Hg^{202}	439.7	963	523	0.13 ± 0.03	Bo 59			
	0.7	2	2					
Po^{212}	727.2	1512.6	785.4	1.6*	Se 57			
	0.5	0.5	0.5					
Po^{214}	609.4	1281.3	(672)	≲1	Dz 56b			
	0.2							

TABLE 4

(Continued)

Nucl.	$E_1(2+)$ (keV)	$E_2(2+)$ (keV)	$E_\gamma(2'\to 2)$ (keV)	$r = \frac{\text{Crossover}}{\text{Cascade}}$	Ref. r	δ	% E2	Ref. δ
Rn^{222}	187	447	260	<0.05	Ha 56a			
	1	5	5					
Th^{228}	57.5	965	908	0.57*	Ky 53			
	0.1	1	1	1.1*	Ho 57			
				0.45	Bj 57			
				0.52 ± (0.1)				
Th^{232}	52.8	790	740	0.65 ± (0.1)	Mc 57		(E2)	Mc 58a
		(10)	(10)				M1 or E2+E0 †	Re 59
Pu^{238}	44.03	1031	987	0.83 ± (0.13)[d]	Ra 55		E2+(M1) †	Ra 55
		1	1					

$E_1(2+)$ and $E_2(2+)$ are the present best values with associated errors for the energies of the first two 2+ levels. $E_\gamma(2'\to 2)$ is the present best value for the energy of the cascade γ-ray transition between these levels. Each best value was obtained from a weighted average of available results. Although no references have been specifically listed for these energy determinations, some of the references given in columns 6 and 9 will contain such measurements. r is the γ-ray branching for the second 2+ level, equal to the ratio of the intensities of the cross over to cascade γ-rays. δ is the ratio of the matrix elements for E2 and M1; δ^2 is the mixing ratio of E2 to M1.

* This branching ratio was calculated from the observed intensities of conversion electrons. If the E2 to M1 mixing ratio for the $(2'\to 2)$ cascade transition is not known, then 100 % E2 is assumed. (Exception: W^{182} where 100 % E2 was assumed [f]).

† This estimate of the multipolarity of the $(2'\to 2)$ cascade transition was made from a knowledge of the K conversion coefficient, or the K/L ratio, rather than from a $\gamma-\gamma$ angular correlation measurement.

[a]) The branching ratio for Ni^{60} given by (Nu 54) is the ratio of the intensities of the 2.16 and 0.83 MeV γ-rays seen in the Cu^{60} decay. However, (Le 58) have assigned $\approx$ 80 % of the intensity of the 2.16 MeV γ-ray to a 3.39−1.33 MeV transition, from $\gamma-\gamma$ coincidence data. A branching ratio of 0.29 can be calculated from the results of an investigation of the $Ni^{(60)}(n, n'\gamma)$ reaction (Da 56) made at $E_n = 2.56$ MeV, in which the 3.39 MeV level could not be excited. However, more recent work on this reaction (Na 59a) indicates that the observation of a weak γ-ray in the background of the NaI detector, which can produce a spurious peak at 2.16 MeV if gain shifts are present. Therefore we have chosen the result of (Le 58) as being the most reliable to date.

[b]) The observed intensities of the 1.22 and 0.66 MeV γ-rays in the As^{76} decay give an average ratio of 0.96. Recently all the available results have been analyzed by Gustova and Chubinskii (Gu 58). They find that the intensities of β-rays computed from γ-ray intensities and experimental β intensities are brought into satisfactory agreement if $\approx$ 30 % of the 1.22 MeV γ-rays are attributed to 1.76−0.56 and 2.42−1.21 MeV cascades. Although it seems rather definite that levels at 1.76 and 2.42 MeV are present in Se^{76}, the branching of 0.62 (Gu 58) comes from balancing β and γ intensities, rather than from $\gamma-\gamma$ coincidence data. Until further data are available, we have chosen an intermediate value of $r = 0.8\pm 0.2$, with an error which includes all possibilities.

Note added in proof: The composite 1.22 MeV γ-ray has now been resolved by I. Marklund and G. Backstrom (Ma 59b) who find the second 2+ level in Se^{76} at 1216.6 keV, with a branching ratio of 0.69.

[c]) It is not certain that the 1.83 MeV level is the second 2+ level of Zr^{92}, since there exist levels at 1.38 and 1.48 MeV wnose spins are not yet established.

[d]) A branching of $0.1/13 = 0.008$ can be calculated from the γ-ray intensities listed in the Nuclear Data Sheets in the Rh^{102} decay (Hi 58). This ratio appears to be incorrect in view of Coulomb excitation data (table 2) if the same level is involved. This result has now been corrected by J. D. Kurbatov (Hi 58). However, a re-examination of preliminary data for this decay has provided an estimate of $r < 0.1$ (Go 57). Therefore, the value for the branching of Ru^{102} is considered to be uncertain until further measurements are made.

[e]) Correction has been made for the contribution of the 962 keV γ-ray to the 962+966 keV group in the Tb^{160} decay. The ratio of the e_K intensities for the 966, 962 keV γ-rays is taken as 0.40 from an average of three measurements (Gr 58, Av 59, Ew 59), and it is assumed that both γ-rays have approximately the same conversion coefficient.

[f]) The branching ratios determined from the ratio of the K conversion electrons (Fo 54, Ga 59) depend slightly on the assumption of the percentage of E2 for the 1122 keV cascade γ-ray of W^{182}. As listed, these branching ratios have been calculated assuming 100 % E2. For 90 % E2, the average branching ratio becomes 0.87 ± 0.06 instead of 0.85 ± 0.06.

[g]) The two determinations of the branching for Os^{186} differ by a factor two. There is insufficient information to be able to resolve this discrepancy. We have chosen to omit the result of (Po 56b) in the average branching listed.

[h]) There exists a discrepancy of about a factor two between the branching obtained for the 557 keV level in Os^{190} from radioactivity (At 55, Ni 59) and from Coulomb excitation (Ba 58, Mc 58). The average value for the branching is calculated with all determinations given equal weight.

[i]) A level at 0.947 MeV is seen in Hg^{200} which shows no cross-over γ-ray in the Tl^{200} decay (He 57). On the other hand, a recent study of the $Hg^{(199)}$ (n, $\gamma\gamma$) $Hg^{(200)}$ reaction using $\gamma-\gamma$ coincidences indicates a level at about 0.95 MeV, for which the cascade and cross-over intensities are roughly comparable (Se 58). It is possible that the Tl^{200} decay excites a 4+ level, while a nearby 2+ level is excited in the $Hg^{(199)}$ (n, $\gamma\gamma$) reaction.

[j]) The two most recent level schemes given for Pu^{238} differ considerably (Dz 58a, St 58). The branching for the 1031 keV level depends on the choice of the level scheme. We have chosen the level scheme of St 58; if the alternative scheme were chosen, the value of cross-overs/cascades would have to be increased.

Added Remark: Data for some nuclei are omitted from table 4 for some nuclei which have a second level (or higher level) with a spin of (2+) for two reasons:

(a) The level scheme appears to be too uncertain (Ca^{44}, Yb^{172}, Th^{230})

(b) The level in question may have a spin > 2 (such as 4+) which would account for the failure to observe a cross-over transition to ground (Mo^{94}, Xe^{130}, Gd^{152}, Rn^{218}, Rn^{220})

REFERENCES FOR TABLE 4

(Closed July 1, 1959)

(References are arranged and designated by the first two letters of the author's name, and year. Otherwise duplicate designations are distinguished by a postscript letter).

Ad 55 B. P. Adyasevich, B. D. Groshev and A. M. Demidov, Conf. Acad. Sci. USSR on Peaceful Use of Atomic Energy, Phys. Math. Sci. (1955) 270

Al 55 D. E. Alburger and B. J. Toppel, Phys. Rev. **100** (1955) 1357

Al 57 D. E. Alburger, Phys. Rev. **108** (1957) 812

Ar 58 R. G. Arns and M. L. Wiedenbeck, Phys. Rev. **112** (1958) 229

Ar 59 R. G. Arns, S. E. Sund and M. L. Wiedenbeck, Nuclear Physics **11** (1959) 411

At 55 A. H. W. Aten Jr., G. D. De Feyfer, M. J. Sterk and A. H. Wapstra, Physica **21** (1955) 740; the values of 1.0, 1.7 listed are obtained from the γ intensities observed in the Re^{190} 2.8m and Ir^{190} 11d activities.

Av 58 M. P. Avotina, E. P. Grigor'ev, A. V. Zolotavin, and B. Kratsik, Dokl. Akad. Nauk **119** (1958) 1127; Soviet Physics "Doklady" **3** (1958) 368

Ba 52 A. A. Bashilov, N. M. Anton'eva and B. S. Dzhelepow, Izvest. Akad. Nauk SSSR Ser. Fiz. **16** (1952) 262

Ba 54 A. A. Bashilov, N. M. Anton'eva, M. V. Blinov and B. S. Dzhelepow, Izvest. Akad. Nauk. SSSR Ser. Fiz. **18** (1954) 43

Ba 54a A. A. Bashilov, B. S. Džhelepow and L. S. Chervinskaya, Izvest. Akad. Nauk SSSR Ser. Fiz. **18** (1954) 88

Ba 55 L. L. Baggerly, P. Marmier, F. Boehm and J. M. M. DuMond, Phys. Rev. **100** (1955) 1364

Ba 57 R. Barloutaud, P. Lehmann and A. Lévêque, Comptes Rendus **245** (1957) 523; see also Ba 58

Ba 58 R. Barloutaud, Ph. D. Thesis, University of Paris (1958); and private communication

Be 56 N. Benczer, B. Farrelly, L. Koerts and C. S. Wu, Phys. Rev. **101** (1956) 1027

Be 58 N. Benczer-Koller, CU-177 (1958)

Bj 57 O. Bjørnholm, O. Nathan, O. B. Nielsen and R. K. Sheline, Nuclear Physics **4** (1957) **313**

Bo 57 B. V. Bobykin and K. M. Novik, Izvest. Akad. Nauk SSSR Ser. Fiz. **21** (1957) 1556

Bo 58 H. Bosch, R. Radicella, P. Reyes and T. Urstein, Phys. Rev. **111** (1958) 898

Bo 59 P. Born, J. Molenaur and J. Blok, Physica **25** (1959) 326

Bu 55 M. E. Bunker, J. P. Mize and J. W. Starner, Phys. Rev. **99** (1955) 659A; oral report. This preliminary report is the only source of information for the branching of the 1.34 MeV level, which has been given a tentative spin assignment of (2+) by Dz 58a.

Bu 58 J. W. Butler and C. R. Gossett, Phys. Rev. **112** (1958) 1257

Ca 51 P. Cavanagh, J. Turner, D. Booker and H. Dunster, Proc. Phys. Soc. A **64** (1951) 13

Ca 58 F. Cappellani, U. Farinelli, F. Ferrero and R. Malvano, Physica **24** (1958) 765

Cl 57 M. A. Clark and J. W. Knowles, Bull. Am. Phys. Soc. **2** (1957) 231; revised value given by Ew 59

Co 55 C. F. Coleman, Phil. Mag. **46** (1955) 1132

Co 58 C. S. Cook, Nuclear Physics **7** (1958) 480

Co 58a C. F. Coleman, Nuclear Physics **7** (1958) 488; δ for Se^{76} and Zr^{92} recalculated by Ma 59

Da 56 R. B. Day, Phys. Rev. **102** (1956) 767

Dz 56 B. S. Džhelepow, V. P. Prikhodtseva, A. J. Feoktistov and Iu. V. Khol'nov, Izvest. Akad. Nauk SSSR Ser. Fiz. **20** (1956) 1361

Dz 56a B. S. Džhelepow and Iu. V. Khol'nov, Nuovo Cimento **3**, Suppl. 1 (1956) 49

Dz 56b B. S. Džhelepow and S. A. Sestopalova, Nuovo Cimento **3**, Suppl. 1 (1956) 54. We have estimated a lower limit for the possible cascade 672 keV γ-ray from an examination of the Bi^{214} γ-ray spectrum. The level scheme chosen does not agree with that given by St 58.

Dz 58 B. S. Džhelepow and N. N. Zhukovskii. Nuclear Physics **6** (1958) 655; see Fu 58 for latest level scheme of Cd^{110}

Dz 58a B. S. Džehelpow and L. K. Peker, Decay Schemes of Radioactive Nuclei, Academy of Sciences of the USSR Press, Moscow (1958)

El 54 L. Elliot, M. Preston, and J. Wolfson, Can. J. Phys. **32** (1954) 153

Ew 59 G. T. Ewan, R. L. Graham and J. S. Geiger, Bull. Am. Phys. Soc. **4** (1959) 292; and private communication from G. T. Ewan

Fa 55 B. Farrelly, L. Koerts, N. Benczer, R. van Lieshout and C. S. Wu, Phys. Rev. **99** (1955) 1440

Fo 54 C. M. Fowler, H. W. Kruse, V. Keshishian, R. J. Klotz and G. P. Mellor, Phys. Rev. **94** (1954) 1082L

Fo 55 H. H. Forster and J. S. Wiggins, Nuovo Cimento **2** (1955) 854

Fr 56 H. Frauenfelder, N. Levine, A. Rossi and S. Singer, Phys. Rev. **103** (1956) 352; δ recalculated by Ma 59

Fr 57 P. O. Froman and H. Ryde, Arkiv Fysik **12** (1957) 399

Fu 58 E. G. Funk Jr. and M. L. Wiedenbeck, Phys. Rev. **112** (1958) 1247

Ga 58 C. J. Gallagher, Jr., D. Strominger and J. P. Unik, Phys. Rev. **110** (1958) 725

Ga 59 C. J. Gallagher, Jr., J. O. Newton and V. S. Shirley, Phys. Rev. **113** (1959) 1298

Gi 59 R. K. Girgis and R. van Lieshout, Physica **25** (1959) 590

Gi 59a R. K. Girgis and R. van Lieshout, Physica **25** (1959) 133; the value given comes from an analysis of available results for the γ-ray intensities from the Sb^{124} decay.

Gi 59b R. K. Girgis and R. van Lieshout (to be published); quoted in Gi 59a

Gl 55 M. J. Glaubman, Phys. Rev. **98** (1955) 645

Go 57 N. Goldberg, Bull. Am. Phys. Soc. **2** (1957) 230; and private communication of preliminary value

Gr 56 L. Grodzins and H. Kendall, Bull. Am. Phys. Soc. **1** (1956) 163; verbal report

Gr 57 V. Groshev, A. M. Demidov, V. N. Lutsenko and V. I. Pelekhov, Atomnaya Energiya **3** (1957) 187; Soviet Journ. of Atomic Energy **3** (1957) 970; and private communication from V. Groshev

Gr 57a E. P. Grigor'ev, L. V. Gustova, A. V. Zolotavin, B. Kratsik, T. B. Poleshchuk and O. V. Chubinski, Leningrad State University, Phys. and Chem. Series **10** (1957) 37

Gr 57b K. Ia. Gromov, B. S. Dzhelepow and B. K. Preobrazhenskii, Izvest. Akad. Nauk SSSR Ser. Fiz. **21** (1957) 918; quoted by Dz 58a

Gr 58 E. P. Grigor'ev, B. S. Dzhelepow, A. V. Zolotavin, O. E. Kraft, B. Kratsik and L. K. Peker, Izvest. Akad. Nauk SSSR Ser. Fiz. **22** (1958) 101; the branching ratios of 0.60 and 0.86 result from measurements for the Tb^{160} and Ho^{160} decays

Gu 58 L. V. Gustova and O. V. Chubinskii, Zh. Eksp. Teor. Fiz. **35** (1958) 957; Soviet Physics JETP **8** (1959) 1369

Ha 55 R. W. Hayward, D. D. Hoppes and H. Ernst, Phys. Rev. **98** (1955) 231A; verbal report

Ha 56 H. E. Handler and J. R. Richardson, Phys. Rev. **102** (1956) 833

Ha 56a G. Harbottle, M. McKeown and G. Scharff-Goldhaber, Phys. Rev. **103** (1956) 1776. The α branching observed for the Ra^{226} decay is consistent with either a 2+ or 4+ assignment for the 447 keV state in Rn^{222}. If the level has spin 4+, then no crossover γ-ray would be expected, however St 58 assign the spin as (2+)

He 57 C. J. Herrlander and T. R. Gerholm, Nuclear Physics **3** (1957) 161

He 59 R. W. Henry, L. T. Dillman, N. B. Gove and R. A. Becker, Phys. Rev. **113** (1959)1090

Hi 58 H. Hisatake and J. D. Kurbatov, Bull. Am. Phys. Soc. **3** (1958) 315; and private communication from J. D. Kurbatov.

Ho 56 O. P. Hok and E. Arbman, Arkiv Fysik **11** (1956) 193. This value for the branching has been omitted from the average because the contribution of the 960 keV γ-ray from the Pa^{228} decay has not been subtracted

Ho 58 D. J. Horen and W. E. Meyerhof, Phys. Rev. **111** (1958) 559

Ho 59 D. J. Horen, Phys. Rev. **113** (1959) 572

Ho 59a D. J. Horen, W. E. Meyerhof, J. J. Kraushaar, D. O. Wells, E. Brun and J. E. Neighbor, Phys. Rev. **113** (1959) 875

Hu 57 S. Hultberg and A. Hedgran, Arkiv Fysik **11** (1957) 369

Ja 58 K. P. Jacob, J. W. Mihelich, B. Harmatz, and T. H. Handley, Bull. Am. Phys. Soc. **3** (1958) 358. The branching ratio listed have been calculated from the $B(E2; 2' \rightarrow 2)/B(E2; 2' \rightarrow 0)$ ratio given by B. Harmatz (private communication)

Ja 58a T. Jacobi, as quoted by Ho 59, and private communication from R. Richardson

Ja 58b P. S. Jastram (1958), private communication to Ki 59

Jo 54 M. W. Johns and S. V. Nablo, Phys. Rev. **96** (1954) 1599

Jo 55 M. W. Johns, B. Chidley and I. R. Williams, Phys. Rev. **99** (1955) 1645A; revised intensities given by Kr 56

Jo 56 M. W. Johns, C. C. McMullen, I. R. Williams and S. V. Nablo, Can. J. Phys. **34** (1956) 69; error for branching ratio given in Ki 59

Jo 57 N. R. Johnson and G. D. O'Kelley, Phys. Rev. **108** (1957) 82. The two branching ratios listed are obtained from γ-ray intensities in the Br^{84} and Rb^{84} decays. From their $\gamma\gamma(\theta)$ measurement, they find the 1.01 MeV γ-ray is 99.9 % E2, provided that the 1.89 MeV level has spin 2+

Jo 59 N. R. Johnson and G. D. O'Kelley, Phys. Rev. **114** (1959) 279

Ka 58 M. Kawamura, A. Aoki and T. Hayashi, J. Phys. Soc. Japan **13** (1958) 1071

Ka 58a S. Katcoff, Phys. Rev. **99** (1958) 1618. No crossover is seen from a level at $1.41 \pm (0.02)$ MeV excited in the Tc^{98} decay. This level may have spin 4+, occurring at nearly the same energy as the 2+ level at 1.402 ± 0.010 MeV seen by Coulomb excitation (see table 2)

Ke 55 G. L. Keister, E. B. Lee and F. H. Schmidt, Phys. Rev. **97** (1955) 451

Ke 57 V. M. Kelman, R. Ya. Metskhvarishvili, V. A. Romanov and V. V. Tuchkevich, Nuclear Physics **4** (1957) 240

Ki 59 W. J. King and M. W. Johns, Can. J. Phys. **37** (1959) 755

Ko 55 L. Koerts, P. Macklin, B. Farrelly, R. van Lieshout and C. S. Wu, Phys. Rev. **98** (1955) 1230

Kr 56 J. J. Kraushaar, E. Brun and W. E. Meyerhof, Phys. Rev. **101** (1956) 139

Ku 55 J. D. Kurbatov, B. B. Murray and M. Sakai, Phys. Rev. **98** (1955) 674
Ky 53 J. Kyles, C. Campbell and W. Henderson, Proc. Phys. Soc. A **66** (1953) 519
La 56 N. H. Lazar, E. Eichler and G. D. O'Kelley, Phys. Rev. **101** (1956) 727
Le 58 N. Levine, H. Frauenfelder and A. Rossi, Zeits. Physik **151** (1958) 241
Li 57 T. Lindqvist and I. Marklund, Nuclear Physics **4** (1957) 189
Li 59 R. W. Lide and M. L. Wiedenbeck, Phys. Rev. **113** (1959) 840
Ma 53 L. Marquez, Phys. Rev. **92** (1953) 1511
Ma 55 C. E. Mandeville, J. Varma and B. Saraf, Phys. Rev. **98** (1955) 94; δ recalculated by Ma 59
Ma 59 S. S. Malik, V. R. Potnis and C.E. Mandeville, Nuclear Physics **11** (1959) 691 and private communication of calculation of δ for Se^{76}
Ma 59a Preliminary value given by S. S. Malik, C. E. Mandeville, N. Nath, M. A. Rothman and D. M. Van Patter, Bull. Am. Phys. Soc. **4** (1959) 259
Ma 59b I. Marklund and G. Backstrom, Arkiv Fysik **16** (1959)
Mc 57 F. K. McGowan and P. H. Stelson, Bull. Am. Phys. Soc. **2** (1957) 207; value for branching slightly revised in private communication (1958)
Mc 58 F. K. McGowan and P. H. Stelson, Bull. Am. Phys. Soc. **3** (1958) 228; ORNL-2501 (Feb. 15, 1958) p. 14
Mc 58a F. K. McGowan, paper given at the Paris conference (1958). The angular distribution of the 740 keV γ-ray from Coulomb excitation is consistent with E2 radiation, however it could be fitted by E2/M1 = 0.16 ± 0.05 (14 % E2)
Mc 59 F. K. McGowan and P. H. Stelson, Bull. Am. Phys. Soc. **4** (1959) 232; preliminary value by Eichler
Me 53 F. R. Metzger and W. B. Todd, Phys. Rev. **92** (1953) 904; δ recalculated by Ma 59
Mo 56 H. T. Motz, Phys. Rev. **104** (1956) 1353
Mr 57 J. Mraz, Nuclear Physics **4** (1957) 457. This value of δ assumes that the 921 keV level of Pt^{192} has spin 4+
Mu 55 J. J. Murray, F. Boehm, P. Marmier and J. W. M. Dumond, Phys. Rev. **97** (1955) 1007
Na 57 O. Nathan and W. Waggoner, Nuclear Physics **2** (1956/57) 548
Na 57a O. Nathan, Nuclear Physics **4** (1957) 125
Na 59 O. Nathan and S. Hultberg, Nuclear Physics **10** (1959) 118
Na 59a N. Nath, S. S. Malik, M. A. Rothman and D. M. Van Patter, Bull. Am. Phys. Soc. **4** (1959) 258
Ni 58 K. O. Nielsen and O. B. Nielsen, Nuclear Physics **5** (1958) 319
Ni 59 O. B. Nielsen, N. O. R. Poulsen, R. K. Sheline and B. S. Jensen, Nuclear Physics **10** (1959) 475
Nu 54 R. H. Nussbaum, R. van Lieshout, A. H. Wapstra, N. F. Verster, F. E. L. Ten Haaf, G. I. Nijgh and L. T. M. Ornstein, Physica **20** (1954) 555
Of 57 S. Ofer, Nuclear Physics **4** (1957) 477
Of 57a S. Ofer, Nuclear Physics **5** (1957) 331; error for branching given by Ar 59
Pe 54 M. L. Perlman and J. Welker, Phys. Rev. **95** (1954) 133
Po 55 A. J. Poe, Phil. Mag. **46** (1955) 1165
Po 56 V. R. Potnis, V. S. Dubey and C. E. Mandeville, Phys. Rev. **102** (1956) 459; δ recalculated by Ma 59
Po 56a V. R. Potnis, Phys. Rev. **104** (1956) 722
Po 56b F. T. Porter, M. S. Freedman, T. B. Novey and F. Wagner, Jr., Phys. Rev. **103** (1956) 921
Po 56c V. R. Potnis, Indian J. Phys. **30** (1956) 375; δ recalculated by Ma 59
Pr 58 V. P. Prikhodtseva and Iu. V. Khol'nov, Izvest. Akad. Nauk SSSR Ser. Fiz. **22** (1958) 176
Ra 55 J. O. Rasmussen, H. Slatis and T. O. Passell, Phys. Rev. **99** (1955) 42;
J. O. Rasmussen, F. S. Stephens, Jr., D. Strominger and B. Astrom, Phys. Rev. **99** (1955) 47
Re 59 D. H. Rester, F. E. Durham and C. M. Class, Bull. Am. Phys. Soc. **4** (1959) 98. The measured K/L+M ratio is compatible with a pure multipole of ≤ 1, or E2 plus a strong E0 admixture.
Ro 59 R. L. Robinson, F. K. McGowan and W. G. Smith, Bull. Am. Phys. Soc. **4** (1959) 279; ORNL-2718 (June 10, 1959) p. 8. The values listed for the branching come from the Ag^{106} and Rh^{106} decay. The value of 0.49 ± 0.14 from the Rh^{106} decay assumes 100 % E2 for the 618 keV cascade transition.

Sa 58 M. Sakai, H. Ikegami, T. Yamazaki and K. Sugiyama, J. Phys. Soc. Japan **14** (1959) 983 and private communication from M. Sakai. δ for Te^{126} has been recalculated by Ma 59.

Sc 53 D. Schiff and F. R. Metzger, Phys. Rev. **90** (1953) 849

Sc 53a C. D. Schrader, Phys. Rev. **92** (1943) 928

Sc 56 R. P. Scharenberg, M. G. Stewart and M. L. Wiedenbeck, Phys. Rev. **101** (1956) 689

Sc 57 B. L. Schram, H. L. Polak, W. Schoo, R. K. Girgis and R. van Lieshout, unpublished data (1957) quoted by St 58.

Sc 59 R. P. Schuman, E. H. Turk and R. L. Heath, Phys. Rev. **115** (1959) 185

Se 57 A. G. Sergeev, E. M. Krisuik, G. D. Latyshev, Iu. N. Trofimov and A. S. Remmenvi, Zh. Eksp. Teor. Fiz. **33** (1957) 1140; Soviet Physics JETP **6** (1958) 878

Se 58 R. E. Segel, Phys. Rev. **111** (1958) 1620

St 53 R. M. Steffen, Phys. Rev. **89** (1953) 665L; error given by St 56a

St 56 G. S. Stanford and G. F. Pieper, Phys. Rev. **103** (1956) 637

St 56a R. M. Steffen; quoted by M. T. Thieme and E. Bleuler, Phys. Rev. **101** (1956) 1031

St 58 D. Strominger, J. M. Hollander and G. T. Seaborg, Revs. Mod. Phys. **30** (1958) 585

St 59 M. J. Stimac, W. L. Skeel and P. S. Jastram, Bull. Am. Phys. Soc. **4** (1959) 56

Su 57 O. I. Sumbaev, Zh. Eksp. Teor. Fiz. **32** (1957) 247; Soviet Physics JETP **5** (1957) 170. Correction for the contribution of the 1231 keV γ-ray to the 1222+1231 keV group in the Ta^{182} decay has been made by taking the ratio of the e_K intensities for the 1231, 1222 keV γ-rays as 0.52 from the results of Mu 55 and Fr 57. Then, assuming that both γ-rays are pure E2, a correction can be applied to the γ-ray spectrum.

Su 57a O. I. Sumbaev, Izvest. Akad. Nauk SSSR Ser. Fiz. **21** (1957) 987

Ta 55 H. W. Taylor and R. W. Pringle, Phys. Rev. **99** (1955) 1345

Ve 54 J. Verhaeghe and J. Demuynck, Comptes Rendus **239** (1954) 1374

Vo 56 J. Volpe and G. Hinman, Phys. Rev. **104** (1956) 753

Wa 56 R. C. Waddell and E. N. Jensen, Phys. Rev. **102** (1956) 816

We 59 H. I. West, Jr., L. G. Mann and G. M. Iddings, Phys. Rev. **113** (1959) 881

Wi 56 R. C. Williams and K. J. Roulston, Can. J. Phys. **34** (1956) 1087

Zo 56 A. V. Zolotavin, E. P. Grigorev and M. A. Aborian, Izvest. Akad. Naud SSSR Ser. Fiz. **20** (1956) 289

1.D.2:
1.E.4

Nuclear Physics **14** (1959/60) 70—77; © *North-Holland Publishing Co., Amsterdam*
Not to be reproduced by photoprint or microfilm without written permission from the publisher

EVEN NUCLEI WITHOUT AN AXIS OF SYMMETRY

N. MACDONALD

Atomic Weapons Research Establishment, Aldermaston

Received 12 August 1959

Abstract: The low lying levels of even nuclei, and the electric quadrupole transition probabilities between certain of these levels, are discussed in terms of the rotation of a nucleus without axial symmetry. The moments of inertia of the nucleus are not restricted to those prescribed by the hydrodynamical model. Rather we use a prescription due to Moszkowski. This contains a parameter p whose value depends on the residual interaction, and which in varying from 0 to 1 causes the moments of inertia to vary from the rigid body values to approximately the hydrodynamical values. We find that to obtain agreement with the experimental data on the transitions it is necessary to have p larger than the values which give the correct values of the energy of the first excited state in the case of nuclei having a small deviation from axial symmetry.

1. Introduction

A great number of medium mass and heavy even nuclei fall into two categories. In one the sequence of states is 0^+ (ground state), 2^+, 4^+, with the energies of the first two excited states in the ratio $E_{41}/E_{21} \approx 3.3$. The properties of these nuclei have been successfully accounted for [1]) by consideration of the rotational collective motion of a spheroidal nucleus. The other class of even nuclei have the sequence 0^+ (ground state), 2^+, 2^+, with $E_{22}/E_{21} = 2$ to 2.5. It has been proposed [2]) that these excited states correspond to vibrational motion. If the nucleus has spherical equilibrium shape there is an excited 2^+ state and above it a degenerate triplet (0^+, 2^+, 4^+) with $E_{22}/E_{21} = 2$. If the equilibrium shape is spheroidal, then [3]) the 0^+ member of this triplet is raised above the others, and E_{22}/E_{21} increases to about 2.5.

No work has been published using this model to make detailed predictions about the electric quadrupole transitions between these levels, on which there is now a considerable amount of experimental data [4]). Davydov and Fillipov [5]) have proposed another interpretation of these nuclei which allows one, knowing E_{22}/E_{21}, to predict the ratio of the electric quadrupole transition probabilities between the various levels. Their suggestion is that the level spectra of these nuclei are rotational, and that the nuclei have no axis of symmetry. This situation was previously discussed by Marty [6]). The predictions of this theory for these ratios have had some success [4]) as our graphs show.

Davydov and Fillipov have used the nuclear moments of inertia of the hydrodynamical model [7]). It is our intention in this paper to examine how sensitive

the predictions of this theory are to the form of moment of inertia used. In obtaining an alternative form we make use of the work of Inglis [8]) and Moszkowski [9]). We make no other change in the theory; in particular we derive the transition probabilities using the electric quadrupole operator for a uniform charge distribution throughout the ellipsoidal nucleus [5]). We do not discuss the question [10]) of how the nucleus comes to have an equilibrium form which is not axially symmetric.

2. Predictions of the Theory of Davydov and Fillipov

An ellipsoidal nucleus can be described [7]) by parameters β, γ, which are related to the principal axes R_λ by

$$R_\lambda = R_0\left\{1+\left(\frac{5}{4\pi}\right)^{\frac{1}{2}}\beta\cos\left(\gamma-\frac{2\pi\lambda}{3}\right)\right\} \qquad \lambda = 1, 2, 3. \tag{2.1}$$

where $R_1R_2R_3 \approx R_0^3 =$ constant, for incompressible nuclear matter. Axial symmetry is obtained when $\gamma = \frac{1}{3}n\pi$, n an integer. The moment of inertia of a liquid drop rotating about λ has the form

$$\mathscr{I}_\lambda^{\mathrm{H}} = \beta^2\sin^2\left(\gamma-\frac{2\pi\lambda}{3}\right). \tag{2.2}$$

This form for $\mathscr{I}_\lambda$ implies that the predictions of [5]) are symmetric about $\gamma = \frac{1}{6}\pi$ and that the ratios of energies or of transition probabilities do not depend on β. Thus, for a given value of E_{22}/E_{21} we have unique values of $B(\mathrm{E2};\ 22 \to 21)/B(\mathrm{E2};\ 2j \to 01)$, writing $B(\mathrm{E2}; Ij \to I'j')$ for the reduced electric quadrupole transition probability from the jth state with spin I to the j'th state of spin I'. The main results of this theory are as follows.

There are two excited states with $I = 2$. The value of E_{22}/E_{21} for maximum asymmetry ($\gamma = \frac{1}{6}\pi$) is 2. This ratio increases monotonically to ∞ as $\gamma \to 0$. The state 22 can lie below the state 41. There is one excited state with $I = 3$. This state always lies above the state 41. For any value of γ,

$$E_{31} = E_{21}+E_{22}. \tag{2.3}$$

Nine cases are given in ref. [5]) in which this result holds. However, seven of these are in nuclei in which $E_{41} \ll E_{22}$ (γ small). In this situation it has been proposed [11]) that the states 21 and 41 are members of the usual rotational band based on the ground state of an axially symmetric nucleus, and 22 is a vibrational level on which is based another rotational band, the next member being 31. If one assumes the same moment of inertia for the two bands the result (2.3) holds. The other two cases given in ref. [5]) are nuclei with $E_{22}/E_{21} \approx 2$. It would be interesting to have further evidence on the presence of states with $I = 3$ in such nuclei.

We show in figs. 1, 2, 3 the ratios $B(\mathrm{E2};\, 22 \to 21)/B(\mathrm{E2};\, 22 \to 01)$, $B(\mathrm{E2};\, 22 \to 21)/B(\mathrm{E2};\, 21 \to 01)$ and $B(\mathrm{E2};\, 22 \to 01)/B(\mathrm{E2};\, 21 \to 01)$, plotted against E_{22}/E_{21}, and compared with the experimental data of ref. [4])†. Fig. 1 is included to show how this ratio goes from the value ∞ at $E_{22}/E_{21} = 2$, as in the

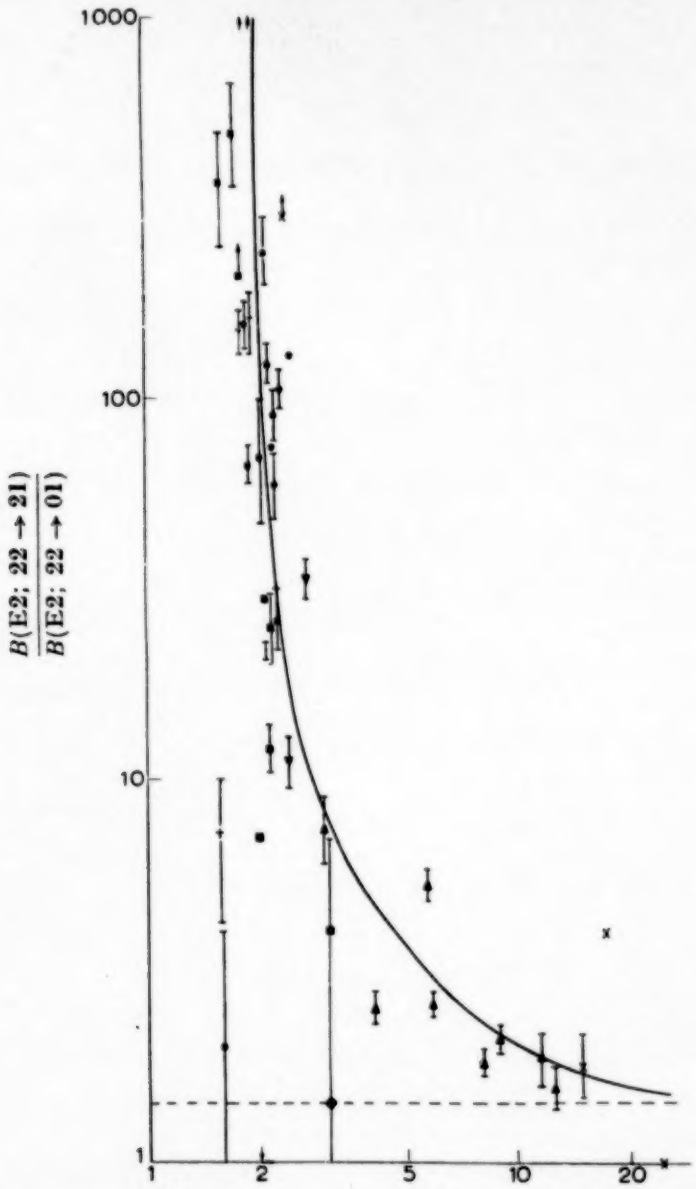

Fig. 1. The ratio $B(\mathrm{E2};\, 22 \to 21)/B(\mathrm{E2};\, 22 \to 01)$ according to the hydrodynamical model, compared with experimental data.

theory of ref. [2]), to $\frac{10}{7}$ for $E_{22}/E_{21} \gg 1$, as in the theory of ref. [11]). The agreement with the experimental data is more marked in figs. 2 and 3. The theory of ref. [2]) predicts $B(\mathrm{E2};\, 22 \to 21)/B(\mathrm{E2};\, 21 \to 01) = 2$ for $E_{22}/E_{21} = 2$.

† In the final version of Van Patter's paper, there are several changes in the best values for these ratios. These do not alter the general character of the results.

Davydov and Fillipov find that as γ varies from 0 to $\frac{1}{6}\pi$, E_{21} increases only by about 50 %, if β remains unaltered. Also the value of $B(\mathrm{E2};\ 21 \to 01)$ does not vary much with γ. Thus, we can estimate, as is usual for the case of $\gamma = 0$, E_{21} from the value of β obtained from the ratio F of $B(\mathrm{E2};\ 21 \to 01)$ to its single

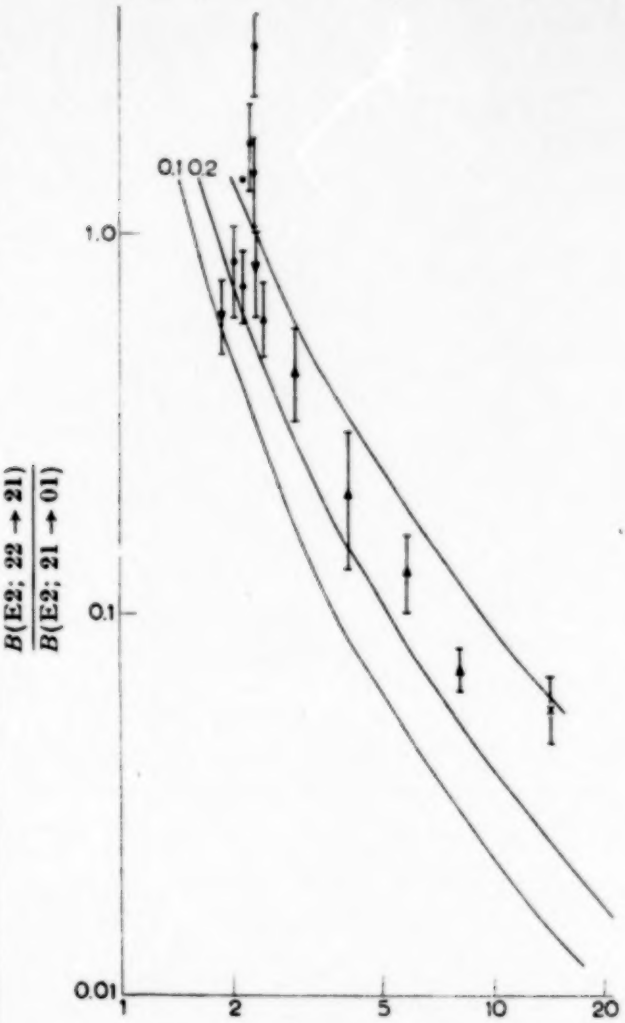

Fig. 2. The ratio $B(\mathrm{E2};\ 22 \to 21)/B(\mathrm{E2};\ 21 \to 01)$ compared with experimental data. The unlabelled curve is that of the hydrodynamical model. The other two are obtained using (4.4) with $p = 0.1$ and 0.2 respectively.

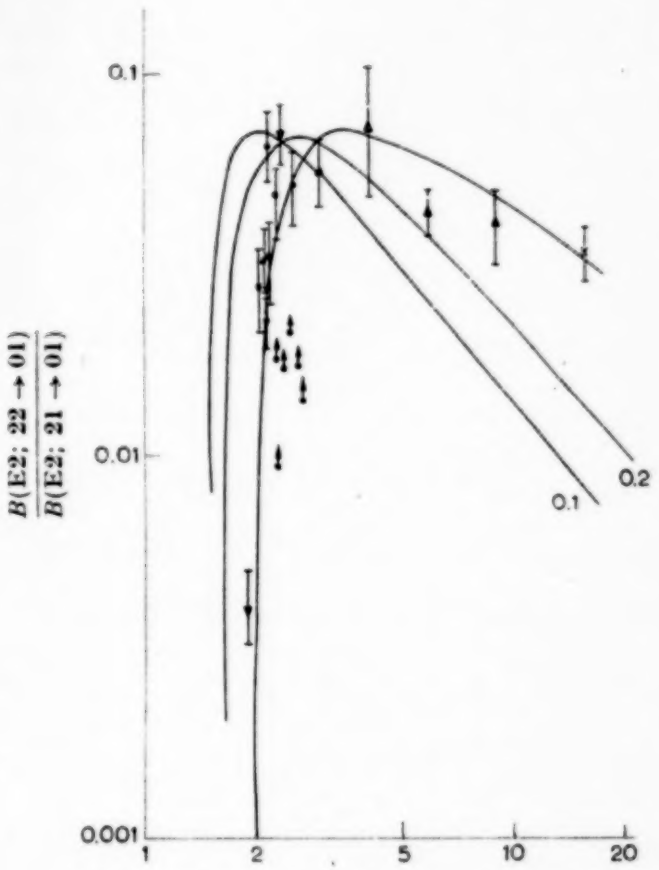

Fig. 3. The ratio $B(\mathrm{E2};\ 22 \to 01)/B(\mathrm{E2};\ 21 \to 01)$ compared with experimental data. The curves correspond to those in fig. 2. For some nuclei with $E_{22}/E_{21} \approx 2$ only a lower limit is given. These are isotopes of Ru, Pd and Cd.

particle value, using $E_{21} \propto \beta^{-2}$ and $F \propto \beta^2$. Comparison of the values [12]) of E_{21} and F for the nuclei studied in ref. [4]) shows that for those having $E_{22}/E_{21} > 2.5$ the hydrodynamical model gives E_{21} too great by about a factor 6, while for those with $E_{22}/E_{21} \approx 2$ the model gives E_{21} too great by a factor 4 to 6.

3. General Results

We retain the assumption that the rotational motion can be treated adiabatically, so that the wave functions are the product of a rotational and an intrinsic

wave function. The matrix elements of the rotational energy between states with intrinsic energy E_0, total spin I, $I_Z = M$ and $I_3 = K$ are [6,13])

$$\begin{aligned}\langle E_0IMK|H_r|E_0IMK\rangle &= I(I+1)a+K^2b,\\ \langle E_0IMK+2|H_r|E_0IMK\rangle &= \tfrac{1}{2}c\{1+\delta_{0K}\}^{\frac{1}{2}}f_I(K)f_I(K+1),\end{aligned} \tag{3.1}$$

all others zero. In these equations

$$a = \tfrac{1}{4}[\mathscr{I}_1^{-1}+\mathscr{I}_2^{-1}], \qquad b = \tfrac{1}{2}\mathscr{I}_3^{-1}-a,$$
$$c = \tfrac{1}{4}[\mathscr{I}_1^{-1}-\mathscr{I}_2^{-1}], \qquad f_I(K) = [I(I+1)-K(K+1)]^{\frac{1}{2}}.$$

For $\gamma = 0°[\mathscr{I}_3 = 0,\ \mathscr{I}_1 = \mathscr{I}_2]$ K is a good quantum number. In an even nucleus the possible values of K are

I	0	1	2	3	4
K	0	–	0, 2	2	0, 2, 4

and so on. From (3.1) we have

$$E_{31} = 12a+4b,$$

E_{21}, E_{22} the roots of $(E-6a)(E-6a-4b)+12c^2 = 0$,

$$\therefore E_{31} = E_{21}+E_{22}.$$

Writing A_j, B_j for the components of the eigenvectors for $I = 2$, and using the E2 operator for a uniform distribution of charge, we have

$$\begin{aligned}B(\mathrm{E2};\ 2j \to 01) &= \frac{e^2Q_0^2}{16\pi}[A_j\cos\gamma+B_j\sin\gamma]\varphi(\beta,\gamma),\\ B(\mathrm{E2};\ 22 \to 21) &= \frac{e^2Q_0^2}{16\pi}[(A_1A_2-B_1B_2)\cos\gamma-(A_1B_2+B_1A_2)\sin\gamma]\tfrac{10}{7}\varphi(\beta,\gamma);\end{aligned} \tag{3.2}$$

φ is a factor depending on the intrinsic state of the nucleus, which is the same for all rotational states; Q_0 is the intrinsic electric quadrupole moment of an axially symmetric nucleus with deformation parameter β,

$$Q_0 = \frac{3ZR^2\beta}{\sqrt{5}\pi}.$$

There is little information about the E2 transitions from 31 to the states with $I = 2$. We simply draw attention to the result, which is independent of the form of $\mathscr{I}_\lambda$, that

$$\frac{B(\mathrm{E2};\ 31 \to 21)}{B(\mathrm{E2};\ 31 \to 22)} = \frac{B(\mathrm{E2};\ 22 \to 01)}{B(\mathrm{E2};\ 21 \to 01)}.$$

4. The Moments of Inertia

For spheroidal nuclei Inglis [8]) has introduced the cranking model, in which the nucleus experiences an externally induced rotation, about an axis λ which is not the axis of symmetry, and the moment of inertia is determined from the energy of rotation in lowest order perturbation theory. The intrinsic wave function is taken as the product of independent particle wave functions in an anisotropic harmonic oscillator potential,

$$V = \tfrac{1}{2}M(\omega_1^2X^2+\omega_2^2Y^2+\omega_3^2Z^2), \quad \omega_1\omega_2\omega_3 = \omega_0^3 = \text{constant}.$$

(Inglis took $\omega_1 = \omega_2$ but the theory is readily extended to the general case.) At equilibrium deformation, when unfilled oscillator shells are involved, $\mathscr{I}_\lambda = \mathscr{I}_\lambda^{\mathrm{R}}$, the rigid body value. Moszkowski [9]) has given a method of allowing for the residual interaction of the nucleons, the part of the two-nucleon interaction which is not represented by the oscillator well. Moszkowski's result is

$$\mathscr{I}_\lambda = \mathscr{I}_\lambda^{\mathrm{H}}/\varepsilon^2, \tag{4.1}$$

$\varepsilon\hbar\omega_0$ being a suitably defined average value of the denominator in the cranking model expression

$$\mathscr{I}_\lambda = 2\hbar^2 \sum_b \frac{\left|\left(b\left|\frac{\partial}{\partial\theta_\lambda}\right|a\right)\right|^2}{E_b - E_a}. \tag{4.2}$$

Defining ε_0 as the value of ε when the residual interaction is ignored, and using Inglis' result in this case, we have

$$\mathscr{I}_\lambda^{\mathrm{R}} = \mathscr{I}_\lambda^{\mathrm{H}}/\varepsilon_0^2. \tag{4.3}$$

Setting $\varepsilon = \varepsilon_0 + p$ we have

$$\mathscr{I}_\lambda = \mathscr{I}_\lambda^{\mathrm{H}}\left[\frac{1}{\left(\frac{\mathscr{I}_\lambda^{\mathrm{H}}}{\mathscr{I}_\lambda^{\mathrm{R}}}\right)^{\frac{1}{2}} + p}\right]^2. \tag{4.4}$$

Moszkowski finds the value of p needed to give E_{21} correctly for even axially symmetric nuclei. For $\beta = 0.2$, $p = 0.2$, and for $\beta = 0.4$, $p = 0.15$. We treat p as a parameter independent of β and γ, and have obtained results for $p = 0.1$ and 0.2, with various values of β. Like Moszkowski we use $\mathscr{I}_\lambda^{\mathrm{R}}$ for a uniform distribution of nucleons.

It should be pointed out that although we discuss the result (4.1) in the context of the cranking model, Moszkowski [14]) has obtained a form like (4.1) with a quite different approach.

An advantage of the form (4.4) is that, for $p \neq 0$, $\gamma \to 0$ implies $\mathscr{I}_3 \to 0$, and $\beta \to 0$ implies all $\mathscr{I}_\lambda \to 0$, as they must for rotation about an axis of symmetry.

5. Results and Discussion

With our form for $\mathscr{I}_\lambda$ we do not have symmetry about $\gamma = 30°$. However, our results for β, γ are identical with those for $-\beta, 60°-\gamma$. The main difference in the energy levels from the hydrodynamical case is that for $\gamma \approx 30°$, E_{22}/E_{21} can fall below 2, and E_{31} can be less than E_{41}. Again, E_{21} varies little with γ for fixed β and p. We have now the possibility of fitting the values of E_{21} for both the (0, 2, 2) and (0, 2, 4) nuclei by having p increase with γ.

We show in figs. 2 and 3 our results for $B(\mathrm{E2}; 22 \to 21)/B(\mathrm{E2}; 21 \to 01)$ and $B(\mathrm{E2}; 22 \to 01)/B(\mathrm{E2}; 21 \to 01)$ for $\beta = 0.2$, compared with the results of Davydov and Fillipov and the experimental data [4]). The curves for $\beta = -0.2$ are roughly similar, and as β increases the curves lie further from the Davydov and Fillipov curves. We consider two sets of nuclei separately.

For $E_{22}/E_{21} > 2.5$ the nuclei are, in decreasing order of this ratio, Th^{232}, W^{184}, W^{186}, Os^{188}, Os^{190}. These are known to have $\beta \approx 0.2$ (ref.[11]), table 5.2). It is clear from the figures that to get as good or better agreement with the experimental data as in the hydrodynamical case it is necessary to have $p > 0.2$, the value found by Moszkowski to correspond to $\beta = 0.2$. The best agreement is obtained for $p = 0.3$ to 0.5, which gives E_{21} too great by a factor $\frac{3}{2}$ to 3. Thus the failure of this model to give correct absolute values of excitation energies is not removed by our treatment.

For $E_{22}/E_{21} < 2.5$ the values of F indicate that β can fall to 0.1—0.15. Therefore, without going to $p > 0.2$ we can fit the data as well in our case as in the hydrodynamical case. The agreement with experiment is not very good in this region anyway.

I wish to thank Dr. A. M. Lane for his comments on the manuscript of this paper, Mr. F. J. Birkin for calculating the energy eigenvalues and eigenvectors, and Dr. D. M. Van Patter for sending me his compilation of experimental data.

References

1) A. Bohr and B. R. Mottelson, Mat. Fys. Medd. Dan. Vid. Selsk. **27**, no. 16 (1953)
2) G. Scharff-Goldhaber and J. Weneser, Phys. Rev. **98** (1955) 212
3) L. Wilets and M. Jean, Phys. Rev. **102** (1956) 788
4) D. M. Van Patter, Bull. Am. Phys. Soc. **4** (1959) 233
5) A. S. Davydov and G. F. Fillipov, Nuclear Physics **8** (1958) 237
6) C. Marty, Nuclear Physics **1** (1956) 85; **3** (1957) 193
7) A. Bohr, Mat. Fys. Medd. Dan. Vid. Selsk. **26** (1952) 14
8) D. R. Inglis, Phys. Rev. **103** (1950) 1786
9) S. A. Moszkowski, Phys. Rev. **103** (1956) 1328
10) M. Gursky, Phys. Rev. **98** (1955) 1205(A); (see ref. [3]));
B. T. Geilikman, Zhur. Exp. Theor. Fiz. **35** (1958) 989;
T. D. Newton, Rehovoth Conference Proceeding (1957) 118;

D. A. Zaikin, Zhur. Exp. Theor. Fiz. **35** (1958) 529;
A. S. Davydov and G. F. Fillipov, Nuclear Physics **10** (1959) 654
11) K. Alder *et al.*, Revs. Mod. Phys. **28** (1956) 432
12) C. A. Mallmann, Proceedings of Second Geneva Conference (1958) A/CONF. 15/P/1971; W. Scheuer and E. Aisenberg, Proceedings of Second Geneva Conference (1958) A/CONF. 15/P/2513
13) L. D. Landau and E. M. Lifshitz, Quantum Mechanics (Pergamon Press, 1958) Ch. 13.
14) S. A. Moszkowski, Phys. Rev. **110** (1958) 403

1.E.1:
2.L:3.A

Nuclear Physics **14** (1959/60) 78—96; © *North-Holland Publishing Co., Amsterdam*
Not to be reproduced by photoprint or microfilm without written permission from the publisher

INELASTIC NEUTRON SCATTERING IN Nb^{93}

N. NATH †, M. A. ROTHMAN ††, D. M. VAN PATTER and C. E. MANDEVILLE †††
Bartol Research Foundation of the Franklin Institute, Swarthmore, Pa. *

Received 6 August 1959

Abstract: Study of gamma ray spectra following inelastic neutron scattering in Nb^{93} has been made at bombarding energies ranging from 0.81 to 2.25 MeV. Measurement of thresholds for the gamma rays and the gamma-gamma coincidence spectra has enabled us to work out a level scheme for Nb^{93}. The energies of the two levels previously reported have been revised to 0.741 and 0.958 MeV. In addition, levels have been found at 0.809, 1.08, 1.28, 1.34, 1.48, 1.67 and 1.92 MeV. In all, fourteen gamma-ray transitions have been detected and the possibility of a few more is indicated. In suitable cases, branching ratios have been calculated. Gamma ray production cross-sections have also been tabulated. Theoretical calculations of the cross sections for the first five levels, using a diffuse-edge potential well, give fairly good agreement with the experiment. Probable spin assignments for the second to fifth excited states have been discussed.

1. Introduction

In a previous publication [1]) we reported two energy levels in Nb^{93}, found through the study of the gamma rays excited by inelastic neutron scattering. Since that time our technique has been improved by the incorporation of a 100-channel pulse-height analyzer, a slow-fast coincidence circuit, and a scintillator with better resolution.

A preliminary study of Mn^{55} showed that very useful information concerning the spins of excited states could be obtained by measuring the branching ratios of the gamma rays arising from these levels, together with measurements of the inelastic scattering cross sections [2]).

In our previous work with Nb^{93} we had drawn the conclusion that the gamma rays from the 764 and 977 keV levels cascaded through the 29 keV isomeric state, and as a result of this had given tentative spin assignments to the two higher levels. However, theoretical cross-section calculations based on these spin assignments gave results which were much lower than the measured cross sections.

In view of these discrepancies it was decided to pursue the study of Nb^{93} further for the purpose of clarifying the situation. As a result of the improved experimental arrangement, it was found possible to detect the presence of six

† Present address: Physics Dept. Louisiana State University, Baton Rouge, La.
†† Present address: Project Matterhorn, Princeton University, Princeton, New Jersey.
††† Present address: Physics Department, University of Alabama, Tuscaloosa, Alabama.
* Assisted by the U. S. Atomic Energy Commission.

higher levels, in addition to a level located between the two previously observed. Further cross-section calculations have been made, using a diffuse-edge nuclear potential.

2. Experimental Arrangement

The gamma ray detectors and slow-fast coincidence circuit used in this experiment were the same as those previously described in connection with the study of Mn^{55} [2]). The neutron beam was produced by the $Li^7(p, n)Be^7$ reaction in the Bartol-ONR Van de Graaff generator. Lithium targets were 40 to 80 keV thick, for $E_p = 1.88$ MeV, except for certain threshold measurements during which 5 to 10 keV targets were employed.

The NaI crystal used on the 100-channel side of the circuit was 35 mm in diameter and 40 mm long, with a resolution of 8 % for the Cs^{137} 662 keV gamma ray. On the single-channel side the crystal was 35 mm in diameter and 30 mm long, with a resolution of about 10 %.

The niobium scatterer was a square piece, $2'' \times 2'' \times \frac{1}{4}''$, weighing 128 grams. The NaI crystals were located $\frac{1}{8}''$ from each face of the scatterer, and were shielded from the neutron source by Mallory Metal wedges 5" long. In addition $\frac{1}{8}''$ of Mallory Metal was placed immediately in front of the neutron source to attenuate the 478 keV gamma rays from the lithium target and thus reduce Compton scattering of these gamma rays from the niobium into the crystals. Fig. 1 of our previous publication [2]) shows the experimental set-up along with the block diagram of the electronic equipment used.

3. Analysis of Gamma Ray Spectra

In this section will be discussed the "singles" spectra, obtained with one detector and attenuating wedge in place. Discussion of the coincidence spectra will be deferred to the next section.

Singles spectra were taken at a number of bombarding energies, so that the gamma rays from each level could be observed to appear at the appropriate threshold. Because of this ability to observe the levels being excited one at a time, it was possible to analyze a relatively complicated level scheme in a fairly unambiguous way.

Background subtraction was accomplished by replacing the niobium with a graphite scatterer, and performing an automatic subtraction on the 100-channel analyzer while running for a time equal to the original niobium run (after correcting for the difference in average dead-times of the analyzer for the two runs).

Figs. 1(a) and (b) show typical subtracted spectra obtained at bombarding energies varying from 1.06 to 2.12 MeV. The detailed analysis of each spectrum was done on the basis of known spectra obtained from suitable monoenergetic gamma rays of various energies. Empirical techniques were worked out for

constructing correct shapes for the photopeak, pair, and Compton distributions for a given energy gamma ray.

Analysis was aided by the fact that the first time a given gamma ray was observed, at a bombarding energy just above its threshold, the energy of this gamma ray could be established without interference from higher energy gamma rays. Then, when spectra taken at higher bombarding energies were analyzed,

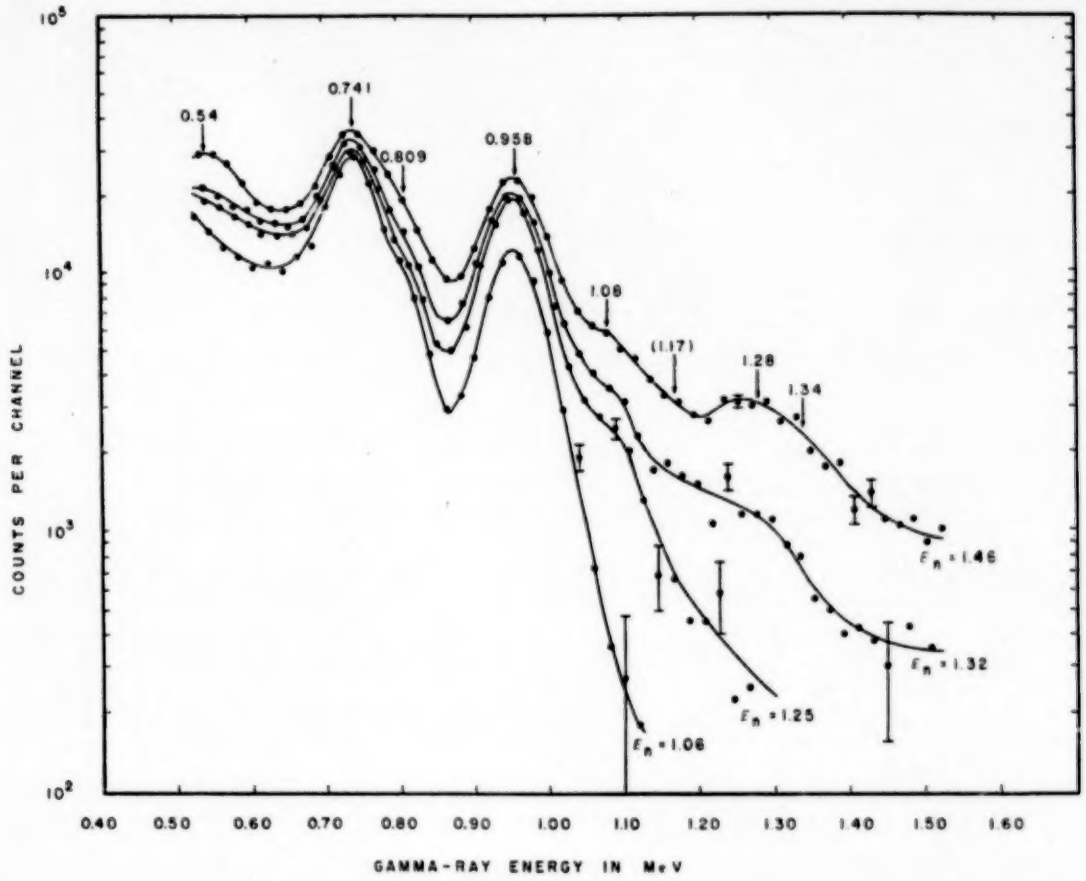

Fig. 1(a).
Gamma ray spectra from Nb^{93} (singles); E_n varying from 1.06 to 1.46 MeV.

the presence of the first gamma ray was already established, even though it might be hidden under the distribution of higher energy gamma rays.

In the region of the spectrum below 800 keV, it is important to consider the effect of the peaks in the background caused by inelastic scattering in iodine. Over or under-subtraction of background will cause anomalous effects. Likewise shifts in gain between the niobium and graphite runs will cause improper subtraction to occur in the neighbourhood of these background peaks, creating false peaks in the difference spectrum.

Table 1 summarizes the gamma rays observed and gives the best estimate of their energies. These are listed together with the results of Boley, Thorndike, and Moffet [3]), which were published after the completion of our experimental data.

Considerable effort was given to the accurate calibration of the 741 and 958 keV peaks, since this is important in assigning the position of the corresponding levels (see later discussion concerning threshold measurements). Repeated measurements were made, alternating with calibration runs using Cs^{137} and Co^{58} sources.

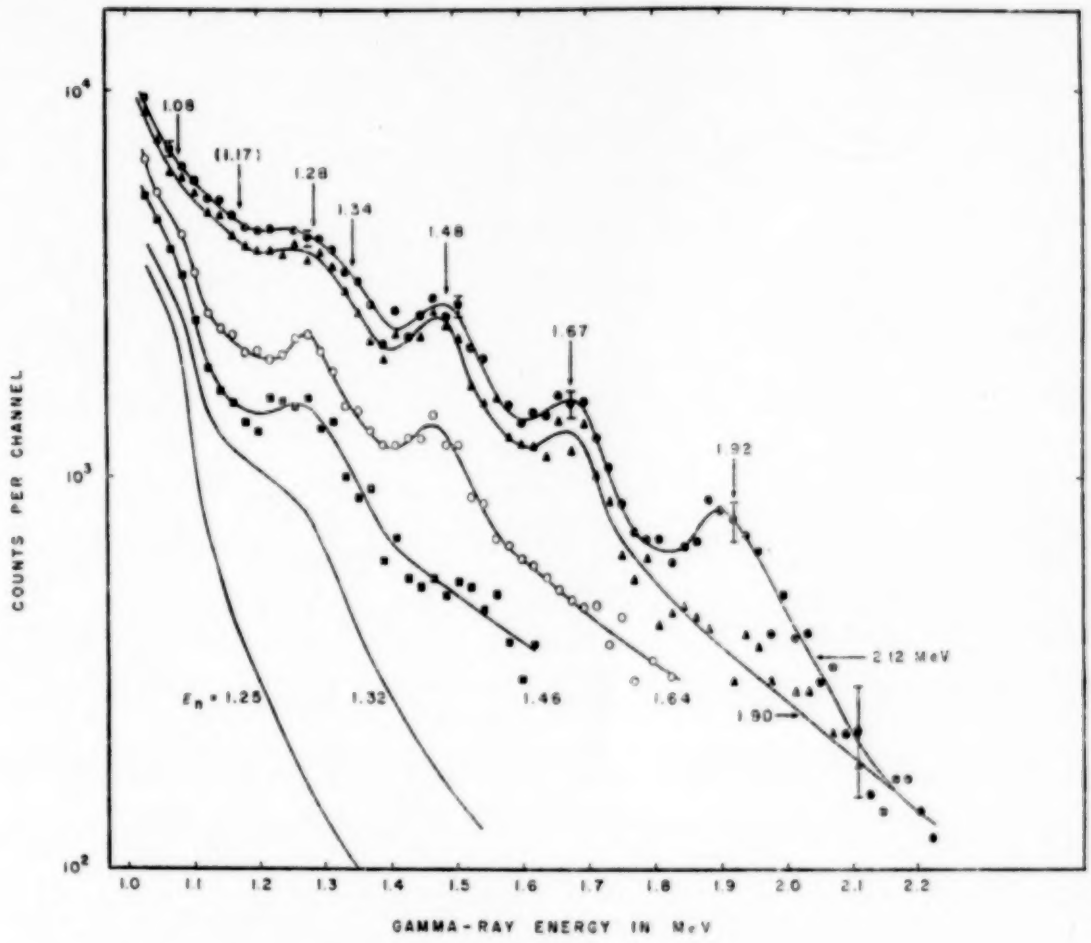

Fig. 1(b).
Gamma ray spectra from Nb^{93} (singles); E_n varying from 1.46 to 2.12 MeV.

The 741 and 958 keV gamma rays are the two prominent ones which we reported previously. Subsequent analysis, using proper spectrum shapes, indicated that the first photopeak was a superposition of two peaks close together. A gamma ray of 809 keV energy was established in this manner. This was verified by making runs at bombarding energies just below the thresholds for this gamma ray and the 0.958 MeV gamma ray, as shown in fig. 2. Comparison of these two spectra shows clearly the existence of 809 keV gamma ray.

In fig. 2, the peak at 0.63 MeV is attributed to gamma rays from inelastic neutron scattering in the iodine of the crystal. It is seen that this peak is less prominent at the higher bombarding energy. Since neutrons scattered from the niobium or the graphite contributes to the flux incident on the NaI crystal, and

since this scattering is a function of neutron energy, it is difficult to compensate exactly for this scattering at all energies.

With only a knowledge of the gamma ray energies, there is an ambiguity as to the actual level energies, since there is a possibility that the gamma rays may arise from cascade transitions through the 29 keV metastable state.

TABLE 1

Niobium gamma rays observed

Bartol	Boley *et al.* [3])
singles	
0.335±0.010	0.345±0.017
0.54 ±0.02	
0.741±0.005	0.73 ±0.02
0.809±0.005	
0.958±0.005	0.95 ±0.02
1.08 ±0.01	
(1.17 ±0.02)	
1.28 ±0.015	
1.34 ±0.02	
1.48 ±0.015	1.52 ±0.04
1.67 ±0.02	
1.92 ±0.03	1.94 ±0.07
2.13 ±0.04	2.11 ±0.08
coincidence with 741 keV	
0.335±0.010	
0.54 ±0.02	
0.92 ±0.03	
coincidence with 958 keV	
0.31 ±0.01	
0.38 ±0.01	
0.52 ±0.02	
0.71 ±0.02	

From earlier threshold measurements [1]) we had drawn the conclusion that the transitions were of the cascade type, so that the level energy was given as being 29 keV higher than the gamma ray energy.

However, more recent measurements, using 5 keV lithium targets and a better geometry than before, show the thresholds for the production of the 741 and 958 keV gamma rays to be 755±12 and 966±10 keV, respectively. Correction for centre-of-mass motion results in excellent agreement between the gamma ray energy and the level energy, leading to the conclusion that the gamma rays arise from ground state transitions. This data is summarized in table 2.

The error in our earlier work is attributed to the fact that the scatterer had been closer to the neutron source and subtended a fairly large angle. Spread of the neutron energy due to this subtended angle lowered the average neutron

energy, and thus caused the thresholds to be measured too high. The fact that the threshold for appearance of the 0.845 MeV gamma ray in iron could be measured correctly even in the poor geometry was misleading. This is explained by noting that the yield of the 0.845 MeV gamma ray rises very abruptly above

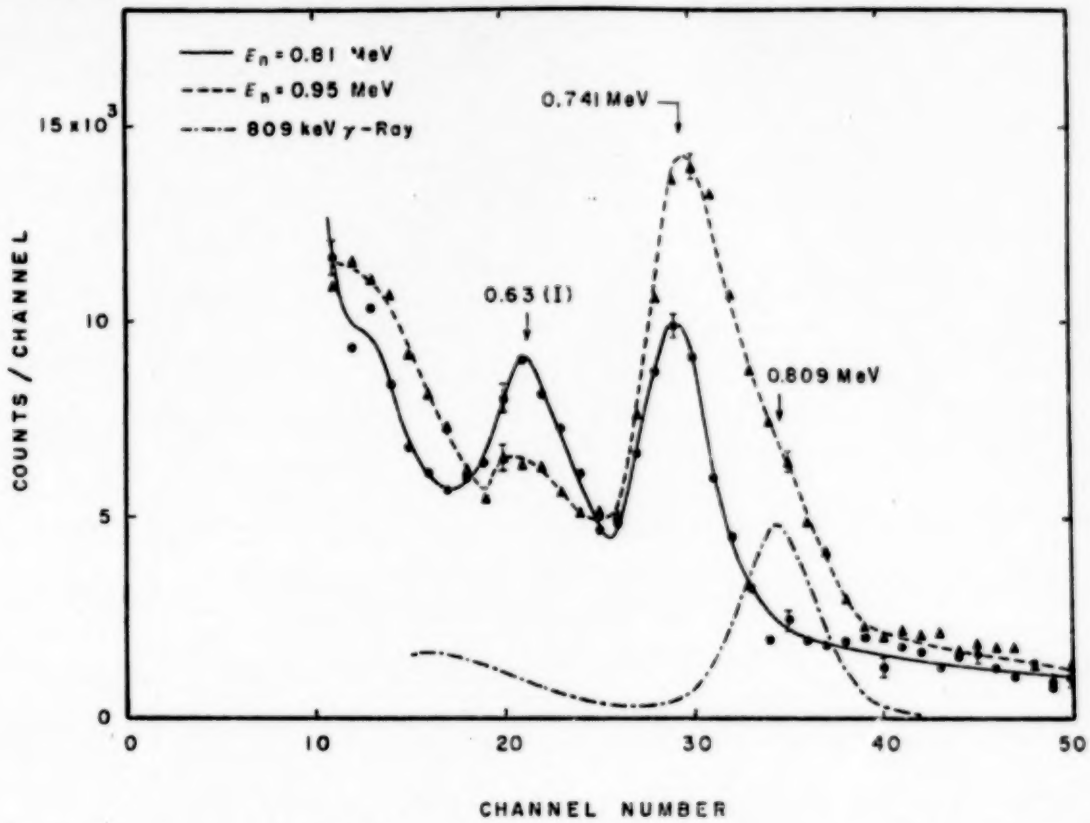

Fig. 2. Singles spectra at $E_n = 0.81$ and 0.95 MeV, indicating the existence of 0.809 MeV gamma ray.

TABLE 2
Thresholds for 741 and 958 keV gamma rays

	First gamma ray	Second gamma ray
Threshold energy	755±12	966±10
Level energy	747±12	956±10
Gamma-ray energy	741± 5	958± 5

Level energy $= -Q = E_{th}A/(A+1)$.
Energies in keV.

its threshold, and reaches a maximum within about 10 keV due to a resonance at that point. The yield of the niobium gamma rays rises much more gradually, so that an error of about 30 keV in the threshold could arise due to improper knowledge of the average neutron energy.

With the 0.741 and 0.958 MeV levels now defined, the positions of some of the higher levels could be determined by a knowledge of the gamma ray transitions.

The 1.08 MeV gamma ray was not easily resolved from the 0.958 MeV peak. In fact, the presence of this level was first indicated by the appearance of the 0.335 MeV gamma ray in coincidence with the 0.741 MeV gamma ray. Subsequent close examination showed the peak at 1.08 MeV in the singles spectrum.

The 0.335 MeV gamma ray was also seen in the singles spectrum, and by means of threshold measurements it was verified that this gamma ray originated from the 1.08 MeV level. In a like manner, the 0.54 MeV gamma ray was seen both in coincidences and in singles, while its threshold established it as originating in the 1.28 MeV level. Cascade gamma rays of these low energies are difficult to observe, since they are located in the high background part of the spectrum, and since they are always accompanied by the back-scattering and Compton distributions from higher energy gamma rays.

In spite of these difficulties the 0.54 MeV gamma ray could be seen clearly enough to note that its intensity increased somewhat abruptly at a bombarding energy of about 1.5 MeV, indicating the presence of a transition from the 1.48 MeV level to the 0.958 MeV level.

A gamma ray of 1.17 MeV energy is listed in parentheses, since its presence could not be established beyond doubt. The yield for this gamma ray seemed quite low up to neutron bombarding energy of 1.92 MeV. However, above this neutron energy the yield showed an abrupt rise, indicating probable cascades from higher levels or else the presence of a likely cascade transition from the 1.92 MeV to 0.741 MeV level.

4. Gamma-Gamma Coincidences

In this experiment coincidences were observed between gamma rays cascading through the 0.741 and 0.958 MeV levels. At the time this was done, the 0.809 MeV level had not yet been established, so that no special effort was made to resolve the 0.809 MeV gamma ray from the others. However, in every case a gamma ray found in the coincidence spectra could be identified with a level observed in the singles measurements, so that the results were fairly unambiguous.

Special problems arising in these coincidence measurements have been discussed in connection with inelastic neutron scattering in Mn^{55} [2]). It was shown there that effects could be found due to multiple scattering in the scatterer and in the sodium iodide crystals. These give a high background in the coincidence spectra which cannot be accounted for simply by measuring the chance rates.

Further background arises from Compton scattering of gamma rays between the two crystals, and also due to summation of two gamma rays which reach one crystal simultaneously. For example, if gamma rays A and B are in true coincidence, while C by chance arrives in one of the crystals simultaneously with

B, then A will appear to be in coincidence with the sum pulse B+C. This gives a continuous background which cannot be subtracted out by considering the chance rates occurring in either the fast or slow coincidence circuits.

Because the gamma rays from the niobium gave counting rates which were low compared to the rates induced directly by the neutrons incident on the counters, it was felt inadvisable to move the crystals farther back from the scatterer so that proper absorbers could be used to eliminate scattering between the crystals.

The following scheme was adopted to give at least a qualitative indication of the background due to multiple scattering and Compton scattering between the crystals. If the niobium is replaced by an iron scatterer, and the single-channel analyzer is set to cover the 0.845 MeV gamma ray from the iron, then there should be no true coincidences for bombarding energies up to 2.12 MeV, which is the threshold for the second excited state in iron. Coincidences observed will be the result of background effects such as: 1) multiple scattering of neutrons in the iron, giving two simultaneous gamma rays from two different nuclei, 2) events in which a neutron scattered inelastically in the iron produces an inelastic event in one of the NaI crystals, so that the 0.845 MeV gamma ray is in coincidence with one of the iodine gamma rays, 3) events in which the 0.845 MeV gamma ray and the inelastically scattered neutron simultaneously enter one crystal, forming a sum pulse, while a Compton-scattered quantum at the same time goes over to the other crystal, giving a distribution in the low energy region.

The procedure was as follows: coincidence runs were made with the niobium scatterer, at a bombarding energy E_n, with the single-channel analyzer set first on the 0.741 MeV peak (run A) and then on the 0.958 MeV peak (run B). This gave the spectra of the gamma rays in coincidence with each of these two gamma rays in turn. With the iron scatterer in place, a run was made at a bombarding energy $E_n+0.1$ MeV (run C). The energy of the inelastically scattered neutron in run A is approximately $E_n-0.74$ MeV, while in run C the corresponding energy is $E_n+0.1-0.84$ MeV. The scattered neutrons have roughly the same energy in the two cases, so that run C makes an appropriate background for run A. If a run with the iron scatterer is made at a bombarding energy $E_n-0.1$ MeV, then the inelastically scattered neutrons have an energy $E_n-0.1-0.84$ MeV, which is roughly the same as the energy of the neutrons scattered in run B.

In this way the bombarding energy for the background runs was chosen so that the energy of the inelastically scattered neutrons was the same as in the corresponding niobium runs. Thus approximately the same multiple scattering effects should be observed. Because the scattering cross sections differ, the background is incorrect quantitatively; however the curves were arbitrarily normalized so that upon subtraction a reasonably shaped spectrum resulted.

The contribution of the peak caused by 0.845—0.845 MeV coincidences due to multiple scattering in the iron was subtracted from the background spectrum.

Runs were made at intervals of 0.2 MeV over the energy range from 1.07 to

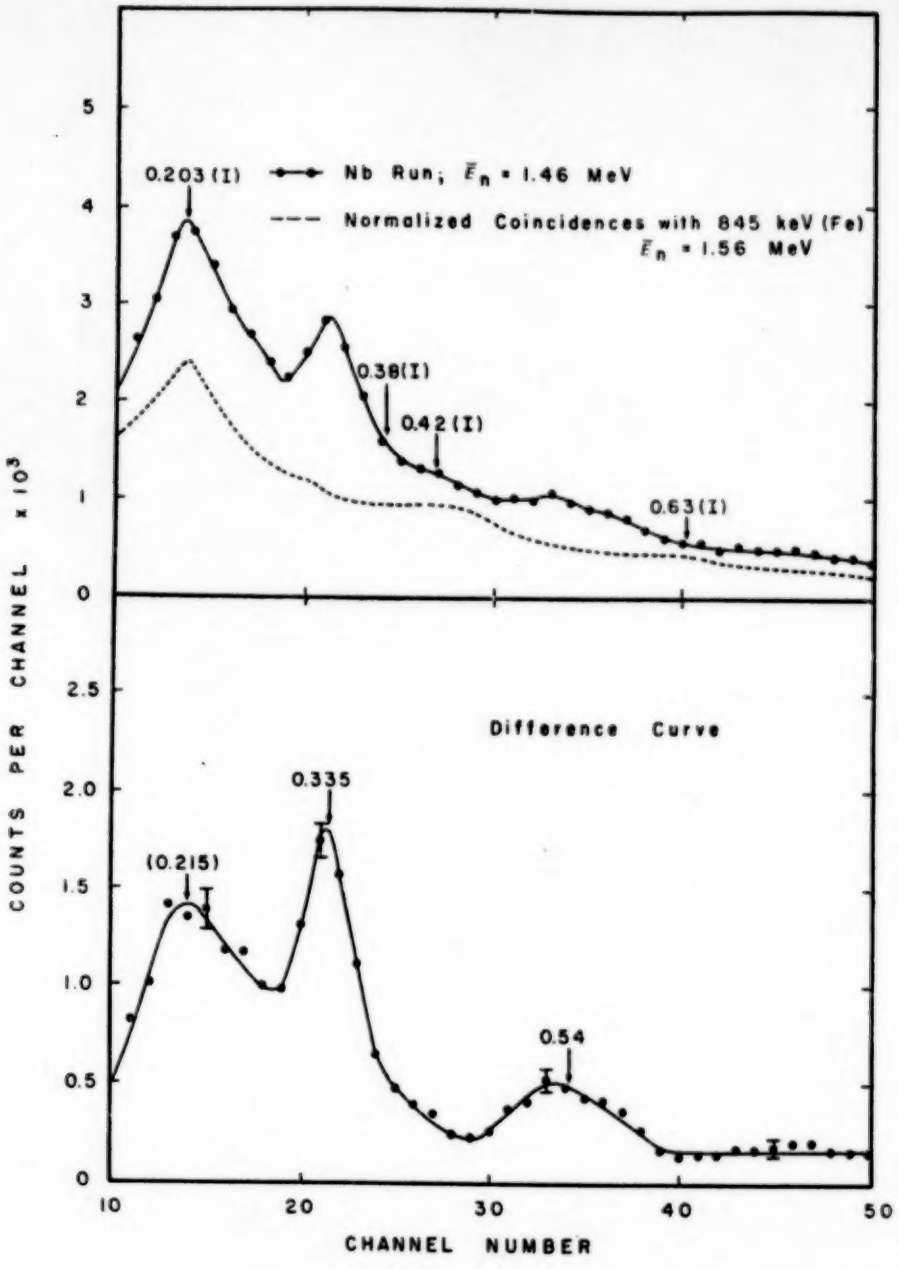

Fig. 3(a).

Coincidences with 0.741 MeV gamma ray from Nb^{93}; $E_n = 1.46$ MeV.

2.67 MeV so that cascades from higher levels could be observed making their appearance as the various levels were reached.

Figs. 3(a) and (b) show typical coincidence spectra obtained at average bombarding energies of 1.46 and 1.66 MeV. The former was taken in coincidence with the 0.74-MeV gamma ray, while the latter was in coincidence with the

0.958 MeV gamma ray. The normalized spectra obtained from iron are shown in dotted lines, while the difference curves are drawn below on a separate scale. Figs. 4(a) and (b) display the same information for a bombarding energy of

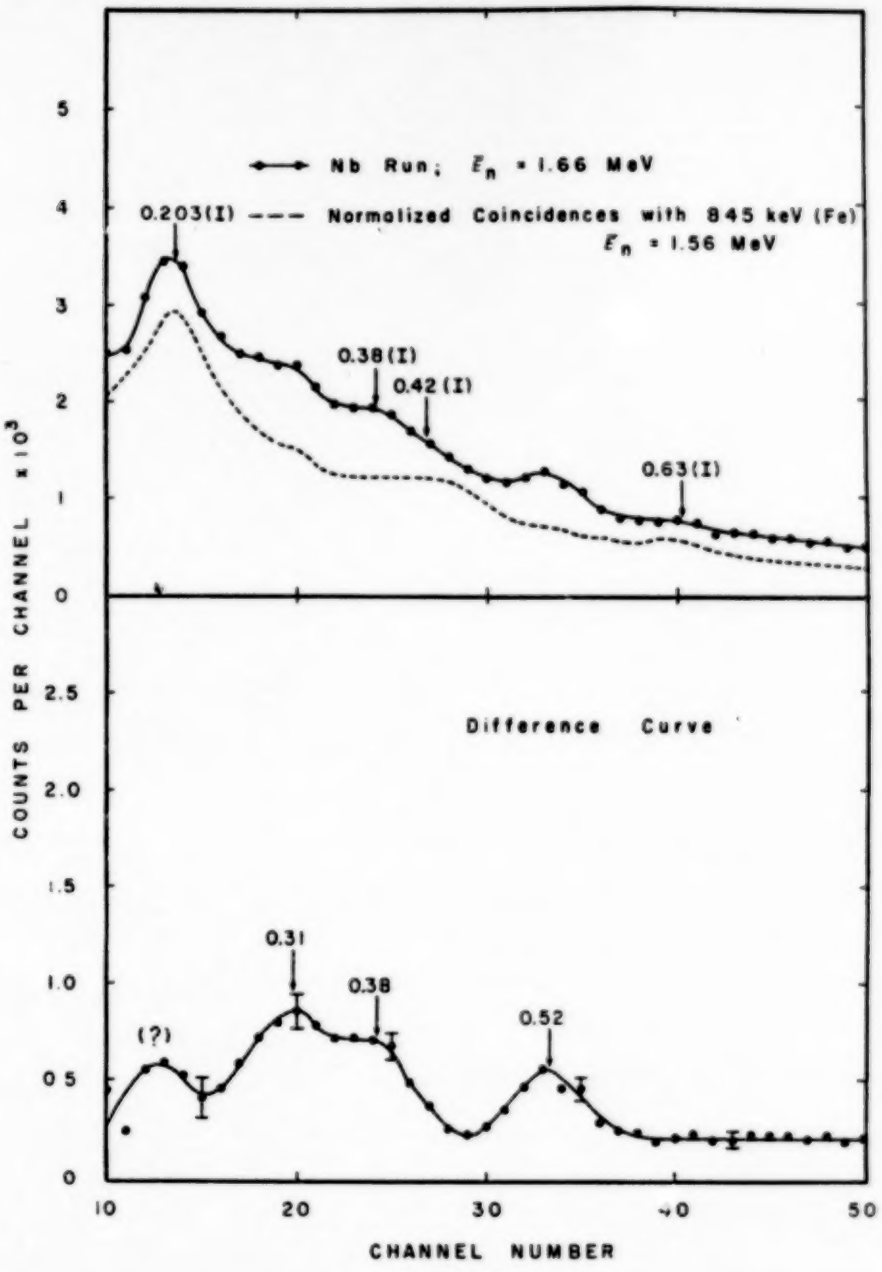

Fig. 3(b).

Coincidences with 0.958 MeV gamma ray from Nb^{93}; E_n = 1.66 MeV.

2.28 MeV. The peaks due to multiple scattering in iodine of the scintillator have been designated by the symbol '(I)' in these figures.

Due to the difficulty of making proper background subtraction, this coincidence data has not been used for quantitative yield measurements. However, some of the gamma rays observed in these coincidence measurements have

served as useful indicators of energy levels. In particular, the 0.335 MeV gamma ray was seen clearly in coincidence with 0.741 MeV before the presence

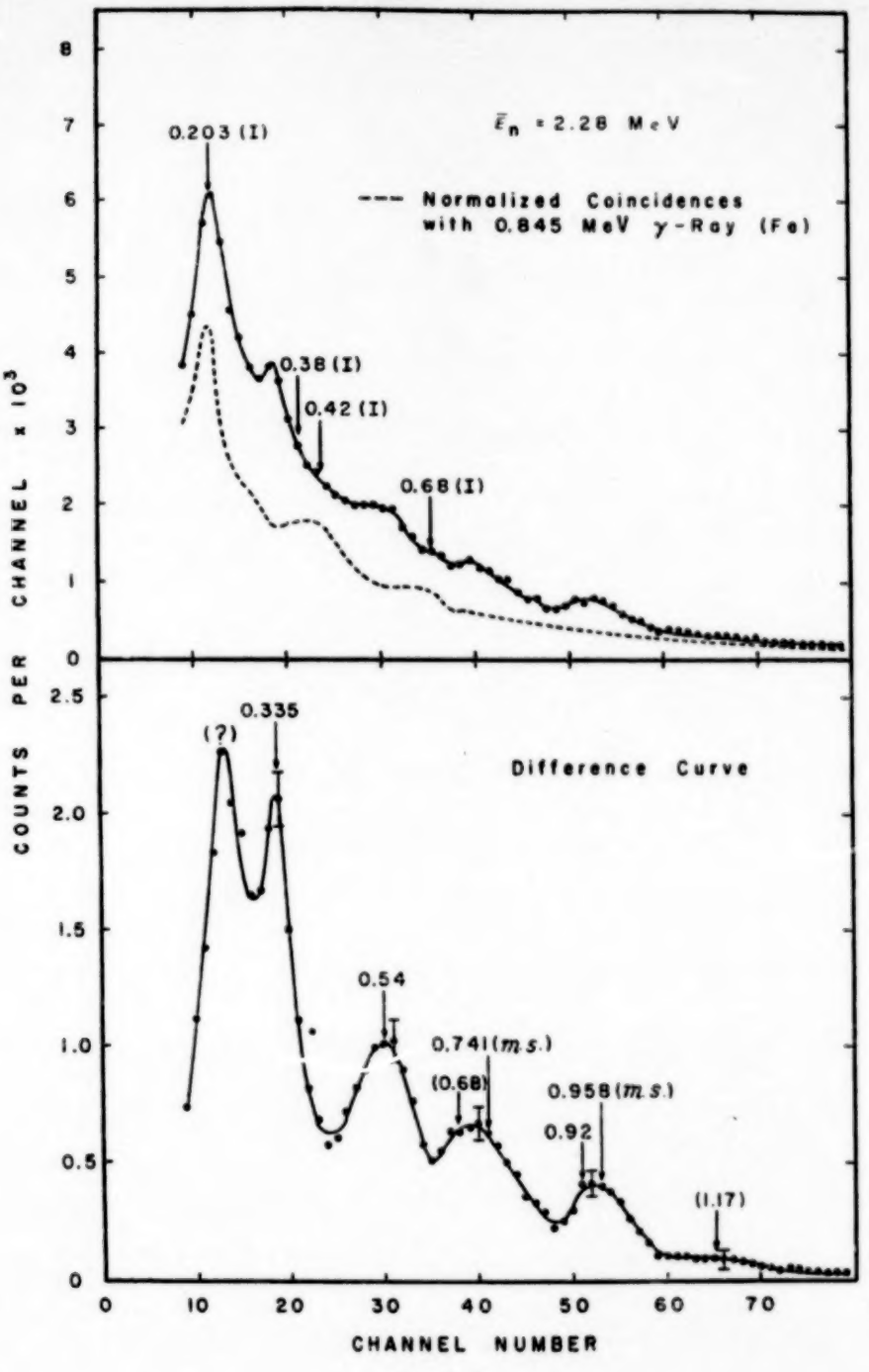

Fig. 4(a).

Coincidences with 0.741 MeV gamma ray from Nb^{93}; $E_n = 2.28$ MeV.

of the corresponding 1.08 MeV level was known. Also, the presence of a 0.38 MeV gamma ray in coincidence with 0.958 MeV transition provided the first evidence of a level at 1.34 MeV.

The results of the coincidence measurements have been summarized in table 1.

There is the possibility of a 0.74 MeV cascade transition arising from a level at 1.48 MeV to be in coincidence with the 0.741 MeV gamma ray. Likewise, a level at 1.92 MeV would give rise to a 0.96 MeV transition in coincidence with

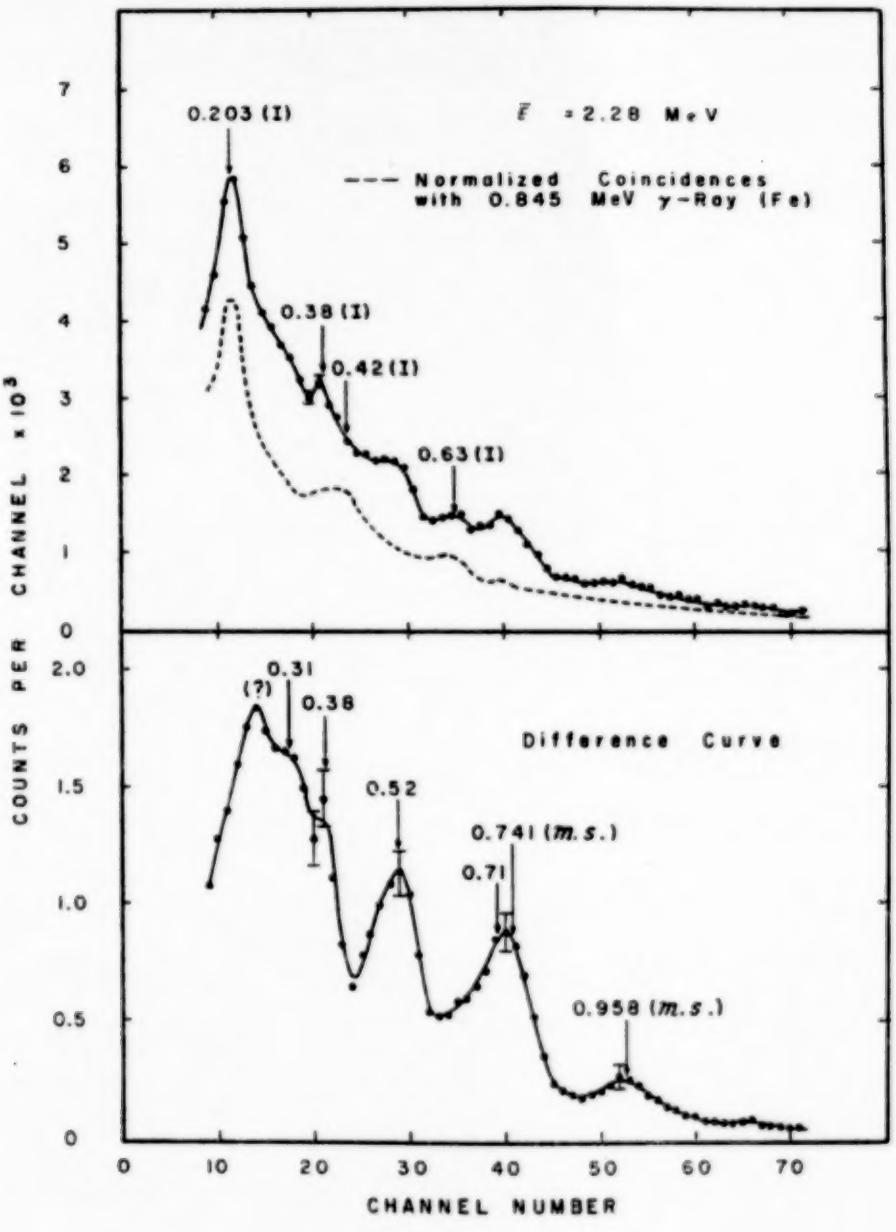

Fig. 4(b).

Coincidences with 0.958 MeV gamma ray from Nb^{93}; $E_n = 2.28$ MeV.

0.958 MeV gamma ray. These could not be resolved in the coincidence spectra from events due to multiple neutron scattering in niobium. Peaks arising due to such events have been indicated by the symbol 'm.s.' in figs. 3 and 4. Such peaks

in these figures must be considered at least in part due to multiple scattering.

There is some indication of a gamma ray at 0.68 MeV in the coincidence spectrum with 0.74 MeV. This may result due to a transition between the 1.48 and 0.81 MeV level. Since no effort was made to resolve the coincidences resulting from the 0.809 MeV gamma ray, this along with other possible cascades to the 0.81 MeV level could not be established unambiguously.

In fig. 3(a) a peak appears at an energy of 0.215 MeV. This may arise due to a

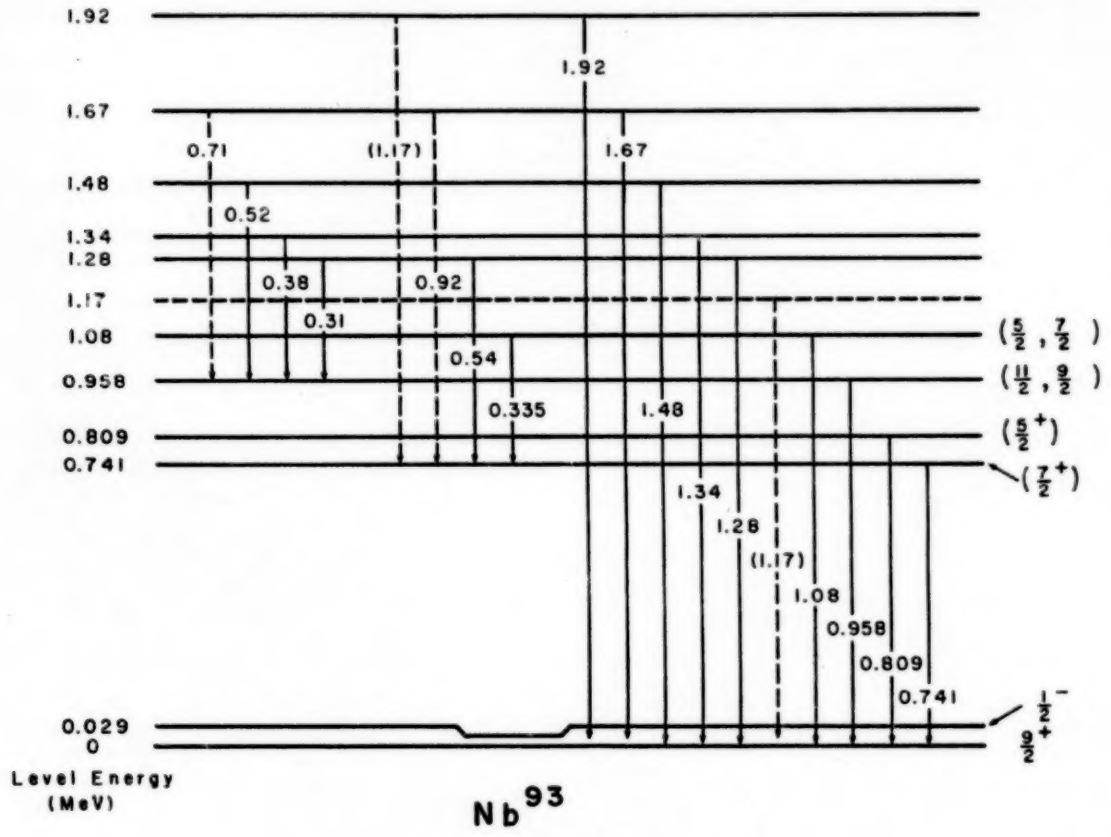

Fig. 5. Proposed Level Scheme of Nb^{93}.

cascade transition from the 0.958 MeV level. Large background due to back scattered gamma rays in this region and the possibility of imperfect subtraction of the iodine gamma ray at 0.203 MeV makes it difficult to draw any definite conclusion. However, an attempt was made to reduce the background by using $\frac{1}{8}''$ Pb-absorbers between the scatterer and each of the two detectors. Spectra in coincidence with 0.74 MeV gamma ray were taken at $E_n = 1.26$ MeV with and without the Pb-absorber in front of the detector on the 100-channel side. The subtraction of these two spectra resulted in a very conspicuous peak at 0.335 MeV and a hump in the neighbourhood of 0.22 MeV which may in part correspond to the cascade transition from the 0.958 MeV level. A run was also taken at $E_n = 1.08$ MeV. This data could provide us qualitative informa-

tion regarding the possible branching of 0.958 MeV level. It will be discussed further in the next section.

A peak at 1.17 MeV is indicated in fig. 4(a). Due to its low intensity it could not definitely be assigned to a possible cascade transition between the 1.92 and 0.741 MeV levels.

The peaks designated by a question mark in figs. 3 and 4 may arise due to imperfect subtraction of 0.203 MeV iodine peak or the back scattered gamma rays in that neighbourhood. A gradual cut-off of the coincidence circuit for the low energy gamma rays is also expected.

Fig. 5 shows the level-scheme for Nb^{93} indicating the various cascade and ground-state transitions observed in our singles or gamma-gamma coincidence spectra. Dotted vertical lines indicate transitions whose existence could not be established with certainty.

A comparison of our level scheme with the study of inelastic proton groups in Nb made by Cohen and Rubin [4]) indicate good agreement with their level positions of 0.74, 0.95, 1.32 and 1.47 MeV.

5. Branching ratios

The 0.741 and 0.958 MeV levels have been shown (by threshold measurements) to decay primarily by transitions to the ground state. In the case of the 0.809 MeV gamma ray it is not possible to measure the threshold with accuracy, so that it is not clear whether this gamma ray comes from a level at 0.81 MeV or 0.84 MeV. In the seventh section reasons will be given for preferring the 0.809 MeV assignment.

In the case of the 1.08 and 1.28 MeV levels, it was possible to make estimates of the branching ratios for the cascades through the 0.741 MeV level. The branching ratio is defined as I_0/I_1, where I_0 is the number of ground state transitions from the given level, and I_1 is the number of transitions to the intermediate level.

The decay of the 1.08 MeV level through the 0.741 MeV level gives the 0.335 MeV gamma ray. We have measured the relative intensities of the 0.335 and 1.08 MeV gamma rays in the singles spectrum. Since the counting rates are very high in the lower end of the spectrum compared with the higher end, this comparison was done in two steps. A short run was taken to obtain the intensity of the 0.335 MeV peak in comparison with the 0.741 MeV peak. Then a longer run was made with the lower part of the spectrum suppressed, giving the intensity of the 1.08 MeV peak in comparison with the 0.741 MeV peak. If the comparison had been attempted in one step, the counts in the lower part of the spectrum would have exceeded the storage capacity of the pulse-height analyzer before sufficient statistics had been obtained in the 1.08 MeV peak. Analysis of the data taken at $E_n = 1.25$ MeV resulted in a value of 0.5 ± 0.2 for this

branching ratio after corrections were made for the self-absorption in the scatterer and the crystal efficiency. As pointed out in our earlier publication [2]) the summing effect was taken care of by the use of a $\frac{1}{4}''$ Pb absorber between the scatterer and the detector.

There is some indication of a 0.27 MeV gamma ray resulting from the 1.08—0.81 MeV cascade. Since this peak falls in the region of back-scattered gamma rays in the singles spectrum, it is hard to measure its intensity. However a rough estimate gives a lower limit of 1.3 for the ratio I_0/I_1.

A lower limit for the branching of 0.958 MeV level by way of a possible cascade transition to 0.741 MeV level was estimated to be 15. This experimental value was obtained from the same set of data that was used to get the branching for the 1.08 MeV level. Another value for the branching of 0.958 MeV level was obtained from the coincidence run taken at a bombarding energy of 1.26 MeV using $\frac{1}{8}''$ Pb-absorbers between the scatterer and the detectors. The intensity of 0.22 MeV gamma ray was taken relative to that of 0.335 MeV in the same spectrum. Using relation (3) of our previous paper [2]) the branching ratio was calculated to be of the order of 30. We can thus give a value of $I_0/I_1 > 15$ for the branching of 0.958 MeV level.

Branching of the 1.28 MeV level by a 0.54 MeV cascade to the 0.741 MeV level was estimated from the singles data taken at $E_n = 1.46$ MeV. A value of $I_0/I_1 = 1.1 \pm 0.3$ was obtained. Assuming this branching ratio it was possible to estimate a lower limit of 2.0 for the ratio of the intensities of 1.48 MeV gamma ray to the 0.52 MeV cascade transition resulting from the level at 1.48 MeV. A run at $E_n = 1.64$ MeV was used to get the limiting value for this branching ratio.

6. Gamma Ray Production Cross Sections

As mentioned in section 3, the singles spectra were obtained at various bombarding energies and were analyzed to resolve the individual gamma rays, knowing the proper spectral shapes. Areas under the photopeaks were taken as a measure of the relative intensity of the gamma rays. Corrections were made for dead time in the 100-channel analyzer, as well as for the yield of the neutron monitor. To relate the intensities of each gamma ray from spectra obtained at different bombarding energies, it was necessary to normalize the gamma ray yield to a given number of neutrons in the forward direction. Since the neutron monitor was kept at 90°, a correction for the varying angular distribution of the neutrons was determined and applied.

The yields from the niobium were compared to the previously measured cross section for the 0.845 MeV gamma ray from iron as given by Day [5]) at a bombarding energy of 2.56 MeV. Since Day's measurement was made at an angle of 95°, while our detector subtended an angle ranging from 30° to 150°, it was

estimated that the cross section averaged over our detector was higher by 15 % due to the angular distribution as measured by Cranberg and Levin [6]). The cross section for the gamma ray from iron was taken to be 1.08 b at a bombarding energy of 2.56 MeV.

Using eq. (4) of our previous paper [2]), the cross sections for the niobium gamma rays were calculated. The results are given in table 3. Fig. 6 shows the

TABLE 3

Cross sections for the production of gamma rays by inelastic neutron scattering in Nb^{93}

γ-ray energy (MeV) \ E_n (MeV)	0.933	1.06	1.25	1.32	1.46	1.64	1.90	2.12
0.741	0.45	0.55	0.59	0.57	0.59	0.73	0.71	0.80
0.809	0.17	0.23	0.21	0.26	0.28	0.31	0.32	0.34
0.958	—	0.46	0.83	0.78	0.86	0.97	1.03	1.14
1.08	—	—	0.13	0.14	0.15	0.15	0.15	0.18
(1.17)	—	—	—	0.07	0.07	0.05	0.06	0.13
1.28	—	—	—	0.05	0.12	0.13	0.12	0.14
1.34	—	—	—	—	0.03	0.06	0.05	0.07
1.48	—	—	—	—	—	0.12	0.16	0.16
1.67	—	—	—	—	—	—	0.09	0.11
1.92	—	—	—	—	—	—	—	0.10

Cross-sections in barns.
Approximate probable error: ±30 %.

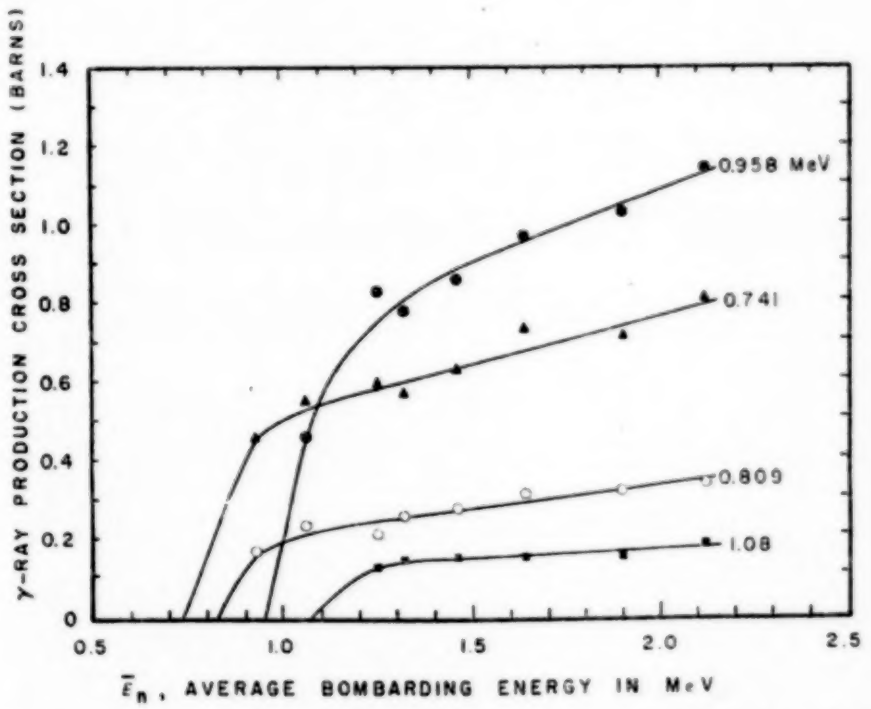

Fig. 6. Gamma-ray production cross sections for (n, n'γ) reaction in Nb^{93}.

yield curves plotted for the four most prominent gamma rays from these experimental values. The curves represent gamma ray yields, and will equal the cross section for excitation of the levels only after cascading has been taken into account. The rise of these yield curves with increasing energy is probably due to such cascades from higher levels.

A probable error of about ± 30 % is estimated for the absolute cross sections, although for the weak gamma rays (1.17, 1.34, and 1.66 MeV) the error may be greater.

7. Comparison with Theory; Probable Spin Assignments

Theoretical calculations based on Hauser-Feshbach theory were made employing the Univac computer at the Franklin Institute. The transmission

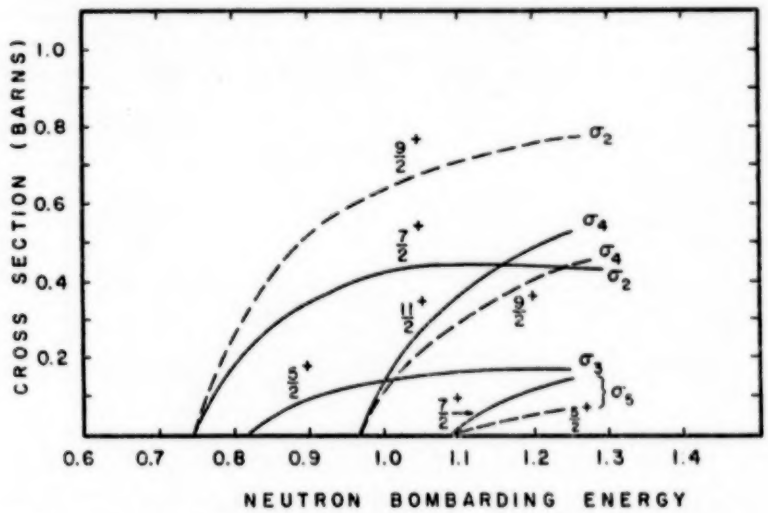

Fig. 7. Theoretical inelastic neutron scattering cross sections for Nb^{93}.

coefficients used in the calculations were based on the diffuse-edge nuclear potential as given in a report by W. S. Emmerich [7]). The various parameters have already been mentioned in our earlier publication [2]). Fig. 7 shows the result of these theoretical calculations for the second to fifth levels up to a bombarding energy of 1.2 MeV. The spins used were $\frac{9}{2}^+$ for the ground state, $\frac{1}{2}^-$ for the first excited (isomeric) state, and the other spins as indicated in the figure. The choice of the spins for the various levels was based on the results of threshold measurements for the 0.741 and 0.958 MeV levels, the qualitative information provided by the branching ratios observed for certain cascades, and the yields of the gamma-rays as outlined in the previous sections.

A comparison of figs. 6 and 7 indicates fairly good agreement between the theoretical and experimental cross-sections for spin assignments of $\frac{7}{2}^+$ and $\frac{5}{2}^+$ for the second and third excited states, respectively. The same spin values are indicated on the basis of shell-model predictions of a $g_{\frac{7}{2}}$ and $d_{\frac{5}{2}}$ excited

states next to the $g_{\frac{9}{2}}$ ground state. Furthermore, the energy separation of these two states is expected to be small [8]). As usually happens when the last odd proton is in the $g_{\frac{9}{2}}$ state, the $p_{\frac{1}{2}}$ state gets raised in energy to form a low-lying isomeric level above the $g_{\frac{9}{2}}$ ground state. The spacings and the spin assignments of the 0.741 and 0.809 MeV levels for $_{41}Nb^{93}$ relative to the $\frac{9}{2}^+$ ground state compare favorably with the level scheme proposed for the $_{41}Nb^{95}$ by Mittelman [8]).

The relative magnitude of the observed cross sections for gamma rays resulting from the second and third excited states and their comparison with theory tend to rule out the possibility of any other spin combination for these states. For example, at $E_n = 0.90$ MeV the ratio of the theoretical cross-sections for the 0.809 and 0.741 MeV levels is calculated to be 0.47, using spins of $\frac{7}{2}^+$ and $\frac{9}{2}^+$ for the respective levels. The same ratio is calculated to be 0.27, using spins of $\frac{5}{2}^+$ and $\frac{7}{2}^+$ for the two levels. The latter compares more favorably with the experimental value of 0.30 ± 0.07.

The shell model spin assignments for the second and third excited states are thus seen to agree with the measured cross sections. The parities for these two levels, on this basis, are both positive. If we consider the transition from the third level, we see that the E2 transition to the ground state is favored over the M3 transition to the isomeric state. This justifies our assumption that the level energy is the same as the gamma ray energy of 0.809 MeV.

For the fourth excited state at 0.958 MeV, the comparison between the theoretical and experimental cross sections near the threshold seems to favour a spin value of $\frac{11}{2}$ as compared to $\frac{9}{2}$. A level with spin $\frac{13}{2}$ will result in a lower theoretical cross section. In considering possible cascades through the 0.741 MeV level, calculations were made for the branching ratio I_0/I_1 using single-particle transition probabilities as given by Siegbahn [8]). Using spins of $\frac{9}{2}^+$ and $\frac{11}{2}^+$ for the 0.958 MeV level, and $\frac{7}{2}^+$ for the 0.741 MeV level, the values of 65 and 3×10^6 respectively were obtained for this branching. Comparing these values with the value of > 15 obtained as a limit in our measurements, the spin value of $\frac{9}{2}$ is suggested for the 0.958 MeV level. However, we give both $\frac{9}{2}$ and $\frac{11}{2}$ as the most likely spin values for the fourth level. Evidence presented here gives no indication about the parity of this state.

For the fifth excited state at 1.08 MeV, the branching ratios of 0.5 ± 0.2 and 1.3 were obtained for the 0.335 and 0.28 MeV cascades, respectively. Considering the various spin possibilities of $\frac{5}{2}^+$, $\frac{7}{2}^+$ and $\frac{9}{2}^+$ for this level, calculations were made for the theoretical ratio I_0/I_1, using the single-particle transition probabilities [8]). The best agreement with the experimental values corresponds to a spin value of $\frac{5}{2}$ for which the theoretical values of I_0/I_1 are 0.12 and 0.43 for the 0.335 and 0.28 MeV cascades, respectively. These theoretical values are based on a E2 ground-state transition and pure M1 cascade transitions. However, a slight deformation from the spherical shape of Nb^{93} nucleus can cause con-

siderable enhancement of the E2 transition due to the increased quadrupole moment of the nucleus. A comparison of the theoretical yield curve with the experimental one for the fifth level indicate a possible spin of $\frac{7}{2}$ or $\frac{5}{2}$. We tentatively propose either of these spin values as possible assignments for the 1.08 MeV level.

The spin assignments for the higher levels become exceedingly complicated to determine because of the existence of many cascade transitions whose intensities are difficult to measure in our type of experiment. In order to properly compare the theoretical cross-sections for the excitation of various levels with the gamma ray production cross-sections, corrections should be made in the latter to take account of the cascade transitions feeding the particular level concerned. It was because of these difficulties that the theoretical calculations were not pursued for the higher levels and for excitation energies above 1.2 MeV.

It may be mentioned here that the theoretical calculations of the cross-sections were also made using the black nucleus model with a square-well potential. The cross-sections were found to be about 80 to 100 percent lower than the experimental ones. Calculations using the cloudy crystal-ball model also yielded similar results. We may thus conclude that the diffuse-edge potential model gives much better agreement with the experimental cross sections than any square-well potential which we have tried. This is supported by our present calculations and the similar ones made for Mn [2]). The theoretical values lie within 30 % of the corresponding values from experiment.

We are grateful to Dr. W. F. G. Swann for his continuing support of this work. The cooperation of Mr. James Welsh, of the Franklin Institute Computing Center, has been greatly appreciated. The untiring help of Mrs. H. Davis, Miss Lillian Ries and Miss Barbara Smith in the preparation of the manuscript is thankfully acknowledged.

References

1) M. A. Rothman, D. M. Van Patter, V. S. Dubey, W. C. Porter and C. E. Mandeville, Phys. Rev. **107** (1957) 155
2) N. Nath, M. A. Rothman, D. M. Van Patter and C. E. Mandeville, Nuclear Physics **13** (1959) 74
3) F. I. Boley, E. H. Thorndike and A. T. Moffet, Phys. Rev. **110** (1958) 915
4) B. L. Cohen and A. G. Rubin, Phys. Rev. **111** (1958) 1568
5) R. B. Day, Phys. Rev. **102** (1956) 767
6) L. Cranberg and J. S. Levin, Phys. Rev. **103** (1956) 343
7) W. S. Emmerich, Westinghouse Research Report 6-94511-6-R19 (1958)
8) P. S. Mittelman, Phys. Rev. **94** (1954) 99
9) K. Siegbahn, Editor, Beta and Gamma Ray Spectroscopy (1955) p. 391

7.A *Nuclear Physics* **14** (1959/60) 97—105; © *North-Holland Publishing Co., Amsterdam*

Not to be reproduced by photoprint or microfilm without written permission from the publisher

A CONTRACTION RULE FOR COMPOSITE PARTICLES

R. BLANKENBECLER †

Palmer Physical Laboratory, Princeton University, Princeton, New Jersey ††

Received 1 August 1959

Abstract: A contraction rule for an arbitrary composite particle is derived, based on results due to Nishijima, and Klein and Zemach. The relation between this contraction rule and the analogous problem in potential scattering is demonstrated by an explicit reduction to the nonrelativistic limit. Applications of these rules are briefly discussed.

1. Introduction

Most of the studies of field theory have dealt with the relationship between free particle scattering states in the remote past and similar states in the remote future. However, there has been considerable progress in the description of reactions involving composite particles in the recent work of Haag [1]), Nishijima [2]), Zimmerman [3]) and Ekstein [4]).

The pourpose of this note is to derive similar, but distinct results based perhaps more closely on the presentation of field theory in terms of multiparticle Green's functions [5]). Use will be made of results due to Nishijima [6]) and Klein and Zemach [7]). In the interest of completeness, these results will be briefly reviewed where necessary. The conclusions of this paper are weaker than those of the first four cited authors, because the description of a composite particle in terms of a local field operator does not naturally arise.

In order to illustrate these two types of contraction rules, consider a bound state of two nucleons, the deuteron. Then the results of ref. [1, 2, 3]) would yield, for example,

$$\langle A|Bd^{(+)}\rangle = i^2\int \mathrm{d}^4x\mathrm{d}^4y\langle A|\mathrm{T}\left(\bar{\psi}(x+\tfrac{1}{2}y)\bar{\psi}(x-\tfrac{1}{2}y)\right)|B\rangle(-\Box_x{}^2+M_\mathrm{D}{}^2)f_d(y)\mathrm{e}^{id\cdot x},$$

where M_D is the deuteron mass and $f_d(y)$ is a suitably normalized, but otherwise almost arbitrary spinor function of y. It has been assumed that A does not contain a deuteron. The results of this paper yield for this case

$$\langle A|Bd^{(+)}\rangle = i^2\int \mathrm{d}^4x\mathrm{d}^4y\langle A|\mathrm{T}(\bar{\psi}(x+\tfrac{1}{2}y)\bar{\psi}(x-\tfrac{1}{2}y))|B\rangle G^{-1}[2]$$
$$\times\langle 0|\mathrm{T}(\psi(\tfrac{1}{2}y)\psi(-\tfrac{1}{2}y))|d\rangle\mathrm{e}^{id\cdot x},$$

† N. S. F. Post-doctoral Fellow.

†† Supported in part by the Air Force Office of Scientific Research and a grant by the National Science Foundation.

where $G^{-1}[2]$ is the inverse two nucleon Green's function; it satisfies the equation

$$G^{-1}[2]G[2] = \left(\gamma\cdot\frac{\partial}{\partial x}+m\right)\left(\gamma\cdot\frac{\partial}{\partial y}+m\right) i^2\langle 0|\mathrm{T}(\psi(x)\psi(y)\bar{\psi}(x')\bar{\psi}(y'))|0\rangle$$
$$-\int \mathrm{d}^4\bar{x}\mathrm{d}^4\bar{y}V(x,y;\bar{x},\bar{y})i^2\langle 0|\mathrm{T}(\psi(\bar{x})\psi(\bar{y})\bar{\psi}(x')\bar{\psi}(y'))|0\rangle$$
$$=\delta(x-x')\delta(y-y'),$$

where V is the two-nucleon interaction kernel and the Pauli principle has been neglected. While this latter form of the contraction rule would seem to be vastly more complicated than the former, it seems to be quite convenient for the explicit evaluation of certain matrix elements (see ref. [10])). The difficult problem in the former approach is the normalization of the function $f_d(y)$ because here also, a knowledge of the two-body amplitude $\langle 0|\mathrm{T}(\psi(\frac{1}{2}y)\psi(-\frac{1}{2}y))|d\rangle$ is required.

In sec. 2 the relation between the S-matrix and multiparticle Green's functions is reviewed. This leads naturally to the contraction rules for general bound systems. In sec. 3 these rules are used to derive some familiar results and also an integral equation relating the two-nucleon interaction kernel to a six-point vacuum expectation value. This equation may be of interest in inferring properties of the kernel from the presumably simpler properties of this six-point function. Finally, the non-relativistic limit of the contraction rule is thoroughly discussed.

2. Contraction Rules

The following discussion will be mainly concerned with establishing the relationship between the S-matrix and the set of multiparticle Green's functions which are conveniently defined as [4])

$$G[n,m] = i^n i^{[\frac{1}{2}m]}\langle 0|\mathrm{T}(\psi(x_1)\ldots\psi(x_n)\bar{\psi}(x'_1)\ldots\bar{\psi}(x'_n)\phi(y_1)\ldots\phi(y_m))|0\rangle \quad (1)$$

where $\psi(\phi)$ is a renormalized fermion (boson) field and $[\frac{1}{2}m]$ means the nearest, smaller integer in $\frac{1}{2}m$. The Wick chronological ordering symbol [8]) is denoted by T. In analogy with the treatment of the single particle case it is convenient to introduce amplitudes with the aid of which the G's can be constructed:

$$\chi_\alpha^{(\pm)} = \langle 0|\mathrm{T}(\psi\ldots\bar{\psi}\ldots\phi\ldots)|\alpha^\pm\rangle,$$
$$\bar{\chi}_\alpha^{(\pm)} = \langle\alpha^\pm|\mathrm{T}(\psi\ldots\bar{\psi}\ldots\phi\ldots)|0\rangle. \quad (2)$$

In order to spare the reader a seeming hodge-podge of multiparticle functions, and in order to illustrate the physical simplicity of this discussion, it is convenient to consider a simple yet non-trivial example. We choose to discuss inelastic nucleon-deuteron scattering to fulfil these purposes.

The S-matrix element of interest is therefore

$$S = \langle abc^{(-)}|ed^{(+)}\rangle, \tag{3}$$

where a, b, c are the final nucleons, e the initial free nucleon, and d the initial deuteron state. The relevant Green's function is

$$G[3] = i^3\langle 0|\mathrm{T}(\psi_a\psi_b\psi_c\bar{\psi}_e\bar{\psi}_N\bar{\psi}_P)|0\rangle, \tag{4}$$

which is assumed to be expressible in the form

$$\begin{aligned} G[3] = {} & G[1]\ G[1]\ G[1]H\ G[1]\ G[1]\ G[1]+G[1]\ G[2]\ IG[1]\ G[1]\ G[1] \\ & +G[1]\ G[1]\ G[1]\ JG[2]\ G[1]+G[1]\ G[2]\ KG[2]\ G[1]. \end{aligned} \tag{5}$$

This assumption would seem to be equivalent to the assumption that scattering theory is applicable, namely, that the particles eventually get out of the interaction region. Here we have introduced the scattering operators H, I, J and K to represent the interaction between the deuteron and the nucleons and defined the one-and two-particle Green's function as

$$\begin{aligned} G_{\mathrm{N}}^{-1} &= i\gamma\cdot N+m \\ G_{\mathrm{D}}^{-1} &= G_{\mathrm{N}}^{-1}G_{\mathrm{P}}^{-1}-V, \end{aligned} \tag{6}$$

where V is the interaction kernel between the bound nucleons [9, 5]) and is in reality an integral operator. While (5) would not seem to be correctly anti-symmetrized, the final results will be seen to posses the correct symmetry.

The nucleon and deuteron amplitudes are introduced as

$$\begin{aligned} \langle 0|\psi_N|N\rangle &= \chi_N \\ \langle 0|\mathrm{T}(\psi_N\psi_P)|d\rangle &= \chi_d, \end{aligned} \tag{7}$$

with similar definitions for the conjugate amplitudes. The normalization condition to be imposed on the two-body amplitude has been discussed elsewhere [6, 7]). The amplitudes satisfy the homogeneous integral equations

$$\begin{aligned} G_{\mathrm{N}}^{-1}\chi_N &= 0 \\ G_{\mathrm{D}}^{-1}\chi_D &= 0. \end{aligned} \tag{8}$$

In order to connect the Green's function and the S-matrix, it is clear that a limiting operation must be performed and a suitable asymptotic condition imposed. Following Klein and Zemach [7]) the operation $L(t';t)$ is introduced and defined by

$$L(t';t)G[3] = i^3\langle 0|\mathrm{T}(\psi\psi\psi)_{t'}T(\bar{\psi}\bar{\psi}\bar{\psi})_t|0\rangle, \tag{9}$$

where t' and t are the centre-of-mass times of their respective groups of fields. These times are assumed to approach $+\infty$ and $-\infty$, respectively, while the relative times in each group are kept finite. By inserting two complete sets of

physical states, this can be written in terms of many-body amplitudes and the S-matrix, namely,

$$L(t';t)G[3] = i^3 \sum_{\alpha\beta} \langle 0|\mathrm{T}(\psi\psi\psi)_{t'}|\beta^{(-)}\rangle S_{\beta\alpha}\langle\alpha^{(+)}|T(\bar{\psi}\bar{\psi}\bar{\psi})_t|0\rangle, \tag{10}$$

where $S_{\beta\alpha} = \langle\beta^{(-)}|\alpha^{(+)}\rangle$.

Since we are interested at the moment in inelastic scattering only, the state α is taken to represent asymptotically a deuteron and a nucleon, while β represent three free nucleons. In the limit as t approaches $-\infty$, the $\alpha^{(+)}$ amplitude must break up into a product of nucleon and deuteron amplitudes,

$$\lim_{t\to-\infty} \langle\alpha^{(+)}|\mathrm{T}(\bar{\psi}\bar{\psi}\bar{\psi})_t|0\rangle = \bar{\chi}_N{}^{\alpha}(t)\bar{\chi}_D{}^{\alpha}(t),$$

where the other space-time arguments have been suppressed. This is, in fact, the meaning of the outgoing wave boundary condition indicated by $(+)$. For the ingoing wave state β, we have an analogous condition,

$$\lim_{t'\to+\infty} \langle 0|\mathrm{T}(\psi\psi\psi_{t'})|\beta^{(-)}\rangle = \chi_a{}^{\beta}(t')\chi_b{}^{\beta}(t')\chi_c{}^{\beta}(t').$$

Thus we see that

$$L(t';t)G[3] = i^3 \sum_{\alpha\beta} \chi_a{}^{\beta}(t')\chi_b{}^{\beta}(t')\chi_c{}^{\beta}(t')S_{\beta\alpha}\bar{\chi}_N{}^{\alpha}(t)\,\bar{\chi}_D{}^{\alpha}(t) + \ldots \tag{11}$$

This limiting operation can also be performed on the explicit form of $G[3]$, eq. (5). Recalling the definition of the one and two body Green's functions, the resulting equation can be written as

$$\begin{aligned} L(t';t)G[3] = {} & i^6 \sum_{\alpha\beta} \chi_a{}^{\beta}\chi_b{}^{\beta}\chi_c{}^{\beta}(t')(\bar{\chi}_a{}^{\beta}\bar{\chi}_b{}^{\beta}\bar{\chi}_c{}^{\beta}|J|\chi_e{}^{\alpha}\chi_D{}^{\alpha}) \\ & \times\bar{\chi}_e{}^{\alpha}\bar{\chi}_D{}^{\alpha}(t) + \ldots \end{aligned} \tag{12}$$

where the round bracket represents a space-time integral over the relevant coordinates, and the . . . stands for terms that will not contribute to the reaction of interest.

Exploiting the equality of eqs. (11) and (12) throughout a semi-infinite time period, which provides a weak form of orthogonality, allows the inference that

$$S_{\beta\alpha} = i^3(\bar{\chi}_a{}^{\beta}\bar{\chi}_b{}^{\beta}\bar{\chi}_c{}^{\beta}|J|\chi_e{}^{\alpha}\chi_D{}^{\alpha}). \tag{13}$$

From the relation between J and $G[3]$, this can be cast into the form

$$S_{\beta\alpha} = i^3(\bar{\chi}_a{}^{\beta}\bar{\chi}_b{}^{\beta}\bar{\chi}_c{}^{\beta}|G_a{}^{-1}[1]G_b{}^{-1}[1]G_c{}^{-1}[1]G[3]G_e{}^{-1}[1]G_d{}^{-1}[2]|\chi_e{}^{\alpha}\chi_d{}^{\alpha}). \tag{14}$$

Since the example considered has only one composite particle present, it is possible to use standard procedures [10]) to "uncontract" the free particles and hence to derive the contraction prescription for the deuteron. This approach cannot be used in the general case however where there are no elementary particles present. A convenient procedure to use here is demonstrated in

appendix A. This proceeds by introducing anticommuting fermion source functions into the Lagrangian and by using the differential action principle [5]).

In the present example if the nucleons are uncontracted the S-matrix achieves the form

$$S_{\beta\alpha} = i^2 \int \langle abc^{(-)}|\mathrm{T}(\bar{\psi}\bar{\psi})|e\rangle G_d^{-1}[2]\chi_d. \tag{15}$$

Reference back to eq. (14) and the commutation relations of the field operators in $G[3]$ shows that the Pauli principle has been correctly maintained in the initial state.

The canonical contraction rule for a bound state C composed of N fermions can be inferred in a similar manner with the aid of appendix A, and is found to be of the form

$$\langle AC^{(-)}|\mathrm{B}\rangle = i^N \int \bar{\chi}_c[N]G^{-1}[N]\langle A|\mathrm{T}(\psi_1 \ldots \psi_N)|B\rangle, \tag{16}$$

and

$$\langle A|CB^{(+)}\rangle = i^N \int \langle A|\mathrm{T}(\bar{\psi}_1 \ldots \bar{\psi}_N)|B\rangle G^{-1}[N]\chi_c[N], \tag{17}$$

plus the usual inhomogeneous term if there is a bound state C present in B or A. The extension to a bound state consisting of any number of particles, antiparticles and bosons is straightforward, provided this state cannot decay, a possibility which would violate the asymptotic assumptions. For the application of these formulae to the particular case of the deuteron, the reader is referred to a discussion of elastic neutron-deuteron scattering by dispersion theory [10]). There the relation between the contraction rule given by eqs. (16) and (17), and a non-relativistic discussion of the transition amplitude is thoroughly discussed for the familiar case of the deuteron.

3. Discussion

In order to clarify the physical content of these contraction rules, they will be used to derive some familiar results. First, it is amusing to note the consistency of these rules by contracting the bound state in the many particle amplitude itself. That is, the operations

$$\begin{aligned}\chi_c[N] &= \langle 0|\mathrm{T}(\psi_1 \ldots \psi_N)|C\rangle \\ &= i^N \int \langle 0|\mathrm{T}(\psi_1 \ldots \psi_N \bar{\psi}_1 \ldots \bar{\psi}_N)|0\rangle G^{-1}[N]\chi_c[N] \\ &= \int G[N]G^{-1}[N]\chi_c[N]\end{aligned}$$

yield an identity.

An application of the contraction rules to the amplitude representing a two-nucleon scattering state $\beta^{(+)}$ yields the result

$$\chi_\beta^{(+)} = \langle 0|\mathrm{T}(\psi\psi)|\beta^{(+)}\rangle = \int G[2]G_N^{-1}G_P^{-1}u_P^\beta u_N^\beta.$$

The equation satisfied by the two-nucleon Green's function leads immediately to the form

$$\chi_\beta^{(+)} = u_P^\beta u_N^\beta + \int G[2] V u_P^\beta u_N^\beta, \tag{18}$$

which is the formal solution of the familiar integral equation

$$\chi_\beta^{(+)} = u_P^\beta u_N^\beta + \int G_P G_N V \chi_\beta^{(+)}. \tag{19}$$

This equation was derived by Salpeter and Bethe and Gell-Mann and Low [9]). This shows the consistency of the contraction rules and the in-put data, eq. (8).

It is also possible to derive an integral equation for the interaction kernel V. Consider a bound state d, then

$$G_P^{-1} G_N^{-1} \chi_d = \langle 0|\mathrm{T}(j_P j_N)|\mathrm{d}\rangle, \tag{20}$$

where the nucleon currents are defined by

$$G_i^{-1} \psi_i = j_i \tag{21}$$

and the equal-time commutator does not contribute. Contracting the deuteron, we achieve the form

$$G_P^{-1} G_N^{-1} \chi_d = i^2 \int \langle 0|\mathrm{T}(j_P j_N \bar{\psi}\bar{\psi})|0\rangle G^{-1}[2] \chi_d.$$

Since by definition the right-hand side of this equation is equal to the interaction kernel applied to the deuteron amplitude, it follows by direct comparison that

$$V = i^2 \langle 0|\mathrm{T}(j_P j_N \bar{\psi}\bar{\psi})|0\rangle (G_P^{-1} G_N^{-1} - V). \tag{22}$$

If the meson-nucleon interaction is of a linear type, the nucleon current is of the form

$$j_i = \Gamma \psi_i \phi, \tag{23}$$

plus renormalization terms. Thus, we see that the kernel V is determined in terms of the six-point multiparticle Green's function $G[2, 2]$. A perturbation expansion of the integral equation (22) shows explicitly that V is the sum of all irreducible diagrams, in agreement with the graphical analysis of Salpeter-Bethe [8]). The function $G[2, 2]$ contains both reducible and irreducible graphs, but the structure of the integral equation is such as to insure the irreducibility of the contributions to V. It should be pointed out that this equation can also be derived directly from a discussion of the relevant four-and six -point Green's functions.

It is both interesting and instructive to perform a nonrelativistic reduction of these contraction rules. In order to carry out this program, the reduction procedure developed by Salpeter [11]) for the two-fermion problem must be generalized to the N-body case. This can be done in a straightforward manner, as follows.

The N-nucleon amplitude satisfies the equation

$$G_1^{-1} \ldots G_N^{-1} \chi[N] = \int V[N] \chi[N] \mathrm{d}^4 x'_1 \ldots \mathrm{d}^4 x'_N, \tag{24}$$

where $V[N]$ is the interaction kernel representing the interaction between all N nucleons. This can also be written in the form

$$G^{-1}[a] G^{-1}[N-a] \chi[N] = \int V[a, N-a] \chi[N] \mathrm{d}^4 x'_1 \ldots \mathrm{d}^4 x'_N, \tag{25}$$

where $V[a, N-a]$ represents the interaction between the two groups (a) and $(N-a)$. The interactions within each group are contained in the Green's functions on the left-hand side of this equation.

From translational invariance it is possible to extract from $\chi[N]$ its exponential dependence on the centre-of-mass coordinate. We assume that this has been done. Then consider eq. (24) in momentum space for an instantaneous potential $v[N]$, that is a potential which does not depend on the fourth component of any relative momentum variable. Defining an equal-time wave function $\varphi[N]$ as the integral of $\chi[N]$ over the fourth component of all the relative coordinates P allows eq. (24) to be written as

$$G_1^{-1} \ldots G_N^{-1} \chi[N] = \int v[N] \varphi[N] \mathrm{d}^3 P'_1 \ldots \mathrm{d}^3 P'_{N-1}.$$

Using the easily proved formula

$$\int \mathrm{d}P_1^0 \ldots \mathrm{d}P_{N-1}^0 G_1 \ldots G_N = (2\pi i)^{N-1} C_{N-1} [E_N - H_1 \ldots - H_N]^{-1},$$

where E_N is the total energy in the centre-of-mass system, the H_i are the Dirac Hamiltonians for the respective particles, C_{N-1} is a constant, and negative energy effects have been neglected, it is seen that $\varphi[N]$ satisfies a Breit-type equation. This equation can be immediately reduced to a Schroedinger equation. Thus $\varphi[N]$ can be identified with the Schroedinger wave function in the non-relativistic limit. If this procedure is applied to eq. (25), it is immediately ascertained that

$$G^{-1}[a] G^{-1}[N-a] \chi[N] = \int v[a, N-a] \varphi[N] \mathrm{d}^3 P'_1 \ldots \mathrm{d}^3 P'_{N-1},$$

or by using the Schroedinger equation

$$G^{-1}[a] G^{-1}[N-a] \chi[N] = (H - H_a - H_{N-a}) \varphi[N], \tag{26}$$

where H is the total Hamiltonian.

Now consider, as an example, a scattering process in which the initial configuration B scatters into two final composite particles a and c, where we assume that $n_a + n_c \equiv n_B = N$. If the two final particles are contracted, the scattering matrix M is of the form

$$M = i^N \int \bar{\chi}[a] \bar{\chi}[c] G^{-1}[a] G^{-1}[c] \chi_B^{(+)}[N] \mathrm{d}^4 x_1 \ldots \mathrm{d}^4 x_N.$$

If the centre-of-mass integration is performed, the delta function conserving the total enrgy-momentum is attained. Using eq. (26), M immediately reduces to

$$M = 2\pi i^N \delta(P_B - P_a - P_c) \int \bar{\varphi}[a]\bar{\varphi}[c](H - E_a - E_c)\varphi_B^{(+)}[N] J \mathrm{d}^3 r_1 \ldots \mathrm{d}^3 r_{N-1}. \quad (27)$$

where the $r_1 \ldots r_{N-1}$ are a set of relative coordinates and J the appropriate Jacobian. This is the non-relativistic result [13]). If the state $\varphi^{(+)}[B]$ satisfies the Pauli principle, then it is obvious that M also does.

It is therefore clear that the inverse of the many-body Greens' function in the contraction rule merely serves to extract from consideration those interactions which produce the asymptotic composite particle.

I wish to thank Drs. M. Baker and F. Zachariasen for conversations which led to this note. Illuminating discussions with Professor R. Haag are gratefully acknowledged.

Appendix A

In order to demonstrate the generality of the approach used here, consider the scattering process $a+b \to c+d$, where any or all of the participating particles may be composite, with nucleon number $n_a \ldots n_d$, where

$$n_a + n_b = n_c + n_d = N.$$

This restriction to fermions is not in any way essential. Using arguments similar to those that led to eq. (14), the S-matrix is found to be

$$(S-1)_{fi} = i^N (\bar{\chi}_c \bar{\chi}_d | G^{-1}[n_c] G^{-1}[n_d] G[N] G^{-1}[n_a] G^{-1}[n_b] | \chi_a \chi_b).$$

If anticommuting external fermion source functions f were added to the Lagrangian in the form $(-\bar{f}\psi + \bar{\psi} f)$, so that nucleon number need not be conserved in a scattering process, we could consider the following reaction:

$$\langle cd^{(-)} | a \rangle = i^{N+n_a} (\bar{\chi}_c \bar{\chi}_d | G^{-1}[n_c] G^{-1}[n_d] \langle 0 | \mathrm{T}(\psi_1 \ldots \psi_N \bar{\psi}_1 \ldots \bar{\psi}_{n_a} | 0 \rangle \times G^{-1}[n_a] | \chi_a).$$

By taking n_b variational derivatives of this equation with respect to the source f, and using the action principle, we find

$$i^{n_b} \langle cd^{(-)} | \mathrm{T}(\bar{\psi}_1 \ldots \bar{\psi}_{n_b}) | a \rangle = i^N (\bar{\chi}_c \bar{\chi}_d | G^{-1}[n_c] G[N] G^{-1}[n_a] | \chi_a).$$

The external sources are now allowed to vanish.

Direct substitution of this equation into the expression for the S-matrix leads to the contraction rule for the system b:

$$(S-1)_{fi} = i^{n_b} \int \langle cd^{(-)} | \mathrm{T}(\bar{\psi}_1 \ldots \bar{\psi}_b) | a \rangle G^{-1}[n_b] \chi_b.$$

It is clear that this type of procedure can be used in any general scattering process.

References

1) R. Haag, Phys. Rev. **112** (1958) 669
2) K. Nishijima, Phys. Rev. **111** (1958) 995
3) W. Zimmerman, Nuovo Cimento **10** (1958) 597
4) H. Ekstein, Nuovo Cimento **4** (1956) 1017
5) J. Schwinger, Proc. Nat. Acad. Sci. U. S. **37** (1951) 452, 455 and unpublished lectures
6) K. Nishijima, Progr. Theoret. Phys. **14** (1955) 175; and previous articles
7) A. Klein and C. Zemach, Phys. Rev. **108** (1957) 126
8) G. C. Wick, Phys. Rev. **80** (1950) 268
9) E. E. Salpeter and H. A. Bethe, Phys. Rev. **84** (1951) 1232;
   M. Gell-Mann and F. Low, Phys. Rev. **84** (1951) 350
10) Lehmann, Symanzik and Zimmerman, Nuovo Cimento **1** (1955) 205
11) Blankenbecler, Goldberger and Halpern, Nuclear Physics **12** (1959) 647
12) E. E. Salpeter, Phys. Rev. **87** (1952) 328
13) W. Brenig and R. Haag, Fortschr. d. Physik (to be published)

4.A:4.C *Nuclear Physics* **14** (1959/60) 106—116; © *North-Holland Publishing Co., Amsterdam*
Not to be reproduced by photoprint or microfilm without written permission from the publisher

γ_5 SYMMETRIES AND RELATIVISTIC CORRECTIONS IN BETA DECAY

MASATO MORITA
Columbia University, New York †

Received 1 August 1959

Abstract: Making the postulate that the four-fermion interaction must be invariant under the mass reversal transformation $\psi \to \gamma_5\psi$ and $m \to -m$, for every pair of the four fields simultaneously, we obtain the V−A interaction where $C_V = -C_A$, $C'_V = -C'_A$ and C_V/C'_V is arbitrary. This invariance property is very useful in finding a similarity between the nth and the $(n \pm 1)$th forbidden transitions in beta decay. In particular, corrections due to the relativistic matrix elements are given for the various formulae describing all kinds of the phenomena in the allowed beta decay. The Coulomb corrections and the finite de Broglie wavelength effect are taken into account simultaneously.

1. Introduction

In the conventional theory of beta decay, the relativistic corrections are omitted for all phenomena of the allowed transitions. This approximation is certainly good, when the maximum electron energy is not too high. In the case of high energy electrons, however, the contribution due to relativistic terms becomes significant.

Recently, Gell-Mann proposed a theory of beta decay in which one considers both direct beta decay of the nucleons and beta decay through the meson cloud of the nucleons [1]). In this theory, the calculated transition probability of beta decay is the same as that of the conventional theory, except for the magnitude of the relativistic corrections. Therefore, it is in principle possible to discriminate between these two theories of beta decay by a precise measurement of the relativistic corrections. For this purpose, Gell-Mann calculated the spectral shape of the beta rays [1]). Directional correlations of the beta ray and gamma or alpha ray were also given by many authors [2, 3, 4]). A similar calculation taking into account the coordinate-type second forbidden matrix elements and the finite de Broglie wavelength effect has been carried out by the present author for the spectral shape and the directional correlations [3]). In that paper, a comparison of the coordinate-type and momentum-type (relativistic) matrix elements has been made. It was shown that the coordinate-type matrix elements are rather small compared with the relativistic ones. A general rule to derive the relativistic corrections has been given [5]).

† This work was partially supported by the U. S. Atomic Energy Commission.

In this paper, we propose a principle by means of which we can introduce the V—A four-fermion interaction. Several invariance properties of this interaction are summarized in section 2. In section 3, we demonstrate a similarity between the nth and the $(n\pm1)$th forbidden transition in beta decay. With this relation the labour of calculation of the transition probability is always reduced by half. The general rule for deriving the relativistic corrections [5]) is reproduced for completeness. Various formulae of the angular correlations and beta-ray spectrum for the allowed beta decay are given in section 4. The electron-neutrino angular correlation and the longitudinal polarization of beta particles are given in sections 5 and 6.

2. γ_5 Symmetries and V—A Interaction

The four-fermion interaction responsible for the weak decays has many interesting symmetries with respect to the transformations of the four fields involving γ_5, such as the mass reversal transformation, $\psi \to \gamma_5\psi$, $m \to -m$ [6]) †, or the chirality transformation [7]) $\psi \to \gamma_5\psi$. In this section, we summarize these properties of the four-fermion interaction studied by many authors. We give also a principle for which the four-fermion interaction is V—A.

First we assume the four-fermion interaction in the usual form

$$\begin{aligned} H_{\text{int}} &= \sum_i (\bar{\psi}_1 O_i \psi_2)[\bar{\psi}_3 (C_i O_i + C'_i O_i \gamma_5)\psi_4] + \text{h.c.} \\ &= a\text{S} + b\text{V} + c\text{T} + d\text{A} + e\text{P}, \end{aligned} \tag{1}$$

satisfying the invariance requirement under proper Lorentz transformations. In the second line of the above equation, a, b, c, d and e are certain constants to be determined by further assumptions. The Dirac equation

$$[i\gamma_\mu(\partial_\mu - iA_\mu) + m]\psi = 0 \tag{2}$$

is invariant under the transformation

$$\psi \to \gamma_5\psi, \quad \bar{\psi} \to -\bar{\psi}\gamma_5, \quad m \to -m. \tag{3}$$

We apply this transformation to two fields out of the four, e.g. $\psi_1 \to \gamma_5\psi_1$ $(\bar{\psi}_1 \to -\bar{\psi}_1\gamma_5)$, $\psi_2 \to \gamma_5\psi_2$, $m_1 \to -m_1$ and $m_2 \to -m_2$. Then the terms of interaction Hamiltonian (1) divide into two classes [8, 9]), namely, VA (invariant) and STP (pseudoinvariant), the phases and relative magnitudes among the members of each group being arbitrary. The invariant (pseudoinvariant) corresponds to the upper (lower) sign of the equation

$$H_{\text{int}}^{\text{transformed}} = \pm H_{\text{int}}. \tag{4}$$

A similar division of the interaction Hamiltonian arises from the transformation for the fields 3 and 4. The results obtained performing the same transformation

† To avoid ambiguity, we assume the phase factor ξ in $\psi \to \xi\gamma_5\psi$ to be equal to unity for all fermions.

for each pair of the four fermion fields are given in table 1. Now, we postulate the following: the four-fermion interaction responsible for a weak decay must be invariant under the transformation eq. (3) for every pair of the four fields.

TABLE 1

Invariance properties of the four-fermion interactions under the mass reversal transformation for two fields, simultaneously.

Fields to be transformed	Interaction	
1 and 2 or 3 and 4	invariant pseudoinvariant	bV+dA aS+cT+eP
1 and 3 or 2 and 4	invariant pseudoinvariant	a(S+P)+cT+b(V−A) a(S−P)+b(V+A)
1 and 4 or 2 and 3	invariant pseudoinvariant	a(S−P)+b(V−A) a(S+P)+cT+b(V+A)
every pair of the four fields	invariant or pseudoinvariant	V−A or V+A or S−P or S+P+cT
	invariant	V−A

Then, the interaction Hamiltonian (1) reduces to V−A:

$$\begin{aligned} 2(\mathrm{V}-\mathrm{A}) = {} & [\bar{\psi}_1\gamma_\mu(1+\gamma_5)\psi_2][\bar{\psi}_3\gamma_\mu(1+\gamma_5)\psi_4](C+C') \\ & + [\bar{\psi}_1\gamma_\mu(1-\gamma_5)\psi_2][\bar{\psi}_3\gamma_\mu(1-\gamma_5)\psi_4](C-C')+\mathrm{h.c.} \end{aligned} \tag{5}$$

Here $C = C_{\mathrm{V}} = -C_{\mathrm{A}}$, $C' = C'_{\mathrm{V}} = -C'_{\mathrm{A}}$. The ratio C'/C is not determined from this postulate, but needs at least an experimental result, such as the polarization of the neutrino, to determine its value. This kind of principle to derive V−A would have a certain importance, although there are some theories which give V−A with C'/C to be unity [10, 11, 12]) and we know that these theories are compatible with all experimental data concerning weak processes among the elementary particles within experimental error †. In fact, one of the γ_5 symmetries of H_{int} is very useful to derive the relativistic corrections to beta decay, as will be shown in the next section. In the paper of Stech and Jensen [8]), the invariance requirement for the interaction Hamiltonian is almost the same as ours. However, they do not distinguish invariant and pseudoinvariant interactions. Their result is that the four-fermion interaction is one of V−A, V+A, S−P, or S+P+cT where c is an arbitrary constant.

As we see from the above, the invariance principle of mass reversal of two

† However, the ratio of the coupling constants in beta decay is different from unity. According to ref. [13]), $|C_{\mathrm{A}}/C_{\mathrm{V}}|^2 = 1.42\pm0.06$ from ft values of the neutron decay and the $0 \to 0$ transitions, and $|C_{\mathrm{A}}/C_{\mathrm{V}}|^2 = 1.16\pm0.05$ from ft values of the $0\to0$ transitions and decays of O^{15} and F^{17}. There is no satisfactory theory to explain these values of the ratio of coupling constants quantitatively.

fields simultaneoulsly is not sufficient to give a unique form for the interaction Hamiltonian. To do this we need a more stringent condition. An ingenious condition was found by Sakurai [10]. He assumed that the four-fermion interaction must be invariant under the transformation (3) for every one of the four fields separately (i.e., not simultaneously). Then we have a unique form of four-fermion interaction

$$H_{\text{int}} = C[\bar{\psi}_1\gamma_\mu(1+\gamma_5)\psi_2][\bar{\psi}_3\gamma_\mu(1+\gamma_5)\psi_4]+\text{h.c.} \tag{6}$$

which is V—A with $C = C'$. The same form of four-fermion interaction has been also obtained by Sudarshan and Marshak by postulating that the wave functions of the four fermions have the same chirality eigenvalue [12], and by Feynman and Gell-Mann who approached the same problem rather differently [11].

3. General Rule

In the last section, we have seen that V—A is invariant under the transformation (3) for every two fields simultaneously. Now, we shall consider a special case of beta decay. In particular, we are interested in the transformation for neutron particles. The interaction Hamiltonian of beta decay is

$$\begin{aligned} H_{\text{int}} = {} & (\psi_{\text{p}}^*\psi_{\text{n}})[\psi_{\text{e}}^*(C_{\text{V}}+\gamma_5 C'_{\text{V}})\psi_\nu]-(\psi_{\text{p}}^*\boldsymbol{\alpha}\psi_{\text{n}})[\psi_{\text{e}}^*\boldsymbol{\alpha}(C_{\text{V}}+\gamma_5 C'_{\text{V}})\psi_\nu] \\ & + (\psi_{\text{p}}^*\boldsymbol{\sigma}\psi_{\text{n}})[\psi_{\text{e}}^*\boldsymbol{\sigma}(C_{\text{A}}+\gamma_5 C'_{\text{A}})\psi_\nu]-(\psi_{\text{p}}^*\gamma_5\psi_{\text{n}})[\psi_{\text{e}}^*\gamma_5(C_{\text{A}}+\gamma_5 C'_{\text{A}})\psi_\nu]+\text{h.c.} \end{aligned} \tag{7}$$

Here we do not specify the relative magnitudes of the vector and axial vector coupling constants. If we apply the transformation

$$\begin{gathered} \psi_{\text{n}} \to \gamma_5\psi_{\text{n}}, \quad m_{\text{n}} \to -m_{\text{n}}, \quad \psi_\nu \to \gamma_5\psi_\nu, \quad m_\nu \to -m_\nu, \\ C_{\text{V}} \rightleftarrows -C_{\text{A}}, \quad C'_{\text{V}} \rightleftarrows -C'_{\text{A}}, \end{gathered} \tag{8}$$

to eq. (7), it follows from the invariance of H_{int} that the coupling constants of the vector and axial vector interactions must have a phase difference of π. Furthermore, we can show a similarity between the nth and the $(n\pm1)$th forbidden transitions as follows. Under the same transformation, a term in the transition probability, e.g.

$$(\psi_{\text{p}}^*\boldsymbol{\alpha}\psi_{\text{n}})^*(\psi_{\text{p}}^*\boldsymbol{\sigma}\times\mathbf{r}\psi_{\text{n}})[\psi_{\text{e}}^*(-\boldsymbol{\alpha})(C_{\text{V}}+\gamma_5 C'_{\text{V}})\psi_\nu]^*[\psi_{\text{e}}^*(\boldsymbol{\sigma}\times\mathbf{P})(C_{\text{A}}+\gamma_5 C'_{\text{A}})\psi_\nu], \tag{9}$$

which appears in the first forbidden transition, becomes

$$(\psi_{\text{p}}^*\boldsymbol{\sigma}\psi_{\text{n}})^*(\psi_{\text{p}}^*\boldsymbol{\alpha}\times\mathbf{r}\psi_{\text{n}})[\psi_{\text{e}}^*\boldsymbol{\sigma}(C_{\text{A}}+\gamma_5 C'_{\text{A}})\psi_\nu]^*[\psi_{\text{e}}^*(-\boldsymbol{\alpha}\times\mathbf{P})(C_{\text{V}}+\gamma_5 C'_{\text{V}})\psi_\nu], \tag{10}$$

which appears in the allowed transition. Here $\mathbf{P}$ is the momentum of the electron-neutrino system. These two terms have the same dependence on the electron energy, which can be proved using the identity

$$(\boldsymbol{\sigma}\times\mathbf{P})[1-(\boldsymbol{\alpha}\cdot\mathbf{q}-m_\nu\beta)/E_\nu]\boldsymbol{\alpha} = (\boldsymbol{\alpha}\times\mathbf{P})[1-(\boldsymbol{\alpha}\cdot\mathbf{q}+m_\nu\beta)/E_\nu]\boldsymbol{\sigma} \tag{11}$$

where [ ] is the projection operator for the neutrino; m_ν is not necessarily zero, because m_ν in eq. (9) is transformed into $-m_\nu$ in eq. (10) †. In general, all formulae concerning beta decay retain the same electron energy dependence under the transformation $C_V \rightleftarrows C_A\gamma_5$, $C_V\boldsymbol{\alpha} \rightleftarrows C_A\boldsymbol{\sigma}$, where the Dirac operators act on nucleon wave-functions ††. The same replacement is required for coupling constants with primes. Some examples of the similarity between nuclear matrix elements for the nth and the $(n\pm1)$th forbidden transitions are listed in table 2. Using this fact, the labour of calculation of the transition probabilities in beta decay is always reduced by half.

TABLE 2

Correspondence between nuclear matrix elements

Allowed	First forbidden	Second forbidden	Third forbidden
$C_V\mathfrak{M}(1)$	$C_A\mathfrak{M}(\gamma_5)$		
$C_A\mathfrak{M}(\boldsymbol{\sigma})$	$C_V\mathfrak{M}(\boldsymbol{\alpha})$		
	$C_V\mathfrak{M}(\mathbf{r})$	$C_A\mathfrak{M}(\gamma_5\mathbf{r})$	
	$C_A\mathfrak{M}(\boldsymbol{\sigma}\cdot\mathbf{r})$	$C_V\mathfrak{M}(\boldsymbol{\alpha}\cdot\mathbf{r})$	
	$C_A\mathfrak{M}(\boldsymbol{\sigma}\times\mathbf{r})$	$C_V\mathfrak{M}(\boldsymbol{\alpha}\times\mathbf{r})$	
	$C_A\mathfrak{M}(B_{ij})$	$C_V\mathfrak{M}(A_{ij})$	
		$C_A\mathfrak{M}(\boldsymbol{\sigma}r^2)$	$C_V\mathfrak{M}(\boldsymbol{\alpha}r^2)$
		$C_A\mathfrak{M}((\boldsymbol{\sigma}\cdot\mathbf{r})\mathbf{r})$	$C_V\mathfrak{M}((\boldsymbol{\alpha}\cdot\mathbf{r})\mathbf{r})$
		$C_A\mathfrak{M}(T_{ij})$	$C_V\mathfrak{M}(U_{ij})$
		$C_A\mathfrak{M}(S_{ijk})$	$C_V\mathfrak{M}(V_{ijk})$
		$C_V\mathfrak{M}(r^2)$	$C_A\mathfrak{M}(\gamma_5 r^2)$
		$C_V\mathfrak{M}(R_{ij})$	$C_A\mathfrak{M}(R_{ij}\gamma_5)$
			etc.

Interchanging the nuclear matrix elements on the same line, the formula for the nth forbidden transition is transformed into that for the $(n\pm1)$th forbidden transition, and vice versa. A_{ij}, B_{ij}, R_{ij}, $R_{ij}\gamma_5$, T_{ij} and U_{ij} are the second rank tensors constructed with $\mathbf{r}$ and $\boldsymbol{\alpha}$, $\boldsymbol{\sigma}$, $\mathbf{r}$, $\gamma_5\mathbf{r}$, $\boldsymbol{\sigma}\times\mathbf{r}$, and $\boldsymbol{\alpha}\times\mathbf{r}$, respectively. S_{ijk} (V_{ijk}) is the third rank tensor constructed with $\mathbf{r}$, $\mathbf{r}$, and $\boldsymbol{\sigma}$ ($\boldsymbol{\alpha}$).

An application of this invariance property is given below. A formula with the relativistic corrections for the allowed transition can be obtained from that for the first forbidden transition with the following replacement:

$$\begin{aligned} &\mathfrak{M}(\gamma_5) \to \mathfrak{M}(1), && \mathfrak{M}(\boldsymbol{\sigma}\cdot\mathbf{r}) \to \mathfrak{M}(\boldsymbol{\alpha}\cdot\mathbf{r}), \\ &\mathfrak{M}(\boldsymbol{\alpha}) \to \mathfrak{M}(\boldsymbol{\sigma}), && \mathfrak{M}(\boldsymbol{\sigma}\times\mathbf{r}) \to \mathfrak{M}(\boldsymbol{\alpha}\times\mathbf{r}), \\ &\mathfrak{M}(\mathbf{r}) \to \mathfrak{M}(\gamma_5\mathbf{r}), && \mathfrak{M}(B_{ij}) \to \mathfrak{M}(A_{ij}), \\ &C_V \rightleftarrows C_A, && C'_V \rightleftarrows C'_A; \end{aligned} \tag{12}$$

† If we adopt the chirality transformation instead of the mass reversal transformation, m_ν should be zero in order that eq. (11) be correct.

†† In the interchanges of the coupling constants, the minus sign is unnecessary, because the transition probability is a function of the square of the coupling constants.

and vice versa. The formula given by this rule does not involve the corrections due to the coordinate-type matrix elements of the second forbidden transition, which are smaller than relativistic corrections but not negligible in some cases[3]). If the formula for the first forbidden transition involved the corrections due to the third forbidden transition, especially $\mathfrak{M}(\boldsymbol{\alpha}r^2)$, $\mathfrak{M}((\boldsymbol{\alpha}\cdot\mathbf{r})\mathbf{r})$, and $\mathfrak{M}(\gamma_5 r^2)$ in the fourth column of table 2, we could derive the formula for the allowed transition with relativistic corrections as well as corrections due to the coordinate-type matrix elements, $\mathfrak{M}(\boldsymbol{\sigma}r^2)$, $\mathfrak{M}((\boldsymbol{\sigma}\cdot\mathbf{r})\mathbf{r})$ and $\mathfrak{M}(r^2)$, by the same rule given above; and vice versa. Since the formulae already published in many papers involve the matrix elements in the second column of table 2 only, we investigate the relativistic corrections alone in the following sections.

The content of this section can also be developed using the invariance property of the interaction Hamiltonian (7) under the transformation $\psi_n \to \gamma_5\psi_n$, $m_n \to -m_n$, $C_V \rightleftarrows -C'_A$, $C'_V \rightleftarrows -C_A$.

4. Formulae

As we have shown in section 3, we can derive all formulae for allowed transitions in beta decay with the relativistic corrections, by inspection, from those for the first forbidden transition, which have been published in many papers. Although we could find the second power terms of the relativistic matrix elements very easily, they are neglected here. The coordinate-type matrix elements are also omitted, for the reason mentioned at the end of section 3. The finite de Broglie wavelength effect is taken into account only for L_0 and A_1 in the $|\mathfrak{M}(1)|^2$ and $|\mathfrak{M}(\boldsymbol{\sigma})|^2$ terms, but this is accurate enough in our approximation; L_0 and A_1 are given by

$$L_0 = (2p^2F)^{-1}[g_{-1}^2+f_1^2] = \tfrac{1}{2}(1+\gamma)\mp\tfrac{5}{3}\alpha Z\rho W\mp(\alpha Z\rho/3W)-\tfrac{1}{3}p^2\rho^2 \quad (13)$$

$$\begin{aligned} A_1 &= (2p^2F)^{-1}g_{-1}f_1\sin(\delta_{-1}-\delta_1) = (p/2W)[\tfrac{1}{2}(1+\gamma)\mp\tfrac{5}{3}\alpha Z\rho W-\tfrac{1}{3}p^2\rho^2] \\ &= (p/2W)[1\pm(\alpha Z\rho/3W)]L_0. \end{aligned} \quad (14)$$

In this paper throughout, the upper (lower) sign refers to negaton (positon) decay. The other notations are those used in previous papers [14, 15, 16]). The beta-gamma and beta-alpha angular correlation from the oriented as well as unoriented nuclei and the beta-ray spectrum can be expressed [14]) by parameters $b_{LL'}^{(n)}$. Using our general rule, we find the $b_{LL'}^{(n)}$'s from eqs. (21)—(34) or from eqs. (A15)—(A28) of ref. [14]):

$$b_{00}^{(0)} = |C_V|^2\{|\mathfrak{M}(1)|^2+\tfrac{2}{3}[i\mathfrak{M}^*(\boldsymbol{\alpha}\cdot\mathbf{r})\mathfrak{M}(1)][W_0-(1/W)\pm 3(\alpha Z/2\rho)]\}, \quad (15)$$

$$\begin{aligned} b_{01}^{(1)} = 2(p/W)\{&-\mathrm{Re}(C_V{}^*C_A)[\mathfrak{M}^*(1)\mathfrak{M}(\boldsymbol{\sigma})][1\pm(\alpha Z\rho/3W)] \\ &+\tfrac{1}{3}\mathrm{Re}(C_V{}^*C_A)[i\mathfrak{M}^*(1)\mathfrak{M}(\gamma_5\mathbf{r})][W_0+2W\pm 3(\alpha Z/2\rho)] \\ &-\tfrac{1}{3}\mathrm{Re}(C_V{}^*C_A)[i\mathfrak{M}^*(\boldsymbol{\alpha}\cdot\mathbf{r})\mathfrak{M}(\boldsymbol{\sigma})][W_0\pm 3(\alpha Z/2\rho)] \\ &\mp\tfrac{1}{3}|C_V|^2[\mathfrak{M}^*(1)\mathfrak{M}(\boldsymbol{\alpha}\times\mathbf{r})][W_0-W\mp 3(\alpha Z/2\rho)]\} \\ &+2(\alpha Z/W)\{\tfrac{1}{3}\mathrm{Im}(C_V{}^*C_A)[i\mathfrak{M}^*(\boldsymbol{\alpha}\cdot\mathbf{r})\mathfrak{M}(\boldsymbol{\sigma})] \\ &+\mathrm{Im}(C_V{}^*C_A)[i\mathfrak{M}^*(1)\mathfrak{M}(\gamma_5\mathbf{r})][1+\tfrac{1}{2}p^2]\}; \end{aligned} \tag{16}$$

$$\begin{aligned} b_{11}^{(0)} = -\sqrt{3}\{&|C_A|^2|\mathfrak{M}(\boldsymbol{\sigma})|^2+\tfrac{2}{3}|C_A|^2[i\mathfrak{M}^*(\gamma_5\mathbf{r})\mathfrak{M}(\boldsymbol{\sigma})][W_0-(1/W)\pm 3(\alpha Z/2\rho)] \\ &\pm\tfrac{2}{3}\mathrm{Re}(C_A{}^*C_V)[\mathfrak{M}^*(\boldsymbol{\sigma})\mathfrak{M}(\boldsymbol{\alpha}\times\mathbf{r})][W_0-2W+(1/W)\mp 3(\alpha Z/2\rho)]\}; \end{aligned} \tag{17}$$

$$\begin{aligned} b_{11}^{(1)} = \sqrt{2}(p/W)\{&\pm|C_A|^2|\mathfrak{M}(\boldsymbol{\sigma})|^2[1\pm(\alpha Z\rho/3W)] \\ &+\tfrac{1}{3}\mathrm{Re}(C_A{}^*C_V)[\mathfrak{M}^*(\boldsymbol{\sigma})\mathfrak{M}(\boldsymbol{\alpha}\times\mathbf{r})][2W_0-5W\mp 6(\alpha Z/2\rho)] \\ &\pm\tfrac{2}{3}|C_A|^2[\mathfrak{M}^*(\gamma_5\mathbf{r})\mathfrak{M}(\boldsymbol{\sigma})][W_0-W\pm 3(\alpha Z/2\rho)]\} \\ &-\sqrt{2}\,\mathrm{Im}(C_A{}^*C_V)[\mathfrak{M}^*(\boldsymbol{\sigma})\mathfrak{M}(\boldsymbol{\alpha}\times\mathbf{r})](\alpha Z/W)[1+\tfrac{1}{4}p^2]; \end{aligned} \tag{18}$$

$$\begin{aligned} b_{11}^{(2)} = \sqrt{\tfrac{2}{3}}(p^2/W)\{&\pm\mathrm{Re}(C_A{}^*C_V)[\mathfrak{M}^*(\boldsymbol{\sigma})\mathfrak{M}(\boldsymbol{\alpha}\times\mathbf{r})] \\ &+2|C_A|^2[i\mathfrak{M}^*(\gamma_5\mathbf{r})\mathfrak{M}(\boldsymbol{\sigma})]\}\pm\sqrt{\tfrac{3}{8}}\,\mathrm{Im}(C_A{}^*C_V)p\alpha Z; \end{aligned} \tag{19}$$

$$b_{02}^{(2)} = -\sqrt{\tfrac{2}{3}}|C_V|^2[i\mathfrak{M}^*(1)\mathfrak{M}(A_{ij})](p^2/W); \tag{20}$$

$$b_{12}^{(1)} = -\sqrt{\tfrac{5}{3}}[i\mathfrak{M}^*(\boldsymbol{\sigma})\mathfrak{M}(A_{ij})]\{\mathrm{Re}(C_A{}^*C_V)p+\mathrm{Im}(C_A{}^*C_V)(\alpha Z/W)[1+\tfrac{3}{4}p^2]\}; \tag{21}$$

$$b_{12}^{(2)} = \pm[i\mathfrak{M}^*(\boldsymbol{\sigma})\mathfrak{M}(A_{ij})][\mathrm{Re}(C_A{}^*C_V)(p^2/W)+\mathrm{Im}(C_A{}^*C_V)\tfrac{3}{4}p\alpha Z]; \tag{22}$$

$$b_{12}^{(3)} = b_{22}^{(n)} = 0, \quad n = 0-4. \tag{23}$$

In eqs. (15)—(23), we have assumed $C_V = C'_V$ and $C_A = C'_A$. If this assumption does not hold, we should replace $C_i{}^*C_j$ by $\frac{1}{2}(C_i{}^*C_j+C_i'{}^*C'_j)$ in $b_{LL'}{}^{(\mathrm{even})}$ and $\frac{1}{2}(C_i{}^*C'_j+C_i'{}^*C_j)$ in $b_{LL'}{}^{(\mathrm{odd})}$ (i and j are V or A).

Some of the important formulae are as follows.

A. *Beta-ray spectrum*

$$(2\pi^3)^{-1}[(2j_1+1)/(2j+1)]F(\pm Z, W)pW(W_0-W)^2L_0[b_{00}^{(0)}-\sqrt{\tfrac{1}{3}}b_{11}^{(0)}]\mathrm{d}W. \tag{24}$$

It should be noted that L_0 has some energy dependence given in eq. (13).

B. *Beta-ray angular distribution from oriented nuclei*

$$W(\theta:\beta) = \sum_n \sum_{L\leq L'} \bar{f}_n(j)(-)^{j_1-j+L+L'+n}W(jjLL';nj_1)b_{LL'}^{(n)}P_n(\cos\theta), \tag{25}$$

with

$$\bar{f}_n(j) = \sum_m (-)^{j-m}(jjm-m|n0)a_m.$$

Here, the a_m's are the relative populations of the initial magnetic substates. If we normalize the coefficient of $b_{00}^{(0)}$ to be unity, the $\sum_m a_m$ should be $(2j+1)$.

C. *Angular correlation of beta and gamma rays*

$$W(\theta, \tau : \beta-\gamma) = \sum_n \{[\sum_{L\leqq L'} (-)^{j_1-j+n} b_{LL'}^{(n)} W(j_1 j_1 LL'; nj)(2j_1+1)^{\frac{1}{2}}] \times [\sum_{L_1 L'_1} \tau^n (j_2||L_1||j_1)(j_2||L'_1||j_1) F_n(L_1 L'_1 j_2 j_1)]\} P_n(\cos\theta), \tag{26}$$

with

$$F_n(L_1 L'_1 j_2 j_1) = F_n(L'_1 L_1 j_2 j_1)$$
$$= (-)^{j_2-j_1-1}[(2j_1+1)(2L_1+1)(2L'_1+1)]^{\frac{1}{2}}(L_1 L'_1 1-1|n0) W(j_1 j_1 L_1 L'_1; nj_2).$$

Here $\tau = +1(-1)$ for the right (left) handed circularly polarized gamma ray. The beta-gamma directional correlation will be given by taking n even only. The beta-alpha directional correlation will be given by replacing $(j_2||L_1||j_1)^2 \to |(j_2||L_1||j_1)|^2$ and $(L_1 L'_1 1-1|20)(j_2||L_1||j_1)(j_2||L'_1||j_1) \to -(L_1 L'_1 00|20)(j_2||L_1||j_1)(j_2||L'_1||j_1)^*$ in eq. (26). Various angular correlations from oriented nuclei have been given in ref.[15]) in the forms of geometrical factors with $b_{LL'}^{(n)}$'s, which we do not reproduce here.

For practical use, eq. (26) is simplified considerably by assuming a pure multipolarity of gamma ray:

$$W(\theta, \tau : \beta-\gamma) = [b_{00}^{(0)} - \sqrt{\tfrac{1}{3}} b_{11}^{(0)}]$$
$$+\tau(L+1)^{-1}[b_{01}^{(1)} c_{01}^{(1)} + b_{11}^{(1)} c_{11}^{(1)} + b_{12}^{(1)} c_{12}^{(1)}] P_1(\cos\theta) \tag{27}$$
$$+[3-L(L+1)][(L+1)(2L+3)]^{-1}[b_{02}^{(2)} c_{02}^{(2)} + b_{11}^{(2)} c_{11}^{(2)} + b_{12}^{(2)} c_{12}^{(2)}] P_2(\cos\theta).$$

Here algebraic factors $c_{LL'}^{(n)}$ are given in simple forms as functions of the spin of the parent nucleus, in table 3. The degree of circular polarization of the gamma ray in coincidence with the beta ray is given by

$$P_\gamma = \frac{[\text{the second line of eq. (27) with } \tau = 1]}{[\text{the first plus the third lines of eq. (27)}]}. \tag{28}$$

For purposes of numerical analysis of the experimental data, some relations among nuclear matrix elements have been given in ref. [3]). For the convenience of the reader, they are reproduced here:

$$i\mathfrak{M}(\boldsymbol{\alpha}\cdot\mathbf{r}) = \mp(\Lambda\alpha Z/4\rho)\mathfrak{M}(r^2). \tag{29}$$

$$i\mathfrak{M}(\gamma_5\mathbf{r}) = (1/2M)\mathfrak{M}(\boldsymbol{\sigma}) \mp (\Lambda\alpha Z/4\rho)\mathfrak{M}((\boldsymbol{\sigma}\cdot\mathbf{r})\mathbf{r}). \tag{30}$$

$$\mathfrak{M}(\boldsymbol{\alpha}\times\mathbf{r}) = M^{-1}\mathfrak{M}(\boldsymbol{\sigma}). \tag{31}$$

$$\mathfrak{M}(r^2) = \tfrac{3}{5}\rho^2\mathfrak{M}(1). \tag{32}$$

$$\mathfrak{M}((\boldsymbol{\sigma}\cdot\mathbf{r})\mathbf{r}) = \eta\mathfrak{M}(\boldsymbol{\sigma}r^2) = \tfrac{3}{5}\eta\rho^2\mathfrak{M}(\boldsymbol{\sigma}). \tag{33}$$

TABLE
Algebraic factors $c_{LL'}^{(n)}$ of the Beta-gamma angu

Decay scheme $j \xrightarrow{\beta} j_1 \xrightarrow{\gamma} j_2$	$c_{01}^{(1)}$	$c_{11}^{(1)}$	$c_{12}^{(1)}$
$j \to j-1 \to j-1-L$	0	$-(\frac{1}{2})^{\frac{1}{2}}$	$-[3(j+1)/10(j-1)]^{\frac{1}{2}}$
$j \to j \to j-L$	$[(j+1)/j]^{\frac{1}{2}}$	$(\frac{1}{2})^{\frac{1}{2}}(1/j)$	$-(1/j)[(2j+3)(2j-1)/10]^{\frac{1}{2}}$
$j \to j+1 \to j+1-L$	0	$(\frac{1}{2})^{\frac{1}{2}}[(j+2)/(j+1)]$	$-[1/(j+1)][3j(j+2)/10]^{\frac{1}{2}}$
$j \to j-1 \to j-1+L$	0	$(\frac{1}{2})^{\frac{1}{2}}[(j-1)/j]$	$(1/j)[3(j+1)(j-1)/10]^{\frac{1}{2}}$
$j \to j \to j+L$	$-[j/(j+1)]^{\frac{1}{2}}$	$-(\frac{1}{2})^{\frac{1}{2}}[1/(j+1)]$	$[1/(j+1)][(2j+3)(2j-1)/10]^{\frac{1}{2}}$
$j \to j+1 \to j+1+L$	0	$-(\frac{1}{2})^{\frac{1}{2}}$	$[3j/10(j+2)]^{\frac{1}{2}}$

Here M is the rest mass of a nucleon; η is of the order of unity and depends on the nuclear model; A is given by

$$A = 1 \pm (W_0 \mp 2.5) A^{\frac{1}{3}} Z^{-1}. \tag{34}$$

Eq. (29)—(31) are given in the non-relativistic approximation for nucleons. Eq. (32) and (33) follow, assuming a uniform density of nuclear matter. If we adopt Gell-Mann's theory [1],

$$\mathfrak{M}(\boldsymbol{\alpha} \times \mathbf{r}) \approx M^{-1}(\mu_p - \mu_n)\mathfrak{M}(\boldsymbol{\sigma}) \approx 4\lambda M^{-1}\mathfrak{M}(\boldsymbol{\sigma}) \tag{35}$$

with

$$C_A/C_V \approx C'_A/C'_V \approx -\lambda, \quad \lambda = 1.2.$$

5. Electron-Neutrino Angular Correlation

The electron-neutrino angular correlation of the first forbidden transition was given by the present author assuming a general STPVA interaction and taking into account the Coulomb corrections [16]. To that formula we apply the rule given in section 4. The electron-neutrino angular correlation of the allowed beta decay with the relativistic corrections is then as follows:

$$\begin{aligned} W(\theta)\mathrm{d}W\mathrm{d}\Omega = {} & (2\pi^3)^{-1}[(2j_1+1)/(2j+1)]F(\pm Z, W)pW(W_0-W)^2 L_0 \\ & \times [b_{00}^{(0)} W_F(\theta) - \sqrt{\tfrac{1}{3}} b_{11}^{(0)} W_{GT}(\theta)]\mathrm{d}W\mathrm{d}\Omega \end{aligned} \tag{36}$$

with

$$W_F(\theta) = 1 + (p/W)\{1 \pm (\alpha Z\rho/3W) - (2/3W)[i\mathfrak{M}(\boldsymbol{\alpha}\cdot\mathbf{r})/\mathfrak{M}(1)]\}\cos\theta, \tag{37}$$

$$\begin{aligned} W_{GT}(\theta) = {} & 1 - (p/3W)\{1 \pm (\alpha Z\rho/3W) + \tfrac{2}{3}[i\mathfrak{M}(\gamma_5\mathbf{r})/\mathfrak{M}(\boldsymbol{\sigma})][4W_0 - (1/W)] \\ & \pm \tfrac{2}{3}\mathrm{Re}(C_V/C_A)[\mathfrak{M}(\boldsymbol{\alpha}\times\mathbf{r})/\mathfrak{M}(\boldsymbol{\sigma})][2W_0 - 4W - (1/W)]\}\cos\theta \\ & \pm \tfrac{1}{3}\mathrm{Im}(C_V/C_A)[\mathfrak{M}(\boldsymbol{\alpha}\times\mathbf{r})/\mathfrak{M}(\boldsymbol{\sigma})][W + (1/W)]\alpha Z\cos\theta. \end{aligned} \tag{38}$$

ngular correlation in eq. (27)

$c_{02}^{(2)}$	$c_{11}^{(2)}$	$c_{12}^{(2)}$
0	$-(\frac{1}{8})^{\frac{1}{2}}$	$-[(j+1)/2(j-1)]^{\frac{1}{2}}$
$[(j+1)(2j+3)/j(2j-1)]^{\frac{1}{2}}$	$(\frac{1}{8})^{\frac{1}{2}}[(2j+3)/j]$	$(1/j)[3(2j+3)/2(2j-1)]^{\frac{1}{2}}$
0	$-(\frac{1}{8})^{\frac{1}{2}}[(j+2)(2j+5)/(j+1)(2j+1)]$	$[(2j+5)/(j+1)(2j+1)]$ $\times[j(j+2)/2]^{\frac{1}{2}}$
0	$-(\frac{1}{8})^{\frac{1}{2}}[(j-1)(2j-3)/j(2j+1)]$	$-[(2j-3)/j(2j+1)]$ $\times[(j+1)(j-1)/2]^{\frac{1}{2}}$
$[j(2j-1)/(j+1)(2j+3)]^{\frac{1}{2}}$	$(\frac{1}{8})^{\frac{1}{2}}[(2j-1)/(j+1)]$	$[1/(j+1)][3(2j-1)/2(2j+3)]^{\frac{1}{2}}$
0	$-(\frac{1}{8})^{\frac{1}{2}}$	$[j/2(j+2)]^{\frac{1}{2}}$

Again, L_0 has an energy dependence given by eq. (13); $W_F(\theta)$ and $W_{GT}(\theta)$ are the electron-neutrino angular correlations of the Fermi and Gamow-Teller parts, respectively. If $C_V = C'_V$ and $C_A = C'_A$ do not hold, we should replace $C_i^* C_j$ by $\frac{1}{2}(C_i^* C_j + C_i'^* C'_j)$ in eqs. (37)—(40).

6. Longitudinal Polarization of Beta Particles

Here, we derive the longitudinal polarization of the beta particles from the formulae given by Alder, Stech and Winther in the case of the first forbidden transition in STP interaction [17]. We must transform their formulae from STP to VA interaction. The rule of this transformation has been studied in many papers [14, 16, 18]. Namely

$$C_S\beta \to C_V, \quad C_T\beta\boldsymbol{\sigma} \to C_A\boldsymbol{\sigma}, \quad C_T\beta\boldsymbol{\alpha} \to C_V\boldsymbol{\alpha}, \quad C_P\beta\gamma_5 \to C_A\gamma_5,$$

and the corresponding transformation for coupling constants with primes. Here the Dirac matrices are all in the nuclear matrix elements. Besides, it is necessary to replace K^m (the mth power of the neutrino energy) by $(-)^{m+1}K^m$ $[(-)^m K^m]$ in the numerator (denominator) of eq. (8) of ref.[17]). Finally we perform a transformation which is given in section 4 of this paper. It should be noted that the definition, in ref.[17]), of $\int\beta\boldsymbol{\alpha}$ ($\int\boldsymbol{\alpha}$ in the transformed formulae) has a different sign from ours, which coincides with that of Konopinski and Uhlenbeck [19]). The general rule of transformation between the nth and the $(n\pm1)$th forbidden transition is valid only if we take our definition. The longitudinal polarization of the beta particles for the allowed beta decay with relativistic corrections is given in the following †:

† In the numerator of eq. (39), we may have a term of the form $\mathrm{Im}\,(C_A^* C'_V + C'^*_A C_V)$. This term corresponds to $\mathrm{Im}\,(C_T^* C'_T + C'^*_T C_T) \equiv 0$ in the STP interaction. Therefore, we cannot derive that term from the formulae of ref. [17]). However, since such a term is usually very small, we do not calculate it.

$$P_{\mathrm{L}} = [\text{Numerator}] \div [b_{00}^{(0)} - \sqrt{\tfrac{1}{3}}\, b_{11}^{(0)}] \tag{39}$$

where

$$\begin{aligned}
[\text{Numerator}] = {} & \mp (p/W)|C_{\mathrm{V}}|^2\{|\mathfrak{M}(1)|^2[1 \pm (\alpha Z\rho/3W)] \\
& + \tfrac{2}{3}[i\mathfrak{M}^*(\boldsymbol{\alpha}\cdot\mathbf{r})\mathfrak{M}(1)][W_0 \pm 3(\alpha Z/2\rho)]\} \\
& \mp (p/W)\{|C_{\mathrm{A}}|^2|\mathfrak{M}(\boldsymbol{\sigma})|^2[1 \pm (\alpha Z\rho/3W)] \\
& + \tfrac{2}{3}|C_{\mathrm{A}}|^2[i\mathfrak{M}^*(\gamma_5\mathbf{r})\mathfrak{M}(\boldsymbol{\sigma})][W_0 \pm 3(\alpha Z/2\rho)] \\
& \pm \tfrac{2}{3}\mathrm{Re}(C_{\mathrm{A}}{}^* C_{\mathrm{V}})[\mathfrak{M}^*(\boldsymbol{\sigma})\mathfrak{M}(\boldsymbol{\alpha}\times\mathbf{r})][W_0 - 2W \mp 3(\alpha Z/2\rho)]\}.
\end{aligned}$$

Again, if $C_{\mathrm{V}} = C'_{\mathrm{V}}$ and $C_{\mathrm{A}} = C'_{\mathrm{A}}$ do not hold, we should replace $C_i{}^* C_j$ by $\frac{1}{2}(C_i{}^* C_j + C'_i{}^* C'_j)$ in the denominator and by $\frac{1}{2}(C_i{}^* C'_j + C'_i{}^* C_j)$ in the numerator. For the special case of a pure Gamow-Teller transition with $C_i = C'_i$, P_{L} becomes

$$\begin{aligned}
P_{\mathrm{L}} = {} & \mp (p/W)[1 + (1/3W)\{\pm \alpha Z\rho \mp 2[C_{\mathrm{V}}\mathfrak{M}(\boldsymbol{\alpha}\times\mathbf{r})/C_{\mathrm{A}}\mathfrak{M}(\boldsymbol{\sigma})] \\
& - 2[i\mathfrak{M}(\gamma_5\mathbf{r})/\mathfrak{M}(\boldsymbol{\sigma})]\}].
\end{aligned} \tag{40}$$

The author would like to express his sincere thanks to Professor C. S. Wu for her kind interest in this work, and to Dr. B. Margolis for reading the manuscript.

References

1) M. Gell-Mann, Phys. Rev. **111** (1958) 362
2) M. Morita and M. Yamada, Progr. Theoret. Phys. **13** (1955) 114
3) M. Morita, Phys. Rev. **113** (1959) 1584
4) J. Bernstein and R. R. Lewis, Phys. Rev. **112** (1958) 232
5) M. Morita, Phys. Rev. **114** (1959) 1080
6) D. C. Peaslee, Phys. Rev. **91** (1953) 1447
7) S. Watanabe, Phys. Rev. **106** (1957) 1306
8) B. Stech and J. H. D. Jensen, Zeits. f. Phys. **141** (1955) 175
9) J. Tiomno, Nuclear Physics **1** (1955) 226
10) J. J. Sakurai, Nuovo Cimento **7** (1958) 649
11) R. P. Feynman and M. Gell-Mann, Phys. Rev. **109** (1958) 193
12) E. C. G. Sudarshan and R. E. Marshak, Phys. Rev. **109** (1958) 1860
13) O. C. Kistner and B. M. Rustad, Phys. Rev. **114** (1959) 1329
14) M. Morita and R. S. Morita, Phys. Rev. **109** (1958) 2048
15) M. Morita and R. S. Morita, Phys. Rev. **110** (1958) 461
16) Morita, Progr. Theoret. Phys. **9** (1953) 345; Phys. Rev. **90** (1953) 1005 with erratum **91** (1953) 1580 (E)
17) K. Alder, B. Stech and A. Winther, Phys. Rev. **107** (1957) 728
18) M. Yamada and M. Morita, Progr. Theoret. Phys. **8** (1952) 431
19) E. J. Konopinski and G. E. Uhlenbeck, Phys. Rev. **60** (1941) 308

1.E.1:
3.A

Nuclear Physics **14** (1959/60) 117—119; © *North-Holland Publishing Co., Amsterdam*
Not to be reproduced by photoprint or microfilm without written permission from the publisher

GAMMA RAYS IN THE DECAY OF ^{141}Nd

E. W. CYBULSKA and L. MARQUEZ †

Centro Brasileiro de Pesquisas Fisicas, Rio de Janeiro ††

Received 17 August 1959

Abstract: The gamma rays in the decay of ^{114}Nd have been studied with scintillation spectrometers and coincidences. Seven lines have been established with energies of 38, 145, 420, 510, 880, 1150 and 1300 keV. Their relative intensities are 100, 1.7, 0.6, 9.7, 1.2, 2.3 and 1.5 respectively. The line of 38 keV is due to K-capture in ^{114}Nd and the line of 510 keV is due to annihilation radiation from the positons of ^{141}Nd. The remaining five lines are due to levels in ^{141}Pr. A decay scheme is proposed.

1. Introduction

The gamma ray spectrum in the decay of ^{141}Nd does not seem to be well established. Polak *et al.* [1]) found lines of 1140 keV, 1300 keV, the 38 keV X-ray from the K-capture in ^{141}Nd, and the 511 keV gamma ray from the annihilation of the positons from ^{141}Nd. They did not detect the well known gamma ray of 145 keV from the first excited state in ^{141}Pr. The positrons of ^{141}Nd have been studied only by absorption [2, 3]) with results of 0.7 and 0.8 MeV for the maximum energy.

We made a study of the gamma rays in the decay of ^{141}Nd and found three new lines in addition to the lines found by Polak *et al.*[1]). One of these lines seems to be the 145 keV line from the first excited state in ^{141}Pr.

2. Experimental Method

Our samples were prepared by irradiating natural Nd in the form of Nd_2O_3. The samples were irradiated with gamma rays from the betatron at the University of São Paulo with a maximum energy of 21 MeV and irradiation time of three hours. They were flown immediately to our laboratory where the measurements were carried out. The reaction producing the isotope is ^{142}Nd$(\gamma, n)^{141}$Nd.

The amount of Nd_2O_3 taken for each measurement was the optimum amount needed according to the gamma ray to be studied. It was between 1 g and 8 g. It was spread and compressed over an area of 20 cm^2 having a plastic foil on one side and an Al disc 1 mm thick on the other side. This was placed between

† Present address: Centre d'Études Nucléaires de Saclay.

†† This work was done in part under the auspices of the Conselho Nacional de Pesquisas and the Comissão Nacional de Energia Nuclear of Brazil.

two NaI(Tl) crystals facing each other and as close as possible to the samples. We used crystals of $1\frac{1}{2}''$ diameter by 1'' thickness for the softer gamma rays. For the harder gamma rays we used one crystal with the same dimensions as above and another of 3'' diameter by 3'' thickness. Each detector was connected to a single channel pulse height analyzer and there was a circuit to register the coincidences.

The samples showed the gamma rays from the 2.5 h ^{141}Nd and the gamma rays from the 1.8 h ^{149}Nd, since this is also formed by the reaction ^{150}Nd$(\gamma,n)^{149}$Nd. We found that the lines of ^{141}Nd were strongly enhanced when they were observed in coincidence with the 38 keV X-ray, and this was the criterion that we used to decide if a line decaying with a half life between 1.8 and 2.5 h was from ^{141}Nd or ^{149}Nd. This criterion does not apply to the line of 510 keV. The lines from ^{149}Nd appeared in coincidence with the X-rays because of the secondary X-rays produced in our relatively thick samples.

We found that the decay of ^{141}Nd had gamma rays of 38, 145, 420, 510, 880, 1150 and 1300 keV. Their relative intensities were 100, 1.7, 0.6, 9.7, 1.2, 2.3 and 1.5 respectively. The errors in the energies are estimated as 1 % and the errors in the intensities are estimated as 20 %. The intensity measurements are corrected for background, efficiency, geometry, absorption, fluorescence yield, etc. The 38 keV line comes from the X-ray following the K-capture in ^{141}Nd. The 510 keV line comes from the annihilation radiation of the positons from ^{141}Nd.

We found that the 1300 keV gamma ray was not in coincidence with any other gamma ray. The 1150 keV gamma ray was in coincidence with the 145 keV gamma ray. The 420 keV gamma ray was in coincidence with the 880 keV gamma ray.

3. Discussion

It is very probable that the line of 145 keV that we found comes from the well known first excited state in ^{141}Pr. The coincidence measurements lead us to the decay scheme in fig. 1. The sum of the energies of the cascade gamma rays is equal to the energy of the cross over gamma ray within the experimental error. The order of the gamma rays of 420 keV and 880 keV has been established by the intensity measurements; since their intensities are 0.6 and 1.2, the 880 keV gamma ray must be lower and have 0.6 K-captures going directly to it.

The intensity of the 145 keV gamma ray is 1.7. If we correct this for the conversion coefficient measured by Zorzoli [4]) we get 2.4, which agrees well with the value of 2.3 for the gamma ray of 1150 keV.

The spin and parity of the ground state of ^{141}Pr has been found from measurements [5]) to be $\frac{5}{2}^+$. The spin and parity of the first excited state [6]) is probably $\frac{7}{2}^+$. From our data and the decay scheme in fig. 1, the most likely spins and parities for the second and the third excited states are $\frac{3}{2}^+$ and $\frac{5}{2}^+$ respectively.

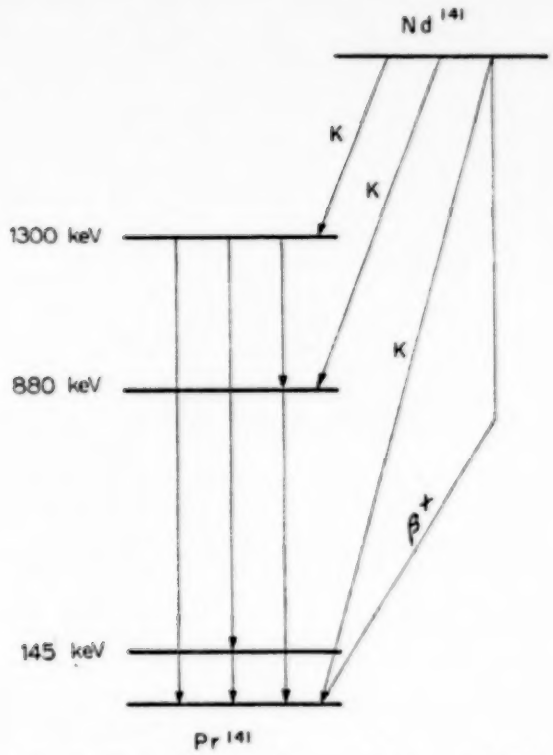

Fig. 1. The proposed decay scheme of ^{141}Nd.

We are greatly indebted to Prof. Jose Goldemberg, in charge of the Laboratorio do Betatron in São Paulo, for making the irradiations without which this work would not have been possible. We are also indebted to S. Oschalins for the installation and maintenance of the electronic equipment.

References

1) H. L. Polak, W. Schoo, B. L. Schram, R. K. Girgis and R. van Lieshout, Nuclear Physics **5** (1958) 271
2) G. Wilkinson and H. H. Hicks, Phys. Rev. **75** (1949) 1687
3) J. D. Kurbatov, D. C. MacDonald, M. L. Pool and L. L. Quill, Phys. Rev. **61** (1942) 106A
4) G. B. Zorzoli, Nuovo Cimento **5** (1957) 289
5) D. Strominger, J. M. Hollander and G. T. Seaborg, Revs. Mod. Phys. **30** (1958) 585
6) E. Ambler, R. P. Hudson and G. M. Temmer, Phys. Rev. **97** (1955) 1212

2.C *Nuclear Physics* **14** (1959/60) 120—130; © *North-Holland Publishing Co., Amsterdam*
Not to be reproduced by photoprint or microfilm without written permission from the publisher

ON THE SPLITTING OF THE PEAK IN THE NEUTRON STRENGTH FUNCTION NEAR $A = 55$

J. M. LEBLANC †, R. E. COTÉ and L. M. BOLLINGER
Argonne National Laboratory, Lemont, Illinois ††

Received 3 August 1959

Abstract: The results of neutron transmission measurements on bromine and selenium and their enriched isotopes are presented. Resonance parameters have been determined for six resonances in Br^{79}, three in Br^{81}, and a total of eight in the various enriched isotopes of selenium. The values of $\bar{\Gamma}_n^0/D$ for Br^{79} and Se^{80} are determined from these parameters. These new values of the strength function are compared with those for neighbouring nucleides. The combined results give a clear indication that the peak in the neutron strength function near nucleon number 55 shows a splitting similar to that of the maximum near $A = 155$.

1. Introduction

The present study was motivated by earlier measurements [1]) of the maximum in the neutron strength function near nucleon number $A = 55$ which had, in addition to experimentally establishing the existence of that maximum, suggested that a secondary maximum might exist near $A = 80$. Some further motivation was provided by the hope of determining some new values of the radiation width Γ_γ which would help complete the picture concerned with the variation of this quantity with A. Both of these ends could be met by the determination of the resonance parameters of bromine and selenium.

In the analysis of the experimental data, the shapes of the resonances are assumed to be given by the single-level Breit-Wigner formula. Because of the low range of energy covered by the present measurements, we need consider only the case of target nucleides which interact by radiative capture or by elastic scattering with neutrons of zero angular momentum. The total cross section σ made up of σ_c, the cross section for radiative capture, and σ_s, the scattering cross section, is then given by [2])

$$\sigma = \sigma_c + \sigma_s$$

with

$$\sigma_c = \sigma_0 \frac{\Gamma_\gamma}{\Gamma} \left(\frac{E_0}{E}\right)^{\frac{1}{2}} \frac{1}{1+x^2}, \qquad (1)$$

† Now at the Lawrence Radiation Laboratory, University of California, Livermore, California.
†† Work performed under the auspices of the U. S. Atomic Energy Commission.

$$\sigma_s = 4\pi R^2 + \sigma_0 \frac{\Gamma_n}{\Gamma} \frac{1 + 2\dfrac{R\Gamma}{\lambda_0 \Gamma_n} x}{1 + x^2}, \tag{2}$$

where

$$\Gamma = \Gamma_n + \Gamma_\gamma, \quad x = (2/\Gamma)(E - E_0), \quad \sigma_0 = 4\pi\lambda_0^2 g \Gamma_n / \Gamma. \tag{3}$$

In these relations E is the kinetic energy of the neutron; E_0 and $2\pi\lambda_0$ are the neutron energy and wavelength at exact resonance; Γ, Γ_γ, and Γ_n are the total, γ-ray, and neutron widths; and σ_0 is the cross section at exact resonance. The statistical factor g is given by

$$g = \tfrac{1}{2}(2J+1)/(2I+1),$$

where I is the spin of the target nucleus and J is the spin of the compound nuclear state. The parameters which we have attempted to measure for each resonance are the quantities E_0, σ_0, and Γ, from which eq. (3) then allows us to deduce Γ_n and Γ_γ for an assumed value of g.

Neutron transmission measurements were made on bromine, selenium, and the enriched isotopes of these elements by use of the Argonne fast choppers. These data were then analyzed by the standard area-analysis method [3]) to determine the various parameters.

The equipment consisted of the old Argonne fast chopper [4]) (Selove type) and a new fast chopper which has been recently described [5]). The resolution of the old chopper was 0.08μsec/m and the new chopper was operated at reduced speed so that its resolution was about 0.07μsec/m. The detector was a boron-loaded liquid scintillator and was located at the end of a 60-meter flight path. In this series of measurements both the 100-channel and 1024-channel time analyzers [6]) were used to record the primary data.

2. Results

2.1. BROMINE

The total neutron cross section of bromine as a function of neutron energy had been measured by Havens and Rainwater [7]). They resolved four resonances in the energy interval from 30 to 150 eV, and their data indicate that there are many unresolved resonances with energies greater than 200 eV.

In the present investigation the transmissions of samples of liquid normal bromine 1.18 and 5.95 g/cm^2 thick and of samples of potassium bromide were measured. The samples of potassium bromide were the following: KBr in D_2O, 0.043 and 0.034 g/cm^2 thick; KBr in which the Br^{79} content was 87 %, 0.171 and 0.342 g/cm^2 thick; and KBr in which the Br^{81} content was 96.8 %, 0.352 g/cm^2 thick. All thicknesses express the number of grams of bromine per cm^2. As a check on the effect of potassium in the samples, the transmission of a

sample of potassium chloride was measured and it was established that, for the thickness of the potassium bromide samples which contained enriched isotopes, no resonance structure of potassium would be observed.

The transmission of a sample of normal bromine (5.95 g/cm^2) is illustrated by the top curve in fig. 1. The transmissions of samples of KBr^{81} and KBr^{79} are

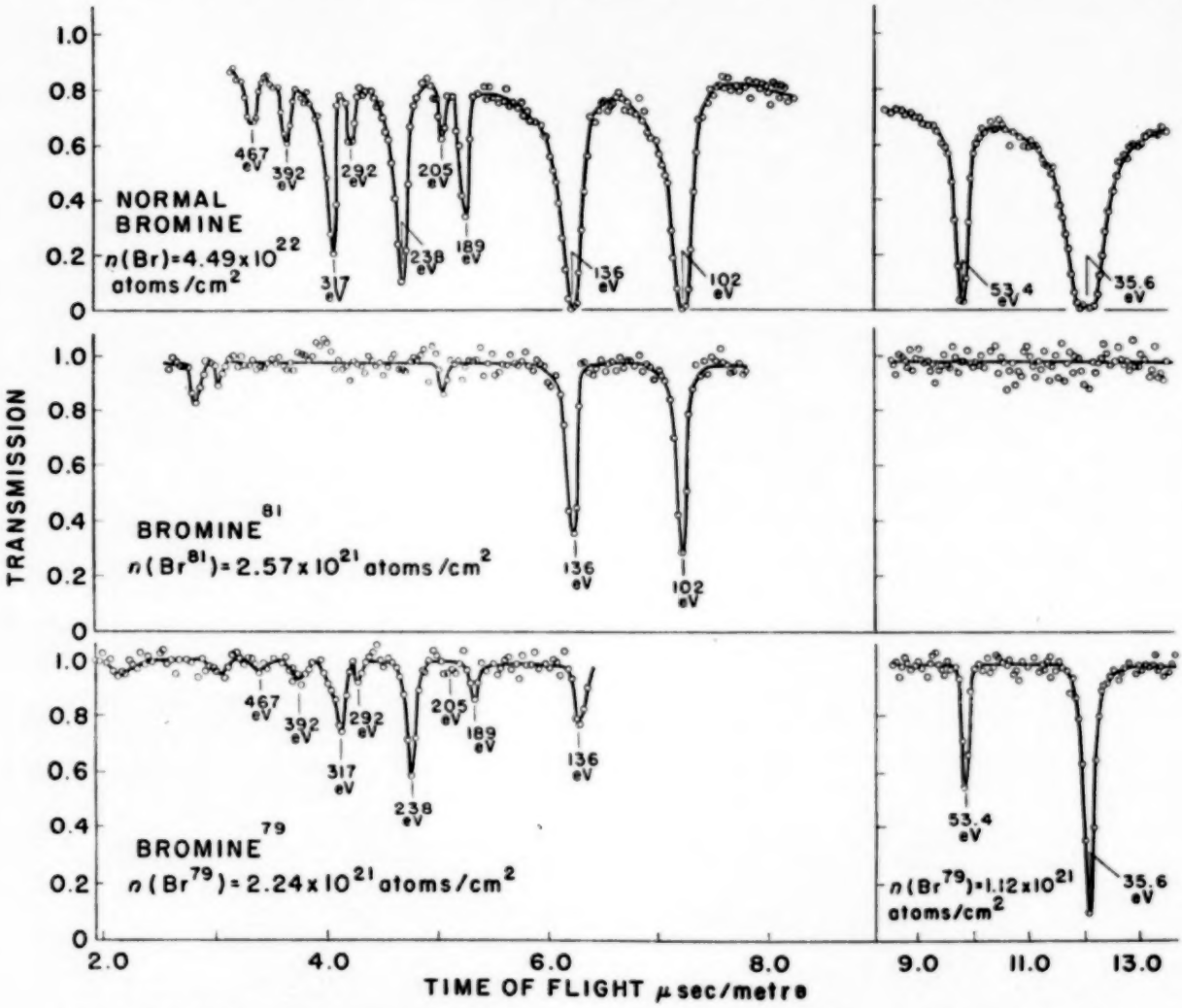

Fig. 1. The total neutron cross sections of a sample of normal bromine and of samples of the isotopes Br^{79} and Br^{81}.

plotted in fig. 1 as the middle and lower curves, respectively. In the interval of energy less than 350 eV there are seven transmission dips which are believed to be due to single resonances. From the data presented in fig. 1, one can conclude that the resonances with energies of 102 eV and 136 eV are associated with Br^{81} and that those with energies of 35.6, 53.4, 189, 238, 292, and 317 eV are associated with Br^{79}. The transmission dip at 136 eV in the lower curve in fig. 1 is due to the 13 % of Br^{81} present in the enriched Br^{79} sample. The transmission

dips at 205 and 392 eV have been tentatively assigned to Br^{81} and Br^{79}, respectively; however, the dip at 392 eV may be due to more than one resonance.

The areas which were obtained with thick and thin samples were analyzed and resonance parameters determined for the nine lowest energy resonances of bromine. In addition, since the data on the resonance at 35.6 eV were well suited to a shape analysis of the type described by Palmer and Bollinger [8]), such an analysis was applied. A value of $\sigma_0 \Gamma^2 = 701 \pm 20$ b · eV^2 was obtained in this manner. The nuclear spin of each of the isotopes of bromine is $\frac{3}{2}$, so the statistical factor g has the values $\frac{5}{8}$ or $\frac{3}{8}$ depending on whether the total angular

TABLE 1

Parameters of neutron resonances in Br^{79} and Br^{81}

E_0 (eV)	σ_0 (b)	Γ (eV)	Γ_n (eV)	Γ_γ (eV)	Γ_n^0 (eV)
		Br^{79} resonances			
35.6	5160± 850	0.37±0.03	0.056±0.004	0.31±0.03	0.0094
53.4	1210± 265	0.45±0.06	0.023±0.002	0.43±0.07	0.0031
189	1000± 450	0.49±0.12	0.078±0.016	0.41±0.14	0.0057
238	3500± 900	1.29±0.25	0.83 ±0.07	0.46±0.30	0.054
292	820± 110	0.43±0.02	0.082±0.007	0.35±0.03(assumed)	0.0047
317	2780± 80	1.09±0.03	0.74 ±0.02	0.35±0.03(assumed)	0.041
		Br^{81} resonances			
102	6500±2300	0.41±0.10	0.20 ±0.03	0.21±0.12	0.020
136	4700±1500	0.70±0.12	0.33 ±0.04	0.37±0.14	0.028
205	330± 40	0.37±0.03	0.015±0.003	0.35±0.03(assumed)	0.0012

A value of $g = \frac{1}{2}$ was used to obtain values of Γ_n and Γ_γ. For the determination of the parameters of the resonances at 205, 292 and 317 eV, Γ_γ was assumed to be equal to a weighted average of the values of Γ_γ deduced for the lower energy resonances in Br^{79}.

momentum associated with each resonance is 2 or 1. Since the value of the total angular momentum is not known for any of the resonances in bromine, a value of $\frac{1}{2}$ has been assumed for g in order to obtain values of Γ_n and Γ_γ. The results for Br^{79} and Br^{81} are summarized in table 1. These results include values of the radiation width Γ_γ for four resonances in Br^{79} and two in Br^{81}. Since it is well established [9]) that these widths show little variation from resonance to resonance, a weighted average of the values for each isotope in table 1 may be considered to represent the radiation width for that nucleide. These average values for Br^{79} and Br^{81} are 0.35±0.03 and 0.28±0.09 eV, respectively. For the resonances at 205, 292 and 317 eV, data of good quality were obtained for only one thickness of sample. In order to obtain values of σ_0, Γ and Γ_n from these data, a value of Γ_γ equal to the weighted average for Br^{79} was assumed.

Because of the small amount of resonance structure observed for Br^{81}, a value for the strength function is given only for Br^{79}. This value was obtained from the resonance parameters listed in table 1 and is equal to $(1.75^{+0.8}_{-0.6}) \times 10^{-4}$.

2.2. SELENIUM

The slow neutron resonance structure of selenium had been investigated previously at this laboratory [10]) with the old Argonne fast chopper located at the old heavy-water reactor (CP-3'). At least eight resonances were observed in the energy interval from 2 eV to 3 keV. The only resonance parameters which could be determined from these data were values of $\sigma_0 \Gamma^2$ for the four resonances of lowest energy. Isotopic assignments of the resonances were not determined. Since the resolution of our chopper located at CP-5 is considerably better than that used in the old measurements, and since the enriched isotopes of selenium have been acquired, we have repeated the measurements.

All the samples, both normal and enriched isotopes, were in the form of metallic selenium. The samples of normal selenium were 0.304, 1.67, 3.56 and

TABLE 2

Relative abundances of the isotopes in the selenium samples

Samples	Percent abundance of various isotopes					
	74	76	77	78	80	82
Se^{76}	0.6	54.8	6.9	12.5	21.5	3.7
Se^{77}	0.4	6.1	49.4	21.4	19.6	3.0
Se^{78}	0.2	2.8	2.9	72.7	18.7	2.7
Se^{80}	0.2	0.8	0.7	2.8	94.6	0.9
Se^{82}	0.5	5.2	4.3	13.7	32.0	44.4
Normal Se	0.9	9.0	7.6	23.5	49.8	9.2

10.9 g/cm^2 thick. Those of Se^{76}, Se^{77}, Se^{78}, Se^{80} and Se^{82} were 0.605, 2.47, 3.17, 3.12 and 0.90 g/cm^2 thick, respectively. All these thicknesses are in terms of the number of g/cm^2 of selenium. The relative abundance of the various isotopes of selenium in each sample is shown in table 2.

The total cross section of normal selenium is presented in fig. 2. The resonance of lowest energy (at an energy of 27.0 eV) is not shown on this graph. All of the resonances in fig. 2 with energies less than 2 keV had been observed previously; however, the group of three resonances in the region of 800 eV are now well enough resolved that their parameters can be determined. Since the time at which the present measurements were made, Good, Neiler and Gibbons [11]) have measured the transmission of a sample of normal selenium over the energy range from 3.8 to 9 keV and have found five resonances, three of which correspond roughly in energy to the three highest reported in the present paper.

The problem of determining the parameters of the resonances observed in selenium is complicated by the fact that normal selenium is made up of many isotopes of which pure individual samples are not available. This means that the mere presence of a resonant dip in the transmission in a measurement made with a sample enriched in a particular isotope does not immediately identify the resonance with that isotope. Furthermore, since the natural widths of the

resonances are comparable to the resolution width associated with the spectrometer, the absolute magnitude of the dip is not a definite means of identification. The only meaningful quantity, in addition to the energy at which the minimum occurs, is the area above the dip in the transmission. Each of these areas may be used, with the aid of the standard curves for area analysis, to construct a

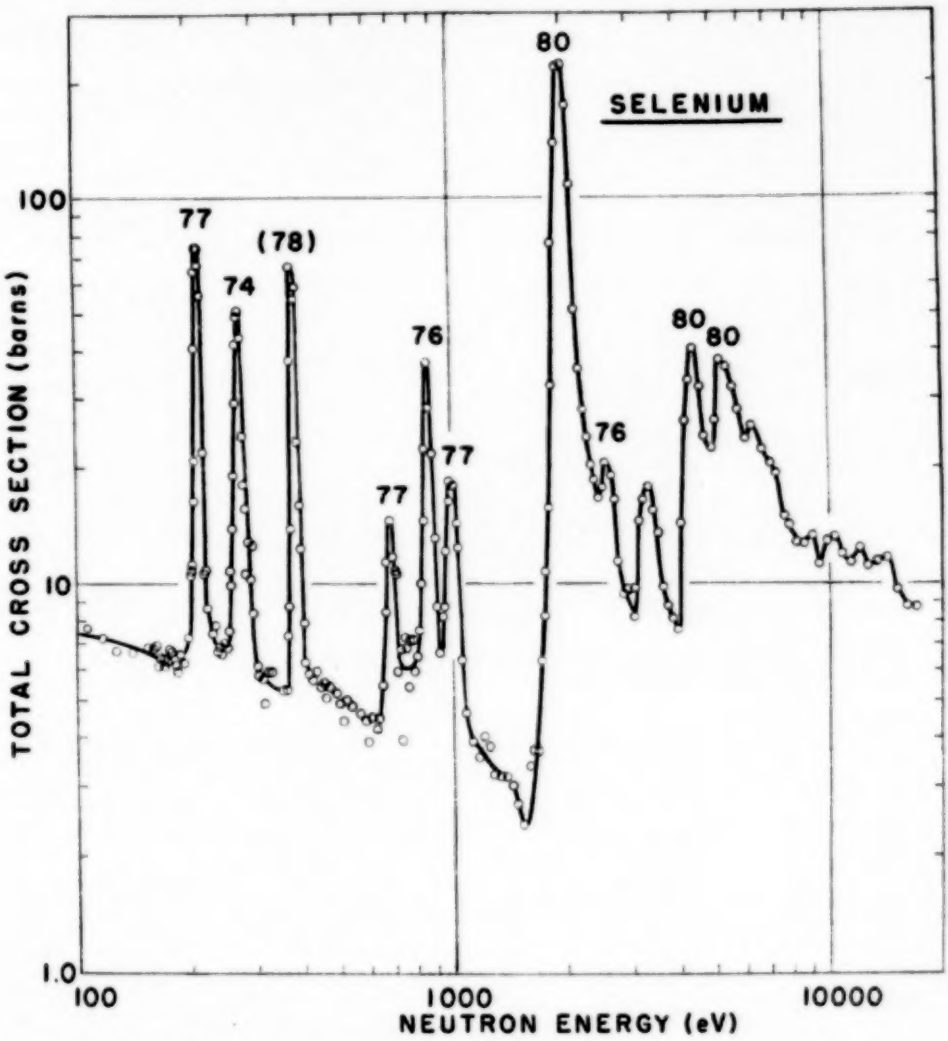

Fig. 2. The total cross section of normal selenium. The numbers associated with the resonant peaks indicate the isotope responsible for the level.

curve of $n\sigma_0$ *vs.* Γ, where n is the sample thickness of the isotope responsible for a transmission dip. The isotopic identification of each resonance may then be made by the determination of the isotopic assignment (i.e., selection of values of n) which caused the curves of σ_0 *vs.* Γ for the different samples to overlap or to intersect at a width corresponding to a reasonable value of Γ_γ. The results of this procedure are given in table 3.

The curves of σ_0 *vs.* Γ were also used to deduce the widths of the levels. For the resonance at 27.0 eV, for which the statistical factor g can have only a

value of unity, the data are complete enough to give values for both Γ_n and Γ_γ. However, for the other levels we have the condition that $\Gamma_\gamma \ll \Gamma_n$, a condition which makes it impossible to determine meaningful values of Γ_γ from the present data. It was, therefore necessary to assume a value for Γ_γ in order to obtain values of Γ_n. For this purpose we use $\bar{\Gamma}_\gamma = 0.25 \pm 0.07$. This value is a somewhat arbitrary average of the radiation width for the 27-eV resonance and of widths for neighbouring nucleides. The parameters obtained from the analysis indicated above are listed in table 3. Since the statistical factor g associated with

TABLE 3

Parameters of neutron resonances in selenium

E_0 (eV)	Isotope	g	σ_0 (b)	Γ (eV)	Γ_n (eV)	Γ_γ (eV)
27.0	74	1	45000±4800	0.355±0.025	0.166±0.008	0.189±0.030
212	77	$\frac{3}{4}$	6860± 400	0.96 ±0.06	0.67 ±0.05	0.25 ±0.07 (assumed)
		$\frac{1}{4}$	2670± 80	1.86 ±0.11	1.61 ±0.11	,,
272	74	1	9000± 110	4.3 ±0.2	4.05 ±0.2	,,
382	(78)	1	4700± 500	0.83 ±0.05	0.58 ±0.04	,,
690	77	$\frac{3}{4}$	2320± 120	1.37 ±0.10	1.12 ±0.10	,,
		$\frac{1}{4}$	845± 20	2.5 ±0.2	2.25 ±0.2	,,
860	76	1	2850± 60	4.0 ±0.25	3.75 ±0.25	,,
998	77	$\frac{3}{4}$	1850± 25	4.9 ±0.6	4.65 ±0.6	,,
		$\frac{1}{4}$	640± 5	8.9 ±1.1	8.65 ±1.1	,,
2000	80	1	1300± 2	48 ±2.0	48 ±2.0	—
2600	76	1	—	—	—	—
3340	—	—	—	—	—	—
4470	80	—	—	—	—	—
5300	80	—	—	—	—	—

A value of $\Gamma_\gamma = 0.25 \pm 0.07$ eV was assumed in order to obtain values of the parameters for all but the first resonance. The isotopic identification of the resonance at 382 eV is enclosed in parentheses to indicate that the assignment is a tentative one, since there is some possibility that the resonance is in Se^{76}.

a resonance in the target nucleide Se^{77} will have one of two widely different values, $\frac{1}{4}$ or $\frac{3}{4}$, parameters are listed for both values. All other isotopes of selenium have spin zero so that only the value $g = 1$ is possible.

Because of the lack of complete separation of the various isotopes of selenium, coupled with a scarcity of observable resonances, a reliable value of the strength function can be given only for Se^{80}. The isotopic purity of the sample enriched in Se^{80} is high enough so that the resonance structure observed at high energy in the transmission measurements on that sample is largely due to Se^{80}. Thus, for this sample, the average area under the transmission curve may be used to determine $\bar{\Gamma}_n^0/D$. The details of the method used in treating the data have been described previously by Coté, Bollinger and LeBlanc [1]). The value of $\bar{\Gamma}_n^0/D$ which was obtained in this manner by averaging over the energy interval from 1 to 15 keV is $(2.43^{+1.20}_{-0.80}) \times 10^{-4}$.

3. Discussion of Results

The experimental data which show the variation of the strength function with nucleon number are displayed in fig. 3. The values which have been selected for this representation have been chosen almost exclusively from results taken with the Argonne fast chopper. This was done because these data offer the advantage of having been obtained in a well understood and systematic way. The main fault with these data is that they are based on a rather small number

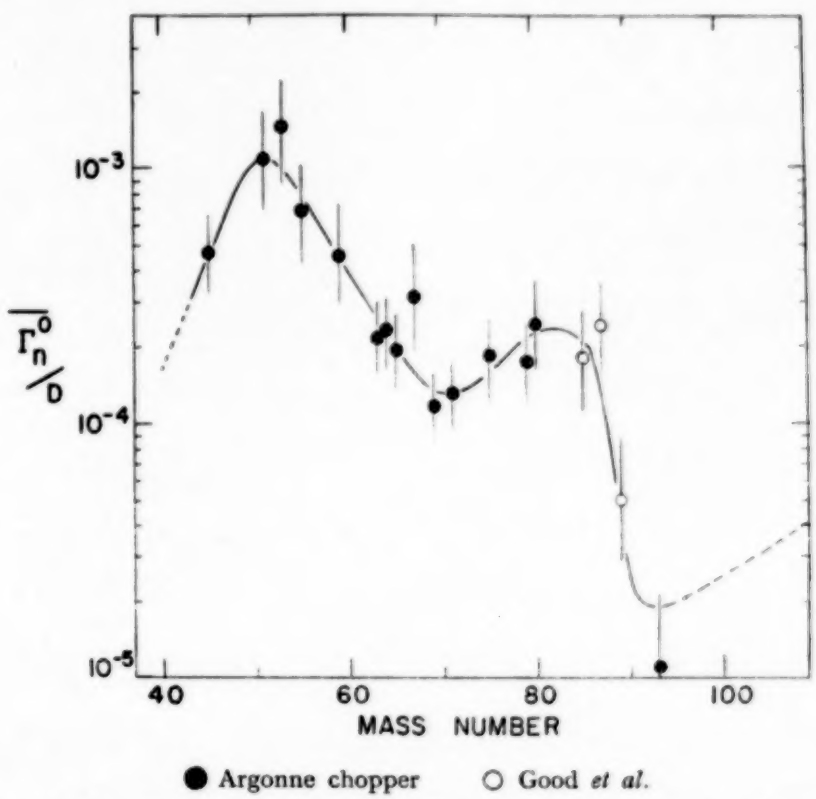

Fig. 3. The variation of the strength function $\overline{\Gamma}_n^0/D$ with nucleon number A. The solid circles indicate data taken with the Argonne fast chopper, while those points marked by open circles are based on the results of Good, Neiler and Gibbons [11]). The curve was drawn through the measured points to emphasize the experimentally determined variation of $\overline{\Gamma}_n^0/D$ with A. The dotted portion above $A = 90$ was drawn to connect with the experimental results for higher A.

of observed resonances, since the data were limited to energies less than 15 keV. However, we feel that this factor is outweighed by the fact that the resonant contribution to the area above the dips in transmission is so large that the effects attributable to potential scattering and to the interference between resonant and potential scattering can be neglected. A meaningful uncertainty in the value of the strength function can then be obtained from well defined statistical arguments.

Although most of the values of $\overline{\Gamma}_n^0/D$ displayed in fig. 3 are the same as those

reported by Coté, Bollinger and LeBlanc [1]), several require some comment. The values for Br^{79} and Se^{80} are those reported in the present paper. The value for Mn^{55} has been changed to $(6.4^{+3.4}_{-2.3})\times 10^{-4}$ as a result of a more recent study of this nucleide by Bollinger, Coté and Thomas [5]), in which better values were obtained for the parameters of the resonances at 7100 and 8800 eV. Finally, we have taken a value of $(0.6^{+0.4}_{-0.2})\times 10^{-4}$ to represent Y^{89}. Good, Neiler and Gibbons [11]) give a value of 0.25×10^{-4} for Γ_n^0/D, but private communication with these authors has revealed that a value of 0.6×10^{-4} is correct. The latter value is consistent with the energies and widths of the resonances observed by them.

The curve shown in fig. 3, which is drawn through the experimental points to emphasize the experimental variation, clearly indicates a splitting of the maximum in the strength function. The presence of experimental evidence for such a splitting was first suggested by the present authors [12]) several years ago on the basis of preliminary measurements on bromine and selenium †. At that time there was little understanding of how such a splitting could occur since the optical model [14]), which had led to the prediction of the maxima, had predicted rather narrow single peaks. Since that time, however, additions have been made to both the theoretical and experimental pictures. As more experimental data were gathered it became clear that the maximum near $A = 155$ was actually a double-peaked maximum [15]). Also, calculations based on the optical model were carried out in which more complicated forms of the potential were assumed. The simple spherically symmetric complex square well used in the earlier calculations was replaced in some calculations by potentials which retained the spherical symmetry but had a diffuse edge [16]), and in other calculations by potentials in which the spherical symmetry was abandoned [17, 18]). Both these changes are in the direction of greater realism, and the calculations based on a spherical potential actually predicted a splitting of the peaks in the strength function.

Let us now consider the relationship of the experimental and calculated values Γ_n^0/D in more detail. The refined calculations of Chase, Wilets and Edmonds [18]), based on a deformed diffuse complex potential in which the deformation is chosen to correspond to experimentally inferred intrinsic quadrupole moments, are in excellent agreement with the experimentally determined values [15]) of the strength function for $A > 120$. Below $A = 120$ the agreement is much less striking and consequently the variation cannot be considered to be as well understood. Between $A = 120$ and $A = 80$ two very deep minima have been observed in the strength function. It appears to be more than mere coincidence that these minima occur for nucleides near the closed shells of 50 neutrons (Nb^{93} with 52) or 50 protons (cadmium and tin with 48 and 50 protons, respec-

† K. Seth [13]) has recently reported some results of Weston, Bilpuch, Newson, and Seth which also suggest a secondary peak.

tively). In fact Lane, Lynn, Melkonian and Rae [19]) have recently pointed out that the imaginary part of the potential might be expected to be low in the region of magic number 50 and that this would result in low values of the strength function.

The discussion of the preceding paragraph provides a basis for an explanation of the observed variation of the strength function with A for $A < 100$, as shown in fig. 3. The two maxima in $\bar{\Gamma}_n^0/D$ may result from deformation of the nucleides in this region of mass, with the sharp drop just above the second maximum being caused by the closing of the shell of 50 neutrons. The importance of nuclear deformations has recently been confirmed by Chase and Wilets [20]), who have extended their calculations with deformed diffuse potentials to nucleides with $A < 120$. They obtain results that are in qualitative agreement with those of fig. 3, although their height of the first maximum seems to be significantly smaller than that of the experimental values, and the second maximum appears to fall at too low a value of A. No detailed comparison between the experimental and calculated values is presented here because the calculated results depend sensitively on the degree of nuclear deformation, and the inferred numerical values of the deformation are quite uncertain for the nucleides considered here. Furthermore, Lane *et al.*[19]) have suggested that the imaginary part of the potential may be smaller for nucleides with A near 50 because of the magic number 28; a decrease in this quantity will result in a higher maximum. Thus too many free parameters are available to make a meaningful fit to the strength function data.

In summary it can be said that a real splitting in the maximum near $A = 55$ does exist in the experimentally determined variation of $\bar{\Gamma}_n^0/D$ and that the main features of that variation, while not completely understood, have some theoretical basis.

References

1) Coté, Bollinger and LeBlanc, Phys. Rev. **111** (1958) 288
2) H. A. Bethe, Revs. Mod. Phys. **9** (1937) 115
3) Melkonian, Havens and Rainwater, Phys. Rev. **92** (1953) 702
4) Bollinger, Coté, Dahlberg and Thomas, Phys. Rev. **105** (1957) 661
5) Bollinger, Coté and Thomas, Proceedings of the Second International Conference on the Peaceful Uses of Atomic Energy, (United Nations, Geneva, 1959) P/686
6) R. W. Schumann, Rev. Sci. Instr. **28** (1957) 489
7) W. Havens, Jr. and L. Rainwater, Phys. Rev. **83** (1951) 1123
8) R. R. Palmer and L. M. Bollinger, Phys. Rev. **102** (1956) 228
9) J. S. Levin and D. J. Hughes, Phys. Rev. **101** (1956) 1328
10) Bollinger, Dahlberg, Palmer and Thomas, Phys. Rev. **100** (1955) 126
11) Good, Neiler and Gibbons, Phys. Rev. **109** (1958) 926
12) LeBlanc, Bollinger and Coté, Phys. Rev. **100** (1955) 1248A; see also ref. [1])
13) Proceedings of the International Conference on the Nuclear Optical Model (The Florida State University, Tallahassee, 1959) p. 172

14) Feshbach, Porter and Weisskopf, Phys. Rev. **96** (1954) 448
15) Hughes, Zimmerman and Chrien, Phys. Rev. Lett. **1** (1958) 461
16) Feshbach, Porter and Campbell (unpublished), quoted by V. F. Weisskopf, Physica **18** (1956) 952
17) B. Margolis and E. S. Troubetzkoy, Phys. Rev. **106** (1957) 105;
V. V. Vladimirskii and I. L. Ilyina, Nuclear Physics **6** (1958) 295
18) Chase, Wilets and Edmonds, Phys. Rev. **110** (1958) 1080
19) Lane, Lynn, Melkonian and Rae, Phys. Rev. Lett. **2** (1959) 424
20) D. M. Chase, private communication

2.I:3.A *Nuclear Physics* **14** (1959/60) 131--139; © *North-Holland Publishing Co., Amsterdam*
Not to be reproduced by photoprint or microfilm without written permission from the publisher

NUCLEAR ABSORPTION OF GAMMA RAYS IN Al, Si, P, S AND Ca

J. DULAR, G. KERNEL, M. KREGAR, M. V. MIHAILOVIĆ, G. PREGL, M. ROSINA and Č. ZUPANČIČ

Institute "J. Stefan", Ljubljana, Yugoslavia

Received 13 August 1959

Abstract: Bremsstrahlung absorption spectra are measured in five elements, using a magnetic Compton spectrometer. By subtracting theoretical atomic absorption cross sections the energy dependence of the nuclear absorption cross sections is obtained. However, the absolute value of the nuclear absorption cross section has not been accurately determined.

1. Introduction

The nuclear absorption cross section of gamma rays is the basic parameter for the photonuclear reaction process and should be the easiest to interpret. Yet most of our present knowledge of the total nuclear absorption stems from investigations on the partial reaction cross sections. In most cases one is obliged to use a differentiating procedure to obtain partial cross sections from bremsstrahlung yield curves. Therefore, it is hard to reveal finer details of the energy dependence of the absorption cross section, especially in the region far above the threshold for the particular reaction. In regions where more than one partial reaction is possible, results are not reliable owing to the difficulty of measuring all partial reactions in the same way.

For these reasons direct measurements of the total nuclear absorption are desirable, though their accuracy is affected by the large atomic absorption. One of the several ways to attempt it, is the measurement of the absorption spectrum of a bremsstrahlung source. The experiment is analogous to the measurement of Fraunhofer lines in optical spectroscopy. Nuclear absorption "lines" show up in the bremsstrahlung absorption spectrum, superimposed on a smooth background of atomic absorption. The first investigations along these lines have been made with the use of NaI total absorption spectrometers [1]). However, their resolution proved to be too poor to give any details about the shape of the absorption curves. Recently, first attempts at using high resolution Compton and pair spectrometers for this purpose have been reported [2, 3]). In a previous paper [4]), the results of such a measurement in Al have been briefly communicated. Here, the experimental procedure will be described in more detail and absorption cross sections in Al, Si, P, S and Ca will be presented.

2. Experimental Arrangement

A block diagram of the experimental set-up is shown in fig. 1.

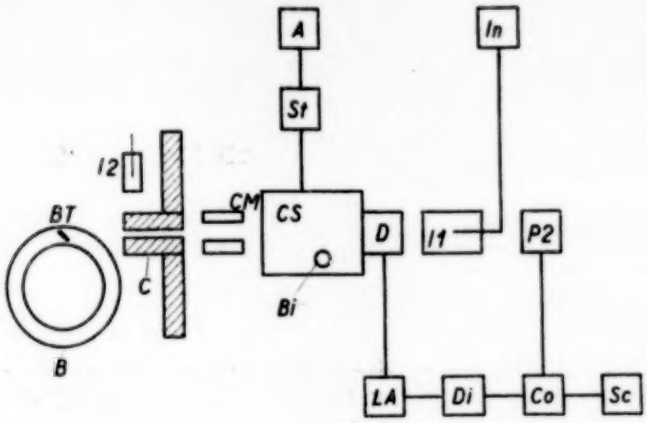

Fig. 1. Block diagram of the experimental set-up.
B — betatron, BT — betatron target, C — lead collimator, CM — magnet for cleaning, CS — Compton spectrometer, A — power supply (batteries) for the magnet, St — current stabilization, D — detector, LA — linear amplifier, Di — discriminator, P2 — photomultiplier for the coincidence pulses, Co — coincidence circuit, Sc — scaler, Bi — bismuth spiral, I1 — ionization chamber, In — current integrator, I2 — ionization chamber.

2.1. BREMSSTRAHLUNG SOURCE

A 30 MeV Brown-Boveri betatron provided the continuous bremsstrahlung spectrum. Its end-point energy was well stabilized and calibrated by known (γ, n) thresholds [5]). Also, the intensity of the bremsstrahlung beam was kept approximately constant by an electronic device. The betatron was as a rule operated at 28.9 MeV, only the highest points were taken at a betatron energy of 30.3 MeV. The beam was collimated by 480 mm of lead. Collimators with different holes, both uniform and partly conical, with an exit diameter of 4 mm were used. The use of different collimators had no effect on the shape of the spectrum.

2.2. ABSORBERS

In order to get an absorption spectrum the collimator hole was filled with the investigated element either in form of powder or solid bars. Bars of Al, S and Ca were available while powdered Si and P were used. Given the time one is prepared to spend on the experiment, the thickness of the absorber has an optimum at which maximum accuracy in the measurement of the cross section is achieved. This optimum depends both on the stability of the experimental arrangement and on the attempted accuracy of the experiment, but it is sufficiently flat that an attenuation by a factor of five or more is satisfactory. In this experiment, minimum attenuation factors were approximately: 14 for Al, 10 for S, 12 for Ca, 5 for Si and 4,5 for P.

2.3. SPECTROMETER

A previously described [6]), but slightly improved, Compton spectrometer was used Such a spectrometer magnetically analyzes the negatons and positons which the bremsstrahlung beam ejects in the forward direction from a foil of light material. The difference between the number of negatons and positons is considered to be the number of Compton electrons. Their spectrum represents the gamma ray spectrum shifted by a small amount and distorted by an energy-dependent efficiency factor, which is, however, immaterial for the measurements of the absorption cross sections.

In our experiment the converter was a 0.114 g/cm² thick polythen foil. A circular lead slit, 14 mm in diameter, at a distance of 50 cm from the converter foil, admitted the ejected electrons to the magnet. The latter was a 70° double-

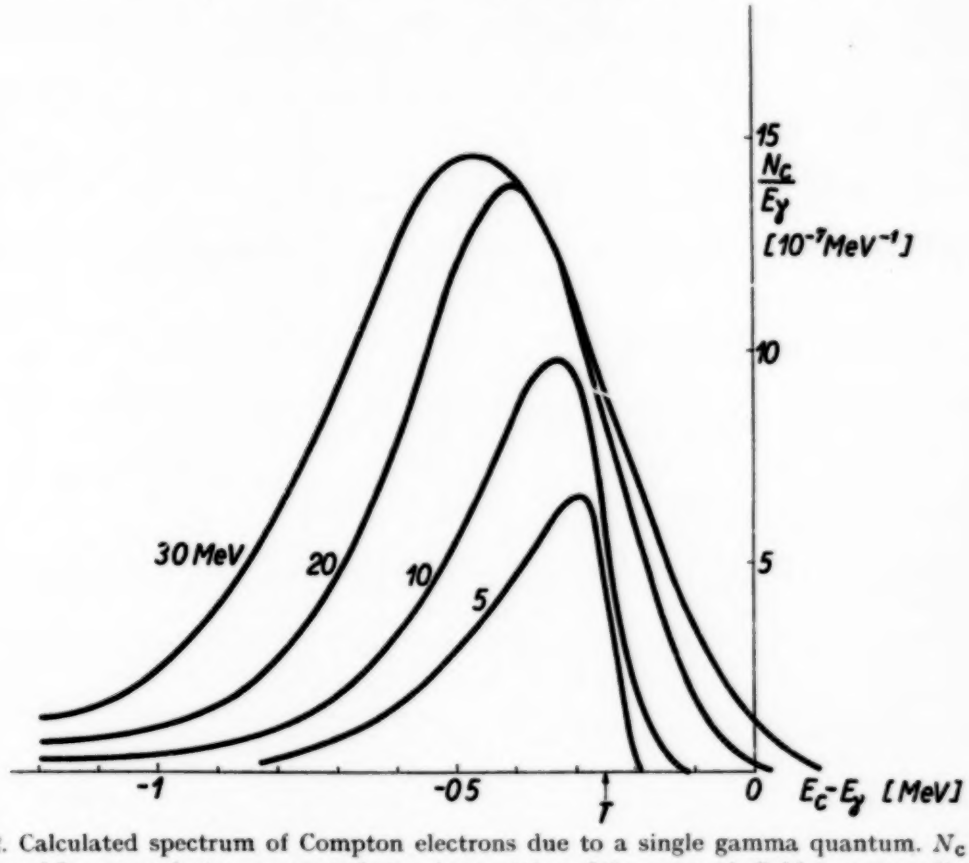

Fig. 2. Calculated spectrum of Compton electrons due to a single gamma quantum. N_c is the number of Compton electrons, counted at a given setting of the magnetic field, corresponding to an electron energy E_c. For convenience N_c/E_γ is plotted versus $E_c - E_\gamma$, E_γ being the energy of the γ-quantum.

focusing type with an equilibrium path radius of 17 cm. The spectrometer was operated at unit magnification. The exit lead slit had a diameter of 10 mm.

The response of the spectrometer has been determined by computing the energy distribution, at the position of the detector, of the Compton electrons caused by a monoenergetic gamma source[7]). In this calculation the angular dependence of the Klein-Nishina cross section, the connection between angle

and energy of the emitted electrons, multiple scattering and energy loss of the electrons in the converter foil, and the finite diameters of the gamma ray beam and of the entrance and exit slits have been taken into account. The result is shown on fig. 2 for four different energies of the gamma ray.

The magnetic field was stabilized to 0.1 % and measured by a bismuth spiral (thermostated to better than 0.1°C) in a bridge circuit. The errors in the magnetic field determination induced by temperature fluctuations were estimated to be of the order of 0.2 % at the upper end of the spectrum and of the order of 2 % at the lowest measured point. The photon energy versus magnetic field calibration was achieved by measuring the end-points of the electron spectrum at several values of the well known betatron energy. The end-points were determined by drawing a straight line through the steeply decreasing upper part of the electron spectrum. This procedure might cause a systematic shift of the energy scale if the bremsstrahlung spectrum flattens off before its end-point, which, however, does not seem to be the case [8]).

2.4. COUNTING SYSTEM

A Čerenkov counter served as the detector of electrons. It consisted of a slightly conical lucite cylinder 25 mm in diameter and 40 mm in length, and an

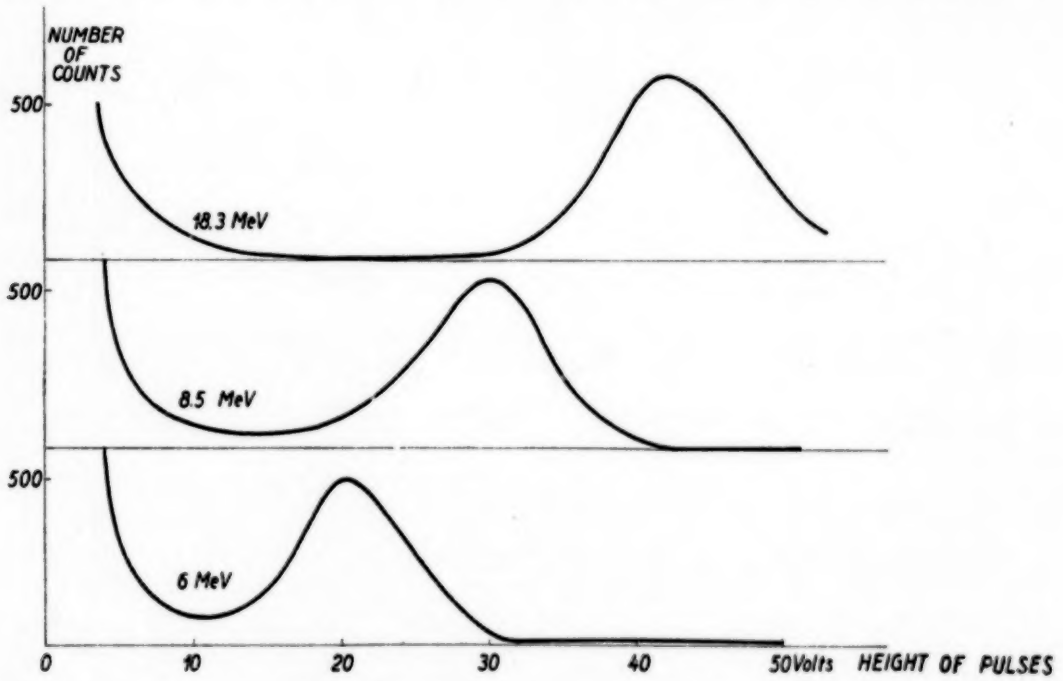

Fig. 3. Height distribution of pulses from the detector due to monoenergetic electrons.

EMI 6262 B photomultiplier. The diameter of the lucite cylinder was chosen large enough to minimize the number of electrons scattered out before they transversed the full length of the cylinder. The photomultiplier had a double mu-metal and a soft iron shield and the hole detector was shielded against stray gamma rays by 10 cm of lead. No neutron shielding was necessary.

The pulses from the photomultiplier were amplified in a conventional Cole amplifier and passed through a pulse height discriminator and a gate to a scaler. The pulses from the discriminator were considerably longer than the betatron bremsstrahlung bursts so that only one or none detector pulse per betatron pulse could be registered. The gate was opened only in coincidence with the bremsstrahlung bursts, which considerably reduced the background.

The discriminator level setting was calibrated by substituting the discriminator by a 100 channel pulse-height analyzer which was also gated in coincidence with the betatron burst. The height distribution of pulses from the detector is shown in fig. 3 for three different electron energies. The pulse height was equal for all electron energies above 11 MeV corresponding to the fact that the range of those electrons was larger than the length of the lucite cylinder.

2.5. BEAM MONITOR

The bremsstrahlung beam intensity was monitored by a large ionization chamber connected to an electronic current integrator. The ionization chamber was placed in the collimated bremsstrahlung beam behind the Compton spectrometer in order to avoid influences of the fluctuations in the operation of the betatron, but resigning thus from an absolute cross section determination. The latter has been attempted by measuring the incoming bremsstrahlung intensity with another ionization cell inside the betatron and outside the main beam, but the results fluctuated by several percent.

3. Measuring Procedure

The standard measuring procedure consisted in counting the numbers of negatons and positons and the respective backgrounds at a given value of the magnetic field and for a given charge collected by the monitor. The background was measured with the converter foil removed from the beam. Since it was found small and smoothly varying, it was in some later measurements counted separately and at larger steps. All these data were corrected for dead time effects which were largest when electrons were counted with no absorber in the beam. In this case they amounted to 20 percent at most. The number of Compton electrons was deduced by subtracting the number of positons and the small difference between negaton and positon background from the total number of negatons. With no absorber this Compton electron spectrum was measured so often in the course of our work that one may consider it to be known with negligible statistical errors.

In view of the limited intensity of the betatron and the small efficiency of the Compton spectrometer all these measurements were extremely time consuming. Though around 200 hours of operation should suffice for one element at the attempted accuracy, it was found in practice that owing to apparatus failure about one month was needed for one element in spite of a working schedule of

18 to 24 hours per day. In such circumstances a rigid control system was found to be very important. In addition to standard checks of the electronic equipment the following controls were accepted. The beam monitor and the detector were checked at intervals of approximately six hours by putting a 10 mC Ra source in appropriate positions. Slow drifts in the beam monitoring and counting equipment could thus be detected and corrected for. The sequence of points to be measured was selected at random but a standard point was repeatedly measured in order to check the reproducibility. The upper end of the spectrum was also traced several times in a week in order to check the magnetic field determination. Upon inspecting all the results the conclusion could be drawn that in this way the systematic errors were kept within one percent.

4. Results and Conclusions

From the measured spectra of Compton electrons the total absorption cross section up to an additive constant was obtained by subtracting the logarithms of the corresponding values of the spectra without and with the absorber. The nuclear absorption cross section up to an additive constant was then obtained by subtracting the theoretical atomic absorption cross section. The latter was interpolated from the data given in Siegbahn's book [9]). The results are presented in figs. 4 to 8. Only statistical errors are indicated; the arrows point out the thresholds for the different partial reactions.

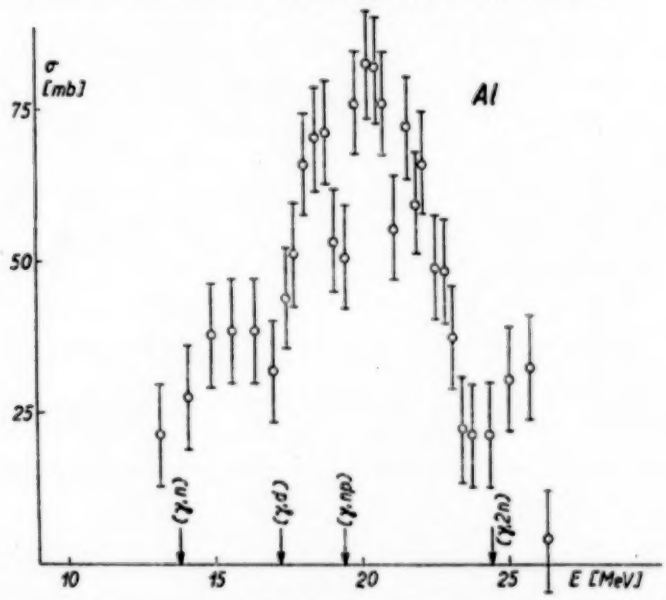

Fig. 4. Nuclear absorption cross section for Al. This figure is essentially the same as in ref. [4]) except for an arbitrary shift of the ordinate scale. It differs somewhat from the figure given in ref. [2]), which is the result of a preliminary evaluation of the experimental data.

In order to determine the additive constant, i.e. to fix the zero point of the ordinate scale the attenuation should be measured absolutely, which has not been achieved with the required accuracy. The theoretical atomic cross sec-

tions are neither believed to be accurate to better than a few percent, which induces a large uncertainty in the position of the zero point of the ordinate scale. In figs. 4 to 8 this position may thus be regarded as more or less arbitrary.

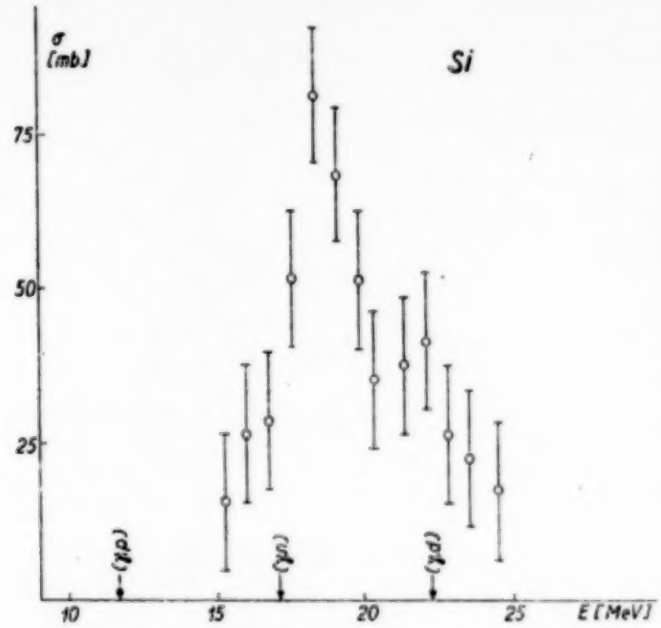

Fig. 5. Nuclear absorption cross section for Si.

On the other hand, the differences between the values of the nuclear cross section at different energies are much less affected by the uncertainties in the atomic cross section, since the latter is slowly varying with energy in all the

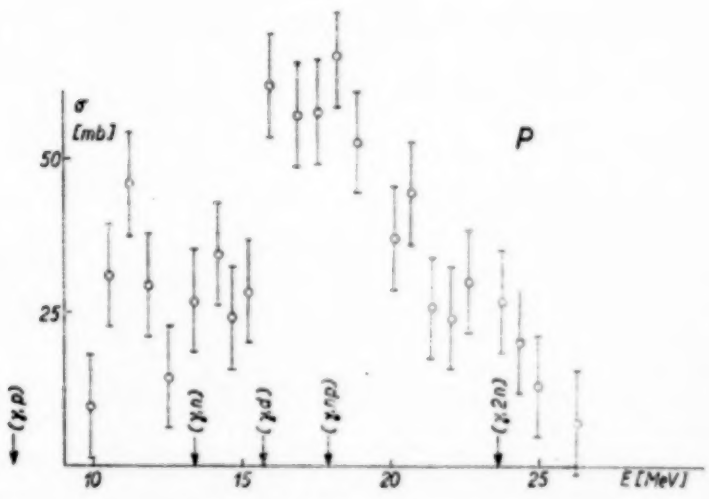

Fig. 6. Nuclear absorption cross section for P.

investigated elements. Experimentally these differences are much more certain too. They may be a little distorted because of uncertainties in the effective length of the absorber and because of secondary radiative effects in the absor-

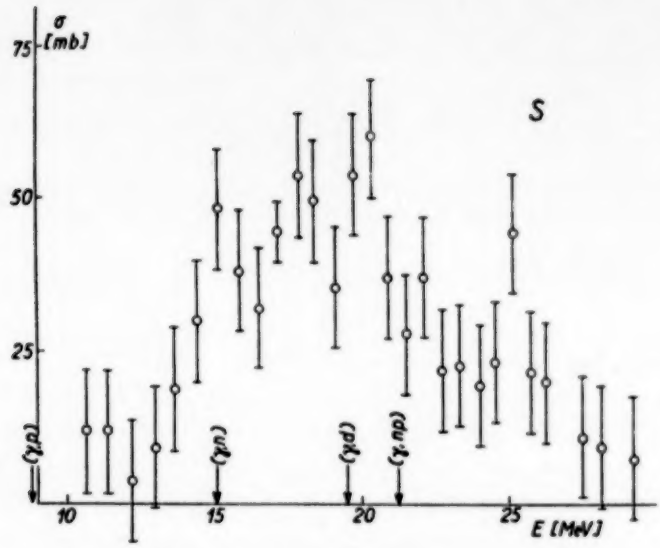

Fig. 7. Nuclear absorption cross section for S.

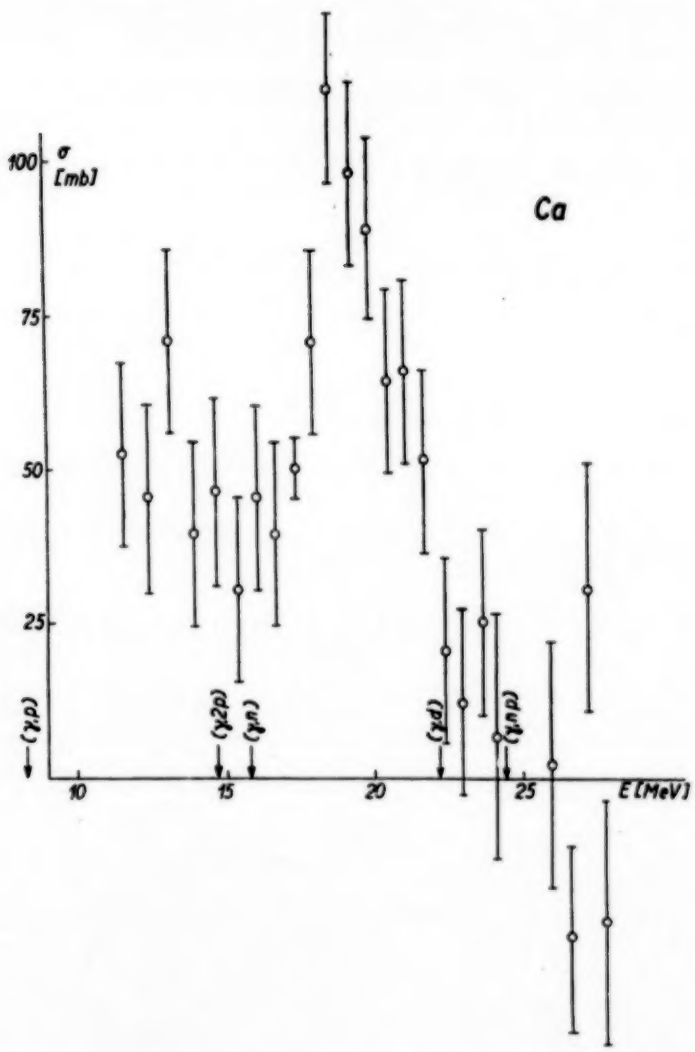

Fig. 8. Nuclear absorption cross section for Ca.

ber. The effective length of the absorber might have been shorter than calculated because of non-uniform density, especially of the powdered absorbers in the conical collimators, and possibly because of some narrow gap between the wall of the collimator and an absorber rod. This might have caused some stretching of the cross section scale but should not be too serious. The influence of gamma quanta scattered in the absorber under small angles and reaching the converter foil, the effect of the bremsstrahlung produced by secondary electrons in the absorber, and the shortening of the effective absorber length by gamma quanta partly traversing the collimator have been estimated and found to be negligible.

A definite indication of considerable structure in the giant resonance appears to be the main result of our measurements. Better resolution and statistics in such and related measurements may reveal an even finer structure. Yet the gross strength function distribution may prove to be of greatest interest. The above results also confirm the known fact that the giant resonance is narrower at magic numbers.

The experimental method can be considerably improved. With higher intensity bremsstrahlung sources or higher efficiency spectrometers better statistics and more favourable geometry could be achieved. The accuracy of the determination of nuclear absorption cross section would then be limited chiefly by present uncertainties in the theoretical atomic cross sections.

We are grateful to Professor A. Peterlin for his kind interest in this work and for many encouragements. We are very indebted to M. Vakselj and J. Šnajder for assistance in the operating of the betatron and development of some parts of the electronic equipment.

References

1) R. S. Foote and H. W. Koch, Rev. Sc. Inst. **25** (1954) 746
2) Comptes rendus du Congrès international de Physique nucléaire (Paris, juillet 1958) 157
3) B. Ziegler, Z. Physik **152** (1958) 566
4) M. V. Mihailović, G. Pregl, G. Kernel and M. Kregar, Phys. Rev. (in press)
5) D. Jamnik, Nuclear Instruments **1** (1957) 324
6) U. Miklavžič and Č. Zupančič, Reports J. Stefan Inst. **5** (1958) 3
7) M. Rosina (to be published)
8) E. G. Fuller, E. Hayward and H. W. Koch, Phys. Rev. **109** (1958) 630
9) Ch. M. Davison, in Beta- and Gamma-Ray Spectroscopy, edited by K. Siegbahn (North Holland Publishing Company, Amsterdam, 1957) 857

2.B:6.A *Nuclear Physics* **14** (1959/60) 140—144; © *North-Holland Publishing Co., Amsterdam*
Not to be reproduced by photoprint or microfilm without written permission form the publisher

AN AID IN THE DETERMINATION OF NUCLEAR SPINS

R. K. SHELINE and H. L. NIELSEN †
Florida State University, Tallahassee, Florida
and
A. SPERDUTO
Laboratory of Nuclear Science, Massachusetts Institute of Technology, Cambridge, Massachusetts ††

Received 4 September 1959

Abstract: Intensities of the α groups collected in the backward angle from the $Al^{27}(d, \alpha)Mg^{25}$ reaction have been analyzed after recording them on nuclear emulsions over an extended range of excitation. Given intensities are determined with an average deviation of ≈ 15 %. Normalizing the intensities by $2I+1$ and barrier penetration factors produces intensities which are the same within an average deviation of 33 %. Use of intensities as an aid in determining spin is suggested.

1. Introduction

The theory of nuclear reactions leads to a very complicated expression for the differential cross section for a given reaction in terms of the nuclear spin of the residual nucleus. However, as the degeneracy of the final state with spin I is $(2I+1)$, the expression must contain the statistical factor $(2I+1)$, in addition to another more involved function of I. If this function of I varies sufficiently slowly, the differential cross section measured by the intensity of the outcoming particle group is approximately proportional to $(2I+1)$. Clearly, a simple I-dependence of the level intensities, together with an exact measurement of the level energies, would lead to an easy and very powerful method for determining nuclear spins. In contrast to the decay-scheme method using beta- and gamma-ray spectroscopy, this method is fast, and in the experiments every level in the nucleus under investigation is populated, whereas in a radioactive decay strong selection rules prohibit population of a number of levels. In certain special cases the differential cross section evaluated from the intensity of the outcoming particle group of a given reaction has proved to be a helpful tool in assigning spins. In these cases a $(2I+1)$ proportionality has been assumed and other spin dependencies considered unimportant. Enge [1]) and Sheline [2]) have

† Now at the Institute for Theoretical Physics, Copenhagen, Denmark.

†† Supported at Florida State University by contracts with the Atomic Energy Commission and the Office of Ordnance Research and at Massachusetts Institute of Technology through Contract No. AEC AT (30-1)-2098 supported by the Atomic Energy Commission, the Office of Naval Research and the Air Force Office of Scientific Research.

applied the $(2I+1)$ rule in the study of jj-doublets and Enge [3]) has used it in stripping reactions.

2. Discussion and Results

In this note an experimental investigation has been carried out in an attempt to test the validity of the $(2I+1)$ proportionality as an approximation for the

TABLE 1

$Al^{27}(d, \alpha)Mg^{25}$ reaction. $Q_0 = 6687 \pm 10$ keV

Level	Excitation energy [a]) (keV)	Spin and parity [b])	Number of tracks [c])				
			Run I [d])	Run II [e])	Run III [f])	Run IV [g])	Run V [h])
0	0 ± 10	$\frac{5}{2}+$	217	121	175	226	–
1	586 ± 5	$\frac{1}{2}+$	59	60	55	67	22
2	975 ± 4	$\frac{3}{2}+$	128	–	110	157	49
3	1608 ± 2	$(\frac{7}{2}+)$	221	150	159	216	74
4	1963 ± 0	$\frac{9}{2}+$	206	173	168	244	72
5	2568 ± 7	$\frac{1}{2}+$	77	58	55	90	21
6	2741 ± 8	$(\frac{7}{2}+)$	124	–	103	127	49
7	2806 ± 7	$(\frac{3}{2}+)$	84	–	53	71	39
8	2404 ± 6	$\frac{3}{2}-(\frac{5}{2}+)$ [i])	293	182	222	–	77
9	3915 ± 4	$\frac{5}{2}+$	99	–	44	102	54
10	3975 ± 3	$(\frac{7}{2}-)$	200	–	147	263	48
11	4061 ± 3						
12	4280 ± 4	$(\frac{1}{2}-)$	55	–	37	73	17

[a]) Measurements are those from present experiments.
[b]) Spins and parities are those of ref. [4]).
[c]) Runs I through V were made on different Al targets. A dash in one of the columns indicates that the peak was obscured by another intense peak or by the plate edge.
[d]) 7.5 MeV bombarding energy; observation angle 130°; beam 3000 μb.
[e]) 7.5 MeV bombarding energy; observation angle 130°; beam 1500 μb.
[f]) 7.5 MeV bombarding energy; observation angle 130°; beam 1500 μb.
[g]) 7.5 MeV bombarding energy; observation angle 130°; beam 2000 μb.
[h]) 8.6 MeV bombarding energy; observation angle 130°; beam 1000 μb.
[i]) Level 8 is assumed to be double. The $\frac{3}{2}-$ component has definitely been established but the $\frac{5}{2}+$ component can only be inferred from the rotational model and from the intensity of the peak.

differential cross section. We have confined ourselves to backwards reaction angles, because experimental evidence indicates that the method fails completely at small reaction angles. The reaction $Al^{27}(d, \alpha)Mg^{25}$ was studied because the residual nucleus, Mg^{25}, has been thoroughly examined by other methods. Twelve levels with spins and parities are known with certainty in this nucleus [4]).

The experiments were carried out as follows: An Al^{27}-target evaporated on Formvar backing was bombarded with 7.52 and 8.54 MeV deuterons from the ONR-MIT Van de Graaff accelerator. The outcoming alpha particle groups were accepted at 130° with respect to the incident beam, analyzed in the field of the magnetic spectrograph, and detected on nuclear track plates.

Table 1 lists the ground state Q-value for the reaction $Al^{27}(d, \alpha)Mg^{25}$ and the excitation energies of the first 12 levels as measured in the present experiments. Uncertainties in the energies listed are the root mean square of five determinations. These values are in good agreement with those previously reported [5]). The spins and parities from ref. [4]) are also listed.

An evaluation of the intensity of each group was made by counting the total number of tracks in a peak corrected for background and solid angle variation along the plate. The reproducibility of the intensity of a level is fairly good;

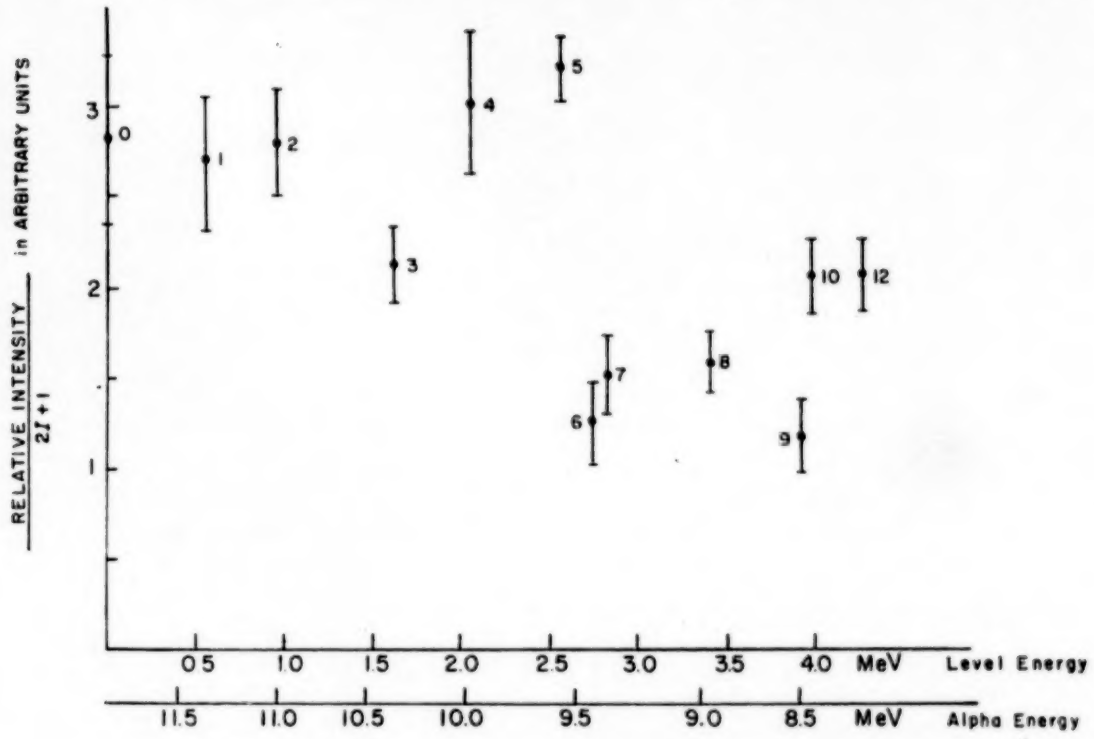

Fig. 1. The relative intensities of alpha particle groups from the reaction $Al^{27}(d, \alpha)Mg^{25}$ divided by $(2I+1)$, where I is the spin of the corresponding level in Mg^{25}. The abscissa shows level energy in Mg^{25} as well as energy of outcoming alpha groups (in centre-of-mass system). The intensities are weighed averages of normalized values from five experiments.

in four runs at 7.52 MeV deuterons the deviation from the average of the normalized intensities was less than 15 %. The normalized intensities for each alpha particle group for each of five runs are listed in the last five columns of table 1.

Fig. 1 shows the intensities divided by $(2I+1)$ as a function of the energy of the level in Mg^{25} and the corresponding energy of the alpha particle group. The level marked 8 at 3.40 MeV is assumed to be double on the basis of collective model considerations, consisting of a $\frac{9}{2}+ (K = \frac{5}{2})$ level and a $\frac{3}{2}+ (K = \frac{1}{2})$ level. At small alpha energies of the order of the Coulomb barrier, the intensities become considerably lower. This can be explained largely as a barrier effect and corrections were made. Using a radius 1.2×10^{-13} cm for the alpha particle[6])

and $R = 1.2\ A^{\frac{1}{3}} \times 10^{-13}$ cm for the Mg^{25} daughter-nucleus, we arrive at a Coulomb barrier value 8.6 MeV. The centrifugal barrier is neglected. The penetrability of the alpha particle through the barrier can be evaluated from Morrison's nomogram [7]).

The corrected intensities are plotted in fig. 2 against $(2I+1)$. There are significant deviations from the least squares fit, originating from individual effects. However, it can be seen that the $(2I+1)$ statistical factor largely accounts for the dependence of the intensities on spin. Normalizing each of the intensities by the factor $(2I+1)$ and the barrier penetration factors produces

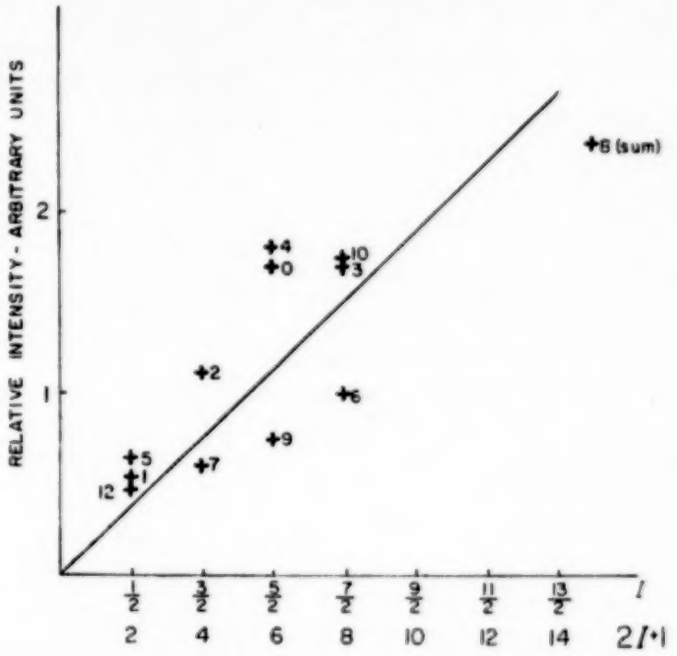

Fig. 2. The relative intensities corrected for barrier penetrability and plotted against $(2I+1)$. The straight line is a least square fit through the origin.

intensities which are the same within an average deviation of 33 %. Since the experimental intensities have an average deviation of about 15 % it seems probable that the intensities are not uniquely determined by spin. Nonetheless, intensities which varied by a factor of 5 to 6 are effectively normalized by this simple procedure, and it is obvious at once that these are the major factors. It is perhaps reasonable to note also the periodicity in the deviations. The first 6 levels (0—5) are all too intense, the next 4 (6—9) too weak and the last two (10 and 12) too intense.

The versatility of this statistical approach is also seen from the fact that in these experiments the same general trend has been observed in (d, d'), (p, p') and (d, p) reactions on Al^{27}. In these cases the resulting nuclei, namely Al^{27} and Al^{28}, have many fewer states with known spin. For this reason their results will not be presented here. It should be noted, however, that in most cases reported

in this research the compound nucleus has been the same, namely Si^{29}. This method like many others for determining nuclear spin does not determine it uniquely. Nonetheless these experiments seem to indicate the method's potential use expecially in those cases when the application of a model such as the collective model allows a choice between only a few spin possibilities in fitting the systematics of the model.

The simultaneous recording on nuclear emulsions of reaction particle groups over an extended range of excitation such as is afforded by a broad-range high-resolution magnetic spectrograph now provides an excellent means for integrating and comparing of intensities such as described here.

The results observed thus far should justify investigation of other nuclei in order to test further the suggested interpretation. It is hoped, too, that these results may give impetus to further theoretical treatment and so perhaps determine the limitations of this method.

We are indebted for the hospitality of Professor W. W. Buechner at the Massachusetts Institute of Technology and for the plate counting of Mr. W. Tripp.

References

1) Harald A. Enge, Phys. Rev. **94** (1954) 730
2) R. K. Sheline, N. R. Johnson, P. R. Bell, R. C. Davis and F. K. McGowan, Phys. Rev. **94** (1954) 1642
3) H. A. Enge, E. J. Irwin and D. H. Weaner, to be published in Phys. Rev.
4) Litherland, McManus, Paul, Bromley and Gove, Can. Journ. Phys. **36** (1958) 378
5) P. M. Endt and C. M. Braams, Revs. Mod. Phys. **29** (1957) 683
6) J. M. Blatt and V. F. Weisskopf, Theoretical Nuclear Physics (J. Wiley and Sons, 1952) **353**
7) P. Morrison, A Survey of Nuclear Reactions in E. Segrè, Experimental Nuclear Physics (1953) 198

1.E.1:
4.E

Nuclear Physics **14** (1959/60) 145—154; © *North-Holland Publishing Co., Amsterdam*
Not to be reproduced by photoprint or microfilm without written permission from the publisher

DECAY OF ^{140}Ba

P. BOSKMA and H. DE WAARD

Natuurkundig Laboratorium der Rijksuniversiteit, Groningen, Netherlands

Received 21 August 1959

Abstract: The decay of ^{140}Ba to ^{140}La has been investigated by means of a coincidence magnetic spectrometer and β- and γ-scintillation coincidence techniques. A uniquely determined level scheme (fig. 1B) can be given.

1. Introduction

^{140}La is a nucleus with 57 protons and 83 neutrons. The study of odd nuclei is very interesting to get information on the coupling of the odd particles. As this nucleus has 83 neutrons, some trends of the shell model may also be expected to be present.

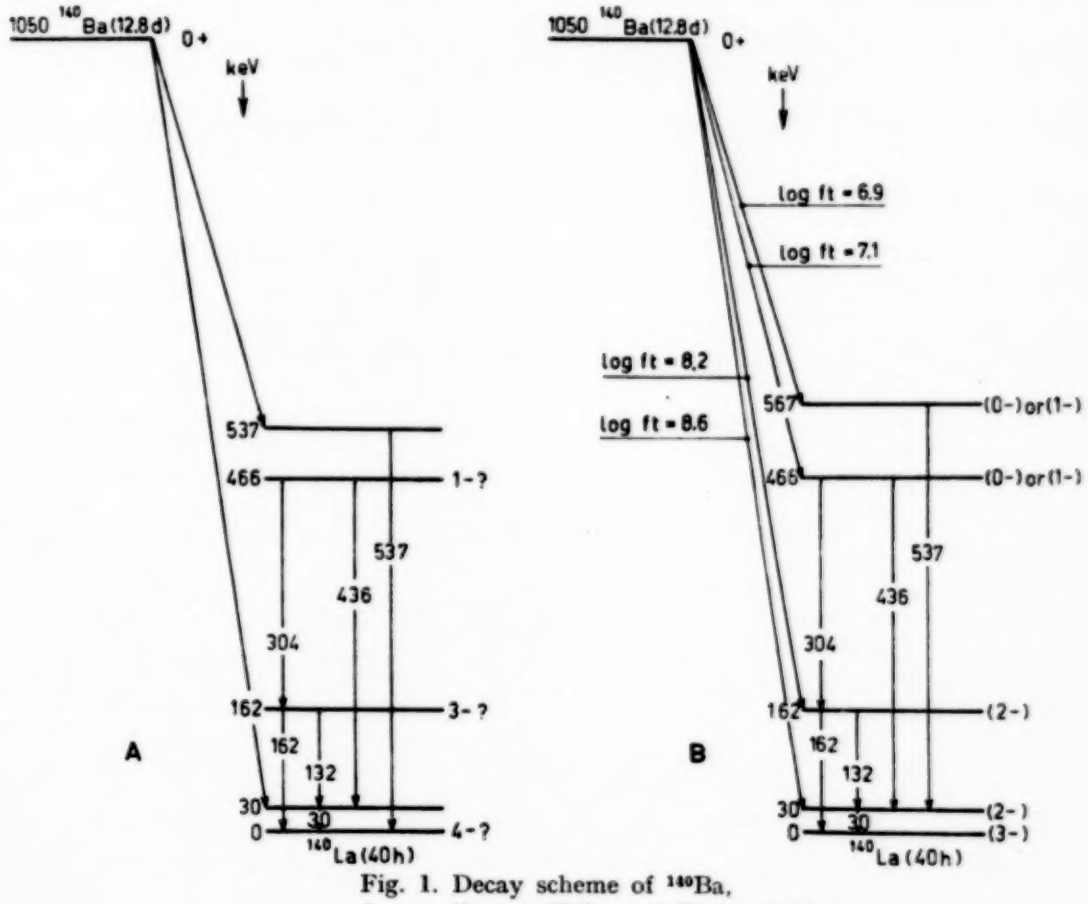

Fig. 1. Decay scheme of ^{140}Ba,
A-according to Kelly and Wiedenbeck,
B-according to this paper.

The decay of ^{140}Ba to ^{140}La has been investigated by several authors [1–5]). Gamma rays of 30, 132, 162, 304, 436 and 537 keV were found and decay schemes were proposed on the basis of intensities and transition energies. The ground state spin of ^{140}La was concluded to be 3— from an investigation of the ^{140}La decay by Bolotin *et al.*[6]), while the 537 keV radiation was determined to have E2 character on the basis of α_K and the K/(L+M) ratio. A more recent investigation was carried out by Kelly and Wiedenbeck [7]) by means of scintillation counter and directional correlation measurements. Coincidence experiments, using the summing method in a NaI(Tl) crystal established a decay scheme with levels at 30, 162, 466 and 537 keV. The directional correlation measurements on the 304—162 keV cascade gave as a most favoured sequence 1(Q)3 (D, Q)4 for the levels at 466, 162 and 0 keV. Other combinations, partly including double mixtures could not be absolutely excluded. However, the results uniquely indicate a spin $\geqq 2$ for the intermediate level. Fig. 1A shows the decay scheme and level assignments proposed by Kelly and Wiedenbeck. Finally, a study by Silant'ev [8]), which came to our notice after the completion of our own measurements, leads to a decay scheme different from that of Kelly and Wiedenbeck but in good agreement with our measurements.

2. Preparation of Sources

^{140}Ba was obtained as a fission product from Harwell. A chemical purification of the $^{140}BaCl_2$ was necessary to separate the Ba from its daughter ^{140}La, which decays with a 40 h half life to ^{140}Ce. Inactive La-carrier was added and the La was then precipitated as the hydroxyde. After centrifuging the solution was removed with a pipette from the Ba precipitated as $BaCO_3$ or $BaSO_4$. Sources for β-spectroscopic measurements were made by drying a drop of a suspension of this precipitate on a 0.4 mg/cm^2 teflon backing.

The effectiveness of the separation was estimated by comparing the intensities of the photopeaks at 820 keV in the La-decay and at 537 keV in the Ba-decay. The amount of La in a purified Ba sample shortly after the separation was about 6 per cent of that in the equilibrium mixture. This degree of separation is of the same order as that of Kelly and Wiedenbeck. The Ba-spectrum could be corrected for the small contribution of the 490, 820 and 1600 keV lines from the remaining La-activity. The sources could, however, not be used for more than about 40 h, due to the ingrowth of the La-activity.

3. Gamma and Conversion Spectra

A pure single count gamma spectrum of ^{140}Ba in a $1\frac{3}{4}'' \times 2''$ NaI(Tl) crystal is shown in fig. 2. It was obtained by subtracting the gamma spectrum of a purified La source from that of a purified Ba source, relating the intensities of both

spectra by means of the 820 keV La line. Photopeaks corresponding to gamma transitions of 162, 304, 436 and 537 keV were clearly observed. The 30 keV line together with the X-rays can also be seen on the low energy side but it is not

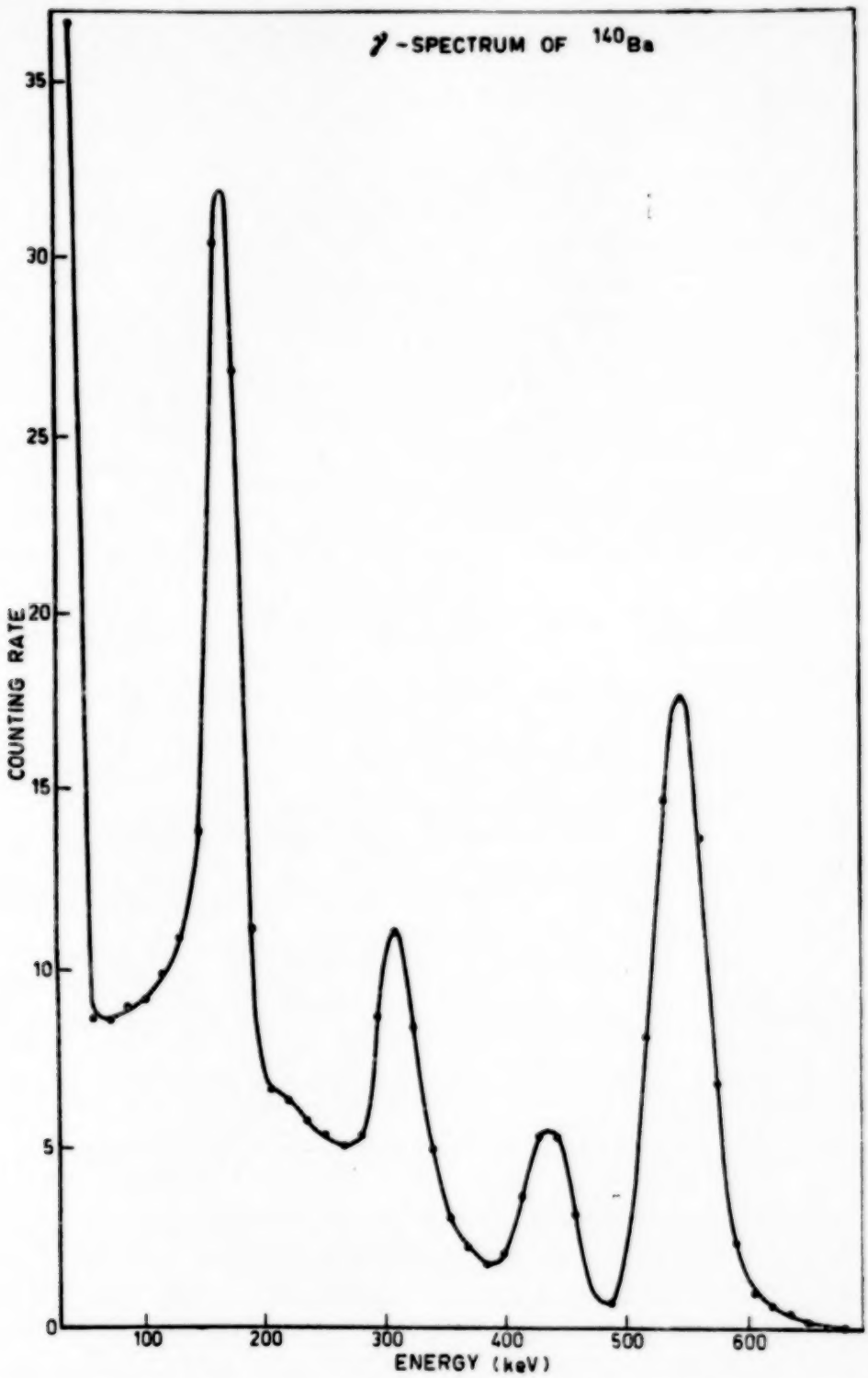

Fig. 2. A pure single count gamma spectrum of ^{140}Ba.

completely resolved from the noise. An analysis of the spectrum also reveals the existence of a 130 keV line. The slight bump at about 200 keV may be due to back scattering. Relative intensities of the gamma rays can be calculated from the areas under the photopeaks correcting for the efficiency and photofraction of the crystal. The results are listed in table 1. A single count β-spec-

TABLE 1
Relative intensities of the gamma lines

Gamma energy (keV)	Relative intensity (%)
132	3
162	22
304	10
436	10
537	55

trum shows conversion lines corresponding to transitions in La of 29.6, 131, 162.0, 304, 436 and 537 keV. The data of these lines and their interpretation is given in table 2. From a Kurie plot of the continuous β-spectrum the maximum

TABLE 2
Conversion lines and their identification

Energy of conversion line (keV)	Identification
23.1	L 29.6
27.5	M 29.6
29.3	N 29.6
91.7	K 131
123	K 162
156	L 162
269	K 304
390	K 436
498	K 537

energies of the β-components could be estimated. Four components with maximum energies of 1020, 870, about 580 and 450 keV were visible. A more reliable determination was, however, obtained from the β—γ coincidence measurements reported in section 4. In order to study the conversion lines more closely, coincidences were registered between electrons detected by an anthracene crystal placed directly behind the source and electrons analyzed in the solenoidal β-spectrometer. The background of the continuous β-spectrum is then very small. Figs. 3a and 3b show the conversion lines of the 30 and 162 keV

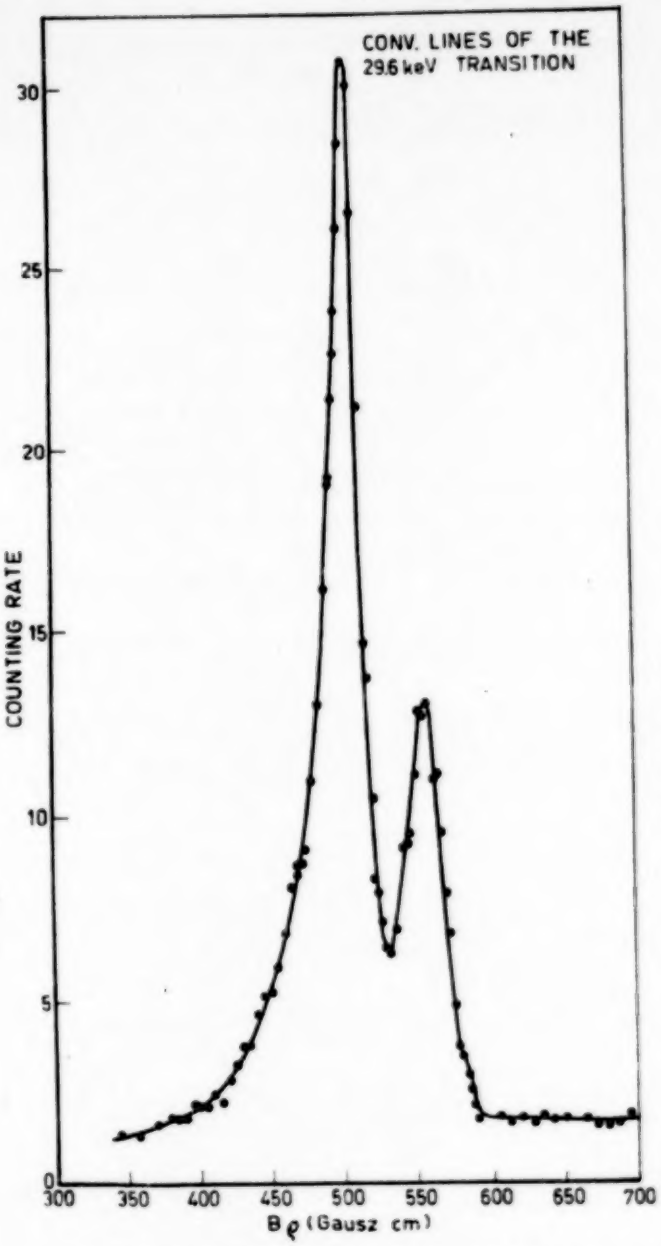

Fig. 3a. $\beta-e^-$ coincidences on the 29.6 keV line.

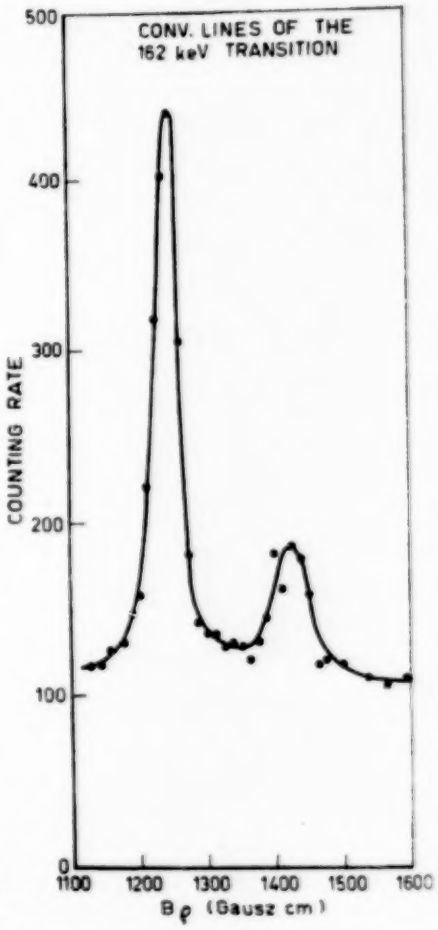

Fig. 3b. $\beta-e^-$ coincidences on the 162 keV line.

TABLE 3

Conversion ratios of the 29.6 and 162 keV transitions

Gamma energy (keV)	Conversion ratio	Theoretical value (Rose)				Experimental value	Multipolarity
		α_1	α_2	β_1	β_2		
29.6	L/(M+N)	2.6	2.1	2.2	1.8	2.4±0.3	E1, M1, E2
162	K/(L+M)	7.9	2.8	8.1	5.6	3.5±0.8	E2 (+M1)

transitions thus obtained. The conversion ratios of these lines were determined and compared with the theoretical values for the different radiation characteristics (see table 3).

4. Coincidence Spectra

In order to check the level schemes proposed by the previous authors, γ—γ coincidences were measured with two $1\frac{3}{4}'' \times 2''$ NaI(Tl) crystals. The gamma spectrum, recorded with the pulse-height analyzer, was successively gated on the different photopeaks. The lower limit of the coincidence spectrum was about 50 keV, so no coincidences with the 30 keV line were registered. When the gating channel was adjusted on the photopeaks of the 537 and 436 keV lines, no coincidences were found. The 304 keV line proved to be the only line in coincidence with the 162 keV transition. The 132 and 162 keV photopeaks were found in the spectrum coincident with the 304 keV line.

The spectrum coincident with the 30 keV gamma rays was found by taking the difference of coincidence spectra recorded with the gating channel on top and just beside the 30 keV peak. This difference spectrum is shown in fig. 4 together with the single count spectrum. The very small intensity of the 162 keV line in the coincidence spectrum shows that it is not coincident with the 30 keV line. It should be noted, that the K X-rays of ^{140}La have an energy of 39 keV and therefore cannot be separated from the 30 keV gamma rays. This circumstance explains the presence of such a high peak at 304 keV, which cannot be understood as due to coincidences via the 132 keV line.

In order to check this result in a different way, coincidences were also measured between L conversion electrons of the 29.6 keV transition selected in the magnetic β-spectrometer and the gamma spectrum from a $1\frac{3}{4}'' \times 2''$ NaI(Tl) crystal, placed directly behind the source. Also in this experiment, the 537 and 436 keV lines were found to be coincident with the 30 keV line, while the 304 keV line is practically absent. So the place of the 30 keV transition in the decay scheme of Kelly and Wiedenbeck is believed to be incorrect, while the results of the measurements of Silant'ev are in good agreement with our experiments.

The structure of the β-spectrum was more closely investigated by means of β—γ coincidence techniques. The β-particles were detected in a 10 mm thick anthracene crystal and the γ-particles in a $1\frac{3}{4}'' \times 2''$ NaI(Tl) crystal. The gamma channel was adjusted on the different photopeaks and the coincident β-spectrum was recorded on the pulse height analyzer. These coincident β-spectra were drawn on double logarithmic paper and compared with the 880 keV β-spectrum in the ^{170}Tm decay coincident with the 84.2 keV line, in order to get a determination of the maximum energies of the different β-components. The end point of the spectrum coincident with the 537 keV gamma's was determined to be at 460 ± 50 keV, that of the spectrum coincident with the 304 keV line at 590 ± 50

keV, while the endpoint of the spectrum coincident with the 162 keV line was at 830±50 keV. The 30 keV line is coincident with the 1020 keV β-component. The conclusion can be drawn that every level except the ground state is fed by

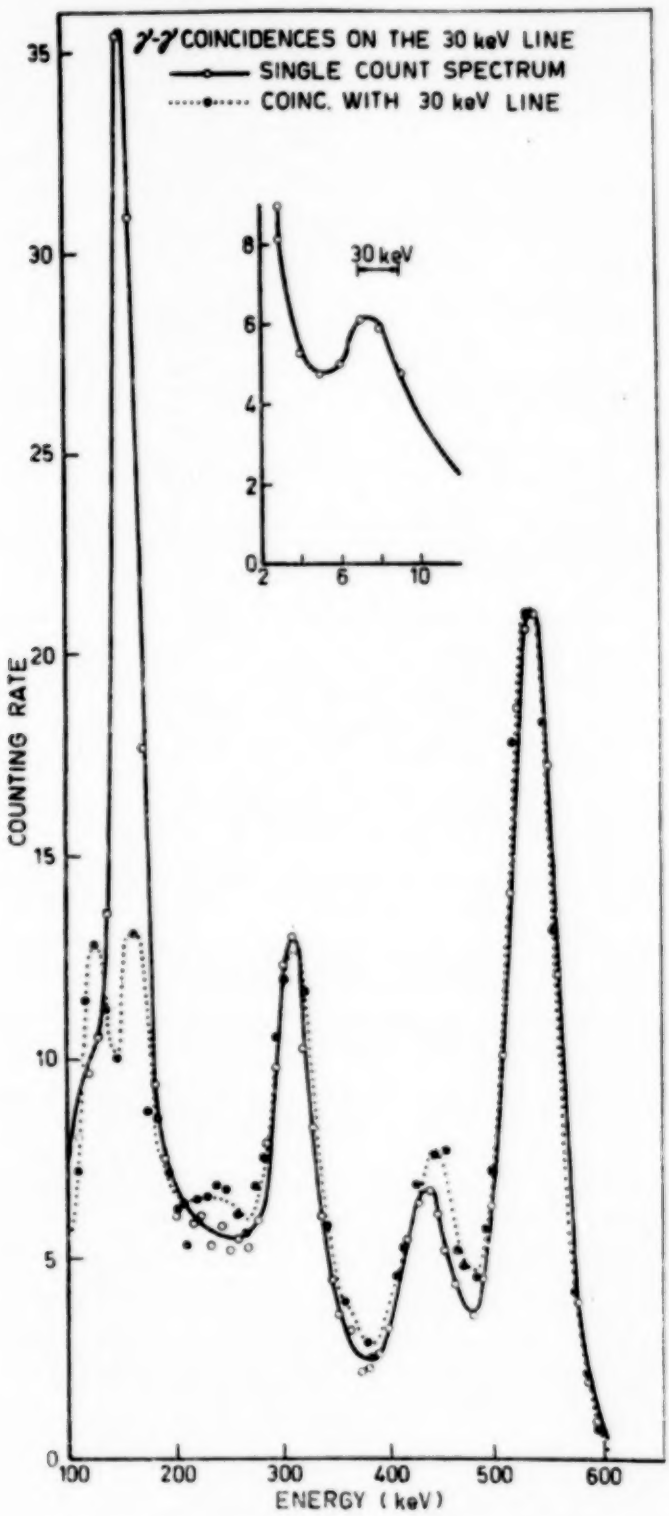

Fig. 4. $\gamma-\gamma$ coincidences with the 30 keV line

a separate β-component. Fig. 5 shows the two new components. The log ft values are given in table 4. Beekhuis † determined an *upper limit* of 30×10^{-10} sec for the half life of the 30 keV level. A delayed coincidence measurement in the β-spectrometer between the β-particles detected in a stilbene crystal placed directly behind the source and K 162 conversion electrons selected in the mag-

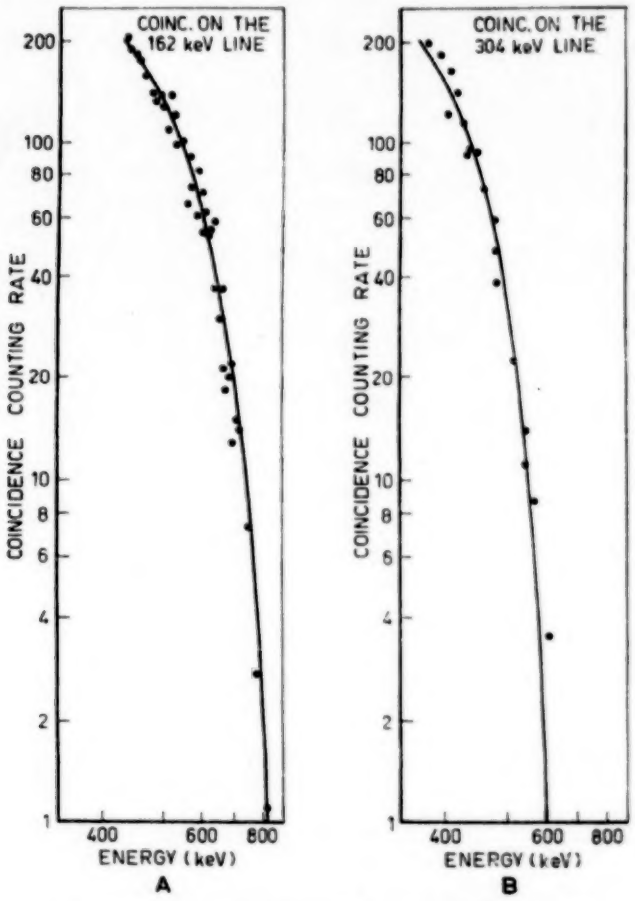

Fig. 5. $\beta-\gamma$ coincidences in the ^{140}Ba-decay.
A. β-spectrum coincident with the 162 keV line.
B. β-spectrum coincident with the 304 keV line.
The drawn line has the form of the ^{170}Tm coincidence spectrum.

TALBE 4

β-components and log ft values

Max. energy β-comp. (keV)	log ft value	Classification
480	6.9	first forbidden
590	7.1	first forbidden
830	8.2	unique first forb.
1020	8.6	unique first forb.

† Thanks are due to Mr. H. Beekhuis who carried out this measurement using a delayed coincidence technique with accelerated conversion electrons, earlier described by him for another case [9]).

netic spectrometer gives an *upper limit* for the half life of the 162 keV state of 8.5×10^{-10} sec.

5. Discussion of the level Scheme

The decay scheme shown in fig. 1B is uniquely determined by the previous measurements. It differs from that of Kelly and Wiedenbeck [7]) in the following respects:

1. The 537 keV transition is in cascade with the 30 keV line.
2. Two more β-components, of 590 and 830 keV, are present.

According to Bolotin *et al.*[6]) the ground state of ^{140}La must have an assignment 3—. The parent nucleus ^{140}Ba is even with quantum numbers 0+. The log *ft* value of 8.6 for the 1020 keV β-component to the 30 keV level indicates a unique first forbidden transition. The assignment of this level should therefore be 2—. The L/(M+N) ratio of the 29.6 keV transition gives no unique decision about the multipolarity of this radiation. However, an E2 character can be excluded on the basis of the measured upper limit of 30×10^{-10} sec for the half life. The calculated value for a single particle E2-transition, using Rose's values for the conversion coefficients, is 6.7×10^{-7} sec, and there is probably no strong enhancement since ^{140}La has 83 neutrons and thus lies very close to the magic number 82. An E1 character should involve a positive parity for the 30 keV state, and this can therefore also be excluded. The M1 character is in agreement with all experimental results. The K/L ratio of the 162 keV transition agrees best with a predominantly E2 character of this radiation. The log *ft* value of 8.2 for the β-component to this level again indicates a unique first forbidden transition. Thus the assignment of the 162 keV level is very probably 2—. The spin values of the 466 and 567 keV levels can be 0 or 1 on the basis of the log *ft* values of the β-components, both with negative parity.

It is very difficult to understand the ground state spin 3— of ^{140}La. This nucleus has 83 neutrons and 57 protons: the deformation should thus be small and the shell model should be applicable. The 83rd neutron should then populate an $f_{\frac{7}{2}}$ state; while the seven protons above the magic number 50 would be in a $d_{\frac{5}{2}}$ or $g_{\frac{7}{2}}$ state, which compete in this region.

An effort to understand the ground state and the low energy excited states as particle configurations of these protons and the 83rd neutron, using the results of the theoretical considerations given by De Shalit [10]) and Schwartz [11]), had no success.

The authors wish to thank Professor H. Brinkman for providing them with excellent facilities to perform these measurements. They further acknowledge the unrelenting assistance of Mr. H. Beekhuis and Mr. K. G. Dik during the experiments and the help of Mr. E. Houtman and Mr. W. G. Mook in making the chemical separations.

References

1) L. A. Beach, C. L. Peacock and R. G. Wilkinson, Phys. Rev. **76** (1949) 1624
2) J. M. Cork, J. M. LeBlanc, A. E. Stoddard, D. W. Martin, C. E. Branyan and W. J. Childs, Phys. Rev. **83** (1951) 856
3) J. M. Hollander, I. Pearlman and G. T. Seaborg, Revs. Mod. Phys. **25** (1953) 469
4) R. E. Maerker and R. D. Birkhoff, Phys. Rev. **89** (1953) 1159
5) R. C. Rohr and R. D. Birkhoff, Phys. Rev. **98** (1955) 1266
6) H. H. Bolotin, C. H. Pruett, P. L. Roggenkamp and R. G. Wilkinson, Phys. Rev. **99** (1955) 62
7) W. H. Kelly and M. L. Wiedenbeck, Phys. Rev. **102** (1956) 1130
8) A. N. Silant'ev, JETP **7** (1958) 394
9) H. Beekhuis and H. de Waard, Physica **24** (1958) 767
10) A. de Shalit, Phys. Rev. **91** (1953) 1479
11) C. Schwartz, Phys. Rev. **94** (1954) 95

8.B *Nuclear Physics* **14** (1959/60) 155—168; © *North-Holland Publishing Co., Amsterdam*

Not to be reproduced by photoprint or microfilm without written permission from the publisher

THE UNIVERSAL FERMI INTERACTION AND HEAVY MESONS

SEITARO NAKAMURA †

Service de Physique Mathématique, Centre d'Études Nucléaires, Saclay, Gif-sur-Yvette, S. & O, France ††

Received 11 June 1959

Abstract: By postulating interchange ability of the fermions, forty-four kinds of new heavy bosons are introduced which were not included in the Gell-Mann-Nishijima scheme. It is aimed thus to understand the β-decay and the other processes by the universal Fermi interaction in terms of the competitive processes involving the intermediary of boson groups. The existence of new kinds of muons with extraordinary long life-times of 1 to 100 days is also conjectured.

1. General Theory

It is a general trend in the physics of elementary particles that the specific quantum numbers of these particles, such as charge, hypercharge and baryon number, are no longer considered as preventing particles from being interchangeable. We know two types of reactions which illustrate this statement. One is the decay of the unstable particles, the other the strong interactions. In the terminology of the classical physics, the decay is comparable to an irreversible process, while the strong interaction is comparable to the energy exchange in a system of two resonators. In quantum theory, we conceive the decay as a transition from the higher level to the lower level in the mass multiplet of the particles, while the strong interaction is the internal coupling between components of the same level. In other words, if we have some reasons to regard a number of particles as belonging to the same group, we have to expect that among them there must be certain processes of strong interaction, and vice versa.

i) The typical example for this is the meson theory proposed by Yukawa [1]). We know that the neutron and the proton can be considered as different states of the same particle because they interact strongly; and also, they show a striking resemblance in nuclear reactions.

The nucleon-pion phenomena present the remarkable feature of charge independence; both the direction and length of the isovector **I** are conserved, which is in accordance with the requirement of the symmetrical meson theory.

† On leave of absence from the Department of Physics, University of Tokyo.

†† The outline of the present work was first presented at the annual meeting of the Physical Society of Japan held at Nagoya University (May, 1958).

ii) In the baryon group, Ξ, $\Sigma\Lambda$ and nucleons are considered as three states of the same particle, each differing in the hypercharge S [2]). They can change into each other by emitting the K-mesons with $S = +1$ or $S = -1$. Here we notice that while pions are found in the three types $Q/e = +1, 0, -1$, in accordance with the requirement of the symmetrical meson theory, the K-mesons with $S = 0$ are not found. We postulate, therefore, the necessary existence of new types of K-mesons having the hypercharge $S = 0$, for the sake of symmetrical argument. We suppose these new K-mesons with $S = 0$ to act as intermediaries between the same members of $\Xi(S = -1)$, $\Sigma\Lambda(S = 0)$ and nucleon $(S = +1)$ in baryon groups, just as the neutral pion transmits the interaction between P—P or N—N. Thus, we have the following strong interactions in the K-meson theory symmetrical with respect to the hypercharge:

$$\Xi_{S=-1} \rightarrow \Xi_{S=-1} + \mathrm{K}_{S=0}, \tag{1}$$

$$\Sigma_{S=0} \rightarrow \Sigma_{S=0} + \mathrm{K}_{S=0}, \tag{2}$$

$$\Lambda_{S=0} \rightarrow \Lambda_{S=0} + \mathrm{K}_{S=0}, \tag{3}$$

$$\mathrm{N}_{S=1} \rightarrow \mathrm{N}_{S=1} + \mathrm{K}_{S=0}. \tag{4}$$

If we assume that these K-mesons are composed of a charge triplet and a charge singlet, we can easily show that the conservation law for **I** holds for (1), (2), (3) and (4).

iii) As the third step, possible processes in which a baryon can change into a lepton will be considered. Following Heisenberg and Pauli, we denote both baryons and leptons by the general name of isofermions. We shall take as an analogy the meson theory of Yukawa in this case. Just as the positive (negative) pion can be emitted when the nucleon changes its state from the proton (neutron) into the neutron (proton), we shall assume that a boson X with baryonic charge $+1(-1)$ can be emitted when an isofermion jumps from the baryon state (lepton state) into the lepton state (baryon state):

$$\mathrm{B}(1) \rightarrow \mathrm{L}(0) + \mathrm{X}(1), \tag{5}$$

$$\mathrm{L}(0) \rightarrow \mathrm{B}(1) + \mathrm{X}(-1). \tag{6}$$

Here (1), (0) and (-1) indicate the baryonic charge. In order to keep the stability of the baryon, we must suppose the mass M_{X} of the X-meson to be heavier than that of the baryon, M_{B}:

$$M_{\mathrm{X}} > M_{\mathrm{B}}. \tag{7}$$

Further, if we extend the idea of the symmetrical meson theory to this case, we have to assume the existence of a boson with the baryonic charge zero:

$$\mathrm{B}(\pm 1) \rightarrow \mathrm{B}(\pm 1) + \mathrm{X}(0), \tag{8}$$

$$\mathrm{L}(0) \rightarrow \mathrm{L}(0) + \mathrm{X}(0). \tag{9}$$

We see, however, that the properties of the X(0)-meson are displayed by the K-meson group, and by the pion and photon groups. Therefore, we need not introduce other unknown mesons for the sake of a symmetric theory.

It is interesting to note that the anomalous electron-neutron scattering discovered by the Stanford group [3]) could be, in principle, in direct connection with the X-mesons. We can in fact expect the X-process to contribute to the phenomenon through the following two processes:

$$\mathrm{N} \rightarrow \mathrm{X}^{+}_{S=1}(1)+\mathrm{e}^{-}, \tag{10}$$

$$\mathrm{N} \rightarrow \mathrm{X}^{0}_{S=0}(0)+\mathrm{N}, \tag{11}$$

$$\mathrm{e}^{-} \rightarrow \mathrm{X}^{0}_{S=0}(0)+\mathrm{e}^{-}. \tag{12}$$

If we assume that the anomalous part of the electron-neutron scattering can only be explained by the process (5), we have the following relationship:

$$\frac{e^2}{M_\pi{}^2} \approx \frac{g_\mathrm{X}{}^2}{M_\mathrm{X}{}^2}. \tag{13}$$

This is a rough estimate based on the consideration of the potential volume for the electron-neutron scattering in the anomalous part. Here g_X is the coupling constant for the process (5) and M_X is the mass of X particle. If we take $g_\mathrm{X}{}^2/\hbar c \approx 1$, we have $M_\mathrm{X} \approx 3000\, m_e$, m_e being the mass of the electron. At present, we cannot say anything definite about these masses and coupling constants.

Next the question may be asked: How many kinds of particles could ever exist which could be called X-mesons? At a first estimate, if we imagine them to be analogous to those in the K-meson (X(0)-meson) group, we would have 32 kinds, of which there would be 16 kinds with $B = 1$ and 16 with $B = -1$.

In our scheme, we intend to assume that the three groups of heavy mesons (K with $B = 0$, X with $B = +1$, and X with $B = -1$) will make the components of a vector **B**. Let us denote

$$\begin{aligned} &\mathrm{n}_1 = (\mathrm{P}, \mathrm{N}) && \mathrm{n}_2 = \left(\Sigma^{+}, \frac{1}{\sqrt{2}}(\Lambda^0-\Sigma^0)\right) \\ &\mathrm{n}_3 = \left(\Sigma^{-}, \frac{1}{\sqrt{2}}(\Lambda^0+\Sigma^0)\right), && \mathrm{n}_4 = (\Xi^{-}, \Xi^0). \end{aligned} \tag{14}$$

As long as we confine our attention to the current law of conservation, we have only to assume four kinds of $\mathrm{K}_{S=0}$-mesons, together with four kinds of $\mathrm{K}_{S=\pm 1}$ mesons. If we want, however, to distinguish between the strong interactions of $(\mathrm{n}_1 \leftrightarrow \mathrm{n}_1,\ \mathrm{n}_2 \leftrightarrow \mathrm{n}_2)$ and those of $(\mathrm{n}_3 \leftrightarrow \mathrm{n}_3,\ \mathrm{n}_4 \leftrightarrow \mathrm{n}_4)$, we need to double the number of $\mathrm{K}_{S=0}$-mesons, and similary we need to assume eight kinds of $\mathrm{K}_{S=\pm 1}$-mesons to distinguish between the strong interactions of $(\mathrm{n}_1 \leftrightarrow \mathrm{n}_2,\ \mathrm{n}_1 \leftrightarrow \mathrm{n}_3)$ and those of $(\mathrm{n}_4 \leftrightarrow \mathrm{n}_3,\ \mathrm{n}_4 \leftrightarrow \mathrm{n}_2)$, thus making a total of sixteen kinds of K-mesons.

If we assume further the decay scheme of the X-mesons and the K-mesons, we can in theory deal with the known modes of decay processes. For instance, the decay scheme

$$X^{+}_{S=1}(1) \to P+\tilde{\nu}, \tag{15}$$

$$X^{-}_{S=0}(0) \to e^{-}+\tilde{\nu}, \tag{16}$$

$$X^{0}_{S=0}(0) \to \nu+\tilde{\nu} \tag{17}$$

of the weak iteractions can follow the strong interactions

$$X^{+}_{S=1}(1) \to N+\tilde{e}^{+}, \tag{10a}$$

$$X^{+}_{S=0}(0) \to p+\tilde{N}, \tag{11a}$$

$$X^{0}_{S=0}(0) \to \mu^{\pm}+e^{\mp}, \tag{12a}$$

producing the well-known processes of β-decay and $\mu-e$ decay.

2. β-Decay

Analysis of the β-decay will provide a good test for our scheme for the following two reasons:

Firstly, it is one of the best investigated processes. The final result [4]) for the type of the interaction of β-decay should be the peculiar combination of the vector (V) and the axial vector (A) Fermi interactions

$$\begin{aligned} H_{\beta} &= C_{V}H_{V}+C_{A}H_{A}, \\ H_{V} &= (\bar{P}\gamma_{\mu}N)(\tilde{e}\gamma_{\mu}(1+\gamma_{5})\nu)+\text{h.c.}, \\ H_{A} &= -(\bar{P}\gamma_{\mu}\gamma_{5}N)(\tilde{e}\gamma_{\mu}\gamma_{5}(1+\gamma_{5})\nu)+\text{h.c.}; \end{aligned} \tag{18}$$

$$\alpha = -1.25\pm 0.04, \quad \alpha C_{V} = C_{A}, \tag{19}$$

although, relying on the symmetry argument, we should expect $|\alpha| = 1$.

Secondly, the process of β-decay concerns four fermions, two of which belong to the baryon group, while the other two belong to the lepton group, which indicates that this process includes many particle groups. It will be easily seen that two entirely different types of intermediate bosons must contribute to the β-decay, provided our opinion be accepted that all particles in our symmetric table behave with equal strength. We thus expect the β-decay process through the two channels:

$$N \to P+K^{-}_{S=0}, \tag{11b}$$

$$K^{-}_{S=0} \to e^{-}+\tilde{\nu} \tag{16a}$$

and

$$N \to e^{-}+X^{+}_{S=1}(1), \tag{10a}$$

$$X^{+}_{S=1}(1) \to P+\tilde{\nu}. \tag{15}$$

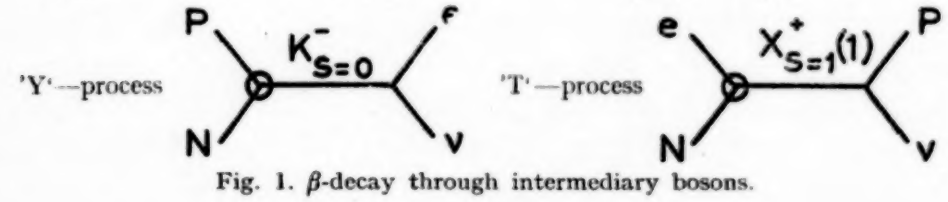

Fig. 1. β-decay through intermediary bosons.

We shall call the first channel given by (11b) and (16a) the 'Y'-process, and the second channel given by (10a) and (15) the 'T'-process. Using the conservation laws of the baryon number and of the hypercharge, we take a K-meson of $B = 0$, $S = 0$ for the 'Y'-process and an X-meson of $B = 1$, $S = 1$ for the 'T'-process. The type of process indicated as the 'Y'-process was originally proposed by Yukawa [5]) twenty years ago, while that of the 'T'-process was put forward by Tanikawa [6]) because of its property of renormalization.

It is interesting to note that, since it became clear that the pion has nothing to do with β-decay, Caianiello [7]) and the present author [8]) have once proposed a theory of β-decay through an unknown heavy meson of the vector type, which can be considered as a prototype of the present 'Y'-scheme [9]). It must also be mentioned that Tanikawa and Watanabe [10]) recently developed the 'T'-scheme in the Watanabe theory of the chiral boson.

Now, in our scheme, both intermediary boson processes ('Y') and ('T') are supposed to contribute simultaneously to β-decay. This is the essential point in our argument for the total symmetry. In fact, we cannot find any other process than the 'Y' and 'T' ones to contribute to the β-decay through any boson in our symmetric table.

To formulate the interaction Hamiltonian for the β-decay, we have to know the properties of the fields describing the K-mesons for the 'Y'-process and of those describing the X-mesons for the 'T'-process. As we have mentioned above, we suppose them to be parity twins in our scheme. Therefore, the interaction Hamiltonian which describes the β-decay will be formulated in general as follows:

$$H_1^{Y} = g_1^{K}\,\overline{P}\gamma_\mu(1+\gamma_5)N\cdot\phi_K{}^\mu + f_1^{K}\,\bar{e}\gamma_\mu(1+\gamma_5)\nu\cdot\phi_K{}^\mu + \text{h.c.} \tag{20}$$

$$H_1^{Y'} = g_1^{K'}\,\overline{P}\gamma_\mu(1-\gamma_5)N\cdot\phi_{K'}^\mu + f_1^{K'}\,\bar{e}\gamma_\mu(1-\gamma_5)\nu\cdot\phi_{K'}^\mu + \text{h.c.} \tag{21}$$

$$H_0^{Y} = g_0^{K}\,\overline{P}\quad(1+\gamma_5)N\cdot\phi_K + f_0^{K}\,\bar{e}\quad(1+\gamma_5)\nu\cdot\phi_K + \text{h.c.} \tag{22}$$

$$H_0^{Y'} = g_0^{K'}\,\overline{P}\quad(1-\gamma_5)N\cdot\phi_{K'} + f_0^{K'}\,\bar{e}\quad(1-\gamma_5)\nu\cdot\phi_{K'} + \text{h.c.} \tag{23}$$

$$H_1^{T} = g_1^{X}\,\overline{P}\gamma_\mu(1+\gamma_5)N\cdot\phi_X{}^\mu + f_1^{X}\,\bar{e}\gamma_\mu(1+\gamma_5)\nu\cdot\phi_X{}^\mu + \text{h.c.} \tag{24}$$

$$H_1^{T'} = g_1^{X'}\,\overline{P}\gamma_\mu(1-\gamma_5)N\cdot\phi_{X'}^\mu + f_1^{X'}\,\bar{e}\gamma_\mu(1-\gamma_5)\nu\cdot\phi_{X'}^\mu + \text{h.c.} \tag{25}$$

$$H_0^{T} = g_0^{X}\,\overline{P}\quad(1+\gamma_5)N\cdot\phi_X + f_0^{X}\,\bar{e}\quad(1+\gamma_5)\nu\cdot\phi_X + \text{h.c.} \tag{26}$$

$$H_0^{T'} = g_0^{X'}\,\overline{P}\quad(1-\gamma_5)N\cdot\phi_{X'} + f_0^{X'}\,\bar{e}\quad(1-\gamma_5)\nu\cdot\phi_{X'} + \text{h.c.} \tag{27}$$

Here $\phi_K{}^\mu$ and $\phi_{K'}^\mu$ stand for the wave functions of the $K_{S=0}$-mesons with spin 1, ϕ_K and $\phi_{K'}$ for those of the $K_{S=0}$-mesons with spin 0, $\phi_X{}^\mu$ and $\phi_{X'}^\mu$ for hose of the X-mesons with spin 1, and ϕ_X and $\phi_{X'}$ for those of the X-mesons with spin 0. g_1^{K}, $g_1^{K'}$, g_0^{K}, $g_0^{K'}$ are the coupling constants for the process (11b), f_1^{K}, $f_1^{K'}$, f_0^{K}, f_0^{K} for the process (16a), g_1^{X}, $g_1^{X'}$, f_0^{X}, $g_0^{X'}$ for the process (10a) and f_1^{X}, $f_1^{X'}$, f_0^{X}, $f_0^{X'}$ for the process (15.) The singns of $1\pm\gamma_5$ in the Hamiltonians

TABLE 1

Symmetric table of the elementary particles

Fermions		Bosons	
		$B=1$	$B=1$
		$\underbrace{X^0X^-}_{S=-1}$ $\underbrace{X^0X^+}_{S=+1}$	$\underbrace{X^0X^-}_{S=-1}$ $\underbrace{X^0X^+}_{S=+1}$
		$\underbrace{X^+X^0X^-}_{S=0}$ $\underbrace{X^-X^0X^+}_{S=0}$	$\underbrace{X^+X^0X^-}_{S=0}$ $\underbrace{X^-X^0X^+}_{S=0}$
		$\underbrace{X^0X^0}_{S=0}$	$\underbrace{X^0X^0}_{S=0}$
		$\underbrace{X^+X^0}_{S=+1}$ $\underbrace{X^-X^0}_{S=-1}$	$\underbrace{X^+X^0}_{S=+1}$ $\underbrace{X^-X^0}_{S=-1}$
$B=+1$	$B=-1$		
$\underbrace{\Xi^0\Xi^-}_{S=-1}$	$\underbrace{\tilde{\Xi}^0\tilde{\Xi}^+}_{S=+1}$		
$\underbrace{\Sigma^+\Sigma^0\Sigma^-}_{S=0}$	$\underbrace{\tilde{\Sigma}^-\tilde{\Sigma}^0\tilde{\Sigma}^+}_{S=0}$		
$\underbrace{\Lambda^0}_{S=0}$	$\underbrace{\tilde{\Lambda}^0}_{S=0}$		
$\underbrace{P\,N}_{S=+1}$	$\underbrace{\tilde{P}\,\tilde{N}}_{S=-1}$		
		$B=0$	
		$\underbrace{K_{\Xi^0}K_{\Xi^-}}_{S=-1}$ $\underbrace{K_{\tilde{\Xi}^0}K_{\tilde{\Xi}^+}}_{S=+1}$	
		$\underbrace{K_{\Sigma^+}K_{\Sigma^0}K_{\Sigma^-}}_{S=0}$ $\underbrace{K_{\tilde{\Sigma}^-}K_{\tilde{\Sigma}^0}K_{\tilde{\Sigma}^+}}_{S=0}$	
		$\underbrace{K_{\Lambda^0}}_{S=0}$ $\underbrace{K_{\tilde{\Lambda}^0}}_{S=0}$	
		$\underbrace{K_PK_N}_{S=+1}$ $\underbrace{K_{\tilde{P}}K_{\tilde{N}}}_{S=-1}$	
$B=0$	$(B=0)$	$B=0$ $(\lvert\mathbf{B}\rvert=0)$	
$\underbrace{\mu^-\nu\mu^+}_{S=0}$	$\underbrace{\tilde{\mu}^+\tilde{\nu}\tilde{\mu}^-}_{S=0}$	$\underbrace{\pi^+\pi^0\pi^-}_{S=0}$	
$(B=0)$	$(B=0)$	$(B=0)$ $(\lvert\mathbf{B}\rvert=0)$	
$\underbrace{e^-}_{S=0}$	$\underbrace{\tilde{e}^+}_{S=0}$	$\underbrace{\gamma}_{S=0}$	

are taken to be same for each boson, in view of the conservation law for the neutrino charge [11]).

We can limit the general formulation for the Hamiltonian by introducing several assumptions. First, if we take into account the two-component theory with the neutrino of the left-hand screw and the antineutrino of the right-hand screw [4]), we put

$$(1-\gamma_5)\nu = 0. \tag{28}$$

Therefore, we expect no contribution from (21), (23), (25) and (27) to β-decay. Next, if we assume charge independence [12]) for the strong intraction between the nucleons and $K_{S=0}$ (triplet), we have

$$\bar{P}\gamma_\mu N \cdot \phi_K{}^\mu = 0. \tag{29}$$

Now, by means of perturbation calculations, we can easily obtain the expressions for the interaction Hamiltonian of β-decay in terms of the five forms of Fermi interactions:

$$H_1{}^V(\beta) \Rightarrow -H_A, \tag{30}$$

$$H_0{}^V(\beta) \Rightarrow H_P+H_S, \tag{31}$$

$$H_1{}^T(\beta) \Rightarrow H_V-H_A, \tag{32}$$

$$H_0{}^T(\beta) \Rightarrow H_S+H_T+H_P, \tag{33}$$

where

$$\begin{aligned} H_S &= (\bar{P}N)(\bar{e}(1+\gamma_5)\nu)+\text{h.c.}, \\ H_T &= (\bar{P}\sigma_{\mu\tau}N)(\bar{e}\sigma_{\mu\nu}(1+\gamma_5)\nu)+\text{h.c.}, \\ H_P &= (\bar{P}\gamma_5 N)(\bar{e}\gamma_5(1+\gamma_5)\nu)+\text{h.c.} \end{aligned} \tag{34}$$

and we obtain the energy spectrum of β-decay:

$$W(\varepsilon)d\varepsilon = d\varepsilon f_0(\varepsilon)\left[\frac{C_V(\varepsilon)}{\tau_V}|M_A|^2+\frac{C_T(\varepsilon)}{\tau_T}(|M_V|^2+|M_A|^2)\right], \tag{35}$$

$$C_V(\varepsilon) = 1+\frac{p^2+q^2}{M_K{}^2-2M_K\varepsilon+\varepsilon^2}, \tag{36}$$

$$C_T(\varepsilon) = \frac{M_N{}^2}{M_X{}^2-M_N{}^2+2M_N\varepsilon}; \tag{37}$$

τ_V and τ_T are numerical constants. It is quite clear from (31) and (33) that the bosons of spin 0 type cannot yield results in agreement with the experiments (18) and (19). In fact, these coupling types lead us to the scalar, tensor and pseudoscalar interactions, which must, however, have a factor of $\approx 10^{-1}$, compared to the vector and axial vector interactions.

On the other hand, if we take (30) and (32), we get $H_V - \alpha_t H_A$. By assuming

$$\alpha_t^2 = 1 + \left(\frac{g_1^K f_1^K}{g_1^X f_1^X}\right)^2 \left(\frac{M_X}{M_K}\right)^4 = 1.56, \tag{38}$$

$$\frac{1}{\tau_T} = \frac{1}{2\pi^3} \frac{m_e c^2}{\hbar} \left(\frac{g_1^X f_1^X}{\hbar c}\right)^2 \left(\frac{m_e}{M_X}\right)^4 = \frac{1}{\tau_0}, \tag{39}$$

we obtain

$$\begin{aligned} W(\varepsilon)\mathrm{d}\varepsilon &\approx \mathrm{d}\varepsilon \left\{\frac{1}{\tau_0} f_0(\varepsilon)[|M_V|^2 + \alpha_t^2 |M_A|^2]\right\}, \\ f_0(\varepsilon) &= (\varepsilon_0 - \varepsilon)^2 \varepsilon (\varepsilon^2 - 1)^{\frac{1}{2}}, \\ \frac{1}{\tau_0} &= \frac{1}{2\pi^3} \frac{m_e c^2}{\hbar} \left[\frac{G_\beta}{m_e c^2 \left(\frac{\hbar}{m_e c}\right)^3}\right]^2. \end{aligned} \tag{40}$$

This means that the ratio of the bare coupling constants, α_t, must be

$$\alpha_t = -1.25. \tag{41}$$

One must not, however, compare this result uncritically with the experiments. In fact, the renormalization of the coupling constants might modify the value of α_t quite appreciably. Symanzik [13]) has recently deduced the expression for α_t by dispersion theory. If we take into account in his expression the total symmetry [11]), incuding the global symmetry hypothesis of Gell-Mann and Pais [14]), we might expect the effects from the renormalization to cancel out. Only in this case could we say that the contribution of the two intermediary boson processes 'Y' and 'T' yields the correct ratio α for β-decay, provided the following properties are assumed to the K-meson and the X-meson:

$$\begin{aligned} &\mathrm{K}: B = 0, \quad S = 0, \quad \text{spin } 1; \\ &\mathrm{X}: B = 1, \quad S = 1, \quad \text{spin } 1. \end{aligned}$$

It is interesting to note that the factors given in (36) and (37) could be tested by comparison with the energy spectra of the β-decay. As is shown in (36) and (37), the β-decay spectra in the allowed transition are predicted to show a slight deviation of about $\approx 1/1000$ in both the lower and the higher energy regions. In order to check our result, the β-emitters with a large maximum energy of the electron are preferable. Thus, we could expect an experimental decision between our intermediate boson theory and the universal Fermi interaction.

3. Universal Fermi Interaction

Now we shall consider the universal Fermi interaction in general. Before discussing the actual decay processes, let us introduce some assumptions which can define the possible decay schemes in greater detail:

a) All the universal Fermi interactions are assumed to go through the intermediary bosons found in our symmetric table.

b) Conservation of the particle number must hold without exception.

c) All the processes accompanied by emission of any number of neutrinos or anti-neutrinos must be caused by weak interactions.

It must be noted here that the lepton number cannot be conserved for the processes involving the emission or the absorption of X-mesons. We consider that the present assumption b) together with the law of the conservation of the baryon number are sufficient to determine these processes.

3.1. MUON DECAY

According to our assumptions, the possible modes of muon decay are limited to the following:

$$\mu^- \rightarrow \mathrm{K}^0_{S=0}+\mathrm{e}^-, \qquad \tilde{\mu}^+ \rightarrow \mathrm{K}^0_{S=0}+\tilde{\mathrm{e}}^+, \tag{42}$$

$$K^0_{S=0} \rightarrow \nu+\tilde{\nu}. \tag{43}$$

The conceivable process involving intermediary X-mesons is excluded by the selection rule on the baryon number.

By analogy with the β-decay, the interaction-Hamiltonian which describes the muon decay will be assumed to be

$$H_1^{\mathrm{Y}}(\mu) = g\ \tilde{\mathrm{e}}\gamma_\mu(1+\gamma_5)\mu\cdot\phi_{\mathrm{K}}{}^\mu + f\ \tilde{\nu}\gamma_\mu(1+\gamma_5)\nu\cdot\phi_{\mathrm{K}}{}^\mu + \mathrm{h.c.} \tag{44}$$

$$H_1^{\mathrm{Y}}(\mu') = g'\tilde{\mathrm{e}}\gamma_\mu(1-\gamma_5)\mu\cdot\phi^\mu_{\mathrm{K}'} + f'\tilde{\nu}\gamma_\mu(1-\gamma_5)\nu\cdot\phi^\mu_{\mathrm{K}'} + \mathrm{h.c.} \tag{45}$$

Here g and g' are the coupling constants for the process (42) and f and f' those for the process (43). If we take into account the two-component theory given by the relation (28), we expect no contribution from the Hamiltonian (45) to the muon decay. From the remaining terms (44), we obtain

$$H(\mu) \Rightarrow (\tilde{\mathrm{e}}\gamma_\mu(1+\gamma_5)\mu)(\tilde{\nu}\gamma_\mu(1+\gamma_5)\nu)+\mathrm{h.c.} \tag{46}$$

It is interesting to note that we have the pure form of the V—A theory for the muon decay. In this scheme, the Michel parameter ρ is expected [15]) to be $< \frac{3}{4}$.

From the consideration of lepton number conservation and from the two-component theory of the neutrino, it was concluded that the muon produced in the decay of the positive pion is $\tilde{\mu}^+$, while that produced in the decay of the negative pion is μ^- [4]). One may then ask the question: Is there another pair of muons, μ^+ and $\tilde{\mu}^-$? Only by an argument of symmetry can we conjecture the possible existence of such a pair of muons. For instance, the present author has

recently drawn up a symmetric table of the elementary particles on the assumption that the mass multiplets must be in general the same for fermions, anti-fermions and bosons. According to this assumption, it is concluded that any group of fermions must have their counterparts in the boson families, and also any group of bosons must have their counterparts in the fermion and anti-fermion families. A typical example is the group of negaton, positon and its photon counterpart. In order to find the fermions and the anti-fermions corresponding to the isotriplet boson group of pions, we are led to assume the possible existence of four kinds of muons (instead of the two kinds ordinarily accepted) and to form the isotriplet group of fermions and anti-fermions

$$\mu^-, \nu, \mu^+; \quad \tilde{\mu}^+, \tilde{\nu}, \tilde{\mu}^-.$$

Now, if we take into account the three assumptions mentioned above, the usual processes for the decay of the new muons would be forbidden because of the assumption b):

$$\mu^+ \not\rightarrow \mathrm{K}^0_{S=0}+\tilde{\mathrm{e}}^+, \quad \tilde{\mu}^- \not\rightarrow \mathrm{K}^0_{S=0}+\mathrm{e}^-.$$

The only process in which they can decay through the intermediary bosons would be limited to the following case:

$$\mu^+ \rightarrow \mathrm{K}^+_{S=0}+\nu, \quad \tilde{\mu}^- \rightarrow \mathrm{K}^-_{S=0}+\tilde{\nu}, \quad . \tag{47}$$

$$\mathrm{K}^+_{S=0} \rightarrow \tilde{\mathrm{e}}^+ + \nu, \qquad \mathrm{K}^-_{S=0} \rightarrow \mathrm{e}^- + \tilde{\nu}, \tag{48}$$

$$\therefore \ \mu^+ \rightarrow \tilde{\mathrm{e}}^+ + 2\nu, \qquad \tilde{\mu}^- \rightarrow \mathrm{e}^- + 2\tilde{\nu}. \tag{49}$$

According to the assumption b), it is clear that the rates of their decay are described by the doubly weak interaction since both (47) and (48) involve the emission of a neutrino or anti-neutrino. Thus we have

$$\tau_{\mu^+} = \tau_{\tilde{\mu}^-} = \left(\frac{g}{f}\right)^2 \tau_{\tilde{\mu}^+} = \left(\frac{g}{f}\right)^2 \tau_{\mu^-}.$$

If

$$\left(\frac{g}{f}\right)^2 \approx 10^{11} \text{ to } 10^{13}, \quad \tau_{\tilde{\mu}^+} = \tau_{\mu^-} = 2.5\times 10^{-6} \text{ sec},$$

we obtain

$$\tau_{\mu^+} = \tau_{\tilde{\mu}^-} \approx 2.5\times 10^{5} \text{ to } 2.5\times 10^{7} \text{ sec}. \tag{50}$$

Therefore, we could distinguish between the ordinary muons and the new muons by measuring their life times. Another difference between the two muons is to be found in the expected values for the Michel parameter ρ. It is easily seen that the Michel parameter must be 0 for the processes (49), because two identical neutrinos or anti-neutrinos will appear in the final states. Also, we can discriminate between the ordinary muons and the new muons by

measuring their helicity directly. It is interesting to note that these muons, if they exist, may play a useful catalytic role in fusion reactions, because of their extraordinarily long life-times of 1 to 100 days.

3.2. LEPTONIC MODES OF DECAY OF HYPERONS

Decay of hyperons accompanied by emission of leptons can be caused by the intermediary bosons in our scheme. As for the β-decay, we have, for the present case, to consider in general two possibilities mediated by a X-meson and a K-meson. The modes of decay thus obtained are illustrated by the Feynman diagrams of table 2. In several cases one of the corresponding diagrams through K-mesons or X-mesons is excluded by the selection rules of the hypercharge. It must also be noticed that in our scheme the alternative modes of decay with the muons of the new kinds are added to the ordinary muon modes.

Following the example of the β-decay mentioned above, we shall assume that the universal Fermi interactions have one vertex described by the strong interaction and the other vertex by the weak interaction:

$$H_{\mathrm{Y}}^{1} = g_{\mathrm{K}}^{1}\bar{\psi}_2\gamma_\mu(1+\gamma_5)\psi_1\cdot\phi_{\mathrm{K}}^{\mu}+f_{\mathrm{K}}^{1}\bar{\psi}_4\gamma_\mu(1+\gamma_5)\psi_3\cdot\phi_{\mathrm{K}}^{\mu}+\mathrm{h.c.}, \tag{51}$$

$$H_{\mathrm{Y}}^{0} = g_{\mathrm{K}}^{0}\bar{\psi}_2(1+\gamma_5)\psi_1\cdot\phi_{\mathrm{K}}+f_{\mathrm{K}}^{0}\bar{\psi}_4\gamma_\mu(1+\gamma_5)\psi_3\cdot\partial_\mu\phi_{\mathrm{K}}+\mathrm{h.c.}, \tag{52}$$

$$H_{\mathrm{T}}^{1} = g_{\mathrm{X}}^{1}\bar{\psi}_4\gamma_\mu(1+\gamma_5)\psi_1\cdot\phi_{\mathrm{X}}^{\mu}+f_{\mathrm{X}}^{1}\bar{\psi}_2\gamma_\mu(1+\gamma_5)\psi_3\cdot\phi_{\mathrm{X}}^{\mu}+\mathrm{h.c.}, \tag{53}$$

$$H_{\mathrm{T}}^{0} = g_{\mathrm{X}}^{0}\bar{\psi}_4(1+\gamma_5)\psi_1\cdot\phi_{\mathrm{X}}+f_{\mathrm{X}}^{0}\bar{\psi}_2\gamma_\mu(1+\gamma_5)\psi_3\cdot\partial_\mu\phi_{\mathrm{X}}+\mathrm{h.c.} \tag{54}$$

Theoretically, it is an open question which types of interaction should be chosen for the individual processes. Experimentally, there are several pieces of evidence which may serve to determine the interaction types. First, we know that the spin of $\mathrm{K}_{S=\pm1}$-mesons is 0. Secondly, the rate of decay for $\mathrm{K}\to\mathrm{e}+\nu$ is found to be negligible compared to that of $\mathrm{K}\to\mu+\nu$. This fact is in favour of the assumption that these processes are described by the V—A type interactions, since in this case we would have

$$\frac{W(\mathrm{K}\to\mathrm{e}+\nu)}{W(\mathrm{K}\to\mu+\nu)} \approx \left(\frac{m_{\mathrm{e}}}{m_\mu}\right)^2 = 6\times10^{-5}.$$

In the preceding section, we have taken the spins of $\mathrm{X}_{S=1}$-mesons and of $\mathrm{K}_{S=0}$-mesons to be 1, in order to explain the β-decay by their intermediary. At present we have no clue to determine the spin of $\mathrm{X}_{S=0}$-mesons. Thus, we obtain the following figures for the spins of the unknown bosons:

boson	$X_{S=0}$	$X_{\lvert S\rvert=1}$	$K_{S=0}$	$K_{\lvert S\rvert=1}$
spin	0, 1	1	1	0

By means of perturbation calculations, we can deduce the rate of decay for

TABLE 2

Feynman diagrams for the universal Fermi interactions through the intermediary bosons

	$A \longrightarrow B+e^-(\mu^-)+\bar{\nu}$ $\longrightarrow B'+\bar{e}^+(\bar{\mu}^+)+\nu$	$A \longrightarrow B+\bar{\mu}+\nu$ $\longrightarrow B'+\mu^++\bar{\nu}$
μ-e decay	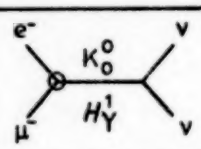	
μ-e decay		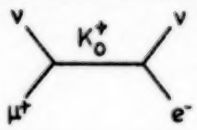
β-decay μ-capture	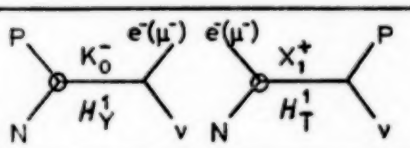	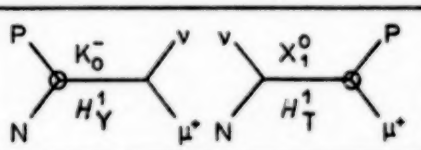
$\Lambda^0(\Sigma^0)$	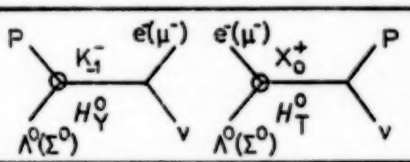	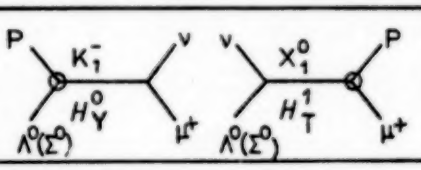
Σ^-	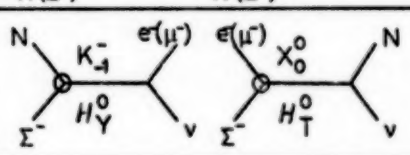	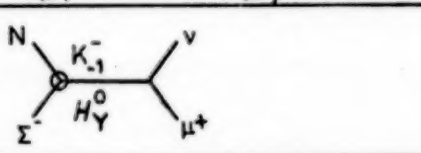
Σ^+	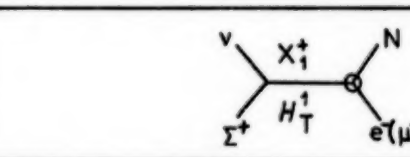	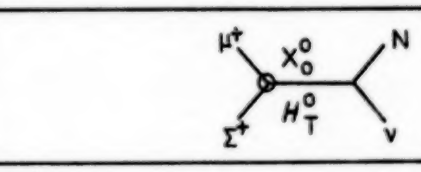
Ξ^0	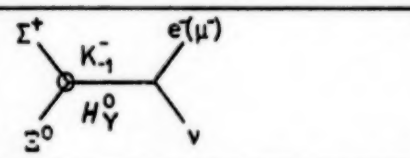	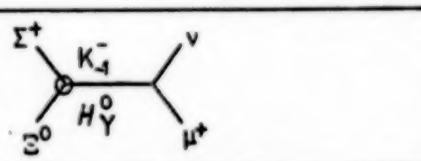
Ξ^0	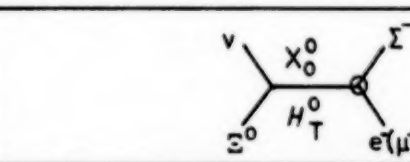	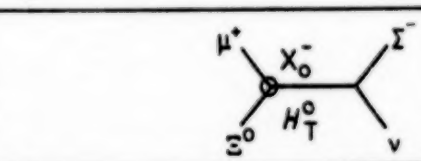
Ξ^-	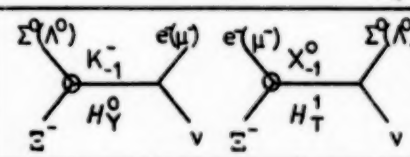	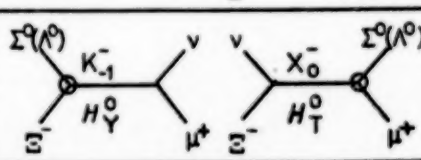

H_V^1, H_T^1: allowed transition, eqs. (55), (57)

H_V^0, H_T^0: forbidden transition, eqs. (56), (58)

each of the hyperon decays:

$$\frac{1}{\tau_{Y^1}} \approx \frac{(g_K{}^1 f_K{}^1)^2}{(\hbar c)^2}\left(\frac{m_e}{M_K}\right)^4\left(\frac{m_e c^2}{\hbar}\right) f(\varepsilon_0), \tag{55}$$

$$\frac{1}{\tau_{Y^0}} \approx \frac{(g_K{}^0 f_K{}^0)^2}{(\hbar c)^2}\left(\frac{m_e}{M_K}\right)^4\left(\frac{m_e c^2}{\hbar}\right) f(\varepsilon_0)\left(\frac{\Delta M}{M_K}\right)^2, \tag{56}$$

$$\frac{1}{\tau_{T^1}} \approx \frac{(g_X{}^1 f_X{}^1)^2}{(\hbar c)^2}\left(\frac{m_e}{M_X}\right)^4\left(\frac{m_e c^2}{\hbar}\right) f(\varepsilon_0), \tag{57}$$

$$\frac{1}{\tau_{T^0}} \approx \frac{(g_X{}^0 f_X{}^0)^2}{(\hbar c)^2}\left(\frac{m_e}{M_X}\right)^4\left(\frac{m_e c^2}{\hbar}\right) f(\varepsilon_0)\left(\frac{\Delta M}{M_X}\right)^2, \tag{58}$$

$$\Delta M = M_1 - M_2.$$

Here we see that the rate of decay for the hyperon is smaller by a factor $(\Delta M/M_K)^2$ or $(\Delta M/M_X)^2 \approx 10^{-1}$ than that of the β-decay, if the interaction Hamiltonians (52) and (54) are assumed. If the present result is really supported by the empirical evidence[16]), it seems likely that the spin of the $X_{S=0}$-mesons is 0. Our assumptions are also in favour of the conclusions given by Furuichi *et al.*[17]), that the tensor interaction is necessary for explaining the angular distribution of the electrons emitted in the decay of $K^{\pm} \to e^{\pm} + \nu + \pi^0$, since in this case we obtain the tensor interaction as a main part from (52) or (54).

The author is grateful to Professor C. Bloch for illuminating discussions and criticisms. He is also endebted to Professor C. Bloch for giving him very kind hospitality at Saclay, where the main part of this work was carried out.

References

1) H. Yukawa, Proc. Phys. Math. Soc. Japan **17** (1935) 48
2) J. Schwinger, Phys. Rev. **104** (1956) 1164
3) R. Hofstadter, Ann. Rev. Nucl. Sci. **7** (1957) 231;
Yennie, Lévy and Ravenhall, Revs. Mod. Phys. **29** (1957) 144;
Ig. E. Tamm, JETP **5** (1957) 154
4) M. Goldhaber, 1958 Ann. Int. Conf. CERN;
C. S. Wu, Int. Conf. Atom. Energy (Genève, 1958)
5) Yukawa, Sakata, Kobayashi and Taketani, Proc. Phys. Math. Soc. Japan **20** (1938) 319;
S. Sakata, ibid **23** (1941) 291
6) Y. Tanikawa, Prog. Theor. Phys. **3** (1948) 338
7) E. R. Caianiello, Phys. Rev. **81** (1951) 625
8) S. Nakamura, Phys. Rev. **85** (1952) 16
9) L. Michel, 1958 Ann. Int. Conf. CERN
10) Y. Tanikawa and S. Watanabe, Phys. Rev.
11) S. Nakamura, Nuovo Cimento
12) B. Stech, Phys. Rev. Letters **2** (1959) 63

13) K. Symanzik, Nuovo Cimento **40** (1959) 269;
B. Ioffe, JETP **7** (1958) 927
14) M. Gell-Mann and A. Pais, Phys. Rev. **97** (1955) 1387
15) T. D. Lee and C. N. Yang, Phys. Rev. **108** (1957) 1615
16) Crawford, Jr., Cresti, Good, Kalbfleish, Stevenson and Ticho, Phys. Rev. Letters **1** (1958) 377
Leitner, Nordheim, Jr., Rosenfeld, Solmitz and Tripp, Phys. Rev. Letters **3** (1959) 186
17) Furuichi, Ogawa, Sugawara, Wakasa and Yonezawa, Progress Theoretical Phys. **17** (1957) 89

10.B *Nuclear Physics* **14** (1959/60) 169—171; © *North-Holland Publishing Co., Amsterdam*

NEWS ITEMS

HIGH ENERGY PARTICLE ACCELERATOR CONFERENCE AT CERN

(Geneva, 13—19 September 1959)

From 14th to 19th September 1959, about 250 scientists from 28 nations attended the CERN International Conference on High Energy Particle Accelerators and Instrumentation.

At midnight, on Wednesday, September 16th, 1959 — third day of the Conference — the Organization's 25 GeV proton synchrotron beamed its first particles once around the 628 metres circumference of the machine. This constitutes a further highlight in the history of CERN, since the event proves that the 100 units of the electromagnet are positioned well within the few tenths of a millimetre radial tolerance over the 200-metre diameter of the machine. Since the accelerating cavities are also installed and tested, the full acceleration cycle will be reached early next year †. This cycle will require one second, during which the protons, with a velocity of about 99.98 % of the speed of light, will make almost 500 000 turns to produce 25 GeV proton energy.

John B. Adams, Director of CERN's Proton Synchrotron Division and Executive Chairman of the Organizing Committee of the Conference, was able to announce this outstanding event on the morning of the fourth day of sessions. Another important scientific event was announced when, in welcoming participants at the opening session of the first day, Professor C. J. Bakker, Director-General of the Organization, asked Soviet scientists attending the Conference "to convey our warmest congratulations to the USSR Academy of Sciences . . . for the great success achieved by their colleagues . . . in landing a rocket on the moon".

Thus, framed between two important though unrelated scientific announcements, the CERN Conference was well set to produce interesting results in the field of accelerating machines and detecting equipment. Also, as during the 1956 Conference, contacts both formal and informal between western scientists and those of eastern countries, as well as scientists of many other parts of the world, were fruitful and uninhibited.

Papers were presented and discussions held on three main fields:

1) *The need for new high-energy accelerators, their building progress, and accelerators projected for the future*

The three new main principles, on the basis of which high-energy accelerators were discussed were (1) the principle of acceleration using fully ionized gases, i.e. plasma betatrons, proposed by Russian scientists and others, work on which has been going on also at CERN contemporaneously with the building of the big machine; (2) stochastic accelerating methods, also invented in Russia, on which much experimental work has been done at CERN; (3) the principle of intersecting or colliding beams and storage ring systems, very extensively studied by the Midwestern Universities Research Association (MURA), and of which an electron model is being studied at CERN.

None of these principles is new; they were elaborated in detail at the 1956 CERN Conference. Thus, though no new accelerator principles emerged from the Conference, a large number of important papers were presented and discussions held on theoretical and experimental research, undertaken since 1956, with a view to putting these principles into practice in building bigger and better high-energy accelerators.

Apart from the world's biggest proton accelerators now building at CERN and Brookhaven, Long Island, New York, USA — both developing 25 to 30 GeV energies — a new Russian machine now planned is expected to produce 50 GeV particles, once it is built at Sepukhov, south-east of Moscow, in some years to come. A 7 GeV model of this is now in its final stage of construction in Moscow. Allusion was also made to an American idea for a 300 GeV accelerator: such a machine would make use of the principle of intersecting or colliding beams and storage rings.

† The full acceleration cycle was reached on 25 November 1959.

Finally, a session was devoted to fundamental limitations imposed on accelerator construction by space charge problems and radiation damping.

2) *Accelerators now under construction*

Other papers and discussions dealt with the high-energy accelerators now being built or planned definitely, throughout the world. Twelve big machines were presented. They involve impressive amounts of work and close collaboration by a large number of physicists, engineers and technicians. Their global cost may be estimated at some 360 million dollars.

3) *Instrumentation for use with high-energy machines*

The third and last part of the Conference dealt with the indispensable instrumentation, likewise costly, used in conjunction with the machines for high-energy nuclear physics research. This includes such apparatus as large "bubble-chambers" of liquid-hydrogen and other types, with their special scanning and computer equipment.

Finally, a session dealt with the production, transport and separation of particles from high-energy machines, counters and other high-energy particle detectors and instrumentation, as well as their attendant high-speed electronics.

Special parallel sessions were devoted to radio-electronics, i.e. radio-frequency systems for high-energy accelerators, as well as linear accelerator techniques and problems of beam storage.

In his concluding remarks at the end of the Conference, Professor V. I. Veksler, head of the Soviet delegation, returned the compliments made by Professor Bakker in his opening remarks, in alluding to the initial success of CERN's alternating gradient proton sychrotron, announced during the sessions. He also expressed his admiration for the extremely efficient organiszation of the Conference with all that this implies, i.e. preparation of papers and other documents for participants, simultaneous translation, transport for the delegates, scientific secretarial services, tape recording, and the many other features which go to make a successful international scientific Conference.

O.E.E.C. INDUSTRIAL CONFERENCE ON NUCLEAR ENERGY

(Stresa, 11—14 May, 1959)

This is the third conference of this type arranged by the Organisation for European Economic Co-operation (O.E.E.C.) to interpret the latest scientific developments in nuclear energy for the benefit of European industry.

The opening address was delivered by Professor Léandre Nicolaidis of Greece, who has been chairman of the Organisation's Steering Committee for Nuclear Energy since its creation in 1956; this Committee is now the controlling body of the European Nuclear Energy Agency (ENEA), which is responsible for the Conference.

He described the Agency's three main joint undertakings in this field: EUROCHEMIC (the European Company for the Chemical Processing of Irradiated Fuels), the HALDEN Boiling Water Reactor in Norway, and the recently agreed joint research and development programme for the investigation of high-temperature gas-cooled reactors, centred round the construction of an experimental reactor (DRAGON) in the United Kingdom. Other achievements of the Agency are the establishment (in agreement with EURATOM) of basic norms for health protection against nuclear radiations, and the exchange of information on radioactivity in the air, water and soil of the various countries of the O.E.E.C.

The Conference was divided into eight sessions at which some fifty papers were presented and discussed. As background information, ENEA has published five detailed studies on nuclear energy in Europe, covering estimates of future production, current methods of financing programmes, special atomic legislation, and markets for nuclear materials and equipment.

In the session on financing nuclear programmes, one of the most interesting points to emerge from the discussion was the very considerable differences from one country to another in the amounts of finance earmarked for pure research. The "big" countries, for reasons of political or military prestige, all have large research budgets usually financed from public funds. Smaller

countries on the other hand depend much more for their research on finance from the private sector, which, in most cases, contributes between 25 % and 50 % of the total investment. In general, research in these smaller countries, however important, progresses more slowly. A universal trend in all countries appears to be for basic research to be directed more and more towards ultimate applications, resulting in a closer association of industry with research work.

Two sessions were devoted to legal problems, one of them to the questions of information and the protection of inventions in the nuclear field. The discussion showed that all states, public bodies and international bodies like EURATOM, undertaking research on their own, are under a legal obligation to put results of such research in the field of peaceful applications of nuclear energy at the disposal of their private industry. A more complex situation, however, was revealed in the field of patents, in particular in those states or territories where a public body undertakes research and may thus acquire patents. Moreover, sometimes the state can obtain, by compulsory means, the use of a private patent. It was pointed out by the representatives of the United States and EURATOM that no use of these compulsory powers has yet been made. If the state or a public body owns a patent, different systems of granting licences may be applied. While in the United States the principle of royalty-free licences for private industry is applied, the European countries, and in particular European industry, favour the commercial sale of licences. The great activity of some states in the field of nuclear energy, and their consequently strong position as owners of patents, gave rise to some concern that the financial value of a patent, one of the most important stimulants of private industrial progress, might become weakened. European industry believes that its important contribution to the development of the peaceful uses of nuclear energy should not be discouraged by endangering the financial value of their industrial advances.

In a panel discussion on management problems facing the nuclear industries, it was pointed out that the main problem was one of assimilating scientists — physicists, chemists and mathematicians, who must also be educated in industrial economics — into management. Nuclear energy was born in state organisations where physics predominated over economics. The problem now was to teach the scientists modern industrial economy, to enable them to step into competitive industry where economics played a vital role.

10.D *Nuclear Physics* **14** (1959/60) 172—176; © *North-Holland Publishing Co., Amsterdam*

BOOK REVIEWS

The University of Texas M. D. Anderson Hospital and Tumor Institute, *Radiation, Biology and Cancer*: a collection of papers presented at the twelfth annual symposium on fundamental cancer research, 1958 (University of Texas Press, Austin, 1959. 433 pages. $ 8.50)

The book contains 34 papers presented at the twelfth annual symposium on fundamental cancer research. There are articles on primary physical and chemical processes in radiobiology; the influence of oxygen upon radiation damage; relative biological effectiveness; integral dose and source size in cobalt-60 teletherapy; dosimetry of interstitial implants of radium, cobalt-60 and cesium-137; radiation effects on the hematopoietic system; induction of neoplasia by ultraviolet light and by ionizing radiations; radiation studies on mutagenesis and carcinogenesis; and on medical applications of radiation, i.e. intracavitary use of radioactive colloidal gold and experience of treatment with cobalt-60 gamma rays and 22 MeV betatron.

The articles are spread over the whole subject of radiation biology and cancer, so that it is not possible to go into details in a short review, but there are so many excellent articles that the book is of great value to everybody interested in the subject.

Sigvard Kaae

C. H. Blanchard, C. R. Burnett, R. G. Stoner and R. H. Weber, *Introduction to Modern Physics* (Prentice-Hall, Inc., Englewood Cliffs, N. J., 1958. xi—414 p. $ 10)

According to the preface it is the purpose of this book to present the qualitative ideas and the simpler quantitative results of atomic physics, and the presentation covers, indeed, a wide field. Starting with a brief survey over Classical Physics it continues with the theories of the Rutherford-Bohr Atom, Quantum Mechanics, Structure of Many Electron Atoms, Molecules and Solids, Nuclear Physics and some of its applications and concludes with a chapter on High-Energy Research. A special chapter is devoted to the theory of restricted relativity.

The exposition is clear and well-planned and followed up by many well-chosen problems and suggestions for further reading. With the restricted space at the authors' disposal, the broad field they have chosen, and the very elementary knowledge presumed in mathematics and physics, it has not been possible to give a deeper discussion and justification of the fundamental ideas of modern physics, but as a first introduction, indicating the wide applicability of these ideas, the book may be useful in a gifted teacher's hand.

Mogens Pihl

A. Messiah, *Mécanique quantique*, vol. I (Dunod, Paris 1959. xv—430 p. 39 fr. nouveaux)

Voici (enfin) un traité de mécanique quantique français que l'on peut sans hésitation placer au rang des meilleurs, — sans excepter le livre de Landau et Lifschitz, sur lequel je me suis récemment répandu en louanges (dans ce journal **9** (1958) 695). En fait, j'inclinerais même à donner la préférence au présent traité sur un point didactique très important. M. Messiah prend soin de développer, d'une manière suffisamment détaillée pour être vraiment instructive, le point de vue de la théorie primitive des quanta, basée sur le principe de correspondance: il parvient ainsi à faire saisir au débutant la contradiction essentielle entre les idées classiques et les postulats quantiques, ainsi que la nécessité d'une conception synthétique éliminant cette contradiction.

Cette présentation historique du sujet paraît indispensable pour préparer l'étudiant à franchir le pas difficile qui sépare la physique classique de la théorie des quanta; je ne crois pas qu'il existe d'autre exposé moderne fait de ce point de vue que celui qu'a tenté ici M. Messiah. Je regrette seulement qu'il n'ait pas rempli cet excellent programme d'une manière assez radicale. Logiquement, il aurait dû souligner le caractère inéluctable et définitif du processus de synthèse que représente la mécanique quantique, et introduire à sa place naturelle la notion de complémentarité qui est l'expression de cette synthèse. Il préfère, avec une timidité coupable (p. 40, note), adopter vis-à-vis de la réaction bohmienne (qui méconnaît complètement cette situation si claire) une attitude agnostique qui enlève beaucoup de sa force à tout le développement qui précède. Sans doute, en disant à propos de cette réaction "qu'elle se situe sur le terrain de la philosophie des sciences", a-t-il trouvé une formule élégante pour signifier qu'elle n'a aucun sens (comme ce personnage des *Thibault* qui exprimait la même opinion en disant: „C'est une vue de l'esprit"). Mais il gâte tout en ajoutant „pour le moment" et surtout „en l'absence de faits expérimentaux susceptibles de trancher le débat". Ce n'est pas, en effet, d'expérience, mais de simple logique qu'il s'agit ici.

Si l'on fait abstraction de cette malheureuse note (que l'auteur, je l'espère, fera disparaître des éditions ultérieures), on ne peut que louer le choix judicieux des matières et la rigueur du traitement, qui se déroule suivant la meilleure tradition de l'école mathématique française. Aussi ce livre est-il recommandé chaleureusement aux étudiants et aux professeurs.

L. R.

Geology of Uranium (Supplement No. 6 of Atomnaya Energiya) (Consultants Bureau, New York 1958. 128 p. $ 6)

Cet ouvrage écrit en collaboration entre plusieurs auteurs comprend des chapitres assez différents se rapportant à la géologie des dépôts uranifères sédimentaires et métamorphiques, à la Minéralogie de l'uranium et à la prospection:

1) *L'uranium dans les formations métamorphiques*

Les dépôts se trouvent en couches dans les parties les plus métamorphiques du paléozoïque supérieur. Il n'est pas possible d'établir une relation entre la présence d'uranium et la nature pétrographique ou chimique des roches, mais il faut souligner le rôle de la porosité. La liaison entre la composition des roches métamorphiques et la localisation de la minéralisation ne conduit pas à des résultats positifs.

2) *Nature de la minéralisation uranifère sédimentaire-métamorphique*

On montre la possibilité de concentration uranifère durant le métamorphisme régional de couches sédimentaires dans une zone géosynclinale.

On distingue quatre phases dans la migration de l'U: sédimentation, diagènèse, métamorphisme, altération. On souligne le rôle important des matières organiques dans les processus de réduction et d'adsorption. L'altération est favorisée par le milieu acide dû à la présence de pyrite.

3) *Origine de la minéralisation uranifère dans les charbons*

La minéralisation est localisée dans les niveaux à gros grain et dans les parties gréseuses perméables.

Les charbons les plus favorables aux concentrations uranifères sont les moins évolués (lignites et charbons bruns). L'origine de l'uranium doit être recherchée dans les granites voisins, dont la radioactivité est supérieure à la normale, et les bicarbonates ont joué un rôle important dans sa migration.

4) *Nouvelles données sur la Nénadkévite* ($U\,SiO_4$)

5) *L'Uramphite* ($NH_4(UO_2)PO_4\,3H_2O$)

6) *L'Ursilite*

7) *Conditions de formation de la Natroautunite*

8) *Synthèse hydrothermale de l'uraninite*

9) *Recherches thermiques sur quelques uranifères*

Ces travaux permettent de compléter les caractères physico-chimiques des uranifères secondaires.

10) *Méthode radiométrique de détermination de l'uranium dans les échantillons de minerais*
Les auteurs exposent la théorie et la pratique d'une méthode $\beta\gamma$ valable pour U et Th, que ces éléments soient en équilibre ou non. Cette méthode fait appel à l'appareillage classique qui sert aux comptages de rayonnement. Les mesures radiométriques de routine donnent une meilleure précision que les analyses chimiques de routine.

11) *Rapport β/γ des produits radioactifs naturels*
Des tableaux résument de nombreuses mesures effectuées avec différents types de compteurs. Des courbes expérimentales représentent l'absorption des β de UX_2, Ra(B+C) et RaE par des écrans d'Al et de Pb. Une table donne les „équivalents" uranium en β et γ pour Th et K.

12) *Méthodes et techniques de prospection aéroportée utilisées dans les pays étrangers*
Les auteurs donnent des indications générales sur les travaux effectués dans ce domaine aux U.S.A., au Canada et en Australie.

P. Le Goff

W. Pauli, *Theory of relativity* (translated by G. Field) (Pergamon Press, London 1959. 241 p. 35 s.)
The publication of an English translation of Pauli's famous Encyclopedia article is the more valuable as it contains substantial additions giving us the author's last opinion about recent developments. The bibliography of textbooks published since the original edition does not pretend to be complete; but it certainly ought to have included Møller's recent treatise. The typographical set-up of this edition is much superior to that of the German edition.

L. R.

U. Fano and G. Racah, *Irreducible tensorial sets* (Academic Press, New York 1959. 171 p. $ 6.80)
The remarkable development of investigation methods based on measurements of angular correlations and polarizations of particles taking part in various reactions and transmutation processes has called forth quite a number of treatises dealing with the mathematical background of these methods; for if the physical conceptions underlying them are straightforward, the laborious computations to which they give rise could not have been carried through to such a large extent without the powerful auxiliary of systematic procedures based on group theory. The authors of the present book have both made essential contributions to the elaboration of these procedures, and their joint efforts have now succeeded in achieving a synthetic presentation of the subject, comprehending its mathematical foundation and main applications, whose elegant concision and lucidity it would be difficult to surpass. The attention of the specialists may be called to the new definitions of V and W symbols, which now seem to have reached the highest degree of symmetry and practical convenience attainable; the use of W and X symbols in recouplings of angular momenta is further illustrated by simple graphical representations, suggesting a remarkable correspondence with fundamental aspects of projective geometry.

L. R.

L. V. Kantorovich and V. I. Krylov, *Approximate methods of higher analysis* (translated by C. D. Benster) (P. Noordhoff, Groningen 1958. xv–681 p. $ 17)
The attention of students of theoretical physics may be called to this textbook, distinguished by special care in the didactic presentation of the subject. The proofs and other developments are given in great detail, which makes the book eminently suitable for self-study. Although it is not written with a view to application to theoretical physics, its contents are of such general scope as to form an indispensable complement to the subject-matter of the more conventional textbooks on higher analysis. In fact, it gives an extensive survey and thorough treatment of the main methods of approximation widely used by physicists. Even the specialist will find it helpful as a book of reference concerning the rigorous mathematical foundation of the tools he sometimes handles with too heavy a hand.

L. R.

J. SCHWINGER (Editor), *Selected papers in quantum electrodynamics* (Dover Publications, New York 1958. xvii—424 p. $ 2.45)

This is one of the well-known series of fac-simile reprints by which the enterprising publishers are rendering such distinguished service to scientific education. We are now presented with an anthology of older and more recent papers which have played an important part in the development of quantum electrodynamics. A selection of this kind is a risky affair: the publishers have been very wise in entrusting it to one of those who have given the most fundamental and original contributions to the theory. Even so, it inevitably reflects the editor's personal conception of the subject and his (conscious or unconscious) preferences for certain of its aspects to the detriment of others.

The editor hints at limitations of space in apology for certain omissions; indeed, I am inclined to think that two volumes of the size of the present one would have done better justice to the subject. In saying this, I am taking it for granted that the function of this collection is not only utilitarian, but also educative: it should not only make easily accessible those papers which are still often quoted and which one therefore likes to have readily within reach, but also those which may well be superseded, but still deserve to be studied as examples of scientific method and creative thought at its best. The present anthology seems to me too incomplete to fulfil adequately the second of these functions.

However this may be, we must be grateful for what we are given. In particular there is, besides the reprints of the papers, a spirited introduction by the editor, in which he presents, in a broad survey, his own view of the growth and prospects of the theory. It is something of a surprise to notice that the author's statements concerning the localizability of electric charge and current are seriously inaccurate; but as a whole, this introduction is a most interesting addition to the literature which it endeavours to summarize.

L. R.

E. J. ÖPIK, *Physics of meteor flight in the atmosphere* (Interscience Publishers, New York 1958. viii—174 p. 15 s. paperbound, 30 s. hard cover)

Owing to the restricted scope of the journal, only too brief a notice can be given here of this most interesting booklet, in which all aspects of the passage of meteors through the atmosphere are analysed in detail, and the present state of our knowledge of the subject authoritatively summed up.

L. R.

M. A. LEONTOVICH (Editor), *Plasma physics and the problem of controlled thermonuclear reactions, Vol. III.* Translated from the Russian by J. B. Sykes (Pergamon Press, London etc., 1959. 422 pages. £ 8 net).

The translations of miscellaneous papers here collected are not typeset, but just reproductions of typescript, like preprints; the typing is rather poor, especially that of the formulae. The binding is good, but the price seems nevertheless extravagant.

L. R.

Report of the fluid fuel reactors task force to the Division of Reactor Development, United States Atomic Energy Commission, February 1959 (United States Atomic Energy Commission, Technical Information Service, 1959. iv—188 pages. $ 1.75)

This volume contains an account of the findings of a Task Force which met continuously during January and February of this year to evaluate critically three fluid fuel reactor concepts.

The Technical Information Service of the U. S. Atomic Energy Commission deserves praise for making available such reports, directly reproduced from typescript, at a reasonable price.

L. R.

Proceedings of the second United Nations international conference on the peaceful uses of atomic energy, held in Geneva 1 *September*—13 *September* 1958.
Vol. 30. *Fundamental physics* (viii—329 pages).
Vol. 31. *Theoretical and experimental aspects of controlled nuclear fusion* (viii—390 pages).
Vol. 32. *Controlled fusion devices* (viii—463 pages).
(United Nations, Geneva, 1958).

These three volumes, out of the thirty-three in which the proceedings of the second Geneva conference are reported, are the most likely to interest physicists concerned with the more fundamental, non-technological aspects of the study of nuclear energy and its applications. The two volumes devoted to nuclear fusion are indeed essential as sources of information on this new branch of development. The volume on fundamental physics contains a large amount of first-rate work, in particular some valuable survey reports, as well as a number of communications which would not easily have found their way into journals run by critically-minded editors.

L. R.

L. D. Landau and E. M. Lifshitz, *The classical theory of fields.* (*Course of theoretical physics, Vol.* 2). Translated from the Russian by Morton Hamermesh (Pergamon Press, London, 1959. ix—354 pages. 70s. net).

This is a re-issue by Pergamon Press of the translation of the excellent textbook of Landau and Lifschitz on classical field theory first published by Addison-Wesley in 1951 (I may be permitted to refer the reader to my review of that edition in Proc. Phys. Soc. A **65** (1952) 567). One would have thought that the publishers of the present issue (which is merely a photostatic reproduction of the previous one) would at least have taken care to make the size of the pages uniform with the other volumes of the author's famous course of theoretical physics, of which they have undertaken the complete translation; but, incredible as it sounds, they have neglected this elementary step to ensure a neat appearance of the whole work on library shelves.

L.R.

Sonderausschuss Radioaktivität, Bundesrepublik Deutschland, Zweiter Bericht (*März* 1959) (Georg Thieme Verlag, Stuttgart, 1959. 117 pages. DM 12.60).

For a review of the first report of the German commission on radioactivity, see this journal **10** (1959) 92. This second report brings a further collection of valuable statistical data concerning the various aspects of radioactive contamination. According to the cautious conclusions of the commission, the material is not yet sufficient to answer the UNO questionnaire on the subject. A 60 % increase in the number of nuclear-weapon tests in the period under investigation had no influence on the radioactivity of the low atmosphere.

L. R.

International directory of radioisotopes, Vol. I: Unprocessed and processed radioisotope preparations and special radiation sources (xiii—264 pages. $ 3.50).
Directory of nuclear reactors, Vol. I: Power reactors (214 pages. $ 3.50)
(International Atomic Energy Agency, Vienna, 1959).

Two useful publications from the new international organism concerned with atomic energy. The selection and arrangement of the material are well conceived and the production very neat, especially that of the reactor directory with its numerous technical drawings. All data contained in the latter directory have been either provided or checked by the authorities in the countries concerned, and can, therefore, be considered as the best available at the present time. Thanks to the co-operation of IAEA's Member States, it has also been possible to include in this volume a number of projects about which no information had hitherto been generally available and many details which have not been included in any previous publication. It is planned to issue periodical supplements to this volume in order to keep it up to date and as complete as possible.

L. R.

NORTH-HOLLAND BOOKS

ANALYTICAL and CANONICAL FORMALISM in PHYSICS

by ANDRÉ MERCIER

Head of the Department of Theoretical Physics University of Berne

6×9″ VIII + 222 pp. Guilders 20.00 (40s.)

CONTENTS

i. LAGRANGIAN FORMALISM
ii. LAGRANGIAN DENSITY
iii. CANONICAL FORMALISM
iv. CANONICAL FORM OF ELECTRODYNAMICS
v. HAMILTONIAN DENSITIES
vi. TRANSFORMATIONS
vii. CANONICAL FORMALISM WITH VANISHING JACOBIAN DETERMINANT

Those who are not highly specialized in these matters but do want to get a fairly broad knowledge of the subject are not aware of the fact that the greater parts of this formalism, including many specific conclusions of physical concern, do not involve in the least quantum theory, i.e. "quantization" of the fields. To show this and to provide the reader with a fairly complete presentation of the ***classical*** (i.e. not yet quantized) theory of fields is one of the main aims of the book.

This formalism is presented with great generality. Some special topics have also been included when they are found to be of importance in connection with the problems raised; however, they are not elaborated with the same generality, but just formulated as far as is found necessary for the understanding of these connections; for instance we can name: tensorial formalism and spinorial formalism.

A special chapter has been devoted to transformations of several kinds including canonical transformations, reversibility and the like as well as their interrelations, so that the ground is prepared for an understanding of the CPT-Theorems.

A short chapter on Dirac's dynamics with vanishing Jacobian closes the book.

The work builds upon the well-known *Principles of Analytical Dynamics* by the same author (in French), where particular weight is laid upon the homogeneous formalism, but it can easily be read with profit without knowledge of the latter by any advanced students in physics, astronomy or mathematics as well as by research workers who want to get a thorough practice in the use of these methods.

Many examples and as many as 124 problems illustrate the formalism exposed.

Sole Agency for U.S.A.: Interscience Publishers Inc.-New York

NORTH-HOLLAND PUBLISHING COMPANY - AMSTERDAM

NORTH-HOLLAND BOOKS

ASYMPTOTIC METHODS in ANALYSIS

by **N. G. DE BRUIJN** *Professor of Mathematics at the University of Amsterdam*

Asymptotics is that part of analysis which considers problems of the type dealt with in this book

Contents

Ch. I. Introduction
Ch. II. Implicit Functions
Ch. III. Summation
Ch. IV. The Laplace Method for Integrals
Ch. V. The Saddle Point Method
Ch. VI. Applications of the Saddle Point Method
Ch. VII. Indirect Asymptotics
Ch. VIII. Iterated Functions
Ch. IX. Differential Equations

6×9" XII+200 pages Guilders 20.00 (40s.)